

New Dual P-Glycoprotein (P-gp) and Human Carbonic Anhydrase XII (hCA XII) Inhibitors as Multidrug Resistance (MDR) Reversers in Cancer Cells

Laura Braconi, Elisabetta Teodori,* Chiara Riganti, Marcella Coronello, Alessio Nocentini, Gianluca Bartolucci, Marco Pallecchi, Marialessandra Contino, Dina Manetti, Maria Novella Romanelli, Claudiu T. Supuran, and Silvia Dei



Cite This: <https://doi.org/10.1021/acs.jmedchem.2c01175>



Read Online

ACCESS |



Metrics & More

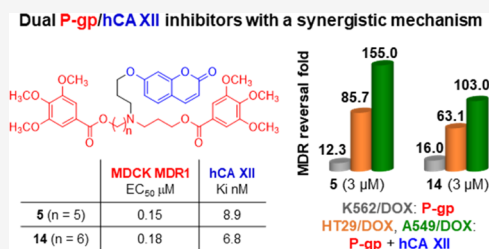


Article Recommendations



Supporting Information

ABSTRACT: In a continuing search of dual P-gp and hCA XII inhibitors, we synthesized and studied new *N,N*-bis(alkanol)amine aryl diester derivatives characterized by the presence of a coumarin group. These hybrids contain both P-gp and hCA XII binding groups to synergistically overcome the P-gp-mediated multidrug resistance (MDR) in cancer cells expressing both P-gp and hCA XII. Indeed, hCA XII modulates the efflux activity of P-gp and the inhibition of hCA XII reduces the intracellular pH, thereby decreasing the ATPase activity of P-gp. All compounds showed inhibitory activities on P-gp and hCA XII proteins taken individually, and many of them displayed a synergistic effect in HT29/DOX and A549/DOX cells that overexpress both P-gp and hCA XII, being more potent than in K562/DOX cells overexpressing only P-gp. Compounds **5** and **14** were identified as promising chemosensitizer agents for selective inhibition in MDR cancer cells overexpressing both P-gp and hCA XII.



INTRODUCTION

The expression of some ATP binding cassette (ABC) transporter proteins on the cell membrane is one of the main features of chemoresistant cancer cells.^{1,2} These energy-dependent transmembrane proteins act as extrusion pumps and reduce the intracellular concentration of anticancer drugs by actively transporting them out of tumor cells and, consequently, lowering their therapeutic efficacy.^{3,4} This phenomenon is one of the main causes of multidrug resistance (MDR), a condition in which cells acquire resistance, over the course of the treatment, to several anticancer drugs with different structures and mechanism of action.⁵ The main human ABC proteins associated with MDR are P-glycoprotein (P-gp), multidrug-resistance-associated protein-1 (MRP1), and breast cancer resistance protein (BCRP) whose expression in tumor cells has been correlated to poor patients' prognosis in numerous studies.^{6,7}

The most highly studied ABC transporter P-glycoprotein (P-gp) is widely overexpressed in human cancer tissues and plays an important role in removing chemotherapeutic agents from cells and decreasing the intracellular drug accumulation.⁸ Because of the importance of P-gp in the regulation of MDR and its clinical correlation, many efforts have been devoted to the development of novel P-gp inhibitors to reverse MDR.^{9,10} These compounds, also known as chemosensitizers, can restore the efficacy of anticancer agents, which are substrates of ABC transporters, when coadministered with them in resistant tumor cells.¹¹ To

date, many P-gp modulators have been identified that can be classified into three generations according to their chronology and characteristics;^{12,13} however, only a few of these compounds have entered clinical trials.¹⁴ The observed problems are mainly due to the presence of P-gp in several healthy tissues where it is responsible for various physiological and pharmacological effects.^{15,16} Furthermore, P-gp modulators could modify the pharmacokinetics of other coadministered substances such as chemotherapeutic agents.¹⁷

To reduce the alteration of the permeability of the normal tissue membranes, it is therefore desirable to develop structurally novel compounds capable of selectively inhibiting the P-gp efflux effect in resistant tumor cells.

A recent work¹⁸ reported that P-gp is colocalized and physically associated with the isoform XII of human carbonic anhydrase (hCA XII) on the membrane of several resistant cancer cells. The metalloenzymes carbonic anhydrases (CAs, EC 4.1.1.1) catalyze the conversion of carbon dioxide to bicarbonate and a proton. Human CAs (hCAs) include 15 isoforms of α -CA with different tissue distributions and cellular localization and

Received: July 22, 2022

play an important role in numerous physiological and pathological processes.¹⁹ Among these isoforms, hCA IX and XII are extracellular membrane-bound CAs overexpressed in many solid and hypoxic tumors and are associated with their progression and metastases formation.^{20–22} hCA IX and XII preserve an alkaline intracellular pH and extracellular acidosis, which promotes the growth of cancer cells, compromising that of normal cells.^{23,24} The intracellular alkalinization maintained by hCA XII is optimal for the efflux activity of P-gp. Therefore, the high expression of hCA XII in some chemoresistant P-gp-positive cancer cells¹⁸ contributes to MDR. Indeed, the pharmacological inhibition of hCA XII causes a decrease in the intracellular pH, which elicits a remarkable reduction in the ATPase activity of P-gp and consequently in the efflux activity of the transporter.^{18,25} Therefore, the development of compounds with a dual inhibition of P-gp and hCA XII could be a useful strategic approach to revert MDR in resistant tumor cells that overexpress both proteins. This synergistic mechanism may allow these compounds to act primarily in resistant tumors without interfering with the physiological function of P-gp.

In a previous study,²⁶ we reported a series of compounds capable of inhibiting P-gp and hCA XII in tumor cells that overexpress both proteins. Indeed, these hybrids are characterized by an *N,N*-bis(alkanol)amine diester group functionalized with a different aryl nucleus (Ar), found in potent P-gp ligands,^{27–30} and a coumarin or benzene sulfonamide group (Y) to inhibit hCA XII^{31–33} (Figure 1, structure A). Many

compounds showed high MDR reversal effects on doxorubicin-resistant human colorectal carcinoma LoVo/DOX cells, which overexpress both P-gp and hCA XII proteins. These compounds were more potent as P-gp inhibitors in LoVo/DOX cells than in K562/DOX cells overexpressing only P-gp, showing a synergistic MDR reversal effect.²⁶

To continue our project on dual P-gp/hCA XII inhibitors, we synthesized new derivatives containing the *N,N*-bis(alkanol)-amine aryl diester scaffold to modulate the P-gp activity and a coumarin group to selectively target hCA XII, as observed in the first series.²⁶ In this new series, the tertiary amino group is linked to two ester groups by a propyl and a 5-, 6-, or 7-methylene chain, while the coumarin moiety is connected through a propyl chain to the nitrogen atom by an ethereal bond. The aromatic ester groups inserted were a combination of (*E*)-3-(3,4,5-trimethoxyphenyl)vinyl, 3,4,5-trimethoxyphenyl, or anthracene residues (a–c) (Figure 1, structure B).

The new compounds 1–27, as hydrochlorides, were first tested for their inhibitory effect on P-gp and hCA XII proteins taken individually. As regards the P-gp inhibition, all of these compounds were tested in the coadministration assay with doxorubicin in K562/DOX cells that overexpress only P-gp.³⁴ To evaluate their hCA selectivity profiles, all of the synthesized compounds were studied on four different hCA isoforms (hCA I, II, IX, and XII).

Selected compounds were also tested in doxorubicin-resistant human adenocarcinoma colon cells (HT29/DOX) and doxorubicin-resistant non-small cell lung cancer cells (A549/DOX), which overexpress both P-gp and hCA XII:¹⁸ thus, the synergistic effect of these compounds was analyzed in a specific environment where these two proteins coexist. Moreover, to confirm the influence of the hCA XII catalytic effect on the P-gp efflux activity in MDR-resistant cells, doxorubicin cytotoxicity was evaluated in P-gp knockout (P-gp KO) and hCA XII knockout (hCA XII KO) HT29/DOX and A549/DOX cell lines. Then, compounds 5 and 14 were tested in the coadministration assay with doxorubicin in the same cell lines. In addition, the intracellular pH and doxorubicin accumulation were evaluated in all studied cell lines.

Finally, the chemical stability of these diester derivatives was investigated in phosphate-buffered solution (PBS) and human plasma samples.

RESULTS AND DISCUSSION

Chemistry. The reaction pathway used to synthesize the designed derivatives 1–27 is reported in Scheme 1. The (hydroxyalkyl)aminoesters 31–37 were previously synthesized by our group,^{28,29,35} while 38–40 were obtained by reaction of the proper bromoesters 28–30^{28,35} with 7-aminoheptan-1-ol³⁶ in dry CH₃CN, following standard procedures. Final compounds 1–27 were obtained starting from ((hydroxyalkyl)-alkylcoumarin)aminoesters 41–50, which were synthesized by the alkylation of the proper (hydroxyalkyl)aminoester with 7-(3-bromopropoxy)-2*H*-chromen-2-one (51) in dry CH₃CN (Scheme 1). Finally, compounds 1–27 were obtained by esterification of 41–50 with the proper carboxylic acid ((*E*)-3-(3,4,5-trimethoxyphenyl)acrylic acid, 3,4,5-trimethoxybenzoic acid, or anthracene-9-carboxylic acid), using 1-ethyl-3-(3'-dimethylaminopropyl)carbodiimide (EDC) hydrochloride and 4-dimethylaminopyridine (DMAP) in dry CH₂Cl₂ or through the acyl chloride obtained by treatment of the suitable acid with SOCl₂ in CHCl₃ (free of ethanol),³⁷ as reported in Scheme 1 (for details, see the Experimental Section). All free bases 1–27

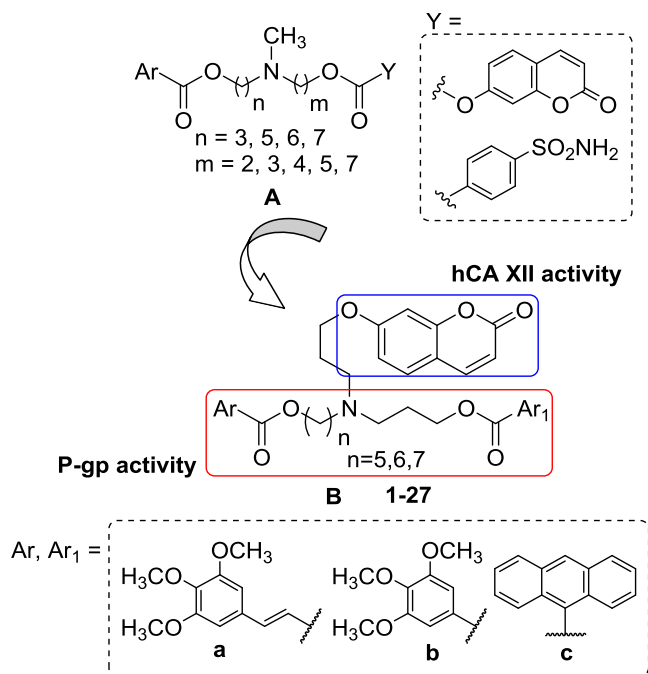
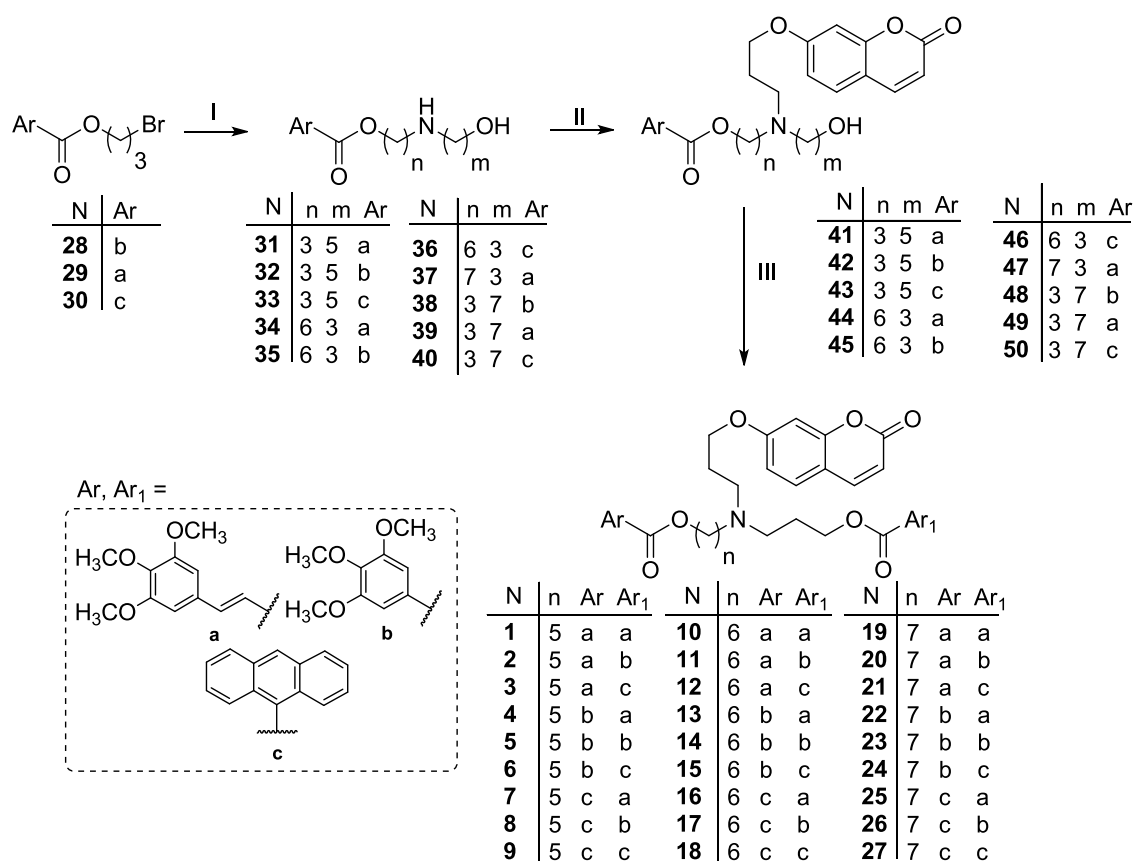


Figure 1. General structure of the leads (structure A) and the (*N*-alkylcoumarin)aminoaryl diester compounds 1–27 synthesized in this study (structure B).

compounds displayed a multitarget activity against hCA XII and P-gp being active in the hCA XII inhibition test and in the rhodamine-123 (Rhd-123) uptake test in doxorubicin-resistant erythroleukemia K562 cells (K562/DOX) that overexpress only P-gp. Derivatives containing a coumarin residue were potent and effective hCA XII inhibitors and exhibited a modest inhibitory effect on P-gp in K562/DOX cells. Moreover, some coumarin

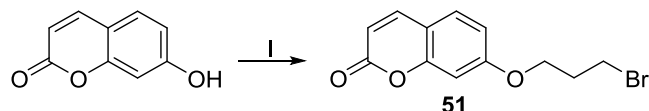
Scheme 1. Reagents and conditions: (I) 7-aminoheptan-1-ol,³⁶ K₂CO₃, dry CH₃CN, 60 °C, overnight (yield 71–72%); (II) 51, K₂CO₃, dry CH₃CN, 60 °C, 20 h (yield 47–69%); (III) Ar₁COOH, EDC hydrochloride, DMAP, dry CH₂Cl₂, rt, 48 h (method A) or Ar₁COCl, CHCl₃ (free of ethanol), rt, 18 h (method B) (yield 14–100%)



were transformed into the corresponding hydrochlorides, which were used in the biological experiments and stability analysis (for details, see the [Experimental Section](#)).

Compound **51** was obtained by reaction of the commercially available 7-hydroxy-2*H*-chromen-2-one with 1,3-dibromopropane in acetone with very good yields, as reported in [Scheme 2](#).

Scheme 2. Reagents and conditions: (I) 1,3-dibromopropane, K₂CO₃, acetone, reflux, overnight (yield 92%)



Chemical Stability Tests. The chemical stability of all of these diester derivatives was evaluated in phosphate-buffered solution (PBS) and human plasma samples. The stability analyses were performed by liquid chromatography coupled with a triple quadrupole mass spectrometry system (LC-MS/MS), operating in multiple reaction monitoring (MRM) mode. The LC-MS/MS instrument and parameters used are reported in the [Supporting Information](#).

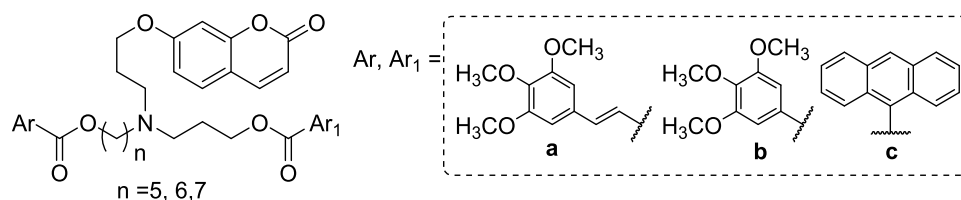
In these assays, we monitored the variation of our diester molecules' concentration at four different incubation times both in PBS and in human plasma samples to evaluate their susceptibility toward spontaneous or enzymatic hydrolysis, respectively. By plotting any variation of analyte concentration

vs the incubation time, the corresponding degradation profiles in both the tested matrices were obtained. The analyte concentration (1 μM) used during the stability tests is generally smaller than its Michaelis–Menten constant (*K_M*), and the enzymatic degradation rate is described by a first-order kinetic. Therefore, by plotting the natural logarithm of the quantitative data versus the incubation time, a linear function can be used, and its slope represents the degradation rate constant (*k*). Accordingly, with the linear function, the half-life (*t*_{1/2}) of each tested compound can be calculated as follows

$$t_{1/2} = (\ln(0.50 \mu\text{M}))/k$$

The plots of the natural logarithm of the quantitative data versus the incubation time of all of the studied compounds were analyzed. Results demonstrated that all of these compounds were stable both in PBS and in human plasma samples. The *k* values of all our compounds were close to 0, yielding extremely high *t*_{1/2} values. Since under the proposed experimental conditions a half-life over 240 min is not properly assessed, it is reasonable to consider that their *t*_{1/2} values could be equal to or greater than 240 min. The degradation profiles of all of these molecules in both the tested media are reported in the [Supporting Information](#). The *t*_{1/2} value ≤ 2 h of ketoprofen ethyl ester (KEE), used as a reference compound, demonstrated that the employed human batch was enzymatically active.

CA Inhibitory Activity. Compounds 1–27 were tested on four hCA isoforms, the cytosolic hCA I and II, and the tumor-associated transmembrane hCA IX and XII isoforms by a stopped-flow CO₂ hydrase assay.³⁸ The hCA inhibition data of

Table 1. Inhibitory Activity on hCA I, II, IX, and XII Isoforms and Doxorubicin Cytotoxicity Enhancement Effect in K562/DOX Cells of Compounds 1–27 and of the Two Reference Compounds Acetazolamide (AAZ) and Verapamil (Ver)

compounds				K_i (nM) ^a				RF ^b	
N	n	Ar	Ar ₁	hCA I	hCA II	hCA IX	hCA XII	1 μ M	3 μ M
1	5	a	a	>10 000	>10 000	39.5	34.6	9.5	25.7
2	5	a	b	>10 000	>10 000	24.2	16.2	3.3	7.7
3	5	a	c	>10 000	>10 000	7.9	44.9	3.1	8.4
4	5	b	a	>10 000	>10 000	58.8	22.3	6.9	25.7
5	5	b	b	>10 000	>10 000	40.7	8.9	5.2	12.3
6	5	b	c	>10 000	>10 000	36.2	30.8	3.1	7.7
7	5	c	a	>10 000	>10 000	104.5	56.4	3.6	8.9
8	5	c	b	>10 000	>10 000	93.7	55.2	2.4	7.1
9	5	c	c	>10 000	>10 000	136.8	73.4	1.0	1.0
10	6	a	a	>10 000	>10 000	8.1	32.4	22.5	30.0
11	6	a	b	>10 000	>10 000	50.2	21.6	8.2	45.0
12	6	a	c	>10 000	>10 000	26.8	66.3	2.2	9.0
13	6	b	a	>10 000	>10 000	71.7	10.1	1.1	11.1
14	6	b	b	>10 000	>10 000	82.7	6.8	6.4	16.0
15	6	b	c	>10 000	>10 000	54.1	43.3	3.9	8.9
16	6	c	a	>10 000	>10 000	148.3	74.0	4.3	13.6
17	6	c	b	>10 000	>10 000	123.2	23.9	4.4	9.3
18	6	c	c	>10 000	>10 000	166.5	90.2	1.2	1.3
19	7	a	a	>10 000	>10 000	27.8	50.9	1.8	26.7
20	7	a	b	>10 000	>10 000	5.2	17.2	8.0	26.7
21	7	a	c	>10 000	>10 000	14.2	37.6	2.0	3.0
22	7	b	a	>10 000	>10 000	43.8	4.6	16.0	22.8
23	7	b	b	>10 000	>10 000	18.3	31.7	8.0	20.0
24	7	b	c	>10 000	>10 000	38.5	62.5	2.3	6.1
25	7	c	a	>10 000	>10 000	71.1	113.1	3.0	6.4
26	7	c	b	>10 000	>10 000	41.3	10.1	2.0	6.1
27	7	c	c	>10 000	>10 000	102.2	83.8	1.0	2.4
AAZ				250.0	12.0	25.0	5.7		
Ver								1.2	3.0

^aMean from three different assays by a stopped-flow technique (errors were in the range of ± 5 –10% of the reported values). ^bInhibition of the P-gp transport activity in K562/DOX cells expressed as RF that is the ratio between the IC_{50} of doxorubicin alone and in the presence of modulators (RF = IC_{50} of doxorubicin – modulator/ IC_{50} of doxorubicin + modulator).

the new compounds are reported in Table 1 together with those of acetazolamide (AAZ), used as a standard inhibitor. Results show that all of these derivatives were inactive against the off-target hCA I and II isoforms, while they inhibited both hCA IX and XII at nanomolar concentrations. As expected, the presence of the coumarin group addresses the activity only to hCA IX and XII.^{39,40} Interestingly, in this series of compounds, the interaction with hCA XII seems to be influenced by the length of the linkers: indeed, derivatives 1–18, carrying a total spacer of 8 or 9 methylenes ($n = 5$ or 6), displayed preference toward hCA XII, except for 3, 10, and 12; compounds characterized by $n = 7$ were generally more active on hCA IX, except for 22, 26, and 27. Compounds 3, 10, and 20 were more potent on the hCA IX isoform than AAZ, showing K_i values < 10 nM.

Notably, compounds 5, 14, and 22 showed the highest potency toward hCA XII, with K_i values < 10 nM ($K_i = 8.9$, 6.8, and 4.6 nM, respectively), as compared with the reference compound AAZ. Compounds 5 and 14 have a 5- or 6-methylene

chain length, respectively, and the 3,4,5-trimethoxyphenyl ester residue (b) for both the aryl moieties; compound 22, with a 7-methylene chain length, shows instead a combination of the (*E*)-3-(3,4,5-trimethoxyphenyl)vinyl (a) and the 3,4,5-trimethoxyphenyl (b) groups.

Doxorubicin Cytotoxicity Enhancement Assay on K562/DOX Cells. The P-gp transport activity inhibition of compounds 1–27 was evaluated on the doxorubicin coadministration assay to assess their effects on the enhancement of the cytotoxicity of the antitumoral drug in the resistant K562/DOX cells, which overexpress only P-gp.³⁴ K562 is a highly undifferentiated erythroleukemia cell line.⁴¹ The P-gp substrate, doxorubicin, is generally inactive in tumor cells, which express the protein, as it is expelled from the membrane by the pump.

Compounds were first studied, at 1, 3, and 10 μ M concentrations, to evaluate their intrinsic cytotoxicity in both the parental K562 and the resistant K562/DOX cell lines, using the 3-(4,5-dimethylthiazolyl-2)-2,5-diphenyl tetrazolium bro-

mid (MTT) assay.⁴² All compounds had no intrinsic cytotoxicity in the parental line and showed a toxicity not exceeding 20% in the resistant cells at the three concentrations tested (Supporting information, Figure S45).

The ability of compounds 1–27 to enhance the doxorubicin cytotoxicity in K562/DOX cells was assessed by evaluating the decrease of doxorubicin IC₅₀ in the presence of 1 and 3 μM concentrations of the tested molecules. The results were expressed as RF (reversal fold) values that are the ratio between the IC₅₀ value of doxorubicin alone and in the presence of the studied compounds: the higher the RF value, the higher the MDR reversal activity. Table 1 reports the RF values of compounds 1–27 in comparison with those of verapamil used as a standard reference. All our compounds enhanced the cytotoxicity of doxorubicin to a different extent and most of them showed higher RF values than those of verapamil. These data showed that the aryl moieties mainly influenced the P-gp inhibitory effects of these compounds since derivatives carrying the (*E*)-3-(3,4,5-trimethoxyphenyl)vinyl (**a**) and the 3,4,5-trimethoxyphenyl (**b**) groups gave the best results. Among these, the most potent compounds were **1**, **4**, and **5** (*n* = 5), **10**, **11**, and **14** (*n* = 6), and **20**, **22**, and **23** (*n* = 7), with RF values higher than 5.0 and 12.0 when used at 1 and 3 μM, respectively. Otherwise, the anthracene derivatives showed in general the lowest effects.

Notably, the potent P-gp inhibitors **5**, **14**, and **22** were also the most potent on hCA XII.

Doxorubicin Cytotoxicity Enhancement Assay in HT29/DOX and A549/DOX Cells. To analyze the effect of these dual P-gp/hCA XII inhibitors in a specific environment where the two target proteins coexist, the most potent P-gp inhibitors bearing the aryl residues **a** and **b** (**1**, **2**, **4**, **5**, **10**, **11**, **13**, **14**, **19**, **20**, **22**, and **23**) were also tested in the doxorubicin cytotoxicity enhancement assay in doxorubicin-resistant human adenocarcinoma colon cells (HT29/DOX) and doxorubicin-resistant non-small cell lung cancer cells (A549/DOX), which overexpress both P-gp and hCA XII.¹⁸ Compounds carrying the anthracene moiety were not selected since they were the least active in the K562/DOX cell line test.

The expression levels of P-gp and hCA XII in sensitive HT29 and A549 cells and their resistant counterparts (HT29/DOX and A549/DOX cells) were checked by immunoblotting analysis, as described in the Experimental Section and reported in the Supporting information (Figure S44). The resistant sublines also showed an increased expression of MRP1 (Supporting information, Figure S44), another transporter involved in doxorubicin resistance, that, however, was not associated with hCA XII nor was affected in its efflux activity by hCA XII.¹⁸

The MTT assay was employed to evaluate the intrinsic cytotoxicity of the selected compounds at 1, 3, and 10 μM concentrations in the parental HT29 and A549 and the resistant HT29/DOX and A549/DOX cells, using the MTT assay.⁴² All compounds had no intrinsic cytotoxicity in the parental lines and showed a toxicity not exceeding 20% in the resistant lines at the three concentrations tested (Supporting information, Figure S46). Similarly, they did not reduce the viability by more than 20–25% in nontransformed epithelial colon EpiCoc and lung BEAS-2B cells at 10 μM (Supporting information, Figure S47). These data suggest that they could be used in the low micromolar range against cancer cells, in combination with classical chemotherapeutic drugs, without inducing toxic effects on nontransformed cells.

To verify this potential use, the ability of our compounds to increase the doxorubicin cytotoxicity was next evaluated by studying them at 1 and 3 μM in combination with the anticancer drug, and the RF values were measured (Table 2). All our

Table 2. RF Values of the 12 Selected Compounds in the Resistant HT29/DOX and A549/DOX Cell Lines

compounds	HT29/DOX		A549/DOX	
	RF ^a		RF ^a	
	1 μM	3 μM	1 μM	3 μM
1	14.9	18.7	21.5	30.2
2	38.4	44.5	54.0	64.3
4	21.7	41.1	39.5	65.0
5	44.4	85.7	70.4	155.0
10	40.2	47.5	65.1	85.4
11	10.8	29.7	17.6	49.8
13	14.1	4.15	16.5	11.6
14	46.2	63.2	67.4	103.0
19	60.5	87.0	92.2	131.6
20	13.1	16.2	19.2	31.5
22	37.6	61.9	61.9	82.4
23	27.2	26.6	37.0	41.3

^aInhibition of the P-gp transport activity on two resistant cell lines, expressed as RF that is the ratio between the IC₅₀ of doxorubicin alone and in the presence of modulators (RF = IC₅₀ of doxorubicin – modulator/IC₅₀ of doxorubicin + modulator).

compounds were able to restore the antineoplastic effect of doxorubicin, a typical substrate of P-gp, with highly reduced cell viability. The best results, in both the resistant cell lines (HT29/DOX and A549/DOX), were obtained for **5** and **14** (Ar, Ar₁ = **b**, *n* = 5 and 6, respectively), **19** (Ar, Ar₁ = **a**, *n* = 7), and **22** (Ar = **b**, Ar₁ = **a**, *n* = 7), with RF values higher than 60 when used at 3 μM. Interestingly, all of these compounds showed RF values higher than those obtained in K562/DOX cells, which overexpress only P-gp, displaying a synergistic effect in the two resistant cell lines (HT29/DOX and A549/DOX) that overexpress both P-gp and hCA XII (see Tables 1 and 2). As an example, when **5** and **14** were tested at 3 μM in the A549/DOX cell line, they displayed RF values about 12 and 6 times higher than in K562/DOX cells, respectively (**5**: RF = 155.0 in A549/DOX and RF = 12.3 in K562/DOX; **14**: RF = 103.0 in A549/DOX and RF = 16.0 in K562/DOX). Compound **13** was the only one not showing a dose-dependent activity; in fact, it displayed a lower RF at 3 μM than at 1 μM in HT29/DOX and A549/DOX cells. This effect, however, was not detected in K562/DOX cells, devoid of hCA XII, differently from HT29/DOX and A549/DOX cells. We may hypothesize that **13** inhibits P-gp at both 1 and 3 μM, reversing doxorubicin resistance as in the case of K562/DOX. When both P-gp and hCA XII coexist, as in the case of HT29/DOX and A549/DOX cells, **13** regularly interfered with the P-gp/hCA XII complex reversing doxorubicin resistance at a low concentration (1 μM). At the higher concentration (3 μM), it may have a paradoxical loss of activity on hCA XII or even an activation, reducing its power as an agent counteracting doxorubicin resistance. Although this aspect requires further investigation, it is noteworthy that **13** is the only exception between the three cellular models analyzed, while all of the other compounds had a dose-dependent RF in all of the cell lines tested.

Thus, compounds **5** and **14** were selected for further studies as the best derivatives based on the results on the hCA XII isoform

and in the K562/DOX, HT29/DOX, and A569/DOX cell lines. Interestingly, both carry the residue **b** as Ar and Ar₁ moieties.

Transport Inhibition of Fluorescent Probes in MDCK Transfected Cells. To further confirm the hypothesis that these derivatives were P-gp inhibitors, we tested the activity of compounds **5** and **14** on P-gp, MRP1, and BCRP in three Madin-Darby Canine Kidney (MDCK) transfected cell lines that overexpress the three proteins (P-gp, MRP1, or BCRP). The inhibiting activity of the two compounds on P-gp and MRP1 was evaluated by measuring the transport inhibition of the profluorescent probe calcein-AM (P-gp and MRP1 substrate) in MDCK-MDR1 and MDCK-MRP1 cells (P-gp- and MRP1-overexpressing cells, respectively). The activity on BCRP was instead evaluated using the fluorescent probe Hoechst 33342 (BCRP substrate) in MDCK-BCRP cells (BCRP-overexpressing cells).⁴³

The results reported in Table 3 showed that compounds **5** and **14** inhibited the P-gp-mediated transport of calcein-AM, with

Table 3. P-gp Interaction Activity of Compounds 5 and 14 in MDCK-MDR1, MDCK-MRP1, and MDCK-BCRP Cells Overexpressing P-gp, MRP1, and BCRP, Respectively

compounds	EC ₅₀ μM ^a		
	MDR1	MRP1	BCRP
5	0.15 ± 0.02	NA	NA
14	0.18 ± 0.03	NA	NA

^aValues are the mean ± standard error of the mean (SEM) of two independent experiments, with samples in triplicate. NA, not active.

EC₅₀ values in the sub-micromolar range. Otherwise, they were completely inactive on the MRP1 and BCRP transporters.

Doxorubicin Cytotoxicity Enhancement Assay in P-gp Knockout (P-gp KO) and hCA XII Knockout (hCA XII KO) HT29/DOX and A549/DOX Cell Lines. To confirm the influence of the hCA XII catalytic effect on the P-gp efflux activity in MDR-resistant cells, P-gp and hCA XII were knocked out (KO) in resistant HT29/DOX and A549/DOX cell lines.

The expression levels of P-gp and hCA XII in P-gp KO and hCA XII KO HT29/DOX and A549/DOX cell lines were checked by immunoblotting, as described in the Experimental Section and reported in the Supporting information (Figure S44).

The results reported in Table 4 highlighted, as expected, that the IC₅₀ doxorubicin values were much lower in P-gp KO cells than in wild-type-resistant HT29/DOX and A549/DOX cells

Table 4. Doxorubicin Cytotoxicity in All Studied HT29 and A549 Cell Lines and RF Values in the Presence of Compounds 5 and 14 in P-gp KO and hCA XII KO HT29/DOX and A549/DOX Cell Lines

treatment ^a	IC ₅₀ μM							
	HT29	HT29/DOX	A549	A549/DOX				
DOX	1.38 ± 0.03	12.00 ± 0.85	2.38 ± 0.009	15.50 ± 0.93				
treatment ^a	HT29/DOX		HT29/DOX		A549/DOX		A549/DOX	
	P-gp KO		hCA XII KO		P-gp KO		hCA XII KO	
	IC ₅₀ μM	RF ^b						
DOX	0.46 ± 0.013		1.30 ± 0.06		0.9 ± 0.013		5.44 ± 1.5	
DOX + 5	0.15 ± 0.044	3.1	1.30 ± 0.11	1	0.16 ± 0.012	6.0	4.79 ± 0.09	1.1
DOX + 14	0.14 ± 0.009	3.3	1.25 ± 0.2	1	0.93 ± 0.015	1.03	4.10 ± 0.012	1.3

^aCompounds **5** and **14** were tested at a 1 μM concentration. ^bInhibition of the P-gp transport activity on knockout cell lines expressed as RF that is the ratio between the IC₅₀ of doxorubicin alone and with modulators (RF = IC₅₀ of doxorubicin – modulator/IC₅₀ of doxorubicin + modulator).

(Table 4). The almost complete absence of the protein determines an increase in the cytotoxicity of doxorubicin also compared to the sensitive HT29 and A549 cells (Table 4), where the basal levels of P-gp confer a weak constitutive resistance to the drug. In P-gp KO HT29/DOX and A549/DOX cells, the coadministration of doxorubicin with 1 μM of the selected compounds **5** and **14** resulted in IC₅₀ values lower than those of doxorubicin alone, except for **14** in P-gp KO A549/DOX cells (Table 4). The reduction of the IC₅₀ values is likely due to the sum of the increase in the accumulation of doxorubicin, caused by the knockout of P-gp, and by an additional effect due to the inhibition of hCA XII exerted by **5** and **14**. The explanation of this effect requires further investigations.

In hCA XII KO cells, doxorubicin IC₅₀ values are similar or even slightly higher than those in the sensitive HT29 and A549 cells, and the coadministration with **5** and **14** did not significantly enhance the cytotoxicity of doxorubicin (Table 4). These results suggest that the complete absence of hCA XII impairs the efflux activity of P-gp that is expressed in these resistant cells; therefore, our dual inhibitors did not show any effect. Based on these results, we propose that our inhibitors show the maximal efficacy in cancer cells expressing both hCA XII and P-gp.

Intracellular pH and Doxorubicin Accumulation. The intracellular pH (pHi) was measured in sensitive, wild-type-resistant, and P-gp KO- and hCA XII KO-resistant HT29 and A549 cells by a pH-sensitive fluorescent probe, and the results are reported in Table 5. The pHi value of the resistant HT29/

Table 5. Intracellular pH (pHi) Values of Sensitive, Wild-Type Resistant, and P-gp KO- and hCA XII KO-Resistant HT29 and A549 Cells

cell lines	pHi ^a	cell lines	pHi ^a
HT29	7.41 ± 0.05	A549	7.39 ± 0.03
HT29/DOX	7.64 ± 0.06	A549/DOX	7.66 ± 0.06
HT29/DOX KO P-gp	7.61 ± 0.08	A549/DOX KO P-gp	7.69 ± 0.05
HT29/DOX KO CAXII	7.42 ± 0.07	A549/DOX KO CAXII	7.41 ± 0.03

^aThe pHi was measured by a pH-sensitive fluorescent probe. Data are means ± standard deviation (SD) (n = 3).

DOX and A549/DOX cell lines was confirmed to be more alkaline than that of the parental counterparts (HT29 and A549). P-gp KO-resistant cells show pHi values like those of the

wild-type-resistant HT29/DOX and A549/DOX cells: this result was expected since P-gp has never been reported to alter pHi. Otherwise, hCA XII KO-resistant cells had a pHi similar to that of sensitive cells, demonstrating the crucial role of hCA XII in regulating the pH of resistant cells, as previously reported.¹⁸

Considering that the slightly alkaline pH maintained by hCA XII promotes the P-gp efflux activity,¹⁸ we next measured the intracellular retention of doxorubicin alone and in the presence of 1 and 3 μM of compounds **5** and **14** in HT29 and A549 in their resistant counterparts (HT29/DOX and A549/DOX) and the corresponding resistant P-gp KO and hCA XII KO cell lines (Figure 2). As expected, HT29/DOX and A549/DOX cells,

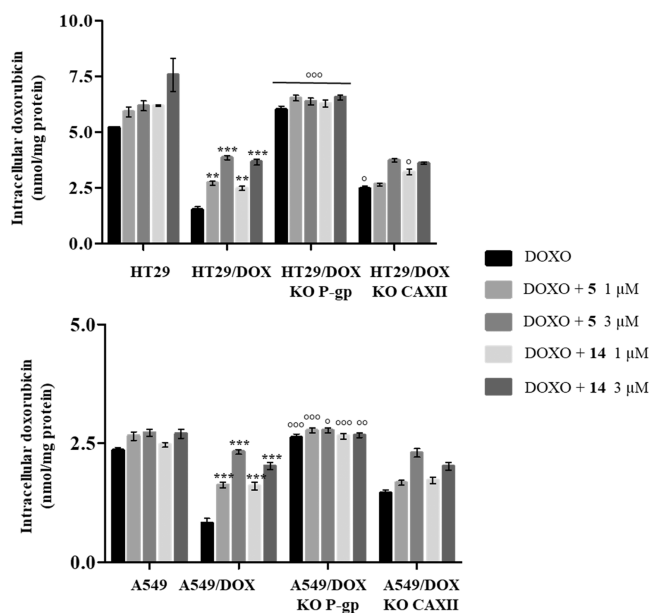


Figure 2. Intracellular accumulation of doxorubicin in sensitive, wild-type-resistant, and P-gp KO- and hCA XII KO-resistant cells. The cells were incubated for 24 h with 5 μM doxorubicin, with and without compounds **5** and **14** at 1 and 3 μM . The intracellular drug retention was measured spectrofluorimetrically. Data are means \pm SD ($n = 3$). ** $p < 0.01$, *** $p < 0.001$: versus wild-type HT29/DOX or A549/DOX cells treated with doxorubicin alone. $^{\circ}p < 0.05$, $^{\circ\circ}p < 0.01$, $^{\circ\circ\circ}p < 0.001$: P-gp KO HT29/DOX or A549/DOX cells versus wild-type HT29/DOX or A549/DOX cells.

compared to HT29 and A549 cells, showed reduced intracellular retention of doxorubicin that was increased by both compounds **5** and **14** in a dose-dependent way. The intracellular accumulation of doxorubicin was lower in A549/DOX cells than in HT29/DOX, likely because of the slightly basal expression of MRP1⁴⁴ (Figure S1), another transporter that can contribute to doxorubicin efflux.⁴ As expected, the accumulation of doxorubicin increased in P-gp KO cells, resembling sensitive counterparts. In these KO cells, compounds **5** and **14** did not significantly increase the retention of doxorubicin because of the absence of their first target P-gp.

In hCA XII KO cell lines, the intracellular concentration of doxorubicin was slightly higher than that in wild-type HT29/DOX and A549/DOX cell lines because the absence of hCA XII impaired the P-gp efflux activity. The presence of compounds **5** and **14** at 1 μM did not significantly increase the retention of doxorubicin, as evidenced also by the low RF values evaluated in these cells (Table 4). At the highest concentration tested (3 μM), our compounds caused an increase in doxorubicin

intracellular concentration compared to doxorubicin administered alone.

Kinetic Parameters of Doxorubicin Efflux in HT29 and A549, Their Wild-Type-Resistant Counterparts (HT29/DOX and A549/DOX), and the Corresponding hCA XII KO Cell Lines. Based on the previous results, we hypothesize that compounds **5** and **14** impaired the efflux kinetics of doxorubicin, thus increasing drug retention and toxicity. The results reported in Table 6 showed that the K_m of doxorubicin was increased by both compounds in the tested cells, suggesting that doxorubicin displayed a reduced affinity for P-gp. In hCA XII KO-resistant cells, they did not modify the K_m of doxorubicin compared to the wild-type-resistant cells, highlighting that the absence of hCA XII did not affect the affinity of doxorubicin for P-gp.

Compounds **5** and **14** reduced the maximal velocity (V_{max}) of the efflux in wild-type doxorubicin-resistant cell lines (HT29/DOX and A549/DOX cells), which was higher than in sensitive counterparts (HT29 and A549). The V_{max} values of doxorubicin in KO hCA XII-resistant cells were intermediate between those of sensitive and resistant cell lines, indicating that the absence of hCA XII reduced the maximal catalytic efficiency of doxorubicin efflux. No additional effects were observed in the presence of compounds **5** and **14** compared to wild-type HT29/DOX and A549/DOX since the compounds lacked one of their targets, hCA XII (Table 6). These data, again, indicated that the maximal efficacy of the compounds is achieved in the cells expressing both P-gp and hCA XII.

Overall, our results suggest that our compounds are maximally active when cancer cells coexpress both P-gp and hCA XII. While P-gp is widely diffused in normal tissues,⁴ hCA XII is an isoform mainly expressed in tumors.⁴⁵ Exploiting this preferential expression, the dual P-gp and hCA XII inhibition proposed in this study is a reasonably safe and selective approach to target mostly cancer cells, sparing nontransformed tissues, with low or no expression of hCA XII. It is worth noting that several small molecules^{46–48} or monoclonal antibodies directed against hCA XII^{49,50} have shown a direct antitumor effect. Indeed, the study of hCA IX and hCA XII interactomes revealed that these enzymes are central regulators in cancer cell proliferation and migration, thanks to their activity on pH control in the tumor microenvironment. As an example, the dual hCA IX/XII inhibitor SLC-0111 is actually in phase Ib/II clinical trials for antitumor and antimetastasing activity,⁵¹ and prompted by these promising results, the first hCA XII small inhibitors conjugated with monoclonal antibodies against hCA XII have been designed and proposed as strong antitumor agents.⁵² However, differently from these latest compounds, we did not observe a direct anticancer effect of our compounds. By contrast, we focused on the compounds used in the low micromolar range and evaluated their behavior in coadministration with classical chemotherapeutic drugs. Indeed, some hCA XII inhibitors also restored chemotherapeutic drug efficacy by controlling the pHi values, as for instance acetazolamide.^{53,54} Also, the activity of P-gp is deeply influenced by pHi, being higher at a slightly alkaline pH.⁵⁵ These findings are in line with our observation, showing a higher V_{max} corresponding to a higher catalytic activity, in HT29/DOX and A549/DOX cells that have higher pHi than their sensitive counterpart, caused by the increased expression of hCA XII.²⁵ By inhibiting the catalytic activity of hCA XII, compounds **5** and **14** create an unfavorable membrane environment for P-gp, contributing to a reduced efflux activity. The results of the present work are in line with several other pieces of evidence reporting that hCA XII

Table 6. Effects of Compounds 5 and 14 on Kinetic Parameters of Doxorubicin Efflux in HT29 and A549, Their Wild-Type-Resistant Counterparts (HT29/DOX and A549/DOX), and the Corresponding hCA XII KO Cell Lines^{ab}

	HT29		HT29/DOX		hCA XII KO HT29/DOX	
	K_m	V_{max}	K_m	V_{max}	K_m	V_{max}
Doxo	0.55 ± 0.028	3.21 ± 0.04	0.54 ± 0.01	8.10 ± 0.15	0.58 ± 0.03	5.47 ± 0.12
Doxo + 5(1 μM)	0.66 ± 0.009	3.29 ± 0.06	0.66 ± 0.009	5.30 ± 0.09	0.66 ± 0.01	4.30 ± 0.06
Doxo + 5(3 μM)	0.72 ± 0.022 ^c	3.12 ± 0.10	0.72 ± 0.009 ^d	3.21 ± 0.05	0.74 ± 0.01 ^d	3.22 ± 0.075
Doxo + 14(1 μM)	0.64 ± 0.014	3.21 ± 0.08	0.63 ± 0.009	4.73 ± 0.25	0.67 ± 0.01	4.27 ± 0.11
Doxo + 14(3 μM)	0.72 ± 0.009 ^d	3.28 ± 0.07	0.73 ± 0.009 ^d	3.80 ± 0.19	0.74 ± 0.008 ^d	3.45 ± 0.075
	A549		A549/DOX		hCA XII KO A549/DOX	
	K_m	V_{max}	K_m	V_{max}	K_m	V_{max}
Doxo	0.47 ± 0.017	2.35 ± 0.08	0.45 ± 0.019	7.51 ± 0.31	0.55 ± 0.028	4.08 ± 0.32
Doxo + 5(1 μM)	0.63 ± 0.013	2.36 ± 0.06	0.61 ± 0.015	5.10 ± 0.068	0.69 ± 0.021	3.75 ± 0.06
Doxo + 5(3 μM)	0.75 ± 0.012 ^c	2.35 ± 0.09	0.73 ± 0.012 ^c	3.98 ± 0.077	0.75 ± 0.012 ^d	2.74 ± 0.077
Doxo + 14(1 μM)	0.64 ± 0.009	2.43 ± 0.09	0.58 ± 0.014	5.27 ± 0.09	0.62 ± 0.012	3.60 ± 0.09
Doxo + 14(3 μM)	0.77 ± 0.02 ^c	2.41 ± 0.07	0.68 ± 0.013 ^c	4.14 ± 0.12	0.74 ± 0.016 ^d	2.92 ± 0.09

^aCells were grown in the absence and presence of compounds 5 and 14 at 1 and 3 μM, respectively, with increasing concentrations of doxorubicin for 24 h. K_m (μM) and V_{max} (μmoles/min) were calculated with the Enzfitter software. ^bData are presented as means ± SD. ^c $p < 0.05$. ^d $p < 0.01$: versus doxo-treated cells.

inhibitors have an indirect inhibition on P-gp activity, as reported in references.^{56,57}

Notably, P-gp and hCA XII are often coexpressed, as demonstrated in doxorubicin-resistant colon, lung, breast cancer, and osteosarcoma cell lines.^{18,25} Moreover, in glioblastoma, the two proteins are expressed in the drug-resistant stem cell component more than in the drug-sensitive, well-differentiated cells.⁵⁷ The novelty of our compounds relies on the fact that they simultaneously inhibit P-gp and hCA XII. As proved by the assay in resistant cells selectively knocked out for P-gp or hCA XII, the inhibitors lost their maximal efficacy if one of these two actors is missing. This feature makes the compounds particularly promising as chemosensitizer agents in the most aggressive and drug-resistant tumors that coexpress both P-gp and hCA XII. This is the case of tumors rich in stem cells, which are often responsible for tumor relapse, metastatization, and generation of drug-resistance clones,^{58–60} or hypoxic tumors that are the most invasive and resistant to the conventional therapies in use,^{61–63} where the transcription factor HIF-1 α transcriptionally upregulates P-gp and hCA XII.¹⁸

CONCLUSIONS

In this study, we reported new dual P-gp/hCA XII inhibitors based on the evidence that in several MDR cancer cells P-gp is colocalized to hCA XII and that the hCA XII catalytic activity modulates the P-gp efflux activity. The structure of these hybrid inhibitors contains both P-gp and hCA XII binding moieties to synergistically overcome the P-gp-mediated MDR in cancer cells that overexpress both proteins; thus, they presented the *N,N*-bis(alkanol)amine aryl diester group carrying a coumarin group on the nitrogen atom. All compounds showed inhibitory activities on P-gp and hCA XII proteins taken individually; in fact, they were able to enhance the cytotoxicity of the anticancer drug doxorubicin in resistant K562/DOX cells that overexpress only P-gp and inhibited hCA XII at nanomolar concentrations.

The doxorubicin cytotoxicity enhancement assays in HT29/DOX and A549/DOX cell lines, which overexpress both P-gp and hCA XII, highlighted a synergistic effect of these compounds since the selected derivatives bearing the aryl residues **a** and **b** were able to restore the antineoplastic effect of doxorubicin with RF values higher than those obtained in K562/

DOX cells that overexpress only P-gp. The P-gp inhibition activity of compounds 5 and 14 was also confirmed by the assay in MDCK transfected cells where the selectivity toward P-gp with respect to the other MDR sister proteins was proved.

The influence of hCA XII catalytic activity on the P-gp efflux activity in MDR-resistant cells was confirmed by the evaluation of the IC₅₀ values of doxorubicin alone or in the presence of the selected two compounds, 5 and 14, in P-gp knockout (P-gp KO) and hCA XII knockout (hCA XII KO) HT29/DOX and A549/DOX cell lines. In P-gp KO cells, the almost complete absence of P-gp determines an expected reduction in doxorubicin IC₅₀ values when used alone; however, in the presence of compounds 5 and 14, an increase in the cytotoxicity of doxorubicin is observed compared to that of resistant wild-type cells, probably due to the increase in the intracellular accumulation of doxorubicin caused by the absence of the transporter and by an additional effect due to the inhibition of hCA XII exerted by 5 and 14. In hCA XII KO cells, doxorubicin IC₅₀ values were similar to those in the sensitive cells, either when doxorubicin was used alone or in the presence of compounds 5 and 14 because the complete absence of hCA XII impairs the P-gp efflux activity and the dual inhibitors did not show any effect. These results confirmed that our inhibitors show the maximal efficacy in cancer cells expressing both hCA XII and P-gp.

Based on these results, we identified a new series of hybrid compounds that act as dual P-gp/hCA XII inhibitors with a synergistic mechanism. These compounds displayed a higher reversing activity in resistant tumor cells overexpressing both P-gp and hCA XII than in cells overexpressing only P-gp, in agreement with our evidence that the efflux activity of P-gp is modulated by the hCA XII catalytic activity.

In particular, compounds 5 and 14 resulted as promising P-gp-mediated MDR reversers characterized by the maximal efficacy in cancer cells expressing both hCA XII and P-gp proteins.

EXPERIMENTAL SECTION

Chemistry. General Information. All melting points were taken on a Büchi apparatus and are uncorrected. NMR spectra were recorded on a Bruker Avance 400 spectrometer (400 MHz for ¹H NMR, 100 MHz for ¹³C NMR). ¹H and ¹³C NMR spectra were measured at room temperature (25 °C) in an appropriate solvent. ¹H and ¹³C chemical

shifts are expressed in ppm (δ) referenced to tetramethylsilane (TMS). Spectral data are reported using the following abbreviations: s = singlet, d = doublet, dd = doublet of doublets, t = triplet, bs = broad singlet, m = multiplet, and coupling constants are reported in Hz, followed by integration. Assignments of the ^{13}C signals were performed using the attached proton test (APT) technique. Chromatographic separations were performed on a silica gel column by flash chromatography (Kieselgel 40, 0.040–0.063 mm; Merck). Yields are given after purification unless otherwise stated. The high-resolution mass spectrometry (HRMS) analysis was performed with a Thermo Finnigan LTQ Orbitrap mass spectrometer equipped with an electrospray ionization source (ESI). The accurate mass/charge ratio measure was carried out by introducing, via a syringe pump at $10\ \mu\text{L}\ \text{min}^{-1}$, the sample solution ($1.0\ \mu\text{g}\ \text{mL}^{-1}$ in mQ water: acetonitrile 50:50), and the signal of the positive ions was acquired. The proposed experimental conditions allowed monitoring the protonated molecules of studied compounds ($[\text{M} + \text{H}]^+$ species), which were measured with a proper dwell time to achieve 60 000 units of resolution at full width at half-maximum (FWHM). The elemental composition of each compound was calculated based on its measured accurate mass/charge ratio, accepting only results with an attribution error of less than 2.5 ppm and a not integer double bond/ring equivalent (RDB) value to consider only the protonated species.⁶⁴ All compounds are >95% pure as determined by high-performance liquid chromatography (HPLC)/diode-array detection (DAD) analysis: the specific analytical method used to determine purity and representative HPLC/DAD traces is included in the Supporting Information.

Compounds were named following IUPAC rules, as applied by ChemBioDraw Ultra 14.0 software. When reactions were performed in anhydrous conditions, the mixtures were maintained under nitrogen. Free bases 1–27 were transformed into the corresponding hydrochlorides by treatment with a solution of acetyl chloride (1.1 equiv) in anhydrous CH_3OH . The salts were crystallized from abs. ethanol/petroleum ether.

General Procedure for the Synthesis of (Hydroxyalkyl)aminoesters (38–40). To a solution of the proper bromoesters 28–30^{28,35} (1 equiv) in the adequate amount of dry CH_3CN , K_2CO_3 (1 equiv) and 7-aminoheptan-1-ol³⁶ (2 equiv) were added. The mixture was stirred at 60 °C overnight; then, the solvent was removed under reduced pressure and the residue was treated with CH_2Cl_2 . The organic layer was washed twice with 10% NaOH solution, dried over Na_2SO_4 , and concentrated under reduced pressure. Finally, the residue was purified by flash chromatography using $\text{CH}_2\text{Cl}_2/\text{CH}_3\text{OH}/\text{NH}_4\text{OH}$ 90:10:1 as an eluent, yielding the desired (hydroxyalkyl)aminoester as a pale yellow oil.

3-((7-Hydroxyheptyl)amino)propyl 3,4,5-Trimethoxybenzoate (38). Following the general procedure, compound 38 (0.10 g, yield: 70.6%) was synthesized from 28³⁵ (0.12 g, 0.37 mmol) and 7-aminoheptan-1-ol³⁶ (0.10 g, 0.74 mmol) in 5.0 mL of dry CH_3CN . ^1H NMR (400 MHz, CDCl_3) δ : 7.25 (s, 2H), 4.35 (t, $J = 6.4$ Hz, 2H), 3.87 (s, 9H), 3.57 (t, $J = 6.8$ Hz, 2H), 2.74 (t, $J = 6.8$ Hz, 2H), 2.59 (t, $J = 7.2$ Hz, 2H), 2.22 (bs, 2H), 1.99–1.93 (m, 2H), 1.50–1.47 (m, 4H), 1.30–1.15 (m, 6H) ppm.

(E)-3-((7-Hydroxyheptyl)amino)propyl 3-(3,4,5-Trimethoxyphenyl)acrylate (39). Following the general procedure, compound 39 (0.17 g, yield: 71.0%) was synthesized from 29²⁸ (0.21 g, 0.58 mmol) and 7-aminoheptan-1-ol³⁶ (0.15 g, 1.17 mmol) in 6.0 mL of dry CH_3CN . ^1H NMR (400 MHz, CDCl_3) δ : 7.51 (d, $J = 16.0$ Hz, 1H), 6.68 (s, 2H), 6.27 (d, $J = 16.0$ Hz, 1H), 4.20 (t, $J = 6.0$ Hz, 2H), 3.81 (s, 6H), 3.80 (s, 3H), 3.52 (t, $J = 6.4$ Hz, 2H), 2.66 (t, $J = 6.8$ Hz, 2H), 2.53 (t, $J = 6.8$ Hz, 2H), 2.06 (bs, 2H), 1.85–1.82 (m, 2H), 1.52–1.39 (m, 4H), 1.30–1.19 (m, 6H) ppm.

3-((7-Hydroxyheptyl)amino)propyl Anthracene-9-carboxylate (40). Following the general procedure, compound 40 (0.33 g, yield: 72.4%) was synthesized from 30³⁵ (0.40 g, 1.17 mmol) and 7-aminoheptan-1-ol³⁶ (0.31 g, 2.33 mmol) in 15.0 mL of dry CH_3CN . ^1H NMR (400 MHz, CDCl_3) δ : 8.49 (s, 1H), 7.99 (t, $J = 9.2$ Hz, 4H), 7.53–7.43 (m, 4H), 4.66 (t, $J = 6.4$ Hz, 2H), 3.62 (bs, 2H), 3.53 (t, $J = 6.4$ Hz, 2H), 2.82 (t, $J = 7.2$ Hz, 2H), 2.59 (t, $J = 7.2$ Hz, 2H), 2.14–2.07 (m, 2H), 1.51–1.37 (m, 4H), 1.29–1.16 (m, 6H) ppm.

7-(3-Bromopropoxy)-2H-chromen-2-one (51). To a solution of 7-hydroxy-2H-chromen-2-one (0.40 g, 2.46 mmol) in 30.0 mL of acetone, K_2CO_3 (1.02 g, 7.39 mmol) and 1,3-dibromopropane (1.25 mL, 12.31 mmol) were added. The reaction was refluxed overnight; then, it was cooled to rt and the solvent was removed under reduced pressure. The residue was dissolved in CH_2Cl_2 and washed twice with water; then, the organic phase was dried over Na_2SO_4 and concentrated under vacuum. 51 (0.64 g, yield 91.5%) was obtained as a pure white solid. TLC: $\text{CH}_2\text{Cl}_2/\text{CH}_3\text{OH}$ 95:5. ^1H NMR (400 MHz, CDCl_3) δ : 7.61 (d, $J = 9.6$ Hz, 1H), 7.35 (d, $J = 8.0$ Hz, 1H), 6.83–6.80 (m, 2H), 6.23 (d, $J = 9.6$ Hz, 1H), 4.14 (t, $J = 6.4$ Hz, 2H), 3.58 (t, $J = 6.4$ Hz, 2H), 2.36–2.29 (m, 2H) ppm.

General Procedure for the Synthesis of ((Hydroxyalkyl)alkylcoumarin)aminoester (41–50). The suitable (hydroxyalkyl)aminoester 31–40 (1 or 1.2 equiv) was dissolved in the adequate amount of dry CH_3CN ; then, K_2CO_3 (3 equiv) and 51 (1 or 1.2 equiv) were added. The mixture was stirred at 60 °C for 20 h; then, it was cooled to rt and the solvent was removed under reduced pressure. The residue was dissolved in CH_2Cl_2 , and then the organic layer was washed twice with 10% NaOH solution, dried over Na_2SO_4 , and concentrated under reduced pressure. The residue was purified by flash chromatography using the proper eluting system, yielding the desired compound as a pale yellow oil.

(E)-3-((5-Hydroxypentyl)(3-((2-oxo-2H-chromen-7-yl)oxy)propyl)amino)propyl 3-(3,4,5-Trimethoxyphenyl)acrylate (41). Following the general procedure, compound 41 (0.30 g, yield: 57.7%) was synthesized from 31²⁸ (0.34 g, 0.89 mmol) and 51 (0.37 g, 1.07 mmol) in 13.0 mL of dry CH_3CN . Chromatographic eluent: $\text{CH}_2\text{Cl}_2/\text{CH}_3\text{OH}/\text{NH}_4\text{OH}$ 97:3:0.3. ^1H NMR (400 MHz, CDCl_3) δ : 7.54 (d, $J = 9.2$ Hz, 1H), 7.51 (d, $J = 16.0$ Hz, 1H), 7.27 (d, $J = 8.4$ Hz, 1H), 6.77–6.75 (m, 2H), 6.68 (s, 2H), 6.25 (d, $J = 16.0$ Hz, 1H), 6.14 (d, $J = 9.2$ Hz, 1H), 4.17 (t, $J = 6.4$ Hz, 2H), 4.02 (t, $J = 6.0$ Hz, 2H), 3.82 (s, 6H), 3.81 (s, 3H), 3.57 (t, $J = 6.4$ Hz, 2H), 2.56 (t, $J = 6.4$ Hz, 2H), 2.50 (t, $J = 6.4$ Hz, 2H), 2.39 (t, $J = 6.4$ Hz, 2H), 2.00–1.83 (m, 3H), 1.82–1.74 (m, 2H), 1.52–1.37 (m, 4H), 1.35–1.26 (m, 2H) ppm.

3-((5-Hydroxypentyl)(3-((2-oxo-2H-chromen-7-yl)oxy)propyl)amino)propyl 3,4,5-Trimethoxybenzoate (42). Following the general procedure, compound 42 (0.16 g, yield: 53.0%) was synthesized from 32²⁸ (0.23 g, 0.64 mmol) and 51 (0.15 g, 0.54 mmol) in 20.0 mL of dry CH_3CN . Chromatographic eluent: $\text{CH}_2\text{Cl}_2/\text{CH}_3\text{OH}/\text{NH}_4\text{OH}$ 95:5:0.5. ^1H NMR (400 MHz, CDCl_3) δ : 7.53 (d, $J = 9.2$ Hz, 1H), 7.26 (d, $J = 8.4$ Hz, 1H), 7.21 (s, 2H), 6.75–6.73 (m, 2H), 6.14 (d, $J = 9.2$ Hz, 1H), 4.26 (t, $J = 6.4$ Hz, 2H), 4.00 (t, $J = 6.4$ Hz, 2H), 3.83 (s, 3H), 3.82 (s, 6H), 3.53 (t, $J = 6.4$ Hz, 2H), 2.56–2.49 (m, 4H), 2.37 (t, $J = 7.2$ Hz, 2H), 2.14 (bs, 1H), 1.90–1.80 (m, 4H), 1.49–1.36 (m, 4H), 1.35–1.26 (m, 2H) ppm.

3-((5-Hydroxypentyl)(3-((2-oxo-2H-chromen-7-yl)oxy)propyl)amino)propyl Anthracene-9-carboxylate (43). Following the general procedure, compound 43 (0.15 g, yield: 46.8%) was synthesized from 33²⁸ (0.25 g, 0.69 mmol) and 51 (0.16 g, 0.58 mmol) in 20.0 mL of dry CH_3CN . Chromatographic eluent: $\text{CH}_2\text{Cl}_2/\text{CH}_3\text{OH}/\text{NH}_4\text{OH}$ 97:3:0.3. ^1H NMR (400 MHz, CDCl_3) δ : 8.46 (s, 1H), 7.97 (t, $J = 8.0$ Hz, 4H), 7.50–7.42 (m, 5H), 7.19 (d, $J = 9.2$ Hz, 1H), 6.73–6.70 (m, 2H), 6.15 (d, $J = 9.2$ Hz, 1H), 4.61 (t, $J = 6.4$ Hz, 2H), 3.97 (t, $J = 6.4$ Hz, 2H), 3.52 (t, $J = 6.4$ Hz, 2H), 2.60–2.54 (m, 4H), 2.40 (t, $J = 7.2$ Hz, 2H), 2.00–1.92 (m, 2H), 1.88–1.82 (m, 2H), 1.47–1.39 (m, 4H), 1.33–1.26 (m, 2H) ppm.

(E)-6-((3-Hydroxypropyl)(3-((2-oxo-2H-chromen-7-yl)oxy)propyl)amino)hexyl 3-(3,4,5-Trimethoxyphenyl)acrylate (44). Following the general procedure, compound 44 (0.27 g, yield: 59.6%) was synthesized from 34²⁹ (0.36 g, 0.91 mmol) and 51 (0.21 g, 0.76 mmol) in 27.0 mL of dry CH_3CN . Chromatographic eluent: $\text{CH}_2\text{Cl}_2/\text{CH}_3\text{OH}/\text{NH}_4\text{OH}$ 97:3:0.3. ^1H NMR (400 MHz, CDCl_3) δ : 7.59 (d, $J = 9.2$ Hz, 1H), 7.56 (d, $J = 16.0$ Hz, 1H), 7.33 (d, $J = 8.8$ Hz, 1H), 6.82–6.77 (m, 2H), 6.73 (s, 2H), 6.32 (d, $J = 16.0$ Hz, 1H), 6.21 (d, $J = 9.2$ Hz, 1H), 4.14 (t, $J = 6.4$ Hz, 2H), 4.03 (t, $J = 6.4$ Hz, 2H), 3.86 (s, 6H), 3.85 (s, 3H), 3.77 (t, $J = 6.4$ Hz, 2H), 2.66–2.59 (m, 4H), 2.44 (t, $J = 7.2$ Hz, 2H), 2.00–1.94 (m, 2H), 1.72–1.62 (m, 4H), 1.51–1.44 (m, 2H), 1.41–1.28 (m, 4H) ppm.

6-((3-Hydroxypropyl)(3-((2-oxo-2H-chromen-7-yl)oxy)propyl)amino)hexyl 3,4,5-Trimethoxybenzoate (**45**). Following the general procedure, compound **45** (0.15 g, yield: 68.7%) was synthesized from **35**²⁶ (0.17 g, 0.47 mmol) and **51** (0.11 g, 0.39 mmol) in 10.0 mL of dry CH₃CN. Chromatographic eluent: CH₂Cl₂/CH₃OH/NH₄OH 93:7:0.7. ¹H NMR (400 MHz, CDCl₃) δ: 7.50 (d, *J* = 9.2 Hz, 1H), 7.23 (d, *J* = 8.4 Hz, 1H), 7.18 (s, 2H), 6.70 (dd, *J* = 8.4, 2.2 Hz, 1H), 6.66 (d, *J* = 2.2 Hz, 1H), 6.09 (d, *J* = 9.2 Hz, 1H), 4.16 (t, *J* = 6.4 Hz, 2H), 3.94 (t, *J* = 6.4 Hz, 2H), 3.78 (s, 9H), 3.65 (t, *J* = 6.4 Hz, 2H), 2.60–2.44 (m, 4H), 2.35 (t, *J* = 7.2 Hz, 2H), 1.93–1.80 (m, 2H), 1.69–1.52 (m, 4H), 1.45–1.34 (m, 2H), 1.33–1.18 (m, 4H) ppm.

6-((3-Hydroxypropyl)(3-((2-oxo-2H-chromen-7-yl)oxy)propyl)amino)hexyl Anthracene-9-carboxylate (**46**). Following the general procedure, compound **46** (0.13 g, yield: 60.4%) was synthesized from **36**²⁶ (0.16 g, 0.43 mmol) and **51** (0.10 g, 0.36 mmol) in 10.0 mL of dry CH₃CN. Chromatographic eluent: CH₂Cl₂/CH₃OH/NH₄OH 97:3:0.3. ¹H NMR (400 MHz, CDCl₃) δ: 8.39 (s, 1H), 7.97 (d, *J* = 8.4 Hz, 2H), 7.91 (d, *J* = 8.4 Hz, 2H), 7.48–7.37 (m, 5H), 7.13 (d, *J* = 9.2 Hz, 1H), 6.66–6.64 (m, 2H), 6.08 (d, *J* = 9.2 Hz, 1H), 4.54 (t, *J* = 6.4 Hz, 2H), 3.87 (t, *J* = 6.4 Hz, 2H), 3.69 (t, *J* = 6.4 Hz, 2H), 2.54–2.47 (m, 4H), 2.34 (t, *J* = 7.2 Hz, 2H), 1.85–1.72 (m, 4H), 1.65–1.53 (m, 2H), 1.49–1.35 (m, 4H), 1.34–1.23 (m, 2H) ppm.

(*E*)-7-((3-Hydroxypropyl)(3-((2-oxo-2H-chromen-7-yl)oxy)propyl)amino)heptyl 3-(3,4,5-Trimethoxyphenyl)acrylate (**47**). Following the general procedure, compound **47** (0.16 g, yield: 63.1%) was synthesized from **37**²⁹ (0.17 g, 0.42 mmol) and **51** (0.14 g, 0.50 mmol) in 7.0 mL of dry CH₃CN. Chromatographic eluent: CH₂Cl₂/CH₃OH/NH₄OH 90:10:1. ¹H NMR (400 MHz, CDCl₃) δ: 7.57 (d, *J* = 9.6 Hz, 1H), 7.53 (d, *J* = 16.0 Hz, 1H), 7.30 (d, *J* = 8.4 Hz, 1H), 6.79–6.74 (m, 2H), 6.70 (s, 2H), 6.29 (d, *J* = 16.0 Hz, 1H), 6.17 (d, *J* = 9.6 Hz, 1H), 4.12 (t, *J* = 6.4 Hz, 2H), 4.01 (t, *J* = 6.0 Hz, 2H), 3.82 (s, 6H), 3.81 (s, 3H), 3.73 (t, *J* = 5.2 Hz, 2H), 2.66–2.61 (m, 4H), 2.44 (t, *J* = 7.2 Hz, 2H), 2.00–1.93 (m, 2H), 1.70–1.59 (m, 4H), 1.51–1.41 (m, 2H), 1.37–1.19 (m, 7H) ppm.

3-((7-Hydroxyheptyl)(3-((2-oxo-2H-chromen-7-yl)oxy)propyl)amino)propyl 3,4,5-Trimethoxybenzoate (**48**). Following the general procedure, compound **48** (0.16 g, yield: 55.1%) was synthesized from **38** (0.18 g, 0.50 mmol) and **51** (0.16 g, 0.56 mmol) in 7.0 mL of dry CH₃CN. Chromatographic eluent: CH₂Cl₂/CH₃OH/NH₄OH 95:5:0.5. ¹H NMR (400 MHz, CDCl₃) δ: 7.58 (d, *J* = 9.6 Hz, 1H), 7.31 (d, *J* = 8.4 Hz, 1H), 6.24 (s, 2H), 6.79–6.77 (m, 2H), 6.20 (d, *J* = 9.6 Hz, 1H), 4.31 (t, *J* = 6.4 Hz, 2H), 4.05 (t, *J* = 6.4 Hz, 2H), 3.88 (s, 3H), 3.81 (s, 6H), 3.58 (t, *J* = 6.4 Hz, 2H), 2.61–2.54 (m, 4H), 2.40 (t, *J* = 7.2 Hz, 2H), 1.93–1.87 (m, 4H), 1.69 (bs, 1H), 1.53–1.45 (m, 2H), 1.44–1.35 (m, 2H), 1.33–1.20 (m, 6H) ppm.

(*E*)-3-((7-Hydroxyheptyl)(3-((2-oxo-2H-chromen-7-yl)oxy)propyl)amino)propyl 3-(3,4,5-Trimethoxyphenyl)acrylate (**49**). Following the general procedure, compound **49** (0.15 g, yield: 59.1%) was synthesized from **39** (0.17 g, 0.42 mmol) and **51** (0.14 g, 0.50 mmol) in 7.0 mL of dry CH₃CN. Chromatographic eluent: CH₂Cl₂/CH₃OH/NH₄OH 95:5:0.5. ¹H NMR (400 MHz, CDCl₃) δ: 7.53 (d, *J* = 9.6 Hz, 1H), 7.50 (d, *J* = 16.0 Hz, 1H), 7.27 (d, *J* = 8.4 Hz, 1H), 6.77–6.73 (m, 2H), 6.67 (s, 2H), 6.24 (d, *J* = 16.0 Hz, 1H), 6.13 (d, *J* = 9.6 Hz, 1H), 4.16 (t, *J* = 6.4 Hz, 2H), 4.01 (t, *J* = 6.0 Hz, 2H), 3.81 (s, 6H), 3.80 (s, 3H), 3.53 (t, *J* = 6.4 Hz, 2H), 2.53 (t, *J* = 6.4 Hz, 2H), 2.47 (t, *J* = 6.8 Hz, 2H), 2.34 (t, *J* = 6.8 Hz, 2H), 1.94 (bs, 1H), 1.90–1.82 (m, 2H), 1.80–1.72 (m, 2H), 1.49–1.40 (m, 2H), 1.39–1.30 (m, 2H), 1.29–1.16 (m, 6H) ppm.

3-((7-Hydroxyheptyl)(3-((2-oxo-2H-chromen-7-yl)oxy)propyl)amino)propyl Anthracene-9-carboxylate (**50**). Following the general procedure, compound **50** (0.32 g, yield: 64.0%) was synthesized from **40** (0.33 g, 0.84 mmol) and **51** (0.28 g, 1.01 mmol) in 15.0 mL of dry CH₃CN. Chromatographic eluent: CH₂Cl₂/CH₃OH/NH₄OH 97:3:0.3. ¹H NMR (400 MHz, CDCl₃) δ: 8.48 (s, 1H), 8.00 (t, *J* = 9.6 Hz, 4H), 7.51–7.41 (m, 5H), 7.21 (d, *J* = 9.2 Hz, 1H), 6.74–6.72 (m, 2H), 6.17 (d, *J* = 9.2 Hz, 1H), 4.64 (t, *J* = 6.4 Hz, 2H), 3.99 (t, *J* = 6.4 Hz, 2H), 3.56 (t, *J* = 6.4 Hz, 2H), 2.62–2.56 (m, 4H), 2.41 (t, *J* = 7.2 Hz, 2H), 2.04–1.96 (m, 2H), 1.94–1.83 (m, 2H), 1.54–1.33 (m, 4H), 1.32–1.16 (m, 6H) ppm.

General Procedures for the Synthesis of Diester Compounds 1–27. Diester compounds were synthesized using two different general procedures:

Method A: in an ice bath, to a solution of the suitable ((hydroxyalkyl)alkylcoumarin)aminoester **41–50** (1 equiv) in the adequate amount of dry CH₂Cl₂, the proper carboxylic acid (1.5 equiv), DMAP (0.8 equiv), and EDC hydrochloride (1.8 equiv) were added in this order. The reaction mixture was stirred at 0 °C for 1 h and then at rt for 48 h. Then, the residue was treated with CH₂Cl₂, and the organic layer was washed twice with water and with a saturated solution of NaHCO₃, dried over Na₂SO₄, and concentrated under reduced pressure. Finally, the residue was purified by flash chromatography using CH₂Cl₂/CH₃OH/NH₄OH 97:3:0.3 as the proper eluting system, obtaining the desired compound as an oil. The final compounds were transformed into the corresponding hydrochloride as a solid. The salts were crystallized from abs. ethanol/petroleum ether.

Method B: the proper carboxylic acid (1.5 equiv) was transformed into the corresponding acyl chloride by treatment with SOCl₂ (15 equiv) in the adequate amount of CHCl₃ (free of ethanol) at 60 °C for 4–6 h. Upon completion of the reaction, the mixture was cooled to rt, and the solvent was removed under reduced pressure. The residue was treated twice with cyclohexane, and the solvent was removed under vacuum. The obtained acyl chloride was dissolved in the proper amount of CHCl₃ (free of ethanol), and the suitable ((hydroxyalkyl)alkylcoumarin)aminoester **41–50** (1 equiv) was added. The mixture was stirred at rt for 18 h; then, the organic layer was washed twice with a saturated solution of NaHCO₃, dried over Na₂SO₄, and concentrated under reduced pressure. Finally, the residue was purified by flash chromatography, using CH₂Cl₂/CH₃OH/NH₄OH 97:3:0.3 as the proper eluting system, yielding the desired compound as an oil. The final compounds were transformed into the corresponding hydrochloride as a solid. The salts were crystallized from abs. ethanol/petroleum ether.

(*E*)-5-((3-((2-Oxo-2H-chromen-7-yl)oxy)propyl)(3-(((*E*)-3-(3,4,5-trimethoxyphenyl)acryloyl)oxy)propyl)amino)pentyl 3-(3,4,5-trimethoxyphenyl)acrylate (**1**). Following **method A**, compound **1** (0.11 g, yield: 72.8%) was synthesized as a pale yellow oil, starting from **41** (0.11 g, 0.19 mmol) and (*E*)-3-(3,4,5-trimethoxyphenyl)acrylic acid (0.067 g, 0.28 mmol) in 4.0 mL of dry CH₂Cl₂. **Free base:** TLC: CH₂Cl₂/CH₃OH/NH₄OH 95:5:0.5. ¹H NMR (400 MHz, CDCl₃) δ: 7.54–7.50 (m, 3H), 7.26 (d, *J* = 9.6 Hz, 1H), 6.76–6.74 (m, 2H), 6.69 (s, 2H), 6.68 (s, 2H), 6.28 (d, *J* = 16.0 Hz, 1H), 6.25 (d, *J* = 16.0 Hz, 1H), 6.13 (d, *J* = 9.6 Hz, 1H), 4.18 (t, *J* = 6.4 Hz, 2H), 4.10 (t, *J* = 6.4 Hz, 2H), 4.02 (t, *J* = 6.4 Hz, 2H), 3.81 (s, 18H), 2.70–2.49 (m, 4H), 2.48–2.35 (m, 2H), 1.97–1.86 (m, 2H), 1.85–1.76 (m, 2H), 1.66–1.59 (m, 2H), 1.52–1.41 (m, 2H), 1.39–1.29 (m, 2H) ppm. ¹³C NMR (100 MHz, CDCl₃) δ: 166.9 (C), 166.8 (C), 162.1 (C), 161.1 (C), 155.9 (C), 153.4 (C), 144.8 (CH), 144.6 (CH), 143.3 (CH), 140.3 (C), 140.2 (C), 129.9 (C), 129.8 (C), 128.8 (CH), 117.4 (CH), 117.1 (CH), 113.0 (CH), 112.6 (CH), 112.5 (C), 105.3 (CH), 104.5 (C), 101.5 (CH), 66.4 (CH₂), 64.4 (CH₂), 62.6 (CH₂), 60.9 (CH₃), 56.2 (CH₃), 53.9 (CH₂), 50.5 (CH₂), 50.2 (CH₂), 28.7 (CH₂), 23.8 (CH₂) ppm. ESI-HRMS (*m/z*) calculated for [M + H]⁺ ion species C₄₄H₅₄NO₁₃ = 804.3590, found 804.3590. **Hydrochloride:** white solid; mp 81–84 °C.

(*E*)-3-((3-((2-Oxo-2H-chromen-7-yl)oxy)propyl)(5-((3-(3,4,5-trimethoxyphenyl)acryloyl)oxy)pentyl)amino)propyl 3,4,5-Trimethoxybenzoate (**2**). Following **method B**, compound **2** (0.058 g, yield: 77.9%) was synthesized as a pale yellow oil, starting from (*E*)-3-(3,4,5-trimethoxyphenyl)acrylic acid (0.034 g, 0.14 mmol) and **42** (0.053 g, 0.096 mmol). **Free base:** TLC: CH₂Cl₂/CH₃OH/NH₄OH 95:5:0.5. ¹H NMR (400 MHz, CDCl₃) δ: 7.52 (d, *J* = 9.6 Hz, 1H), 7.52 (d, *J* = 15.6 Hz, 1H), 7.25 (d, *J* = 8.8 Hz, 1H), 7.20 (s, 2H), 6.75–6.72 (m, 2H), 6.69 (s, 2H), 6.28 (d, *J* = 15.6 Hz, 1H), 6.14 (d, *J* = 9.6 Hz, 1H), 4.28 (t, *J* = 6.4 Hz, 2H), 4.08 (t, *J* = 6.4 Hz, 2H), 4.01 (t, *J* = 6.4 Hz, 2H), 3.83 (s, 3H), 3.82 (s, 6H), 3.81 (s, 6H), 3.81 (s, 3H), 2.62–2.49 (m, 4H), 2.41 (t, *J* = 6.4 Hz, 2H), 1.95–1.82 (m, 4H), 1.63–1.56 (m, 2H), 1.50–1.38 (m, 2H), 1.37–1.30 (m, 2H) ppm. ¹³C NMR (100 MHz, CDCl₃) δ: 167.0 (C), 166.1 (C), 162.2 (C), 161.1 (C), 155.8 (C), 153.4 (C), 152.9 (C), 144.7 (CH), 143.4 (CH), 142.2 (C), 140.1

(C), 129.9 (C), 128.8 (CH), 125.3 (C), 117.4 (CH), 113.0 (CH), 112.6 (CH), 112.5 (C), 106.8 (CH), 105.2 (CH), 101.4 (CH), 66.4 (CH₂), 64.4 (CH₂), 63.3 (CH₂), 60.9 (CH₃), 60.9 (CH₃), 56.2 (CH₃), 56.1 (CH₃), 53.9 (CH₂), 50.4 (CH₂), 50.1 (CH₂), 28.7 (CH₂), 26.8 (CH₂), 26.4 (CH₂), 23.8 (CH₂) ppm. ESI-HRMS (*m/z*) calculated for [M + H]⁺ ion species C₄₂H₅₂NO₁₃ = 778.3433, found 778.3435. Hydrochloride: white solid; mp 128–131 °C.

(*E*)-3-((3-((2-Oxo-2H-chromen-7-yl)oxy)propyl)(5-((3-(3,4,5-trimethoxyphenyl)acryloyl)oxy)pentyl)amino)propyl Anthracene-9-carboxylate (3). Following method B, compound 3 (0.046 g, yield: 74.0%) was synthesized as a pale yellow oil, starting from (*E*)-3-(3,4,5-trimethoxyphenyl)acrylic acid (0.028 g, 0.12 mmol) and 43 (0.045 g, 0.079 mmol). Free base: TLC: CH₂Cl₂/CH₃OH/NH₄OH 95:5:0.5. ¹H NMR (400 MHz, CDCl₃) δ: 8.46 (s, 1H), 7.97 (t, *J* = 7.2 Hz, 4H), 7.54 (d, *J* = 16.0 Hz, 1H), 7.50–7.41 (m, 5H), 7.20 (d, *J* = 8.8 Hz, 1H), 6.73–6.69 (m, 4H), 6.30 (d, *J* = 16.0 Hz, 1H), 6.15 (d, *J* = 9.2 Hz, 1H), 4.62 (t, *J* = 6.4 Hz, 2H), 4.10 (t, *J* = 6.4 Hz, 2H), 3.98 (t, *J* = 6.4 Hz, 2H), 3.83 (s, 3H), 3.80 (s, 6H), 2.62–2.53 (m, 4H), 2.44 (t, *J* = 6.4 Hz, 2H), 2.06–1.95 (m, 2H), 1.94–1.82 (m, 2H), 1.65–1.55 (m, 2H), 1.48–1.40 (m, 2H), 1.39–1.30 (m, 2H) ppm. ¹³C NMR (100 MHz, CDCl₃) δ: 169.6 (C), 167.0 (C), 162.2 (C), 161.2 (C), 155.8 (C), 153.4 (C), 144.7 (CH), 143.3 (CH), 131.0 (C), 129.9 (C), 129.3 (CH), 128.7 (CH), 128.6 (CH), 128.4 (C), 128.0 (C), 126.9 (CH), 125.5 (CH), 124.9 (CH), 117.4 (CH), 112.9 (CH), 112.6 (CH), 112.4 (C), 105.3 (CH), 101.4 (CH), 66.4 (CH₂), 64.4 (CH₂), 64.0 (CH₂), 60.9 (CH₃), 56.1 (CH₃), 54.0 (CH₂), 50.7 (CH₂), 50.2 (CH₂), 28.7 (CH₂), 26.8 (CH₂), 23.9 (CH₂) ppm. ESI-HRMS (*m/z*) calculated for [M + H]⁺ ion species C₄₇H₅₀NO₁₀ = 788.3429, found 788.3429. Hydrochloride: pale yellow solid; mp 94–97 °C.

(*E*)-5-((3-((2-Oxo-2H-chromen-7-yl)oxy)propyl)(3-((3-(3,4,5-trimethoxyphenyl)acryloyl)oxy)propyl)amino)pentyl 3,4,5-Trimethoxybenzoate (4). Following method A, compound 4 (0.10 g, yield: 83.5%) was synthesized as a pale yellow oil, starting from 41 (0.090 g, 0.15 mmol) and 3,4,5-trimethoxybenzoic acid (0.049 g, 0.23 mmol) in 4.0 mL of dry CH₂Cl₂. Free base: TLC: CH₂Cl₂/CH₃OH/NH₄OH 95:5:0.5. ¹H NMR (400 MHz, CDCl₃) δ: 7.53 (d, *J* = 16.0 Hz, 1H), 7.53 (d, *J* = 9.6 Hz, 1H), 7.28 (d, *J* = 9.2 Hz, 1H), 7.23 (s, 2H), 6.78–6.75 (m, 2H), 6.69 (s, 2H), 6.27 (d, *J* = 16.0 Hz, 1H), 6.15 (d, *J* = 9.6 Hz, 1H), 4.23 (t, *J* = 6.4 Hz, 2H), 4.19 (t, *J* = 6.4 Hz, 2H), 4.03 (t, *J* = 6.4 Hz, 2H), 3.85 (s, 9H), 3.83 (s, 9H), 2.72–2.49 (m, 4H), 2.48–2.35 (m, 2H), 2.01–1.87 (m, 2H), 1.86–1.77 (m, 2H), 1.76–1.67 (m, 2H), 1.58–1.45 (m, 2H), 1.44–1.31 (m, 2H) ppm. ¹³C NMR (100 MHz, CDCl₃) δ: 166.9 (C), 166.2 (C), 162.1 (C), 161.1 (C), 155.9 (C), 153.4 (C), 152.9 (C), 144.8 (CH), 143.3 (CH), 142.2 (C), 140.2 (C), 129.8 (C), 128.8 (CH), 125.4 (C), 117.1 (CH), 113.0 (CH), 112.6 (CH), 112.5 (C), 106.9 (CH), 105.3 (CH), 101.5 (CH), 66.4 (CH₂), 65.0 (CH₂), 62.7 (CH₂), 60.9 (CH₃), 60.9 (CH₃), 56.3 (CH₃), 56.2 (CH₃), 53.9 (CH₂), 50.5 (CH₂), 50.2 (CH₂), 28.7 (CH₂), 26.6 (CH₂), 23.8 (CH₂) ppm. ESI-HRMS (*m/z*) calculated for [M + H]⁺ ion species C₄₂H₅₂NO₁₃ = 778.3433, found 778.3434. Hydrochloride: white solid; mp 74–77 °C.

5-((3-((2-Oxo-2H-chromen-7-yl)oxy)propyl)(3-((3,4,5-trimethoxybenzoyl)oxy)propyl)amino)pentyl 3,4,5-Trimethoxybenzoate (5). Following method A, compound 5 (0.055 g, yield: 74.2%) was synthesized as a pale yellow oil, starting from 42 (0.054 g, 0.098 mmol) and 3,4,5-trimethoxybenzoic acid (0.031 g, 0.15 mmol) in 5.0 mL of dry CH₂Cl₂. Free base: TLC: CH₂Cl₂/CH₃OH/NH₄OH 95:5:0.5. ¹H NMR (400 MHz, CDCl₃) δ: 7.52 (d, *J* = 9.6 Hz, 1H), 7.26 (d, *J* = 8.4 Hz, 1H), 7.22 (s, 2H), 7.20 (s, 2H), 6.75–6.72 (m, 2H), 6.14 (d, *J* = 9.6 Hz, 1H), 4.28 (t, *J* = 6.4 Hz, 2H), 4.21 (t, *J* = 6.4 Hz, 2H), 4.01 (t, *J* = 6.4 Hz, 2H), 3.84 (s, 6H), 3.84 (s, 6H), 3.83 (s, 6H), 2.70–2.51 (m, 4H), 2.50–2.35 (m, 2H), 1.97–1.80 (m, 4H), 1.72–1.64 (m, 2H), 1.56–1.42 (m, 2H), 1.41–1.32 (m, 2H) ppm. ¹³C NMR (100 MHz, CDCl₃) δ: 166.2 (C), 166.1 (C), 162.1 (C), 161.1 (C), 155.8 (C), 152.9 (C), 143.3 (CH), 142.2 (C), 128.8 (CH), 125.4 (C), 125.2 (C), 113.0 (CH), 112.6 (CH), 112.5 (C), 106.8 (CH), 106.8 (CH), 101.4 (CH), 66.4 (CH₂), 65.0 (CH₂), 63.3 (CH₂), 60.9 (CH₃), 56.2 (CH₃), 54.0 (CH₂), 50.4 (CH₂), 50.2 (CH₂), 28.7 (CH₂), 26.8 (CH₂), 23.8 (CH₂) ppm. ESI-HRMS (*m/z*) calculated for [M + H]⁺ ion species

C₄₀H₅₀NO₁₃ = 752.3277, found 752.3276. Hydrochloride: white solid; mp 84–87 °C.

3-((3-((2-Oxo-2H-chromen-7-yl)oxy)propyl)(5-((3,4,5-trimethoxybenzoyl)oxy)pentyl)amino)propyl Anthracene-9-carboxylate (6). Following method A, compound 6 (0.044 g, yield: 59.3%) was synthesized as a pale yellow oil, starting from 43 (0.054 g, 0.095 mmol) and 3,4,5-trimethoxybenzoic acid (0.030 g, 0.14 mmol) in 5.0 mL of dry CH₂Cl₂. Free base: TLC: CH₂Cl₂/CH₃OH/NH₄OH 95:5:0.5. ¹H NMR (400 MHz, CDCl₃) δ: 8.45 (s, 1H), 7.97 (t, *J* = 8.0 Hz, 4H), 7.50–7.40 (m, 5H), 7.24 (s, 2H), 7.19 (d, *J* = 8.8 Hz, 1H), 6.73–6.70 (m, 2H), 6.14 (d, *J* = 9.2 Hz, 1H), 4.62 (t, *J* = 6.4 Hz, 2H), 4.20 (t, *J* = 6.4 Hz, 2H), 3.97 (t, *J* = 6.4 Hz, 2H), 3.86 (s, 3H), 3.84 (s, 6H), 2.62–2.55 (m, 4H), 2.43 (t, *J* = 6.4 Hz, 2H), 2.02–1.94 (m, 2H), 1.90–1.83 (m, 2H), 1.70–1.63 (m, 2H), 1.49–1.43 (m, 2H), 1.42–1.33 (m, 2H) ppm. ¹³C NMR (100 MHz, CDCl₃) δ: 169.6 (C), 166.2 (C), 162.2 (C), 161.1 (C), 155.8 (C), 152.9 (C), 143.3 (CH), 142.3 (C), 131.0 (C), 129.3 (CH), 128.7 (CH), 128.6 (CH), 128.4 (C), 128.0 (C), 126.9 (CH), 125.5 (CH), 124.9 (CH), 112.9 (CH), 112.7 (CH), 112.4 (C), 106.9 (CH), 101.4 (CH), 66.5 (CH₂), 65.0 (CH₂), 64.1 (CH₂), 60.9 (CH₃), 56.3 (CH₃), 54.1 (CH₂), 50.7 (CH₂), 50.3 (CH₂), 28.7 (CH₂), 26.9 (CH₂), 26.8 (CH₂), 23.9 (CH₂) ppm. ESI-HRMS (*m/z*) calculated for [M + H]⁺ ion species C₄₅H₄₈NO₁₀ = 762.3273, found 762.3270. Hydrochloride: yellow solid; mp 114–117 °C.

(*E*)-5-((3-((2-Oxo-2H-chromen-7-yl)oxy)propyl)(3-((3-(3,4,5-trimethoxyphenyl)acryloyl)oxy)propyl)amino)pentyl Anthracene-9-carboxylate (7). Following method B, compound 7 (0.020 g, yield: 18.5%) was synthesized as a pale yellow oil, starting from anthracene-9-carboxylic acid (0.046 g, 0.21 mmol) and 41 (0.080 g, 0.14 mmol). Free base: TLC: CH₂Cl₂/CH₃OH/NH₄OH 95:5:0.5. ¹H NMR (400 MHz, CDCl₃) δ: 8.47 (s, 1H), 7.97 (d, *J* = 9.2 Hz, 4H), 7.54 (d, *J* = 16.0 Hz, 1H), 7.51–7.42 (m, 5H), 7.24 (d, *J* = 9.2 Hz, 1H), 6.74–6.71 (m, 2H), 6.69 (s, 2H), 6.26 (d, *J* = 16.0 Hz, 1H), 6.15 (d, *J* = 9.2 Hz, 1H), 4.56 (t, *J* = 6.4 Hz, 2H), 4.18 (t, *J* = 6.4 Hz, 2H), 3.98 (t, *J* = 6.4 Hz, 2H), 3.83 (s, 3H), 3.82 (s, 6H), 2.80–2.34 (m, 6H), 1.91–1.78 (m, 4H), 1.66–1.42 (m, 6H) ppm. ¹³C NMR (100 MHz, CDCl₃) δ: 160.9 (C), 155.7 (C), 153.5 (C), 146.0 (CH), 143.2 (CH), 130.9 (C), 129.5 (CH), 129.0 (CH), 128.7 (CH), 128.3 (C), 127.2 (CH), 125.6 (CH), 124.8 (CH), 116.1 (CH), 113.6 (CH), 113.1 (C), 112.2 (CH), 105.4 (CH), 101.7 (CH), 65.2 (CH₂), 61.0 (CH₂), 61.0 (CH₃), 56.2 (CH₃), 52.7 (CH₂), 50.3 (CH₂), 28.1 (CH₂), 23.7 (CH₂), 23.5 (CH₂), 23.0 (CH₂), 22.9 (CH₂) ppm. ESI-HRMS (*m/z*) calculated for [M + H]⁺ ion species C₄₇H₅₀NO₁₀ = 788.3429, found 788.3430. Hydrochloride: yellow solid; mp 92–95 °C.

5-((3-((2-Oxo-2H-chromen-7-yl)oxy)propyl)(3-((3,4,5-trimethoxybenzoyl)oxy)propyl)amino)pentyl Anthracene-9-carboxylate (8). Following method B, compound 8 (0.063 g, yield: 79.7%) was synthesized as a yellow oil, starting from anthracene-9-carboxylic acid (0.034 g, 0.15 mmol) and 42 (0.058 g, 0.10 mmol). Free base: TLC: CH₂Cl₂/CH₃OH/NH₄OH 95:5:0.5. ¹H NMR (400 MHz, CDCl₃) δ: 8.46 (s, 1H), 7.98–7.95 (m, 4H), 7.51–7.41 (m, 5H), 7.22 (s, 2H), 7.20 (d, *J* = 8.8 Hz, 1H), 6.71–6.68 (m, 2H), 6.13 (d, *J* = 9.2 Hz, 1H), 4.54 (t, *J* = 6.4 Hz, 2H), 4.27 (t, *J* = 6.4 Hz, 2H), 3.94 (t, *J* = 6.4 Hz, 2H), 3.85 (s, 3H), 3.83 (s, 6H), 2.61–2.49 (m, 4H), 2.48–2.38 (m, 2H), 1.90–1.76 (m, 6H), 1.57–1.40 (m, 4H) ppm. ¹³C NMR (100 MHz, CDCl₃) δ: 169.7 (C), 166.1 (C), 162.1 (C), 161.2 (C), 155.8 (C), 152.9 (C), 143.3 (CH), 131.0 (C), 129.3 (CH), 128.7 (CH), 128.6 (CH), 128.3 (C), 128.1 (C), 127.0 (CH), 125.5 (CH), 125.2 (C), 124.9 (CH), 113.0 (CH), 112.6 (CH), 112.5 (C), 106.8 (CH), 101.3 (CH), 66.3 (CH₂), 65.7 (CH₂), 63.2 (CH₂), 60.9 (CH₃), 56.2 (CH₃), 53.9 (CH₂), 50.4 (CH₂), 50.1 (CH₂), 28.6 (CH₂), 24.0 (CH₂) ppm. ESI-HRMS (*m/z*) calculated for [M + H]⁺ ion species C₄₅H₄₈NO₁₀ = 762.3273, found 762.3270. Hydrochloride: pale yellow solid; mp 120–123 °C.

3-((5-((Anthracene-9-carbonyl)oxy)pentyl)(3-((2-oxo-2H-chromen-7-yl)oxy)propyl)amino)propyl Anthracene-9-carboxylate (9). Following method B, compound 9 (0.045 g, yield: 66.8%) was synthesized as a yellow oil, starting from anthracene-9-carboxylic acid (0.029 g, 0.13 mmol) and 43 (0.049 g, 0.086 mmol). Free base: TLC: CH₂Cl₂/CH₃OH/NH₄OH 95:5:0.5. ¹H NMR (400 MHz, CDCl₃) δ:

8.46 (s, 2H), 8.00–7.95 (m, 8H), 7.51–7.40 (m, 9H), 7.12 (d, $J = 8.8$ Hz, 1H), 6.68–6.65 (m, 2H), 6.12 (d, $J = 9.2$ Hz, 1H), 4.60 (t, $J = 6.4$ Hz, 2H), 4.52 (t, $J = 6.4$ Hz, 2H), 3.91 (t, $J = 6.4$ Hz, 2H), 2.59–2.53 (m, 4H), 2.42 (t, $J = 6.4$ Hz, 2H), 2.01–1.92 (m, 2H), 1.86–1.73 (m, 4H), 1.55–1.40 (m, 4H) ppm. ^{13}C NMR (100 MHz, CDCl_3) δ : 169.7 (C), 162.1 (C), 161.2 (C), 155.8 (C), 143.3 (CH), 142.6 (C), 141.9 (C), 131.0 (C), 129.3 (CH), 129.2 (CH), 128.6 (CH), 128.4 (C), 128.0 (C), 126.9 (CH), 125.5 (CH), 125.0 (CH), 124.9 (CH), 112.9 (CH), 112.6 (CH), 112.4 (C), 101.3 (CH), 66.4 (CH₂), 65.7 (CH₂), 64.0 (CH₂), 53.9 (CH₂), 50.6 (CH₂), 50.1 (CH₂), 28.7 (CH₂), 26.7 (CH₂), 26.6 (CH₂), 24.0 (CH₂) ppm. ESI-HRMS (m/z) calculated for $[\text{M} + \text{H}]^+$ ion species $\text{C}_{50}\text{H}_{46}\text{NO}_7 = 772.3269$, found 772.3267. *Hydrochloride*: yellow solid; mp 118–121 °C.

(*E*)-6-((3-((2-Oxo-2H-chromen-7-yl)oxy)propyl)(3-(((*E*)-3-(3,4,5-trimethoxyphenyl)acryloyl)oxy)propyl)amino)hexyl 3-(3,4,5-trimethoxyphenyl)acrylate (10). Following *method A*, compound 10 (0.082 g, yield: 100.0%) was synthesized as a pale yellow oil, starting from 44 (0.060 g, 0.10 mmol) and (*E*)-3-(3,4,5-trimethoxyphenyl)acrylic acid (0.036 g, 0.15 mmol) in 4.0 mL of dry CH_2Cl_2 . *Free base*: TLC: $\text{CH}_2\text{Cl}_2/\text{CH}_3\text{OH}/\text{NH}_4\text{OH}$ 95:5:0.5. ^1H NMR (400 MHz, CDCl_3) δ : 7.55–7.51 (m, 3H), 7.28 (d, $J = 9.2$ Hz, 1H), 6.80–6.76 (m, 2H), 6.71 (s, 2H), 6.70 (s, 2H), 6.30 (d, $J = 16.0$ Hz, 1H), 6.27 (d, $J = 16.0$ Hz, 1H), 6.16 (d, $J = 9.2$ Hz, 1H), 4.19 (t, $J = 6.4$ Hz, 2H), 4.11 (t, $J = 6.4$ Hz, 2H), 4.04 (t, $J = 6.4$ Hz, 2H), 3.84 (s, 9H), 3.84 (s, 9H), 2.56 (t, $J = 6.4$ Hz, 2H), 2.50 (t, $J = 6.4$ Hz, 2H), 2.39 (t, $J = 6.4$ Hz, 2H), 1.93–1.86 (m, 2H), 1.82–1.77 (m, 2H), 1.64–1.57 (m, 2H), 1.43–1.29 (m, 6H) ppm. ^{13}C NMR (100 MHz, CDCl_3) δ : 167.0 (C), 162.3 (C), 155.9 (C), 153.4 (C), 144.7 (CH), 144.6 (CH), 143.4 (CH), 140.1 (C), 129.9 (C), 129.9 (C), 128.7 (CH), 117.4 (CH), 117.2 (CH), 113.0 (CH), 112.8 (CH), 112.4 (C), 105.2 (CH), 101.4 (CH), 66.5 (CH₂), 64.6 (CH₂), 62.9 (CH₂), 61.0 (CH₃), 56.2 (CH₃), 54.1 (CH₂), 50.5 (CH₂), 50.2 (CH₂), 28.7 (CH₂), 27.3 (CH₂), 27.2 (CH₂), 27.0 (CH₂), 26.7 (CH₂), 25.9 (CH₂) ppm. ESI-HRMS (m/z) calculated for $[\text{M} + \text{H}]^+$ ion species $\text{C}_{45}\text{H}_{56}\text{NO}_{13} = 818.3746$, found 818.3748. *Hydrochloride*: white solid; mp 87–90 °C.

(*E*)-3-((3-((2-Oxo-2H-chromen-7-yl)oxy)propyl)(6-((3-(3,4,5-trimethoxyphenyl)acryloyl)oxy)hexyl)amino)propyl 3,4,5-trimethoxybenzoate (11). Following *method B*, compound 11 (0.043 g, yield: 40.6%) was synthesized as a pale yellow oil, starting from 3,4,5-trimethoxybenzoic acid (0.043 g, 0.20 mmol) and 44 (0.080 g, 0.13 mmol). *Free base*: TLC: $\text{CH}_2\text{Cl}_2/\text{CH}_3\text{OH}/\text{NH}_4\text{OH}$ 95:5:0.5. ^1H NMR (400 MHz, CDCl_3) δ : 7.55 (d, $J = 9.6$ Hz, 1H), 7.54 (d, $J = 16.0$ Hz, 1H), 7.28 (d, $J = 9.2$ Hz, 1H), 7.22 (s, 2H), 6.78–6.75 (m, 2H), 6.71 (s, 2H), 6.30 (d, $J = 16.0$ Hz, 1H), 6.17 (d, $J = 9.6$ Hz, 1H), 4.30 (t, $J = 6.4$ Hz, 2H), 4.10 (t, $J = 6.4$ Hz, 2H), 4.03 (t, $J = 6.4$ Hz, 2H), 3.86 (s, 3H), 3.85 (s, 6H), 3.84 (s, 6H), 3.83 (s, 3H), 2.59–2.52 (m, 4H), 2.40 (t, $J = 6.4$ Hz, 2H), 1.91–1.84 (m, 4H), 1.64–1.56 (m, 2H), 1.44–1.36 (m, 2H), 1.35–1.25 (m, 4H) ppm. ^{13}C NMR (100 MHz, CDCl_3) δ : 167.0 (C), 166.1 (C), 162.3 (C), 161.2 (C), 155.9 (C), 153.4 (C), 152.9 (C), 144.6 (CH), 143.4 (CH), 142.2 (C), 140.1 (C), 129.9 (C), 128.7 (CH), 125.3 (C), 117.4 (CH), 113.0 (CH), 112.8 (CH), 112.4 (C), 106.7 (CH), 105.2 (CH), 101.3 (CH), 66.5 (CH₂), 64.5 (CH₂), 63.4 (CH₂), 61.0 (CH₃), 60.9 (CH₃), 56.2 (CH₃), 56.2 (CH₃), 54.1 (CH₂), 50.4 (CH₂), 50.1 (CH₂), 28.7 (CH₂), 27.2 (CH₂), 27.2 (CH₂), 27.0 (CH₂), 26.7 (CH₂), 25.9 (CH₂) ppm. ESI-HRMS (m/z) calculated for $[\text{M} + \text{H}]^+$ ion species $\text{C}_{43}\text{H}_{54}\text{NO}_{13} = 792.3590$, found 792.3589. *Hydrochloride*: white solid; mp 71–74 °C.

(*E*)-3-((3-((2-Oxo-2H-chromen-7-yl)oxy)propyl)(6-((3-(3,4,5-trimethoxyphenyl)acryloyl)oxy)hexyl)amino)propyl Anthracene-9-carboxylate (12). Following *method B*, compound 12 (0.068 g, yield: 56.5%) was synthesized as a pale yellow oil, starting from anthracene-9-carboxylic acid (0.050 g, 0.23 mmol) and 44 (0.090 g, 0.15 mmol). *Free base*: TLC: $\text{CH}_2\text{Cl}_2/\text{CH}_3\text{OH}/\text{NH}_4\text{OH}$ 95:5:0.5. ^1H NMR (400 MHz, CDCl_3) δ : 8.47 (s, 1H), 8.01–7.94 (m, 4H), 7.55 (d, $J = 16.0$ Hz, 1H), 7.52–7.43 (m, 5H), 7.21 (d, $J = 9.2$ Hz, 1H), 6.74–6.72 (m, 2H), 6.71 (s, 2H), 6.30 (d, $J = 16.0$ Hz, 1H), 6.16 (d, $J = 9.6$ Hz, 1H), 4.62 (t, $J = 6.4$ Hz, 2H), 4.10 (t, $J = 6.4$ Hz, 2H), 3.99 (t, $J = 6.4$ Hz, 2H), 3.84 (s, 3H), 3.83 (s, 6H), 2.60–2.55 (m, 4H), 2.40 (t, $J = 7.2$ Hz, 2H), 2.01–1.95 (m, 2H), 1.89–1.83 (m, 2H), 1.62–1.55 (m, 2H), 1.45–1.36 (m, 2H), 1.34–1.25 (m, 4H) ppm. ^{13}C NMR (100 MHz, CDCl_3) δ : 169.6

(C), 167.0 (C), 162.2 (C), 161.2 (C), 155.8 (C), 153.4 (C), 144.6 (CH), 143.4 (CH), 140.1 (C), 131.0 (C), 129.9 (C), 129.3 (CH), 128.7 (CH), 128.4 (C), 128.0 (C), 127.0 (CH), 125.5 (CH), 124.9 (CH), 117.4 (CH), 112.9 (CH), 112.8 (CH), 112.4 (C), 105.2 (CH), 101.3 (CH), 66.4 (CH₂), 64.5 (CH₂), 64.1 (CH₂), 61.0 (CH₃), 56.1 (CH₃), 54.1 (CH₂), 50.6 (CH₂), 50.2 (CH₂), 28.7 (CH₂), 27.2 (CH₂), 26.9 (CH₂), 26.7 (CH₂), 25.9 (CH₂) ppm. ESI-HRMS (m/z) calculated for $[\text{M} + \text{H}]^+$ ion species $\text{C}_{48}\text{H}_{52}\text{NO}_{10} = 802.3586$, found 802.3591. *Hydrochloride*: pale yellow solid; mp 99–102 °C.

(*E*)-6-((3-((2-Oxo-2H-chromen-7-yl)oxy)propyl)(3-((3-(3,4,5-trimethoxyphenyl)acryloyl)oxy)propyl)amino)hexyl 3,4,5-trimethoxybenzoate (13). Following *method B*, compound 13 (0.096 g, yield: 97.7%) was synthesized as a pale yellow oil, starting from (*E*)-3-(3,4,5-trimethoxyphenyl)acrylic acid (0.044 g, 0.19 mmol) and 45 (0.071 g, 0.12 mmol). *Free base*: TLC: $\text{CH}_2\text{Cl}_2/\text{CH}_3\text{OH}/\text{NH}_4\text{OH}$ 95:5:0.5. ^1H NMR (400 MHz, CDCl_3) δ : 7.51 (d, $J = 9.6$ Hz, 1H), 7.50 (d, $J = 15.6$ Hz, 1H), 7.25 (d, $J = 8.8$ Hz, 1H), 7.21 (s, 2H), 6.75–6.72 (m, 2H), 6.66 (s, 2H), 6.24 (d, $J = 15.6$ Hz, 1H), 6.11 (d, $J = 9.6$ Hz, 1H), 4.20–4.14 (m, 4H), 4.00 (t, $J = 6.4$ Hz, 2H), 3.82 (s, 9H), 3.80 (s, 6H), 3.80 (s, 3H), 2.53 (t, $J = 6.4$ Hz, 2H), 2.48 (t, $J = 6.4$ Hz, 2H), 2.36 (t, $J = 6.4$ Hz, 2H), 1.90–1.82 (m, 2H), 1.81–1.72 (m, 2H), 1.71–1.62 (m, 2H), 1.45–1.23 (m, 6H) ppm. ^{13}C NMR (100 MHz, CDCl_3) δ : 166.9 (C), 166.2 (C), 162.3 (C), 161.1 (C), 155.9 (C), 153.4 (C), 152.9 (C), 144.7 (CH), 143.4 (CH), 142.1 (C), 140.1 (C), 129.8 (C), 128.7 (CH), 125.5 (C), 117.2 (CH), 112.9 (CH), 112.7 (CH), 112.4 (C), 106.8 (CH), 105.2 (CH), 101.3 (CH), 66.5 (CH₂), 65.1 (CH₂), 62.8 (CH₂), 60.9 (CH₃), 60.9 (CH₃), 56.2 (CH₃), 56.1 (CH₃), 54.1 (CH₂), 50.5 (CH₂), 50.1 (CH₂), 28.7 (CH₂), 27.1 (CH₂), 26.9 (CH₂), 26.6 (CH₂), 25.9 (CH₂) ppm. ESI-HRMS (m/z) calculated for $[\text{M} + \text{H}]^+$ ion species $\text{C}_{43}\text{H}_{54}\text{NO}_{13} = 792.3590$, found 792.3590. *Hydrochloride*: white solid; mp 78–81 °C.

6-((3-((2-Oxo-2H-chromen-7-yl)oxy)propyl)(3-((3,4,5-trimethoxybenzoyl)oxy)propyl)amino)hexyl 3,4,5-trimethoxybenzoate (14). Following *method A*, compound 14 (0.089 g, yield: 91.7%) was synthesized as a pale yellow oil, starting from 45 (0.072 g, 0.13 mmol) and 3,4,5-trimethoxybenzoic acid (0.040 g, 0.19 mmol) in 5.0 mL of dry CH_2Cl_2 . *Free base*: TLC: $\text{CH}_2\text{Cl}_2/\text{CH}_3\text{OH}/\text{NH}_4\text{OH}$ 95:5:0.5. ^1H NMR (400 MHz, CDCl_3) δ : 7.52 (d, $J = 9.6$ Hz, 1H), 7.25 (d, $J = 8.8$ Hz, 1H), 7.22 (s, 2H), 7.20 (s, 2H), 6.75–6.72 (m, 2H), 6.14 (d, $J = 9.6$ Hz, 1H), 4.27 (t, $J = 6.4$ Hz, 2H), 4.20 (t, $J = 6.4$ Hz, 2H), 4.00 (t, $J = 6.4$ Hz, 2H), 3.84 (s, 9H), 3.83 (s, 9H), 2.58–2.49 (m, 4H), 2.38 (t, $J = 6.4$ Hz, 2H), 1.89–1.81 (m, 4H), 1.69–1.62 (m, 2H), 1.45–1.23 (m, 6H) ppm. ^{13}C NMR (100 MHz, CDCl_3) δ : 166.2 (C), 166.1 (C), 162.2 (C), 161.1 (C), 155.9 (C), 152.9 (C), 143.3 (CH), 142.2 (C), 128.7 (CH), 125.5 (C), 125.3 (C), 112.9 (CH), 112.7 (CH), 112.4 (C), 106.8 (CH), 106.8 (CH), 101.3 (CH), 66.4 (CH₂), 65.1 (CH₂), 63.4 (CH₂), 60.9 (CH₃), 56.2 (CH₃), 56.2 (CH₃), 54.1 (CH₂), 50.4 (CH₂), 50.1 (CH₂), 28.7 (CH₂), 27.1 (CH₂), 26.9 (CH₂), 26.6 (CH₂), 25.9 (CH₂) ppm. ESI-HRMS (m/z) calculated for $[\text{M} + \text{H}]^+$ ion species $\text{C}_{41}\text{H}_{52}\text{NO}_{13} = 766.3433$, found 766.3430. *Hydrochloride*: pale yellow solid; mp 83–85 °C.

3-((3-((2-Oxo-2H-chromen-7-yl)oxy)propyl)(6-((3,4,5-trimethoxybenzoyl)oxy)hexyl)amino)propyl Anthracene-9-carboxylate (15). Following *method B*, compound 15 (0.016 g, yield: 14.2%) was synthesized as a yellow oil, starting from anthracene-9-carboxylic acid (0.049 g, 0.21 mmol) and 45 (0.084 g, 0.15 mmol). *Free base*: TLC: $\text{CH}_2\text{Cl}_2/\text{CH}_3\text{OH}/\text{NH}_4\text{OH}$ 95:5:0.5. ^1H NMR (400 MHz, CDCl_3) δ : 8.47 (s, 1H), 7.99–7.96 (m, 4H), 7.52–7.42 (m, 5H), 7.24 (s, 2H), 7.21 (d, $J = 8.8$ Hz, 1H), 6.73–6.71 (m, 2H), 6.16 (d, $J = 9.2$ Hz, 1H), 4.62 (t, $J = 6.4$ Hz, 2H), 4.20 (t, $J = 6.4$ Hz, 2H), 3.98 (t, $J = 6.4$ Hz, 2H), 3.86 (s, 3H), 3.85 (s, 6H), 2.71–2.57 (m, 4H), 2.52–2.40 (m, 2H), 2.10–1.95 (m, 2H), 1.94–1.85 (m, 2H), 1.71–1.62 (m, 2H), 1.50–1.39 (m, 2H), 1.37–1.25 (m, 4H) ppm. ^{13}C NMR (100 MHz, CDCl_3) δ : 166.2 (C), 162.1 (C), 161.1 (C), 152.9 (C), 143.3 (CH), 142.2 (C), 131.0 (C), 129.3 (CH), 128.7 (CH), 128.4 (C), 127.0 (CH), 125.5 (CH), 124.9 (CH), 113.0 (CH), 112.7 (CH), 112.5 (C), 106.9 (CH), 101.4 (CH), 66.4 (CH₂), 65.1 (CH₂), 64.0 (CH₂), 60.9 (CH₃), 56.3 (CH₃), 54.1 (CH₂), 50.6 (CH₂), 50.3 (CH₂), 28.7 (CH₂), 27.1 (CH₂), 25.9 (CH₂) ppm. ESI-HRMS (m/z) calculated for $[\text{M} + \text{H}]^+$ ion

species $C_{46}H_{50}NO_{10}$ = 776.3429, found 776.3435. *Hydrochloride*: yellow solid; mp 148–151 °C.

(*E*)-6-((3-((2-Oxo-2H-chromen-7-yl)oxy)propyl)(3-((3-(3,4,5-trimethoxyphenyl)acryloyl)oxy)propyl)amino)hexyl Anthracene-9-carboxylate (**16**). Following *method B*, compound **16** (0.060 g, yield: 100.0%) was synthesized as a yellow oil, starting from (*E*)-3-(3,4,5-trimethoxyphenyl)acrylic acid (0.027 g, 0.11 mmol) and **46** (0.043 g, 0.074 mmol). *Free base*: TLC: $CH_2Cl_2/CH_3OH/NH_4OH$ 95:5:0.5. 1H NMR (400 MHz, $CDCl_3$) δ : 8.44 (s, 1H), 7.98 (d, J = 8.4 Hz, 2H), 7.95 (d, J = 8.4 Hz, 2H), 7.54 (d, J = 16.0 Hz, 1H), 7.50–7.40 (m, 5H), 7.17 (d, J = 8.8 Hz, 1H), 6.71–6.69 (m, 2H), 6.68 (s, 2H), 6.27 (d, J = 16.0 Hz, 1H), 6.09 (d, J = 9.2 Hz, 1H), 4.54 (t, J = 6.4 Hz, 2H), 4.18 (t, J = 6.4 Hz, 2H), 3.96 (t, J = 6.4 Hz, 2H), 3.83 (s, 3H), 3.80 (s, 6H), 2.54 (t, J = 6.4 Hz, 2H), 2.49 (t, J = 6.4 Hz, 2H), 2.38 (t, J = 6.4 Hz, 2H), 1.86–1.75 (m, 6H), 1.49–1.27 (m, 6H) ppm. ^{13}C NMR (100 MHz, $CDCl_3$) δ : 169.6 (C), 166.9 (C), 162.2 (C), 161.1 (C), 155.8 (C), 153.4 (C), 144.7 (CH), 143.3 (CH), 141.9 (C), 140.2 (C), 131.0 (C), 129.9 (C), 129.2 (CH), 128.7 (CH), 128.6 (CH), 128.4 (C), 128.2 (C), 126.9 (CH), 125.5 (CH), 125.0 (CH), 117.2 (CH), 112.9 (CH), 112.7 (CH), 112.4 (C), 105.3 (CH), 101.4 (CH), 66.5 (CH₂), 65.8 (CH₂), 62.8 (CH₂), 60.9 (CH₃), 56.2 (CH₃), 54.0 (CH₂), 50.5 (CH₂), 50.2 (CH₂), 28.7 (CH₂), 27.1 (CH₂), 26.9 (CH₂), 26.6 (CH₂), 26.1 (CH₂) ppm. ESI-HRMS (m/z) calculated for $[M + H]^+$ ion species $C_{48}H_{52}NO_{10}$ = 802.3586, found 802.3590. *Hydrochloride*: pale yellow solid; mp 92–95 °C.

6-((3-((2-Oxo-2H-chromen-7-yl)oxy)propyl)(3-((3,4,5-trimethoxybenzoyl)oxy)propyl)amino)hexyl Anthracene-9-carboxylate (**17**). Following *method A*, compound **17** (0.076 g, yield: 77.7%) was synthesized as a yellow oil, starting from **46** (0.074 g, 0.13 mmol) and 3,4,5-trimethoxybenzoic acid (0.040 g, 0.19 mmol) in 5.0 mL of dry CH_2Cl_2 . *Free base*: TLC: $CH_2Cl_2/CH_3OH/NH_4OH$ 95:5:0.5. 1H NMR (400 MHz, $CDCl_3$) δ : 8.44 (s, 1H), 7.98 (d, J = 8.4 Hz, 2H), 7.95 (d, J = 8.4 Hz, 2H), 7.51–7.40 (m, 5H), 7.22 (s, 2H), 7.16 (d, J = 8.8 Hz, 1H), 6.70–6.67 (m, 2H), 6.11 (d, J = 9.2 Hz, 1H), 4.54 (t, J = 6.4 Hz, 2H), 4.27 (t, J = 6.4 Hz, 2H), 3.95 (t, J = 6.4 Hz, 2H), 3.85 (s, 3H), 3.83 (s, 6H), 2.56–2.48 (m, 4H), 2.37 (t, J = 6.4 Hz, 2H), 1.89–1.74 (m, 6H), 1.48–1.28 (m, 6H) ppm. ^{13}C NMR (100 MHz, $CDCl_3$) δ : 169.7 (C), 166.1 (C), 162.2 (C), 161.1 (C), 155.8 (C), 152.9 (C), 143.3 (CH), 142.3 (C), 131.0 (C), 129.2 (CH), 128.7 (CH), 128.6 (CH), 128.4 (C), 128.2 (C), 126.9 (CH), 125.5 (CH), 125.3 (C), 125.0 (CH), 112.9 (CH), 112.7 (CH), 112.4 (C), 106.8 (CH), 101.3 (CH), 66.4 (CH₂), 65.8 (CH₂), 63.4 (CH₂), 60.9 (CH₃), 56.2 (CH₃), 54.0 (CH₂), 50.4 (CH₂), 50.1 (CH₂), 28.7 (CH₂), 27.1 (CH₂), 26.9 (CH₂), 26.6 (CH₂), 26.1 (CH₂) ppm. ESI-HRMS (m/z) calculated for $[M + H]^+$ ion species $C_{46}H_{50}NO_{10}$ = 776.3429, found 776.3425. *Hydrochloride*: yellow solid; mp 87–90 °C.

3-((6-((Anthracene-9-carboxyl)oxy)hexyl)(3-((2-oxo-2H-chromen-7-yl)oxy)propyl)amino)propyl Anthracene-9-carboxylate (**18**). Following *method B*, compound **18** (0.030 g, yield: 44.3%) was synthesized as a pale yellow oil, starting from anthracene-9-carboxylic acid (0.029 g, 0.13 mmol) and **46** (0.050 g, 0.086 mmol). *Free base*: TLC: $CH_2Cl_2/CH_3OH/NH_4OH$ 95:5:0.5. 1H NMR (400 MHz, $CDCl_3$) δ : 8.47 (s, 1H), 8.45 (s, 1H), 8.00–7.94 (m, 8H), 7.51–7.40 (m, 9H), 7.12 (d, J = 9.2 Hz, 1H), 6.68–6.66 (m, 2H), 6.12 (d, J = 9.6 Hz, 1H), 4.60 (t, J = 6.4 Hz, 2H), 4.53 (t, J = 6.4 Hz, 2H), 3.93 (t, J = 6.0 Hz, 2H), 2.58–2.52 (m, 4H), 2.38 (t, J = 7.2 Hz, 2H), 1.99–1.92 (m, 2H), 1.83–1.73 (m, 4H), 1.44–1.30 (m, 6H) ppm. ^{13}C NMR (100 MHz, $CDCl_3$) δ : 169.7 (C), 169.7 (C), 162.2 (C), 161.2 (C), 155.8 (C), 143.4 (CH), 142.7 (C), 141.9 (C), 131.0 (C), 129.3 (CH), 129.2 (CH), 128.6 (CH), 128.4 (C), 128.2 (C), 128.0 (C), 126.9 (CH), 125.5 (CH), 125.0 (CH), 125.0 (CH), 112.8 (CH), 112.7 (CH), 112.3 (C), 101.3 (CH), 66.4 (CH₂), 65.8 (CH₂), 64.1 (CH₂), 54.0 (CH₂), 50.6 (CH₂), 50.2 (CH₂), 28.7 (CH₂), 27.1 (CH₂), 26.9 (CH₂), 26.7 (CH₂), 26.1 (CH₂) ppm. ESI-HRMS (m/z) calculated for $[M + H]^+$ ion species $C_{51}H_{48}NO_7$ = 786.3425, found 786.3424. *Hydrochloride*: yellow solid, mp 136–139 °C.

(*E*)-7-((3-((2-Oxo-2H-chromen-7-yl)oxy)propyl)(3-(((*E*)-3-(3,4,5-trimethoxyphenyl)acryloyl)oxy)propyl)amino)heptyl 3-(3,4,5-Trimethoxyphenyl)acrylate (**19**). Following *method B*, compound **19** (0.050 g, yield: 56.6%) was synthesized as a pale yellow oil, starting

from (*E*)-3-(3,4,5-trimethoxyphenyl)acrylic acid (0.029 g, 0.12 mmol) and **47** (0.050 g, 0.080 mmol). *Free base*: TLC: $CH_2Cl_2/CH_3OH/NH_4OH$ 95:5:0.5. 1H NMR (400 MHz, $CDCl_3$) δ : 7.55–7.51 (m, 3H), 7.28 (d, J = 9.2 Hz, 1H), 6.78–6.75 (m, 2H), 6.70 (s, 2H), 6.68 (s, 2H), 6.29 (d, J = 16.0 Hz, 1H), 6.26 (d, J = 16.0 Hz, 1H), 6.15 (d, J = 9.6 Hz, 1H), 4.18 (t, J = 6.0 Hz, 2H), 4.11 (t, J = 6.0 Hz, 2H), 4.03 (t, J = 6.0 Hz, 2H), 3.83 (s, 18H), 2.67–2.47 (m, 4H), 2.44–2.32 (m, 2H), 1.95–1.85 (m, 2H), 1.84–1.74 (m, 2H), 1.66–1.56 (m, 2H), 1.44–1.35 (m, 2H), 1.34–1.17 (m, 6H) ppm.

^{13}C NMR (100 MHz, $CDCl_3$) δ : 167.0 (C), 166.9 (C), 162.2 (C), 161.2 (C), 155.9 (C), 153.4 (C), 144.8 (CH), 144.6 (CH), 143.4 (CH), 140.2 (C), 140.1 (C), 129.9 (C), 129.8 (C), 128.7 (CH), 117.4 (CH), 117.1 (CH), 113.0 (CH), 112.7 (CH), 112.5 (C), 105.2 (CH), 105.2 (CH), 101.4 (CH), 66.4 (CH₂), 64.6 (CH₂), 62.7 (CH₂), 61.0 (CH₃), 56.2 (CH₃), 54.0 (CH₂), 50.5 (CH₂), 50.2 (CH₂), 29.7 (CH₂), 29.2 (CH₂), 28.7 (CH₂), 27.3 (CH₂), 25.9 (CH₂) ppm. ESI-HRMS (m/z) calculated for $[M + H]^+$ ion species $C_{46}H_{58}NO_{13}$ = 832.3903, found 832.3903. *Hydrochloride*: white solid, mp 90–92 °C.

(*E*)-3-((3-((2-Oxo-2H-chromen-7-yl)oxy)propyl)(7-((3-(3,4,5-trimethoxyphenyl)acryloyl)oxy)heptyl)amino)propyl 3,4,5-Trime-thoxybenzoate (**20**). Following *method B*, compound **20** (0.026 g, yield: 33.0%) was synthesized as a pale yellow oil, starting from (*E*)-3-(3,4,5-trimethoxyphenyl)acrylic acid (0.035 g, 0.15 mmol) and **48** (0.058 g, 0.10 mmol). *Free base*: TLC: $CH_2Cl_2/CH_3OH/NH_4OH$ 95:5:0.5. 1H NMR (400 MHz, $CDCl_3$) δ : 7.59 (d, J = 9.2 Hz, 1H), 7.58 (d, J = 16.0 Hz, 1H), 7.32 (d, J = 8.4 Hz, 1H), 7.26 (s, 2H), 6.81–6.78 (m, 2H), 6.75 (s, 2H), 6.34 (d, J = 16.0 Hz, 1H), 6.21 (d, J = 9.2 Hz, 1H), 4.33 (t, J = 6.4 Hz, 2H), 4.15 (t, J = 6.4 Hz, 2H), 4.06 (t, J = 6.4 Hz, 2H), 3.89 (s, 3H), 3.88 (s, 6H), 3.87 (s, 6H), 3.86 (s, 3H), 2.70–2.50 (m, 4H), 2.49–2.31 (m, 2H), 2.03–1.82 (m, 4H), 1.75–1.57 (m, 2H), 1.51–1.39 (m, 2H), 1.33–1.22 (m, 6H) ppm. ^{13}C NMR (100 MHz, $CDCl_3$) δ : 167.0 (C), 166.1 (C), 162.1 (C), 161.1 (C), 155.9 (C), 153.4 (C), 152.9 (C), 144.6 (CH), 143.3 (CH), 142.2 (C), 140.1 (C), 129.9 (C), 128.8 (CH), 125.2 (C), 117.4 (CH), 113.1 (CH), 112.7 (CH), 112.5 (C), 106.8 (CH), 105.2 (CH), 101.4 (CH), 66.3 (CH₂), 64.5 (CH₂), 63.2 (CH₂), 61.0 (CH₃), 60.9 (CH₃), 56.2 (CH₃), 56.2 (CH₃), 54.0 (CH₂), 50.4 (CH₂), 50.2 (CH₂), 29.2 (CH₂), 28.7 (CH₂), 28.5 (CH₂), 27.3 (CH₂), 25.9 (CH₂) ppm. ESI-HRMS (m/z) calculated for $[M + H]^+$ ion species $C_{44}H_{56}NO_{13}$ = 806.3746, found 806.3749. *Hydrochloride*: white solid, mp 84–87 °C.

(*E*)-3-((3-((2-Oxo-2H-chromen-7-yl)oxy)propyl)(7-((3-(3,4,5-trimethoxyphenyl)acryloyl)oxy)heptyl)amino)propyl Anthracene-9-carboxylate (**21**). Following *method B*, compound **21** (0.080 g, yield: 86.0%) was synthesized as a pale yellow oil, starting from anthracene-9-carboxylic acid (0.038 g, 0.17 mmol) and **47** (0.070 g, 0.11 mmol). *Free base*: TLC: $CH_2Cl_2/CH_3OH/NH_4OH$ 95:5:0.5. 1H NMR (400 MHz, $CDCl_3$) δ : 8.48 (s, 1H), 7.98 (d, J = 8.4 Hz, 4H), 7.57–7.42 (m, 6H), 7.21 (d, J = 9.2 Hz, 1H), 6.73–6.70 (m, 4H), 6.30 (d, J = 16.0 Hz, 1H), 6.16 (d, J = 9.6 Hz, 1H), 4.62 (t, J = 6.4 Hz, 2H), 4.12 (t, J = 6.4 Hz, 2H), 3.98 (t, J = 6.4 Hz, 2H), 3.84 (s, 9H), 2.70–2.53 (m, 4H), 2.50–2.32 (m, 2H), 2.10–1.96 (m, 2H), 1.95–1.79 (m, 2H), 1.66–1.56 (m, 2H), 1.44–1.35 (m, 2H), 1.29–1.12 (m, 6H) ppm. ^{13}C NMR (100 MHz, $CDCl_3$) δ : 169.6 (C), 167.0 (C), 162.2 (C), 161.2 (C), 155.8 (C), 153.4 (C), 144.6 (CH), 143.4 (CH), 131.0 (C), 129.9 (C), 129.3 (CH), 128.7 (CH), 128.4 (C), 127.0 (CH), 125.5 (CH), 124.9 (CH), 117.5 (CH), 112.9 (CH), 112.7 (CH), 112.4 (C), 105.2 (CH), 101.4 (CH), 66.4 (CH₂), 64.6 (CH₂), 64.0 (CH₂), 61.0 (CH₃), 56.1 (CH₃), 54.1 (CH₂), 50.6 (CH₂), 50.2 (CH₂), 29.7 (CH₂), 29.2 (CH₂), 28.7 (CH₂), 27.4 (CH₂), 26.1 (CH₂), 25.9 (CH₂) ppm. ESI-HRMS (m/z) calculated for $[M + H]^+$ ion species $C_{49}H_{54}NO_{10}$ = 816.3742, found 816.3743. *Hydrochloride*: pale yellow solid, mp 100–102 °C.

(*E*)-7-((3-((2-Oxo-2H-chromen-7-yl)oxy)propyl)(3-((3-(3,4,5-trimethoxyphenyl)acryloyl)oxy)propyl)amino)heptyl 3,4,5-Trime-thoxybenzoate (**22**). Following *method A*, compound **22** (0.054 g, yield: 74.5%) was synthesized as a pale yellow oil, starting from **49** (0.055 g, 0.090 mmol) and 3,4,5-trimethoxybenzoic acid (0.029 g, 0.14 mmol). *Free base*: TLC: $CH_2Cl_2/CH_3OH/NH_4OH$ 95:5:0.5. 1H NMR (400 MHz, $CDCl_3$) δ : 7.53 (d, J = 9.6 Hz, 1H), 7.52 (d, J = 16.0 Hz, 1H), 7.27 (d, J = 8.8 Hz, 1H), 7.23 (s, 2H), 6.77–6.74 (m, 2H), 6.68 (s, 2H), 6.26 (d, J = 16.0 Hz, 1H), 6.14 (d, J = 9.6 Hz, 1H), 4.21 (t, J = 6.4

H_z, 2H), 4.17 (t, *J* = 6.4 Hz, 2H), 4.02 (t, *J* = 6.4 Hz, 2H), 3.84 (s, 3H), 3.84 (s, 6H), 3.82 (s, 6H), 3.82 (s, 3H), 2.55 (t, *J* = 6.4 Hz, 2H), 2.49 (t, *J* = 6.4 Hz, 2H), 2.37 (t, *J* = 6.4 Hz, 2H), 1.90–1.85 (m, 2H), 1.80–1.76 (m, 2H), 1.70–1.63 (m, 2H), 1.43–1.22 (m, 8H) ppm. ¹³C NMR (100 MHz, CDCl₃) δ: 166.9 (C), 166.2 (C), 162.3 (C), 161.2 (C), 155.9 (C), 153.4 (C), 152.9 (C), 144.8 (CH), 143.4 (CH), 142.1 (C), 140.1 (C), 129.8 (C), 128.7 (CH), 125.5 (C), 117.2 (CH), 112.9 (CH), 112.7 (CH), 112.4 (C), 106.8 (CH), 105.2 (CH), 101.4 (CH), 66.5 (CH₂), 65.2 (CH₂), 62.8 (CH₂), 61.0 (CH₃), 60.9 (CH₃), 56.2 (CH₃), 56.2 (CH₃), 54.1 (CH₂), 50.5 (CH₂), 50.2 (CH₂), 29.3 (CH₂), 28.7 (CH₂), 27.4 (CH₂), 26.9 (CH₂), 26.0 (CH₂) ppm. ESI-HRMS (*m/z*) calculated for [M + H]⁺ ion species C₄₄H₅₆NO₁₃ = 806.3746, found 806.3751. *Hydrochloride*: white solid, mp 73–76 °C.

7-((3-((2-Oxo-2H-chromen-7-yl)oxy)propyl)(3-((3,4,5-trimethoxybenzoyl)oxy)propyl)amino)heptyl 3,4,5-Trimethoxybenzoate (23). Following *method A*, compound 23 (0.052 g, yield: 69.2%) was synthesized as a pale yellow oil, starting from 48 (0.056 g, 0.10 mmol) and 3,4,5-trimethoxybenzoic acid (0.031 g, 0.14 mmol). *Free base*: TLC: CH₂Cl₂/CH₃OH/NH₄OH 95:5:0.5. ¹H NMR (400 MHz, CDCl₃) δ: 7.57 (d, *J* = 9.6 Hz, 1H), 7.30 (d, *J* = 8.8 Hz, 1H), 7.27 (s, 2H), 7.25 (s, 2H), 6.79–6.76 (m, 2H), 6.19 (d, *J* = 9.6 Hz, 1H), 4.32 (t, *J* = 6.4 Hz, 2H), 4.25 (t, *J* = 6.4 Hz, 2H), 4.05 (t, *J* = 6.4 Hz, 2H), 3.88 (s, 12H), 3.87 (s, 6H), 2.64–2.52 (m, 4H), 2.46–2.35 (m, 2H), 1.97–1.84 (m, 4H), 1.75–1.66 (m, 2H), 1.46–1.24 (m, 8H) ppm. ¹³C NMR (100 MHz, CDCl₃) δ: 166.2 (C), 166.1 (C), 162.2 (C), 161.2 (C), 155.8 (C), 152.9 (C), 143.4 (CH), 142.1 (C), 142.1 (C), 128.7 (CH), 125.5 (C), 125.3 (C), 113.0 (CH), 112.7 (CH), 112.4 (C), 106.7 (CH), 106.7 (CH), 101.3 (CH), 66.4 (CH₂), 65.2 (CH₂), 63.4 (CH₂), 60.9 (CH₃), 56.2 (CH₃), 54.1 (CH₂), 50.4 (CH₂), 50.1 (CH₂), 29.3 (CH₂), 28.7 (CH₂), 27.4 (CH₂), 26.9 (CH₂), 26.5 (CH₂), 26.0 (CH₂) ppm. ESI-HRMS (*m/z*) calculated for [M + H]⁺ ion species C₄₂H₅₄NO₁₃ = 780.3590, found 780.3589. *Hydrochloride*: pale yellow solid, mp 74–77 °C.

3-((3-((2-Oxo-2H-chromen-7-yl)oxy)propyl)(7-((3,4,5-trimethoxybenzoyl)oxy)heptyl)amino)propyl Anthracene-9-carboxylate (24). Following *method A*, compound 24 (0.11 g, yield: 92.3%) was synthesized as a yellow oil, starting from 50 (0.090 g, 0.15 mmol) and 3,4,5-trimethoxybenzoic acid (0.048 g, 0.23 mmol). *Free base*: TLC: CH₂Cl₂/CH₃OH/NH₄OH 95:5:0.5. ¹H NMR (400 MHz, CDCl₃) δ: 8.51 (s, 1H), 8.01 (d, *J* = 8.8 Hz, 4H), 7.55–7.45 (m, 5H), 7.28 (s, 2H), 7.25 (d, *J* = 8.4 Hz, 1H), 6.76–6.74 (m, 2H), 6.19 (d, *J* = 9.2 Hz, 1H), 4.65 (t, *J* = 6.4 Hz, 2H), 4.25 (t, *J* = 6.4 Hz, 2H), 4.01 (t, *J* = 6.4 Hz, 2H), 3.89 (s, 3H), 3.89 (s, 6H), 2.82–2.54 (m, 4H), 2.53–2.38 (m, 2H), 2.13–1.98 (m, 2H), 1.97–1.84 (m, 2H), 1.76–1.66 (m, 2H), 1.53–1.39 (m, 2H), 1.38–1.23 (m, 6H) ppm. ¹³C NMR (100 MHz, CDCl₃) δ: 169.6 (C), 166.2 (C), 162.2 (C), 161.2 (C), 155.8 (C), 152.9 (C), 143.4 (CH), 142.2 (C), 131.0 (C), 129.3 (CH), 128.7 (CH), 128.6 (CH), 128.3 (C), 128.0 (C), 126.9 (CH), 125.5 (C), 125.5 (CH), 124.9 (CH), 112.8 (CH), 112.7 (CH), 112.4 (C), 106.8 (CH), 101.3 (CH), 66.5 (CH₂), 65.2 (CH₂), 64.1 (CH₂), 60.9 (CH₃), 56.2 (CH₃), 54.2 (CH₂), 50.7 (CH₂), 50.2 (CH₂), 29.2 (CH₂), 28.7 (CH₂), 27.4 (CH₂), 27.2 (CH₂), 26.9 (CH₂), 26.8 (CH₂), 26.0 (CH₂) ppm. ESI-HRMS (*m/z*) calculated for [M + H]⁺ ion species C₄₇H₅₂NO₁₀ = 790.3586, found 790.3586. *Hydrochloride*: pale yellow solid, mp 75–77 °C.

(*E*)-7-((3-((2-Oxo-2H-chromen-7-yl)oxy)propyl)(3-((3,4,5-trimethoxyphenyl)acryloyl)oxy)propyl)amino)heptyl Anthracene-9-carboxylate (25). Following *method B*, compound 25 (0.13 g, yield: 93.5%) was synthesized as a pale yellow oil, starting from anthracene-9-carboxylic acid (0.060 g, 0.27 mmol) and 49 (0.11 g, 0.18 mmol). *Free base*: TLC: CH₂Cl₂/CH₃OH/NH₄OH 95:5:0.5. ¹H NMR (400 MHz, CDCl₃) δ: 8.46 (s, 1H), 7.97 (t, *J* = 8.4 Hz, 4H), 7.54 (d, *J* = 16.0 Hz, 1H), 7.51–7.41 (m, 5H), 7.21 (d, *J* = 9.6 Hz, 1H), 6.74–6.71 (m, 2H), 6.69 (s, 2H), 6.28 (d, *J* = 16.0 Hz, 1H), 6.12 (d, *J* = 9.2 Hz, 1H), 4.55 (t, *J* = 6.4 Hz, 2H), 4.19 (t, *J* = 6.4 Hz, 2H), 3.99 (t, *J* = 6.4 Hz, 2H), 3.83 (s, 3H), 3.82 (s, 6H), 2.56–2.48 (m, 4H), 2.39–2.34 (m, 2H), 1.91–1.74 (m, 6H), 1.47–1.21 (m, 8H) ppm. ¹³C NMR (100 MHz, CDCl₃) δ: 169.7 (C), 166.9 (C), 162.2 (C), 161.2 (C), 155.8 (C), 153.4 (C), 144.7 (CH), 143.4 (CH), 140.1 (C), 131.0 (C), 129.9 (C), 129.2 (CH), 128.7 (CH), 128.6 (CH), 128.3 (C), 128.2 (C), 126.9 (CH),

125.5 (CH), 125.0 (CH), 117.2 (CH), 112.8 (CH), 112.6 (CH), 112.4 (C), 105.2 (CH), 101.4 (CH), 66.5 (CH₂), 65.9 (CH₂), 62.8 (CH₂), 61.0 (CH₃), 56.1 (CH₃), 54.1 (CH₂), 50.5 (CH₂), 50.1 (CH₂), 29.2 (CH₂), 28.7 (CH₂), 27.4 (CH₂), 27.1 (CH₂), 26.9 (CH₂), 26.6 (CH₂), 26.1 (CH₂) ppm. ESI-HRMS (*m/z*) calculated for [M + H]⁺ ion species C₄₉H₅₄NO₁₀ = 816.3742, found 816.3744. *Hydrochloride*: pale yellow solid, mp 107–110 °C.

7-((3-((2-Oxo-2H-chromen-7-yl)oxy)propyl)(3-((3,4,5-trimethoxybenzoyl)oxy)propyl)amino)heptyl Anthracene-9-carboxylate (26). Following *method B*, compound 26 (0.073 g, yield: 77.7%) was synthesized as a pale yellow oil, starting from anthracene-9-carboxylic acid (0.040 g, 0.18 mmol) and 48 (0.070 g, 0.12 mmol). *Free base*: TLC: CH₂Cl₂/CH₃OH/NH₄OH 95:5:0.5. ¹H NMR (400 MHz, CDCl₃) δ: 8.47 (s, 1H), 8.01 (d, *J* = 8.4 Hz, 2H), 7.98 (d, *J* = 8.4 Hz, 2H), 7.53–7.43 (m, 5H), 7.25 (s, 2H), 7.21 (d, *J* = 9.2 Hz, 1H), 6.74–6.71 (m, 2H), 6.15 (d, *J* = 9.6 Hz, 1H), 4.58 (t, *J* = 6.4 Hz, 2H), 4.31 (t, *J* = 6.4 Hz, 2H), 3.99 (t, *J* = 6.4 Hz, 2H), 3.88 (s, 3H), 3.86 (s, 6H), 2.58–2.52 (m, 4H), 2.40 (t, *J* = 6.4 Hz, 2H), 1.88–1.79 (m, 6H), 1.48–1.37 (m, 4H), 1.36–1.23 (m, 4H) ppm. ¹³C NMR (100 MHz, CDCl₃) δ: 169.7 (C), 166.1 (C), 162.2 (C), 161.2 (C), 155.8 (C), 152.9 (C), 143.4 (CH), 142.2 (C), 131.0 (C), 129.2 (CH), 128.7 (CH), 128.6 (CH), 128.4 (C), 128.2 (C), 126.9 (CH), 125.5 (CH), 125.3 (C), 125.0 (CH), 112.9 (CH), 112.6 (CH), 112.4 (C), 106.8 (CH), 101.3 (CH), 66.4 (CH₂), 65.9 (CH₂), 63.4 (CH₂), 60.9 (CH₃), 56.2 (CH₃), 54.1 (CH₂), 50.4 (CH₂), 50.1 (CH₂), 29.2 (CH₂), 28.7 (CH₂), 27.4 (CH₂), 26.9 (CH₂), 26.6 (CH₂), 26.1 (CH₂) ppm. ESI-HRMS (*m/z*) calculated for [M + H]⁺ ion species C₄₇H₅₂NO₁₀ = 790.3586, found 790.3585. *Hydrochloride*: yellow solid; mp 97–99 °C.

3-((7-((Anthracene-9-carbonyl)oxy)heptyl)(3-((2-oxo-2H-chromen-7-yl)oxy)propyl)amino)propyl Anthracene-9-carboxylate (27). Following *method B*, compound 27 (0.11 g, yield: 91.1%) was synthesized as a yellow oil, starting from anthracene-9-carboxylic acid (0.050 g, 0.23 mmol) and 50 (0.090 g, 0.15 mmol). *Free base*: TLC: CH₂Cl₂/CH₃OH/NH₄OH 95:5:0.5. ¹H NMR (400 MHz, CDCl₃) δ: 8.48 (s, 2H), 8.05–7.98 (m, 8H), 7.54–7.43 (m, 9H), 7.15 (d, *J* = 8.8 Hz, 1H), 6.71–6.69 (m, 2H), 6.15 (d, *J* = 9.2 Hz, 1H), 4.65 (t, *J* = 6.4 Hz, 2H), 4.58 (t, *J* = 6.4 Hz, 2H), 3.96 (t, *J* = 6.4 Hz, 2H), 2.70–2.49 (m, 4H), 2.42 (m, 2H), 2.07–1.95 (m, 2H), 1.91–1.78 (m, 4H), 1.48–1.36 (m, 4H), 1.34–1.22 (m, 4H) ppm. ¹³C NMR (100 MHz, CDCl₃) δ: 169.8 (C), 169.7 (C), 162.2 (C), 161.3 (C), 155.8 (C), 143.4 (CH), 131.0 (C), 129.3 (CH), 129.2 (CH), 128.7 (CH), 128.4 (C), 128.2 (C), 128.0 (C), 126.9 (CH), 125.5 (CH), 125.0 (CH), 125.0 (CH), 112.8 (CH), 112.7 (CH), 112.4 (C), 101.3 (CH), 66.4 (CH₂), 65.9 (CH₂), 64.1 (CH₂), 54.1 (CH₂), 50.6 (CH₂), 50.2 (CH₂), 29.2 (CH₂), 28.7 (CH₂), 27.4 (CH₂), 27.0 (CH₂), 26.8 (CH₂), 26.7 (CH₂), 26.1 (CH₂) ppm. ESI-HRMS (*m/z*) calculated for [M + H]⁺ ion species C₅₂H₅₀NO₇ = 800.3582, found 800.3578. *Hydrochloride*: pale yellow solid; mp 117–119 °C.

Stability Tests. *Chemicals.* Acetonitrile (Chromasolv), formic acid and ammonium formate (MS grade), NaCl, KCl, Na₂HPO₄·2H₂O, and KH₂PO₄ (Reagent grade), verapamil hydrochloride (analytical standard, used as the internal standard or IS), and ketoprofen (analytical standard) were purchased from Sigma-Aldrich (Milan, Italy). Ketoprofen ethyl ester (KEE) was obtained by Fisher's reaction from ketoprofen and ethanol.

Ultrapure water or mQ water (18 MΩ cm) was obtained from Millipore's Simplicity system (Milan, Italy).

Phosphate-buffered solution (PBS) was prepared by adding 8.01 g L⁻¹ of NaCl, 0.2 g L⁻¹ of KCl, 1.78 g L⁻¹ of Na₂HPO₄·2H₂O, and 0.27 g L⁻¹ of KH₂PO₄. Human plasma was collected from healthy volunteers, pooled in a single batch, and kept at -80 °C until use.

Preparation of Samples. Each sample was prepared by adding 10 μL of working solution 1 (for details, see the [Supporting Information](#)) to 100 μL of the tested matrix (PBS or human plasma) in microcentrifuge tubes. The obtained solutions correspond to 1 μM of the analyte.

Each set of samples was incubated in triplicate at four different times, 0, 30, 60, and 120 min at 37 °C. Therefore, the degradation profile of each analyte was represented by a batch of 12 samples (4 incubation times × 3 replicates). After the incubation, the samples were added with 300 μL of IS solution (for details, see the [Supporting Information](#)) and

centrifuged (room temperature for 5 min at 10 000 rpm). The supernatants were transferred in auto sampler vials and dried under a gentle stream of nitrogen. The dried samples were dissolved in 1.0 mL of 10 mM formic acid in mQ water: acetonitrile 80:20 solution. The obtained sample solutions were analyzed by LC-MS/MS methods described in the [Supporting Information](#).

CA Inhibition Assay. An SX.18MV-R Applied Photophysics (Oxford, U.K.) stopped-flow instrument has been used to assay the catalytic/inhibition of various CA isozymes.³⁸ Phenol Red (at a concentration of 0.2 mM) has been used as an indicator, working at an absorbance maximum of 557 nm, with 10 mM Hepes (pH 7.4) as a buffer, 0.1 M Na₂SO₄ or NaClO₄ (for maintaining constant the ionic strength; these anions are not inhibitory in the used concentration), following the CA-catalyzed CO₂ hydration reaction for a period of 5–10 s. Saturated CO₂ solutions in water at 25 °C were used as a substrate. Stock solutions of inhibitors were prepared at a concentration of 10 μM (in DMSO–water 1:1, v/v), and dilutions up to 0.01 nM were done with the assay buffer mentioned above. At least seven different inhibitor concentrations have been used for measuring the inhibition constant. Inhibitor and enzyme solutions were preincubated together for 10 min at room temperature prior to assay to allow for the formation of the E–I complex. Triplicate experiments were done for each inhibitor concentration, and the values reported throughout the paper are the mean of such results. The inhibition constants were obtained by nonlinear least-squares methods using the Cheng–Prusoff equation, as reported earlier,³² and represent the mean from at least three different determinations. All CA isozymes used here were recombinant proteins obtained as reported earlier by our group, and their concentrations in the assay system were 5.6–12 nM.^{65,66}

Cells. Human chemosensitive colon cancer HT29 cells, lung cancer A549 cells, not-transformed human colon epithelial EpiCoC cells, and lung epithelial BEAS-2B cells were purchased from ATCC (Manassas, VA). The K562 leukemia cells derived from a patient with chronic myelogenous leukemia⁴¹ and the P-gp overexpressing K562/DOX cells were obtained from Prof. J. P. Marie (Hopital Hotel-Dieu, Paris, France). These cells were cultured in RPMI 1640 medium supplemented with 10% fetal calf serum (FCS; GIBCO) at 37 °C in a humidified incubator with 5% CO₂. To maintain the resistance, every month, resistant cells were cultured for 3 days with 400 nM doxorubicin. Human HT29/DOX and A549/DOX were generated by stepwise selection in medium with increasing concentration of doxorubicin, as reported by us,⁶⁷ and maintained in the culture medium with a final concentration of 200 and 100 nM doxorubicin, respectively. All cell lines were authenticated by microsatellite analysis, using the PowerPlex kit (Promega Corporation, Madison, WI; last authentication: January 2022). Cells were maintained in media supplemented with 10% v/v fetal bovine serum, 1% v/v penicillin–streptomycin, and 1% v/v L-glutamine. To generate KO clones, 5 × 10⁵ cells were transduced with 1 μg of RNA vector (CRISPR pCas guide vector) for CAXII, P-gp or 1 μg not-targeting vector, mixed with 1 μg of donor DNA vector (Origene, Rockville, MD), following the manufacturer's instructions. Stable knockout cells were selected in complete medium containing 1 μg/mL of puromycin for 3 weeks. Knockout efficacy was evaluated by immunoblotting, as reported below.

MDCK-MDR1, MDCK-MRP1, and MDCK-BCRP cells are a gift from Prof. P. Borst, NKI-AVL Institute, Amsterdam, The Netherlands. Cells were grown in Dulbecco's modified Eagle's medium (DMEM) high glucose supplemented with 10% fetal bovine serum, 2 mM glutamine, 100 U/mL of penicillin, and 100 μg/mL of streptomycin in a humidified incubator at 37 °C with a 5% CO₂ atmosphere. Cell culture reagents were purchased from Celbio s.r.l. (Milano, Italy). CulturePlate 96/wells plates were purchased from PerkinElmer Life Science (Waltham, MA) and Falcon (BD Biosciences, Bedford, MA). Calcein-AM and Hoechst 33342 (bisbenzimidazole H 33342 trihydrochloride) were obtained from Sigma-Aldrich (Milan, Italy). The other reagents were purchased from Sigma Merck Millipore.

Drugs and Chemicals. Doxorubicin hydrochloride, verapamil hydrochloride, dimethylsulfoxide (DMSO), and 3-(4,5-dimethylthiazol-2-yl)-2,5-diphenyl tetrazolium bromide (MTT) were purchased from Sigma-Aldrich (Milan Italy). Stock solutions of the tested

compounds as hydrochloride salts were prepared in DMSO at 10⁻² M. Stock solutions of doxorubicin hydrochloride and verapamil hydrochloride were prepared in water at 10⁻² M. All of the stock solutions were then diluted with complete medium to obtain the 10x desired final maximum test concentrations.

Immunoblotting. Cells were rinsed with ice-cold lysis buffer (50 mM tris, 10 mM ethylenediamine tetraacetic acid (EDTA), 1% v/v Triton-X100), supplemented with the protease inhibitor cocktail set III (80 μM aprotinin, 5 mM bestatin, 1.5 mM leupeptin, 1 mM pepstatin; Calbiochem, San Diego, CA), 2 mM phenylmethylsulfonyl fluoride, and 1 mM Na₃VO₄, then sonicated and centrifuged at 13 000g for 10 min at 4 °C. Protein extracts (20 μg) were subjected to sodium dodecyl sulfate polyacrylamide gel electrophoresis (SDS-PAGE) and probed with the following antibodies: anti-P-gp (C219, Calbiochem), anti-MRP1 (Abcam, Cambridge, U.K.), anti-CAXII (Abcam, Cambridge, U.K.), and anti-β-tubulin (Santa Cruz Biotechnology Inc., Santa Cruz, CA), followed by a peroxidase-conjugated secondary antibody (Bio-Rad Laboratories). The membranes were washed with tris-buffered saline-Tween 0.1% v/v solution, and the proteins were detected by enhanced chemiluminescence (Bio-Rad Laboratories).

Coadministration Assays in K562/DOX, HT29/DOX, and A549/DOX Cells. K562/DOX cells were incubated for 72 h with compounds (1, 3, 10 μM) alone for intrinsic cytotoxicity and with doxorubicin in combination with 1 or 3 μM of the indicated compounds; HT29/DOX and A549/DOX cells were incubated for 72 h with doxorubicin, in the range from 10 nM to 30 μM, alone or in combination with 1 or 3 μM of the indicated compounds. Cell viability of the three cell lines was measured by the MTT assay, using a Synergy HT microplate spectrofluorimeter (Bio-Tek Instruments, Winooski, VT). The absorbance of untreated cells was considered 100%; results were expressed as the percentage of viable treated cells versus the control untreated cells. IC₅₀ was the concentration killing 50% of cells and was determined graphically from relative survival curves obtained by GraphPad Prism 5 software (GraphPad, San Diego, CA).

pH_i Measurement. pH_i was measured by incubating whole cells with 5 μM 2',7'-bis-(2-carboxyethyl)-5-(and-6)-carboxyfluorescein acetoxyethyl ester for 15 min at 37 °C and reading the intracellular fluorescence by a FACSCalibur flow cytometer (Becton Dickinson). The intracellular fluorescence was converted into pH units according to a titration curve, as described previously.⁶⁸

Intracellular Doxorubicin Accumulation and Kinetic Parameters. Cells were incubated for 3 h with 5 μM doxorubicin, alone or with the selected compounds, washed with PBS, trypsinized, centrifuged at 13 000g for 5 min, and resuspended in 0.5 mL of 1/1 solution ethanol/0.3 N HCl. A 50 μL aliquot was sonicated and used for the measurement of the protein content. The intracellular fluorescence of doxorubicin was measured spectrofluorimetrically using a Synergy HT microplate spectrofluorimeter (Bio-Tek Instruments). Excitation and emission wavelengths were 475 and 553 nm, respectively. Fluorescence was converted in nmol/mg cell proteins using a calibration curve previously set. To calculate the kinetic parameters, cells were incubated for 20 min with increasing (0–100 μM) concentrations of doxorubicin, alone or with the indicated compounds, then analyzed for the intracellular concentration of doxorubicin. A second series of dishes, after the incubation under the same experimental conditions for a further 10 min at 37 °C, were washed and tested for the intracellular drug content. The difference in the doxorubicin concentration between the two series, expressed as nmol doxorubicin extruded/min/mg cell proteins, was plotted versus the initial drug concentration.⁶⁹ Values were fitted to the Michaelis–Menten equation to calculate V_{max} and K_m, using the Enzfitter software (Biosoft Corporation, Cambridge, United Kingdom).

Statistical Analysis. All data in the text and figures are provided as means ± SD. The results were analyzed by one-way analysis of variance (ANOVA) and Tukey's test, using Statistical Package for Social Science (SPSS) software (IBM SPSS Statistics v.19). *p* < 0.05 was considered significant.

■ ASSOCIATED CONTENT

SI Supporting Information

The Supporting Information is available free of charge at <https://pubs.acs.org/doi/10.1021/acs.jmedchem.2c01175>.

¹H NMR (400 MHz), ¹³C-APT-NMR (100 MHz) spectra of compounds 1–27; chemical stability data of compounds 1–27 and reference compound KEE; analytical method used to determine the purity and chromatographic profiles of HPLC–DAD analysis of representative compounds (2, 3, 5, 6, 8, 9, 13–17); UV spectra of compounds 2, 3, 5, 6, 8, 9, 13–17; expression levels of P-gp and hCA XII in sensitive HT29 and A549 human cancer cell lines, in resistant wild-type HT29/DOX and A549/DOX cells, and in their P-gp or hCA XII knockout (KO) counterparts; cytotoxicity on HT29, HT29/DOX, A549, and A549/DOX cell lines of selected compounds (1, 2, 4, 5, 10, 11, 13, 14, 19, 20, 22, 23); and reduction of viability in EpiCoc and BEARS-2B cell lines of selected compounds (1, 2, 4, 5, 10, 11, 13, 14, 19, 20, 22, 23) (PDF)

SMILES format representations of compounds (CSV)

■ AUTHOR INFORMATION

Corresponding Author

Elisabetta Teodori – Department of Neuroscience, Psychology, Drug Research and Child Health - Section of Pharmaceutical and Nutraceutical Sciences, University of Florence, 50019 Sesto Fiorentino (FI), Italy; orcid.org/0000-0002-9705-3875; Email: elisabetta.teodori@unifi.it

Authors

Laura Braconi – Department of Neuroscience, Psychology, Drug Research and Child Health - Section of Pharmaceutical and Nutraceutical Sciences, University of Florence, 50019 Sesto Fiorentino (FI), Italy

Chiara Riganti – Department of Oncology, University of Turin, 10126 Torino, Italy; orcid.org/0000-0001-9787-4836

Marcella Coronello – Department of Health Sciences - Clinical Pharmacology and Oncology Section, University of Florence, 50139 Firenze, Italy

Alessio Nocentini – Department of Neuroscience, Psychology, Drug Research and Child Health - Section of Pharmaceutical and Nutraceutical Sciences, University of Florence, 50019 Sesto Fiorentino (FI), Italy; orcid.org/0000-0003-3342-702X

Gianluca Bartolucci – Department of Neuroscience, Psychology, Drug Research and Child Health - Section of Pharmaceutical and Nutraceutical Sciences, University of Florence, 50019 Sesto Fiorentino (FI), Italy; orcid.org/0000-0002-5631-8769

Marco Pallecchi – Department of Neuroscience, Psychology, Drug Research and Child Health - Section of Pharmaceutical and Nutraceutical Sciences, University of Florence, 50019 Sesto Fiorentino (FI), Italy

Marialessandra Contino – Department of Pharmacy - Drug Sciences, University of Bari “A. Moro”, 70125 Bari, Italy; orcid.org/0000-0002-0713-3151

Dina Manetti – Department of Neuroscience, Psychology, Drug Research and Child Health - Section of Pharmaceutical and Nutraceutical Sciences, University of Florence, 50019 Sesto Fiorentino (FI), Italy; orcid.org/0000-0002-5881-6550

Maria Novella Romanelli – Department of Neuroscience, Psychology, Drug Research and Child Health - Section of Pharmaceutical and Nutraceutical Sciences, University of

Florence, 50019 Sesto Fiorentino (FI), Italy; orcid.org/0000-0002-5685-3403

Claudiu T. Supuran – Department of Neuroscience, Psychology, Drug Research and Child Health - Section of Pharmaceutical and Nutraceutical Sciences, University of Florence, 50019 Sesto Fiorentino (FI), Italy; orcid.org/0000-0003-4262-0323

Silvia Dei – Department of Neuroscience, Psychology, Drug Research and Child Health - Section of Pharmaceutical and Nutraceutical Sciences, University of Florence, 50019 Sesto Fiorentino (FI), Italy; orcid.org/0000-0003-0898-7148

Complete contact information is available at:

<https://pubs.acs.org/10.1021/acs.jmedchem.2c01175>

Author Contributions

These authors contributed equally.

Notes

The authors declare no competing financial interest.

■ ACKNOWLEDGMENTS

This research was supported by grants from the University of Florence (Fondo Ricerca Ateneo RICATEN20 and RICATEN21) and the Italian Association for Cancer Research (Grant IF21408).

■ ABBREVIATIONS USED

AAZ, acetazolamide; BCRP, breast cancer resistance protein; CA, carbonic anhydrase; DMAP, 4-dimethylaminopyridine; Doxo, doxorubicin; EDC, 1-ethyl-3-(3'-dimethylaminopropyl)-carbodiimide; KEE, ketoprofen ethyl ester; KO, knockout; MDCK, Madin-Darby Canine Kidney; MDR, multidrug resistance; MRP1, multidrug-resistance-associated protein-1; MTT, 3-(4,5-dimethylthiazolyl-2)-2,5-diphenyl tetrazolium bromide; PBS, phosphate-buffered solution; P-gp, P-glycoprotein; RF, reversal fold

■ REFERENCES

- (1) Holohan, C.; Van Schaeybroeck, S.; Longley, D. B.; Johnston, P. G. Cancer Drug Resistance: An Evolving Paradigm. *Nat. Rev. Cancer* **2013**, *13*, 714–726.
- (2) Longley, D. B.; Johnston, P. G. Molecular Mechanisms of Drug Resistance. *J. Pathol.* **2005**, *205*, 275–292.
- (3) Gillet, J.-P.; Gottesman, M. M. Mechanisms of Multidrug Resistance in Cancer. In *Methods in Molecular Biology*; Humana Press, 2010; Vol. 596, pp 47–76. DOI: [10.1007/978-1-60761-416-6_4](https://doi.org/10.1007/978-1-60761-416-6_4).
- (4) Gottesman, M. M.; Fojo, T.; Bates, S. E. Multidrug Resistance in Cancer: Role of ATP-Dependent Transporters. *Nat. Rev. Cancer* **2002**, *2*, 48–58.
- (5) Goebel, J.; Chmielewski, J.; Hrycyna, C. A. The Roles of the Human ATP-Binding Cassette Transporters P-Glycoprotein and ABCG2 in Multidrug Resistance in Cancer and at Endogenous Sites: Future Opportunities for Structure-Based Drug Design of Inhibitors. *Cancer Drug Resist.* **2021**, *4*, 784–804.
- (6) Robey, R. W.; Pluchino, K. M.; Hall, M. D.; Fojo, A. T.; Bates, S. E.; Gottesman, M. M. Revisiting the Role of ABC Transporters in Multidrug-Resistant Cancer. *Nat. Rev. Cancer* **2018**, *18*, 452–464.
- (7) Stefan, K.; Schmitt, S. M.; Wiese, M. 9-Deazapurines as Broad-Spectrum Inhibitors of the ABC Transport Proteins P-Glycoprotein, Multidrug Resistance-Associated Protein 1, and Breast Cancer Resistance Protein. *J. Med. Chem.* **2017**, *60*, 8758–8780.
- (8) Szakács, G.; Annereau, J.-P.; Lababidi, S.; Shankavaram, U.; Arciello, A.; Bussey, K. J.; Reinhold, W.; Guo, Y.; Kruh, G. D.; Reimers, M.; Weinstein, J. N.; Gottesman, M. M. Predicting Drug Sensitivity and Resistance: Profiling ABC Transporter Genes in Cancer Cells. *Cancer Cell* **2004**, *6*, 129–137.

- (9) Joshi, P.; Vishwakarma, R. A.; Bharate, S. B. Natural Alkaloids as P-gp Inhibitors for Multidrug Resistance Reversal in Cancer. *Eur. J. Med. Chem.* **2017**, *138*, 273–292.
- (10) Zhang, H.; Xu, H.; Ashby, C. R.; Assaraf, Y. G.; Chen, Z.-S.; Liu, H.-M. Chemical Molecular-Based Approach to Overcome Multidrug Resistance in Cancer by Targeting P-Glycoprotein (P-Gp). *Med. Res. Rev.* **2021**, *41*, 525–555.
- (11) Kathawala, R. J.; Gupta, P.; Ashby, C. R.; Chen, Z.-S. The Modulation of ABC Transporter-Mediated Multidrug Resistance in Cancer: A Review of the Past Decade. *Drug Resist. Updates* **2015**, *18*, 1–17.
- (12) Palmeira, A.; Sousa, E.; Vasconcelos, M. H.; Pinto, M. M. Three Decades of P-gp Inhibitors: Skimming through Several Generations and Scaffolds. *Curr. Med. Chem.* **2012**, *19*, 1946–2025.
- (13) Waghay, D.; Zhang, Q. Inhibit or Evade Multidrug Resistance P-Glycoprotein in Cancer Treatment. *J. Med. Chem.* **2018**, *61*, 5108–5121.
- (14) Coley, H. M. Overcoming Multidrug Resistance in Cancer: Clinical Studies of P-Glycoprotein Inhibitors. In *Methods in Molecular Biology*; Humana Press, 2010; Vol. 596, pp 341–358. DOI: 10.1007/978-1-60761-416-6_15.
- (15) Sarkadi, B.; Homolya, L.; Szakács, G.; Váradi, A. Human Multidrug Resistance ABCB and ABCG Transporters: Participation in a Chemoinnity Defense System. *Physiol. Rev.* **2006**, *86*, 1179–1236.
- (16) Ueda, K. ABC Proteins Protect the Human Body and Maintain Optimal Health. *Biosci., Biotechnol., Biochem.* **2011**, *75*, 401–409.
- (17) Darby, R. A. J.; Callaghan, R.; McMahon, R. M. P-Glycoprotein Inhibition: The Past, the Present and the Future. *Curr. Drug Metab.* **2011**, *12*, 722–731.
- (18) Kopecka, J.; Campia, I.; Jacobs, A.; Frei, A. P.; Ghigo, D.; Wollscheid, B.; Riganti, C. Carbonic Anhydrase XII Is a New Therapeutic Target to Overcome Chemoresistance in Cancer Cells. *Oncotarget* **2015**, *6*, 6776–6793.
- (19) Nocentini, A.; Supuran, C. T. Carbonic Anhydrase Inhibitors as Antitumor/Antimetastatic Agents: A Patent Review (2008–2018). *Expert Opin. Ther. Pat.* **2018**, *28*, 729–740.
- (20) Hynninen, P.; Vaskivuo, L.; Saarnio, J.; Haapasalo, H.; Kivelä, J.; Pastoreková, S.; Pastorek, J.; Waheed, A.; Sly, W. S.; Puistola, U.; Parkkila, S. Expression of Transmembrane Carbonic Anhydrases IX and XII in Ovarian Tumours. *Histopathology* **2006**, *49*, 594–602.
- (21) Rafalko, A.; Iliopoulos, O.; Fusaro, V. A.; Hancock, W.; Hincapie, M. Immunoaffinity Enrichment and Liquid Chromatography-Selected Reaction Monitoring Mass Spectrometry for Quantitation of Carbonic Anhydrase 12 in Cultured Renal Carcinoma Cells. *Anal. Chem.* **2010**, *82*, 8998–9005.
- (22) Monti, S. M.; Supuran, C. T.; De Simone, G. Anticancer Carbonic Anhydrase Inhibitors: A Patent Review (2008–2013). *Expert Opin. Ther. Pat.* **2013**, *23*, 737–749.
- (23) Supuran, C. T. Carbonic Anhydrase Inhibitors as Emerging Agents for the Treatment and Imaging of Hypoxic Tumors. *Expert Opin. Invest. Drugs* **2018**, *27*, 963–970.
- (24) Chiche, J.; Ilc, K.; Laferrère, J.; Trottier, E.; Dayan, F.; Mazure, N. M.; Brahimi-Horn, M. C.; Pouyssegur, J. Hypoxia-Inducible Carbonic Anhydrase IX and XII Promote Tumor Cell Growth by Counteracting Acidosis through the Regulation of the Intracellular pH. *Cancer Res.* **2009**, *69*, 358–368.
- (25) Kopecka, J.; Rankin, G. M.; Salaroglio, I. C.; Poulsen, S.-A.; Riganti, C. P-Glycoprotein-Mediated Chemoresistance Is Reversed by Carbonic Anhydrase XII Inhibitors. *Oncotarget* **2016**, *7*, 85861–85875.
- (26) Teodori, E.; Braconi, L.; Bua, S.; Lapucci, A.; Bartolucci, G.; Manetti, D.; Romanelli, M. N.; Dei, S.; Supuran, C. T.; Coronello, M. Dual P-Glycoprotein and CA XII Inhibitors: A New Strategy to Reverse the P-Gp Mediated Multidrug Resistance (MDR) in Cancer Cells. *Molecules* **2020**, *25*, 1748.
- (27) Martelli, C.; Coronello, M.; Dei, S.; Manetti, D.; Orlandi, F.; Scapecchi, S.; Romanelli, M. N.; Salerno, M.; Mini, E.; Teodori, E. Structure-Activity Relationships Studies in a Series of N,N-Bis(Alkanol)Amine Aryl Esters as P-Glycoprotein (Pgp) Dependent Multidrug Resistance (MDR) Inhibitors. *J. Med. Chem.* **2010**, *53*, 1755–1762.
- (28) Dei, S.; Coronello, M.; Floriddia, E.; Bartolucci, G.; Bellucci, C.; Guandalini, L.; Manetti, D.; Romanelli, M. N.; Salerno, M.; Bello, I.; Mini, E.; Teodori, E. Multidrug Resistance (MDR) Reversers: High Activity and Efficacy in a Series of Asymmetrical N,N-Bis(Alkanol)Amine Aryl Esters. *Eur. J. Med. Chem.* **2014**, *87*, 398–412.
- (29) Dei, S.; Braconi, L.; Trezza, A.; Menicatti, M.; Contino, M.; Coronello, M.; Chiaramonte, N.; Manetti, D.; Perrone, M. G.; Romanelli, M. N.; Udomtanakunchai, C.; Colabufo, N. A.; Bartolucci, G.; Spiga, O.; Salerno, M.; Teodori, E. Modulation of the Spacer in N,N-Bis(Alkanol)Amine Aryl Ester Heterodimers Led to the Discovery of a Series of Highly Potent P-Glycoprotein-Based Multidrug Resistance (MDR) Modulators. *Eur. J. Med. Chem.* **2019**, *172*, 71–94.
- (30) Teodori, E.; Contino, M.; Riganti, C.; Bartolucci, G.; Braconi, L.; Manetti, D.; Romanelli, M. N.; Trezza, A.; Athanasios, A.; Spiga, O.; Perrone, M. G.; Giampietro, R.; Gazzano, E.; Salerno, M.; Colabufo, N. A.; Dei, S. Design, Synthesis and Biological Evaluation of Stereo- and Regioisomers of Amino Aryl Esters as Multidrug Resistance (MDR) Reversers. *Eur. J. Med. Chem.* **2019**, *182*, No. 111655.
- (31) Supuran, C. T. Structure and Function of Carbonic Anhydrases. *Biochem. J.* **2016**, *473*, 2023–2032.
- (32) Maresca, A.; Temperini, C.; Vu, H.; Pham, N. B.; Poulsen, S. A.; Scozzafava, A.; Quinn, R. J.; Supuran, C. T. Non-Zinc Mediated Inhibition of Carbonic Anhydrases: Coumarins Are a New Class of Suicide Inhibitors. *J. Am. Chem. Soc.* **2009**, *131*, 3057–3062.
- (33) Supuran, C. T. Carbonic Anhydrase Inhibitors and Their Potential in a Range of Therapeutic Areas. *Expert Opin. Ther. Pat.* **2018**, *28*, 709–712.
- (34) Yalçintepe, L.; Halis, E.; Ulku, S. Effect of CD38 on the Multidrug Resistance of Human Chronic Myelogenous Leukemia K562 Cells to Doxorubicin. *Oncol. Lett.* **2016**, *11*, 2290–2296.
- (35) Teodori, E.; Dei, S.; Garnier-Suillerot, A.; Gualtieri, F.; Manetti, D.; Martelli, C.; Romanelli, M. N.; Scapecchi, S.; Sudwan, P.; Salerno, M. Exploratory Chemistry toward the Identification of a New Class of Multidrug Resistance Reverters Inspired by Pervilleine and Verapamil Models. *J. Med. Chem.* **2005**, *48*, 7426–7436.
- (36) Versteegen, R. M.; Sijbesma, R. P.; Meijer, E. W. [n]-Polyurethanes Synthesis and Characterization. *Angew. Chem., Int. Ed.* **1999**, *38*, 2917–2919.
- (37) Martelli, C.; Dei, S.; Lambert, C.; Manetti, D.; Orlandi, F.; Romanelli, M. N.; Scapecchi, S.; Salerno, M.; Teodori, E. Inhibition of P-Glycoprotein-Mediated Multidrug Resistance (MDR) by N,N-Bis(Cyclohexanol)Amine Aryl Esters: Further Restriction of Molecular Flexibility Maintains High Potency and Efficacy. *Bioorg. Med. Chem. Lett.* **2011**, *21*, 106–109.
- (38) Khalifah, R. G. The Carbon Dioxide Hydration Activity of Carbonic Anhydrase. I. Stop-Flow Kinetic Studies on the Native Human Isoenzymes B and C. *J. Biol. Chem.* **1971**, *246*, 2561–2573.
- (39) Maresca, A.; Temperini, C.; Pochet, L.; Masereel, B.; Scozzafava, A.; Supuran, C. T. Deciphering the Mechanism of Carbonic Anhydrase Inhibition with Coumarins and Thiocoumarins. *J. Med. Chem.* **2010**, *53*, 335–344.
- (40) Supuran, C. T. How Many Carbonic Anhydrase Inhibition Mechanisms Exist? *J. Enzyme Inhib. Med. Chem.* **2016**, *31*, 345–360.
- (41) Lozzio, C.; Lozzio, B. Human Chronic Myelogenous Leukemia Cell-Line with Positive Philadelphia Chromosome. *Blood* **1975**, *45*, 321–334.
- (42) Alley, M. C.; Scudiero, D. A.; Monks, A.; Hursey, M. L.; Czerwinski, M. J.; Fine, D. L.; Abbott, B. J.; Mayo, J. G.; Shoemaker, R. H.; Boyd, M. R. Feasibility of Drug Screening with Panels of Human Tumor Cell Lines Using a Microculture Tetrazolium Assay. *Cancer Res.* **1988**, *48*, 589–601.
- (43) Teodori, E.; Dei, S.; Bartolucci, G.; Perrone, M. G.; Manetti, D.; Romanelli, M. N.; Contino, M.; Colabufo, N. A. Structure–Activity Relationship Studies on 6,7-Dimethoxy-2-Phenethyl-1,2,3,4-Tetrahydroisoquinoline Derivatives as Multidrug Resistance Reversers. *ChemMedChem* **2017**, *12*, 1369–1379.

- (44) Riganti, C.; Giampietro, R.; Kopecka, J.; Costamagna, C.; Abatematteo, F. S.; Contino, M.; Abate, C. MRP1-Collateral Sensitizers as a Novel Therapeutic Approach in Resistant Cancer Therapy: An In Vitro and in Vivo Study in Lung Resistant Tumor. *Int. J. Mol. Sci.* **2020**, *21*, 3333.
- (45) Waheed, A.; Sly, W. S. Carbonic Anhydrase XII Functions in Health and Disease. *Gene* **2017**, *623*, 33–40.
- (46) Kciuk, M.; Gielecińska, A.; Mujwar, S.; Mojzych, M.; Marciniak, B.; Drozda, R.; Kontek, R. Targeting Carbonic Anhydrase IX and XII Isoforms with Small Molecule Inhibitors and Monoclonal Antibodies. *J. Enzyme Inhib. Med. Chem.* **2022**, *37*, 1278–1298.
- (47) Han, R.; Yang, H.; Lu, L.; Lin, L. Tiliroside as a CAXII Inhibitor Suppresses Liver Cancer Development and Modulates E2Fs/Caspase-3 Axis. *Sci. Rep.* **2021**, *11*, No. 8626.
- (48) Giuntini, G.; Monaci, S.; Cau, Y.; Mori, M.; Naldini, A.; Carraro, F. Inhibition of Melanoma Cell Migration and Invasion Targeting the Hypoxic Tumor Associated CAXII. *Cancers* **2020**, *12*, 3018.
- (49) Gondi, G.; Mysliwicz, J.; Hulikova, A.; Jen, J. P.; Swietach, P.; Kremmer, E.; Zeidler, R. Antitumor Efficacy of a Monoclonal Antibody That Inhibits the Activity of Cancer-Associated Carbonic Anhydrase XII. *Cancer Res.* **2013**, *73*, 6494–6503.
- (50) von Neubeck, B.; Gondi, G.; Riganti, C.; Pan, C.; Parra Damas, A.; Scherb, H.; Ertürk, A.; Zeidler, R. An Inhibitory Antibody Targeting Carbonic Anhydrase XII Abrogates Chemoresistance and Significantly Reduces Lung Metastases in an Orthotopic Breast Cancer Model in Vivo. *Int. J. Cancer* **2018**, *143*, 2065–2075.
- (51) McDonald, P. C.; Swayampakula, M.; Dedhar, S. Coordinated Regulation of Metabolic Transporters and Migration/Invasion by Carbonic Anhydrase IX. *Metabolites* **2018**, *8*, 20.
- (52) Testa, C.; Papini, A. M.; Zeidler, R.; Vullo, D.; Carta, F.; Supuran, C. T.; Rovero, P. First Studies on Tumor Associated Carbonic Anhydrases IX and XII Monoclonal Antibodies Conjugated to Small Molecule Inhibitors. *J. Enzyme Inhib. Med. Chem.* **2022**, *37*, 592–596.
- (53) Vaeteewoottacharn, K.; Kariya, R.; Dana, P.; Fujikawa, S.; Matsuda, K.; Ohkuma, K.; Kudo, E.; Kraiklang, R.; Wongkham, C.; Wongkham, S.; Okada, S. Inhibition of Carbonic Anhydrase Potentiates Bevacizumab Treatment in Cholangiocarcinoma. *Tumor Biol.* **2016**, *37*, 9023–9035.
- (54) Tavares-Valente, D.; Sousa, B.; Schmitt, F.; Baltazar, F.; Queirós, O. Disruption of PH Dynamics Suppresses Proliferation and Potentiates Doxorubicin Cytotoxicity in Breast Cancer Cells. *Pharmaceutics* **2021**, *13*, 242.
- (55) Aänismaa, P.; Seelig, A. P-Glycoprotein Kinetics Measured in Plasma Membrane Vesicles and Living Cells. *Biochemistry* **2007**, *46*, 3394–3404.
- (56) Podolski-Renić, A.; Dinić, J.; Stanković, T.; Jovanović, M.; Ramović, A.; Pustenko, A.; Raivis, Ž.; Pešić, M. Sulfocoumarins, Specific Carbonic Anhydrase IX and XII Inhibitors, Interact with Cancer Multidrug Resistant Phenotype through PH Regulation and Reverse P-Glycoprotein Mediated Resistance. *Eur. J. Pharm. Sci.* **2019**, *138*, No. 105012.
- (57) Salaroglio, I. C.; Mujumdar, P.; Annovazzi, L.; Kopecka, J.; Mellai, M.; Schiffer, D.; Poulsen, S.-A.; Riganti, C. Carbonic Anhydrase XII Inhibitors Overcome P-Glycoprotein-Mediated Resistance to Temozolomide in Glioblastoma. *Mol. Cancer Ther.* **2018**, *17*, 2598–2609.
- (58) Sun, R.; Kim, A. H. The Multifaceted Mechanisms of Malignant Glioblastoma Progression and Clinical Implications. *Cancer Metastasis Rev.* **2022**, DOI: 10.1007/s10555-022-10051-5.
- (59) Mao, X.; Wei, X.; Xu, T.; Li, T.; Liu, K. Research Progress in Breast Cancer Stem Cells: Characterization and Future Perspectives. *Am. J. Cancer Res.* **2022**, *12*, 3208–3222.
- (60) Ju, F.; Atyah, M. M.; Horstmann, N.; Gul, S.; Vago, R.; Bruns, C. J.; Zhao, Y.; Dong, Q.-Z.; Ren, N. Characteristics of the Cancer Stem Cell Niche and Therapeutic Strategies. *Stem Cell Res. Ther.* **2022**, *13*, No. 233.
- (61) Belisario, D. C.; Kopecka, J.; Pasino, M.; Akman, M.; De Smaele, E.; Donadelli, M.; Riganti, C. Hypoxia Dictates Metabolic Rewiring of Tumors: Implications for Chemoresistance. *Cells* **2020**, *9*, 2598.
- (62) Kopecka, J.; Salaroglio, I. C.; Perez-ruiz, E.; Sarmiento-ribeiro, A. B.; Saponara, S.; Las, J.; De; Riganti, C. Hypoxia as a Driver of Resistance to Immunotherapy. *Drug Resist. Updates* **2021**, *59*, No. 100787.
- (63) Salaroglio, I. C.; Belisario, D. C.; Akman, M.; La Vecchia, S.; Godel, M.; Anobile, D. P.; Ortone, G.; Digiovanni, S.; Fontana, S.; Costamagna, C.; Rubinstein, M.; Kopecka, J.; Riganti, C. Mitochondrial ROS Drive Resistance to Chemotherapy and Immune-killing in Hypoxic Non-small Cell Lung Cancer. *J. Exp. Clin. Cancer Res.* **2022**, *41*, No. 243.
- (64) Marshall, A. G.; Hendrickson, C. L. High-Resolution Mass Spectrometers. *Annu. Rev. Anal. Chem.* **2008**, *1*, 579–599.
- (65) Köhler, K.; Hillebrecht, A.; Schulze Wischeler, J.; Innocenti, A.; Heine, A.; Supuran, C. T.; Klebe, G. Saccharin Inhibits Carbonic Anhydrases: Possible Explanation for Its Unpleasant Metallic Aftertaste. *Angew. Chem., Int. Ed.* **2007**, *46*, 7697–7699.
- (66) Tars, K.; Vullo, D.; Kazaks, A.; Leitans, J.; Lends, A.; Grandane, A.; Zalubovskis, R.; Scozzafava, A.; Supuran, C. T. Sulfocoumarins (1,2-Benzoxathiine-2,2-Dioxides): A Class of Potent and Isoform-Selective Inhibitors of Tumor-Associated Carbonic Anhydrases. *J. Med. Chem.* **2013**, *56*, 293–300.
- (67) Riganti, C.; Miraglia, E.; Viarisio, D.; Costamagna, C.; Pescarmona, G.; Ghigo, D.; Bosia, A. Nitric Oxide Reverts the Resistance to Doxorubicin in Human Colon Cancer Cells by Inhibiting the Drug Efflux. *Cancer Res.* **2005**, *65*, 516–525.
- (68) Miraglia, E.; Viarisio, D.; Riganti, C.; Costamagna, C.; Ghigo, D.; Bosia, A. Na⁺/H⁺ Exchanger Activity Is Increased in Doxorubicin-Resistant Human Colon Cancer Cells and Its Modulation Modifies the Sensitivity of the Cells to Doxorubicin. *Int. J. Cancer* **2005**, *115*, 924–929.
- (69) Kopecka, J.; Salzano, G.; Campia, I.; Lusa, S.; Ghigo, D.; De Rosa, G.; Riganti, C. Insights in the Chemical Components of Liposomes Responsible for P-Glycoprotein Inhibition. *Nanomed. Nanotechnol. Biol. Med.* **2014**, *10*, 77–87.

Supporting information

New dual P-glycoprotein (P-gp) and human carbonic anhydrase XII (hCA XII) inhibitors as multidrug resistance (MDR) reversers in cancer cells

Laura Braconi,[§] Elisabetta Teodori,^{*§} Chiara Riganti,[‡] Marcella Coronello,[†] Alessio Nocentini,[§] Gianluca Bartolucci,[§] Marco Pallecchi,[§] Marialessandra Contino,[§] Dina Manetti,[§] Maria Novella Romanelli,[§] Claudiu T. Supuran,[§] Silvia Dei[§]

[§]Department of Neuroscience, Psychology, Drug Research and Child Health - Section of Pharmaceutical and Nutraceutical Sciences, University of Florence, via Ugo Schiff 6, 50019 Sesto Fiorentino (FI), Italy.

[‡]Department of Oncology, University of Turin, Via Santena 5/bis, 10126 Torino, Italy.

[†]Department of Health Sciences - Clinical Pharmacology and Oncology Section, University of Florence, Viale Pieraccini 6, 50139 Firenze, Italy

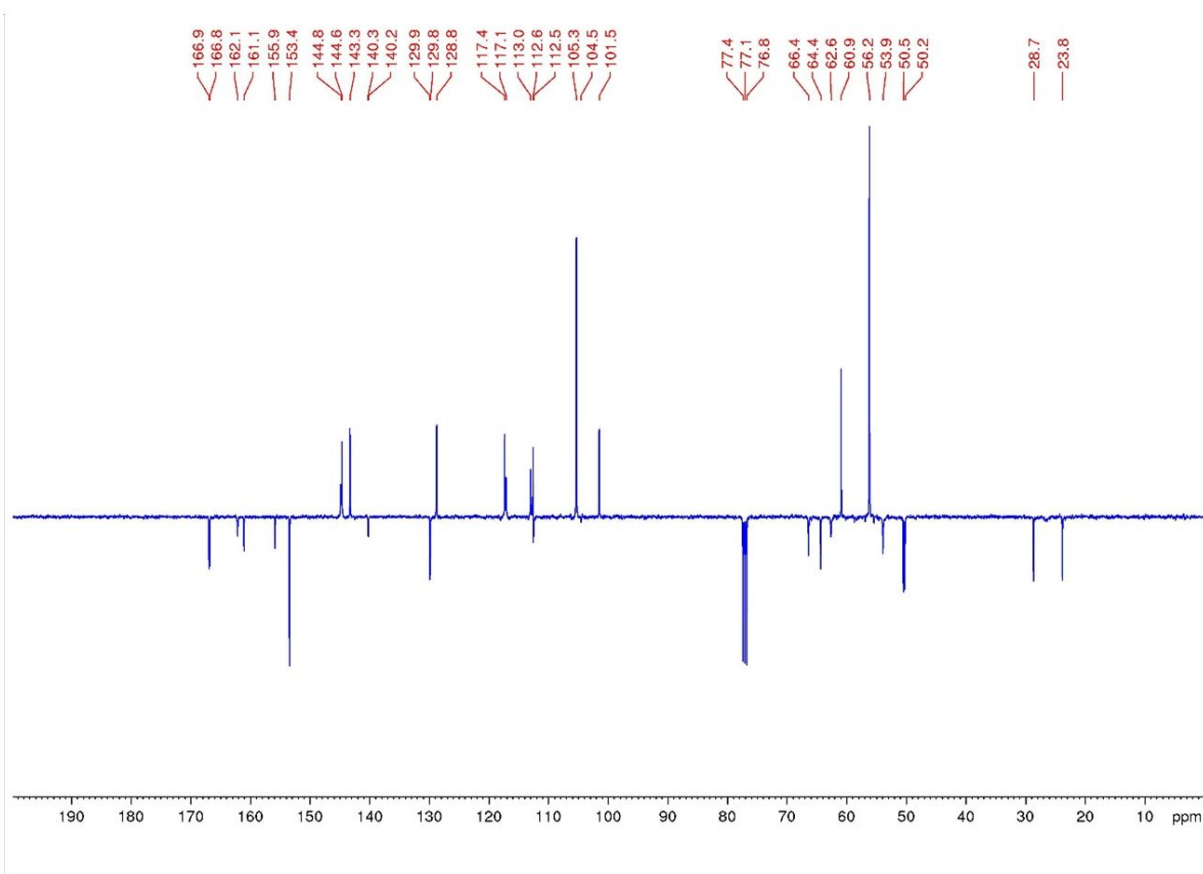
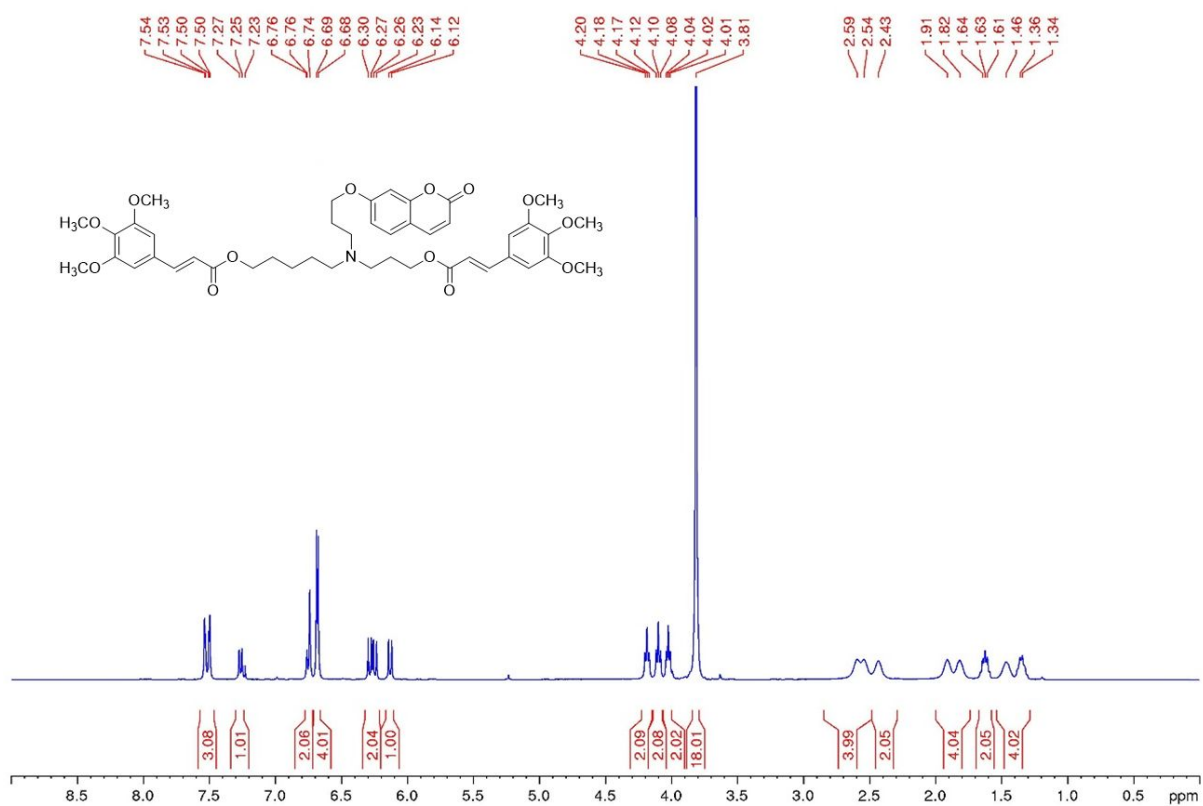
[§]Department of Pharmacy - Drug Sciences, University of Bari "A. Moro", via Orabona 4, 70125, Bari, Italy.

Corresponding Author: Elisabetta Teodori: e-mail, elisabetta.teodori@unifi.it

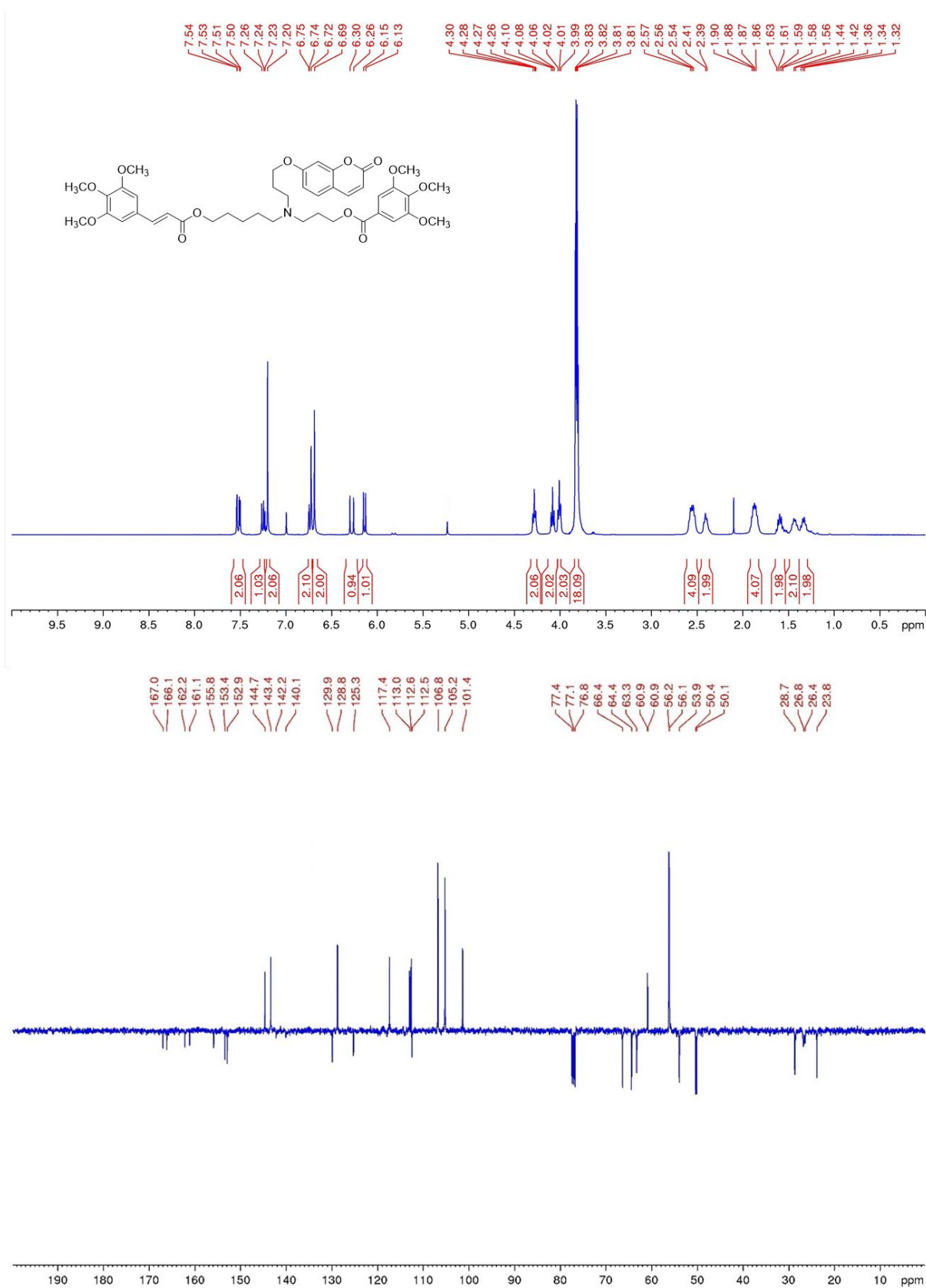
Table of Contents

- ¹ H-NMR (400 MHz), ¹³ C-APT- NMR (100 MHz) spectra of compounds 1-27	S2
- Chemical stability data of compounds 1-27 and reference compound KEE	S29
- Analytical method used to determine purity and chromatographic profiles of HPLC-DAD analysis of representative compounds (2, 3, 5, 6, 8, 9, 13-17)	S45
- UV spectra of compounds 2, 3, 5, 6, 8, 9, 13-17	S51
- Expression levels of P-gp and hCA XII in sensitive HT29 and A549 human cancer cell lines, in resistant wild-type HT29/DOX and A549/DOX cells, and in their P-gp or hCA XII knock-out (KO) counterparts	S54
- Cytotoxicity on K562/DOX cells of compounds 1-27	S55
- Cytotoxicity on HT29, HT29/DOX, A549, A549/DOX cell lines of selected compounds 1, 2, 4, 5, 10, 11, 13, 14, 19, 20, 22, 23	S56
- Reduction of viability EpiCoc and BEARS-2B cell lines on data of selected compounds 1, 2, 4, 5, 10, 11, 13, 14, 19, 20, 22, 23	S57

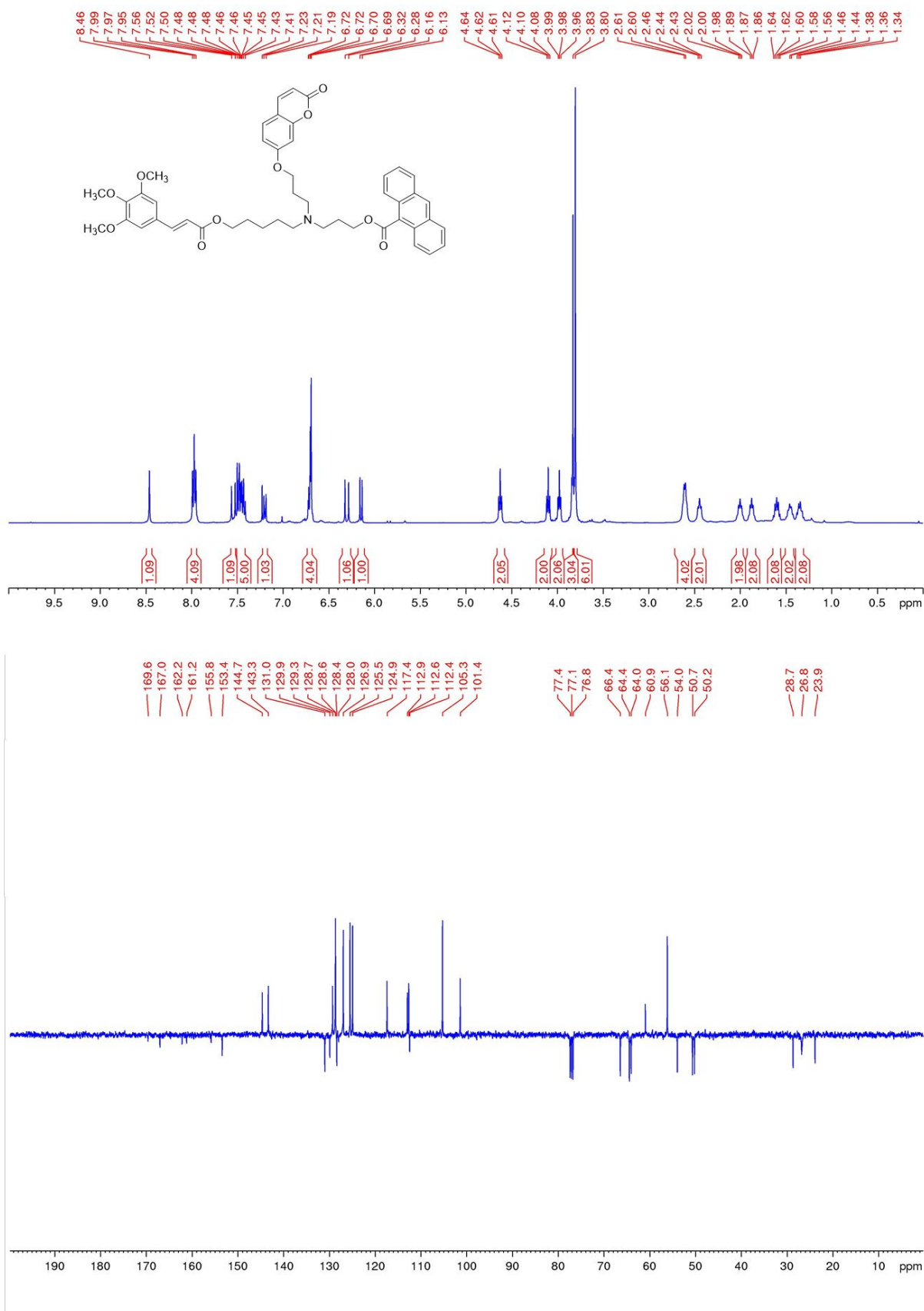
^1H -NMR and ^{13}C -APT-NMR spectra of compound **1**



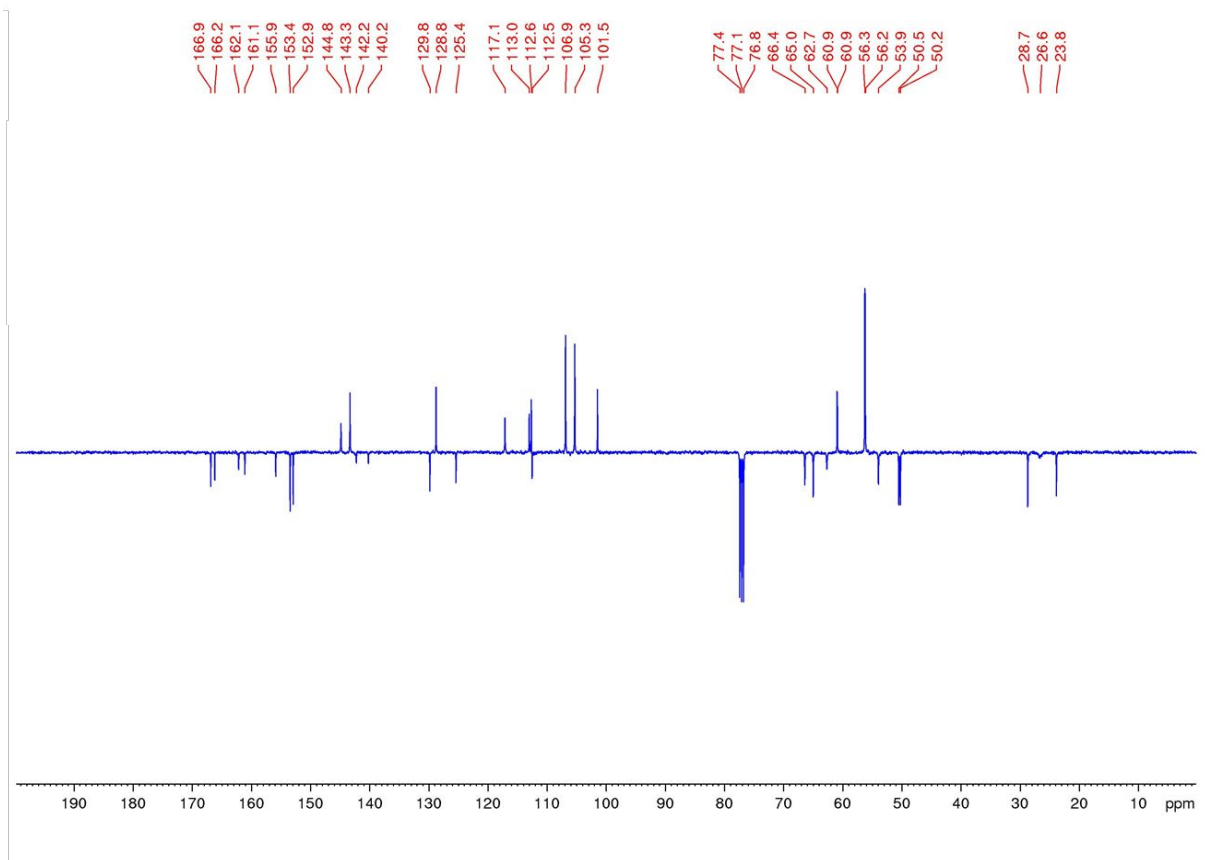
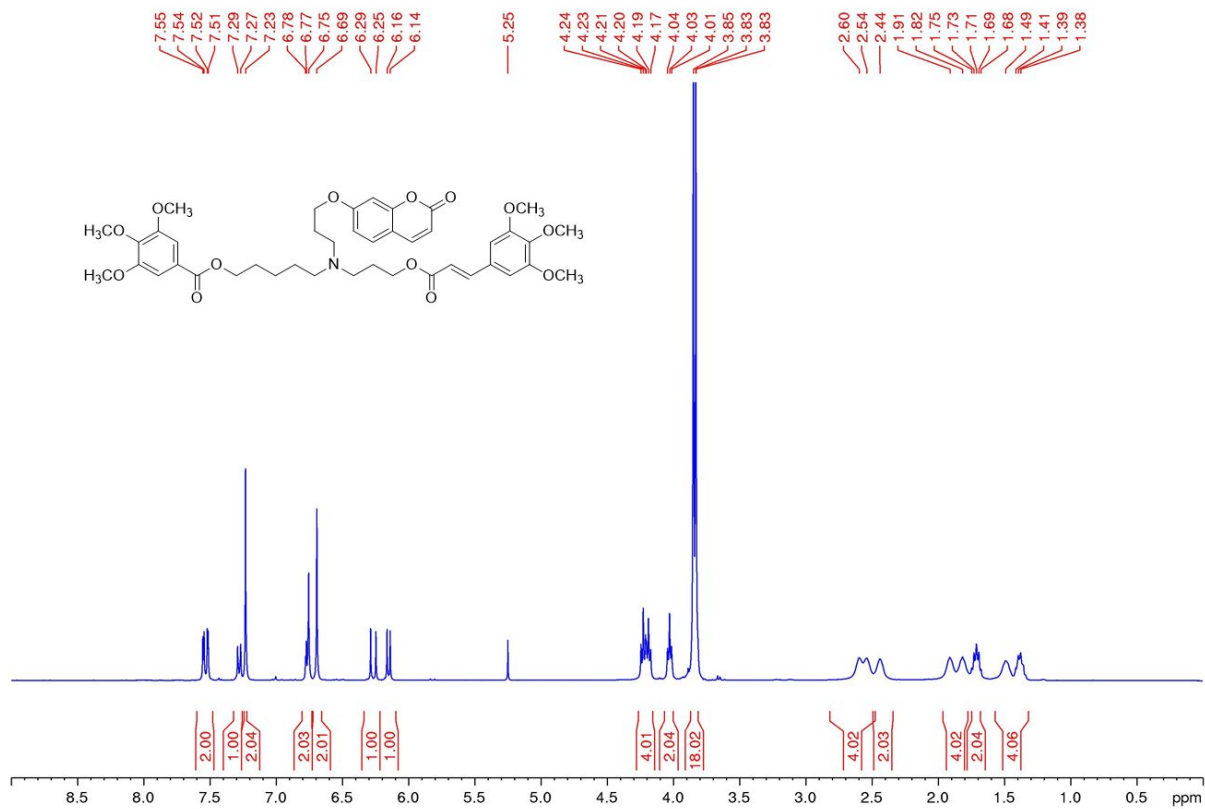
^1H -NMR and ^{13}C -APT-NMR spectra of compound 2



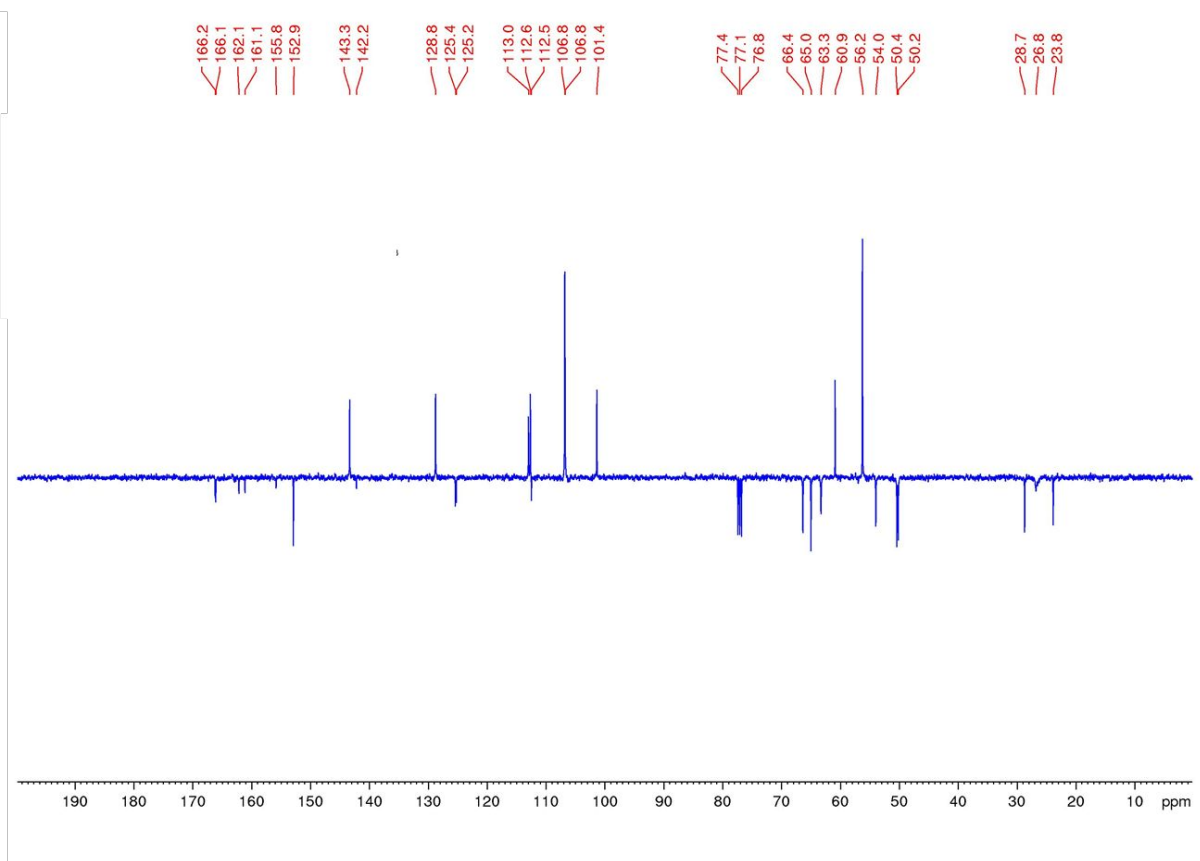
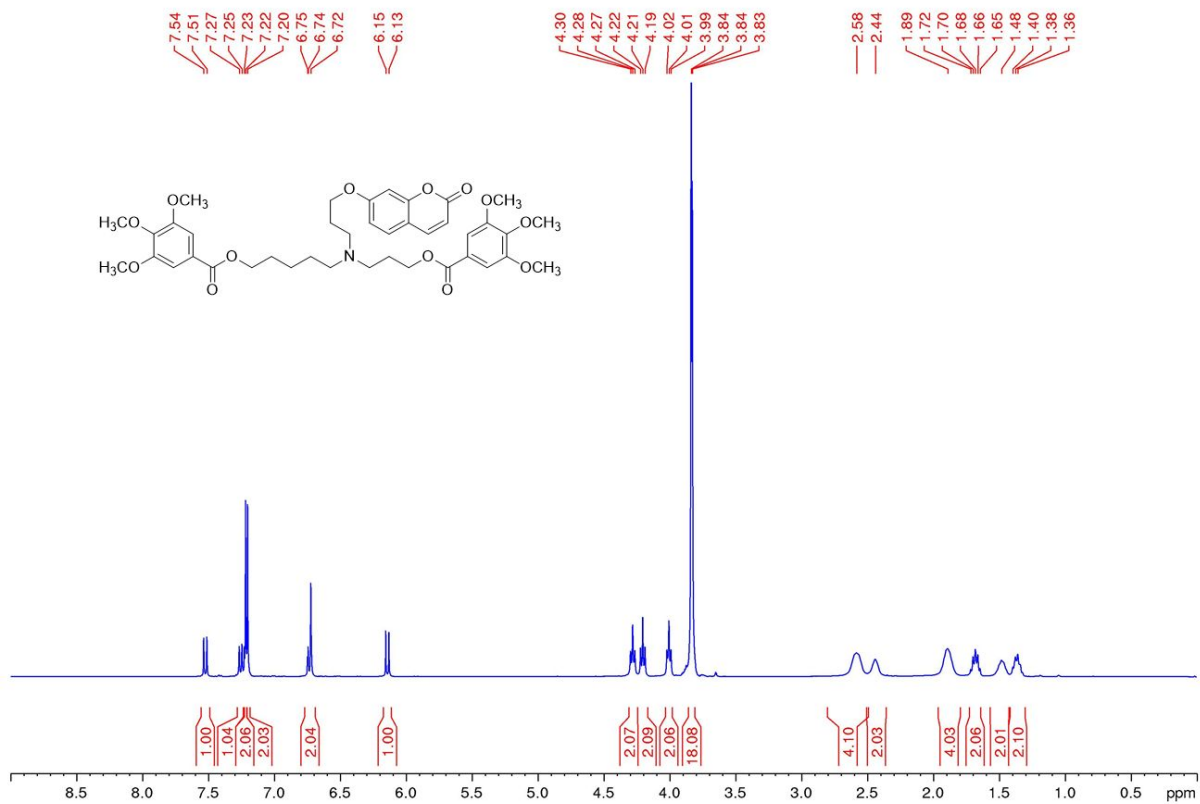
$^1\text{H-NMR}$ and $^{13}\text{C-APT-NMR}$ spectra of compound **3**



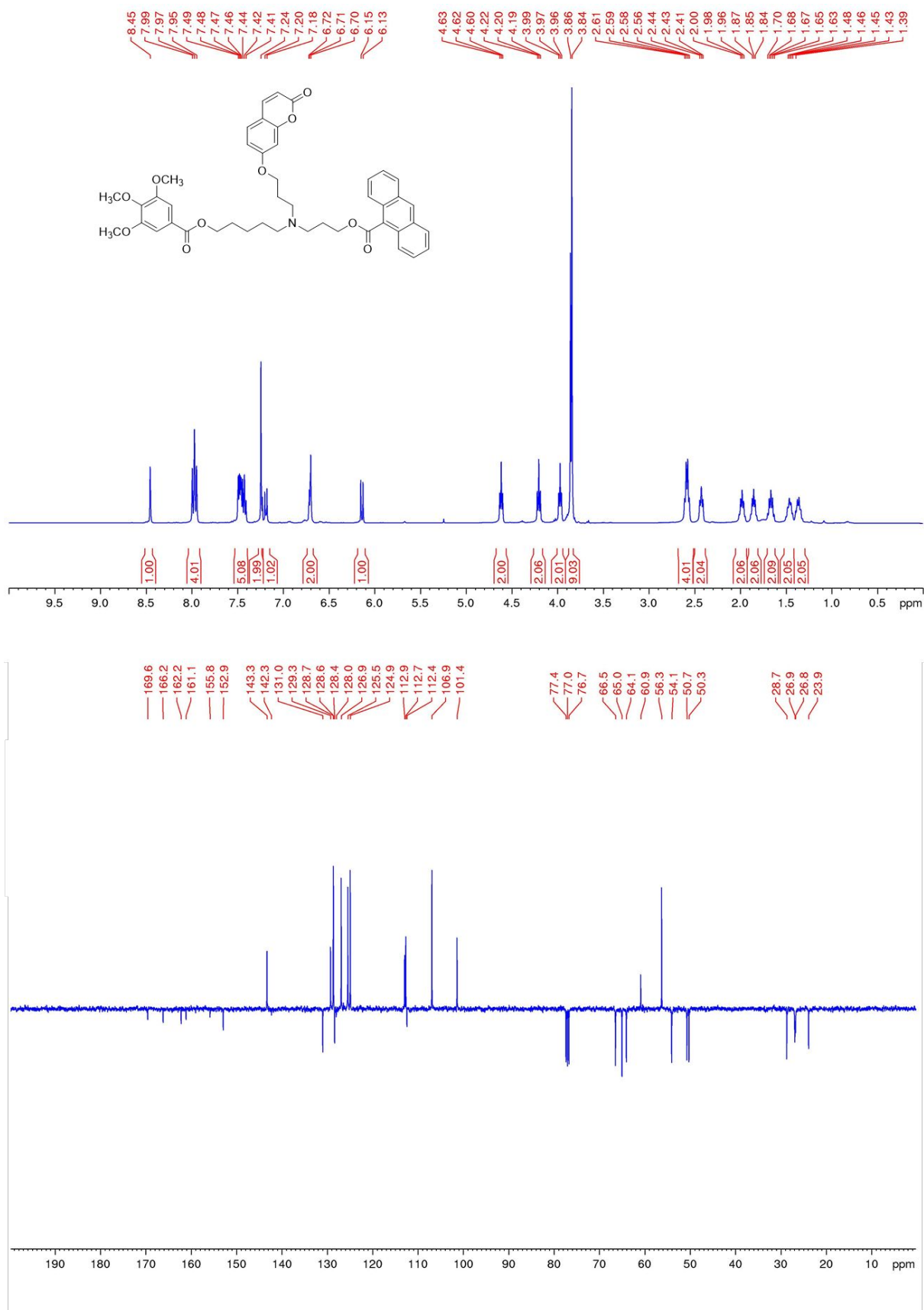
^1H -NMR and ^{13}C -APT-NMR spectra of compound 4



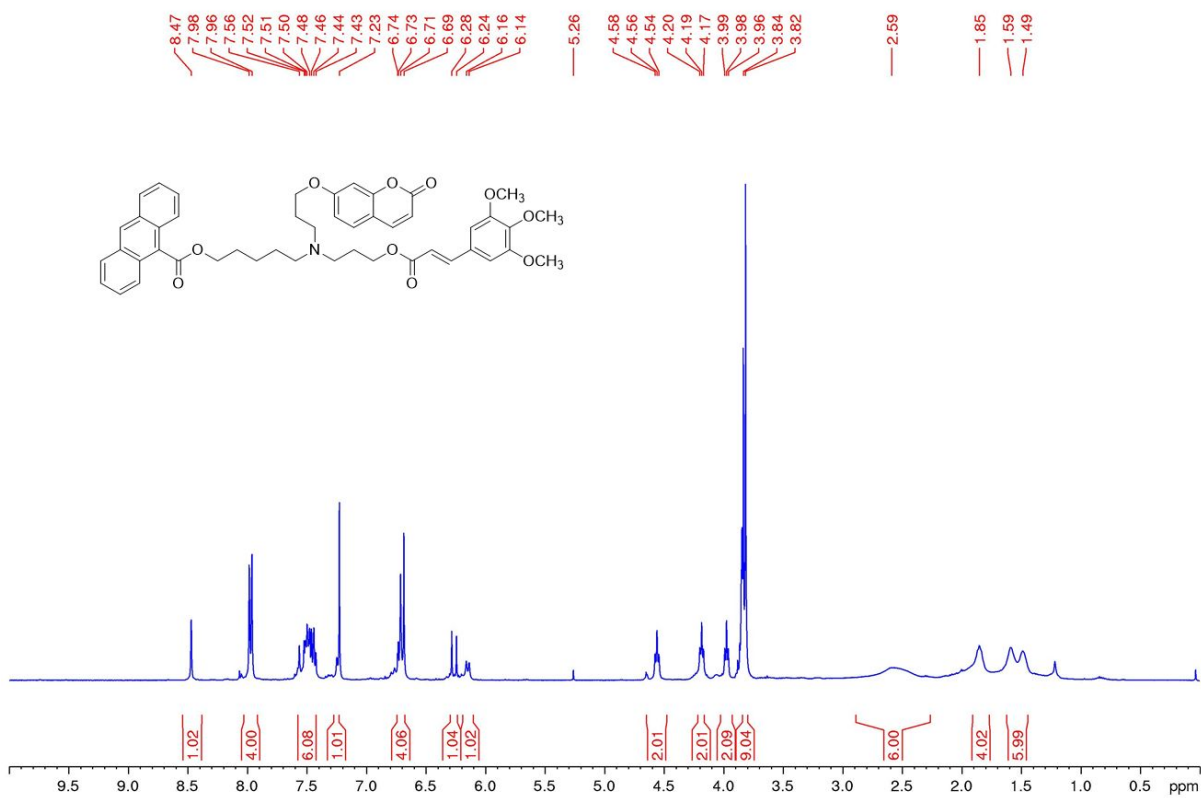
¹H-NMR and ¹³C-APT-NMR spectra of compound 5



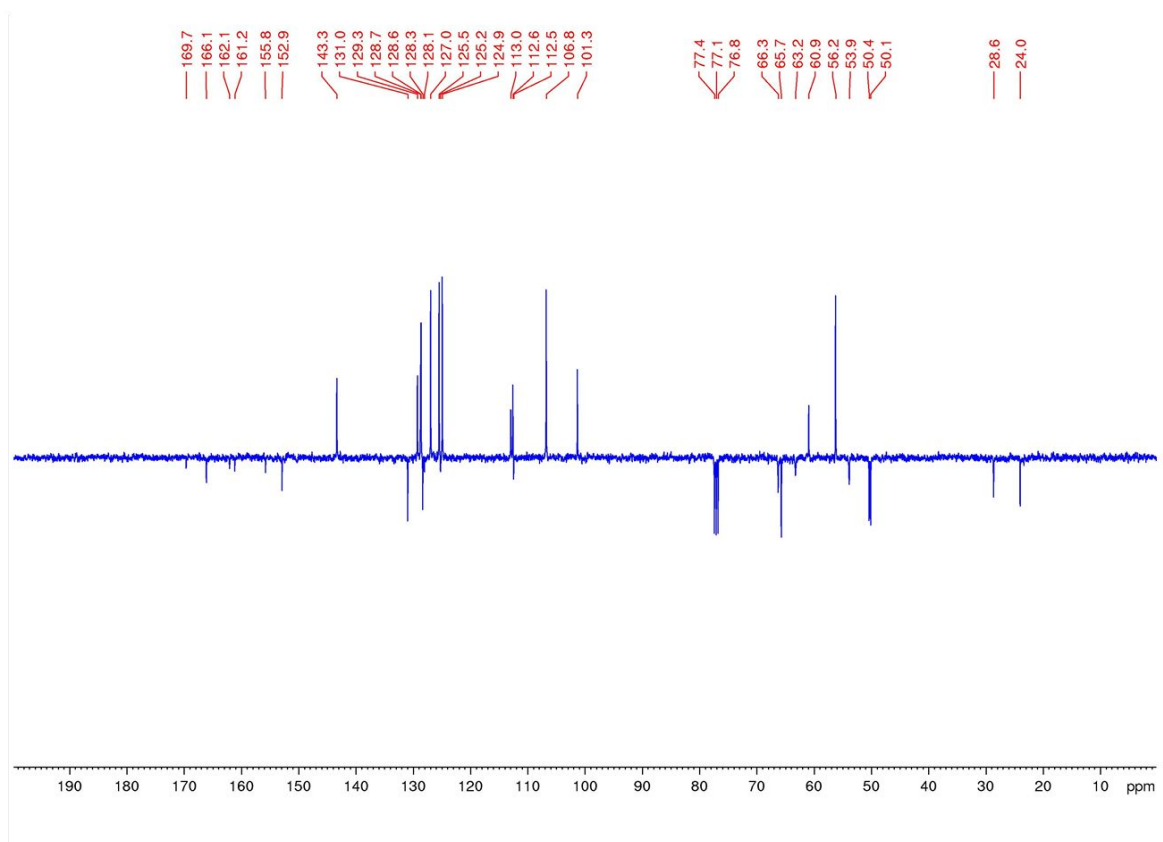
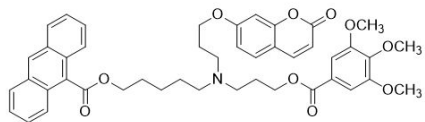
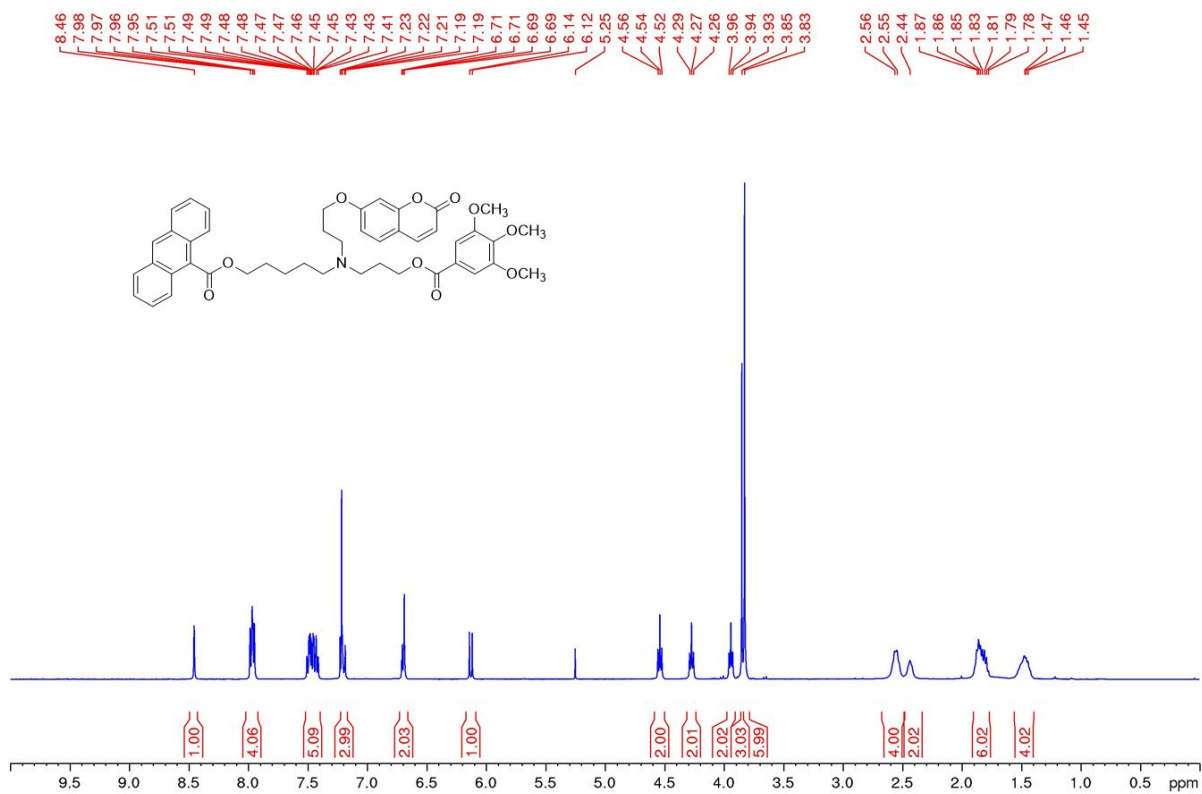
$^1\text{H-NMR}$ and $^{13}\text{C-NMR}$ spectra of compound **6**



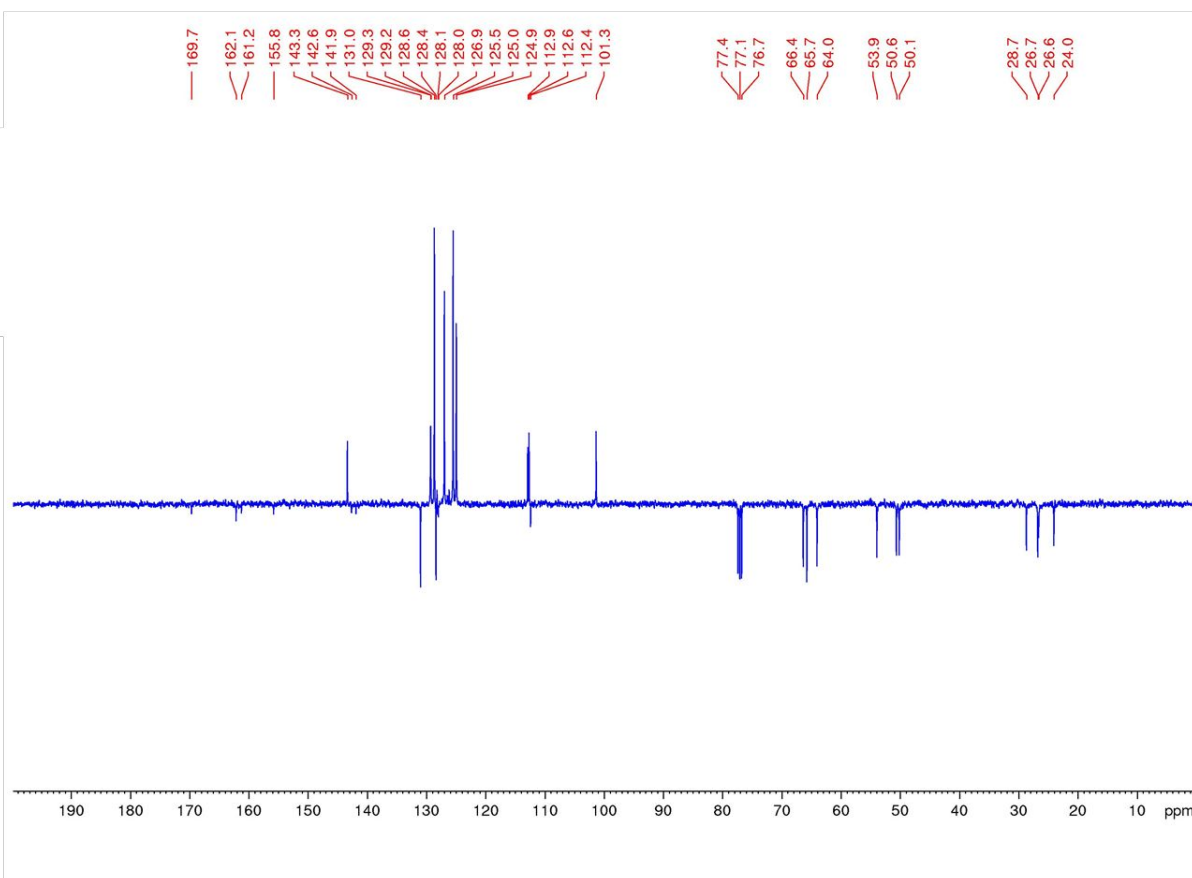
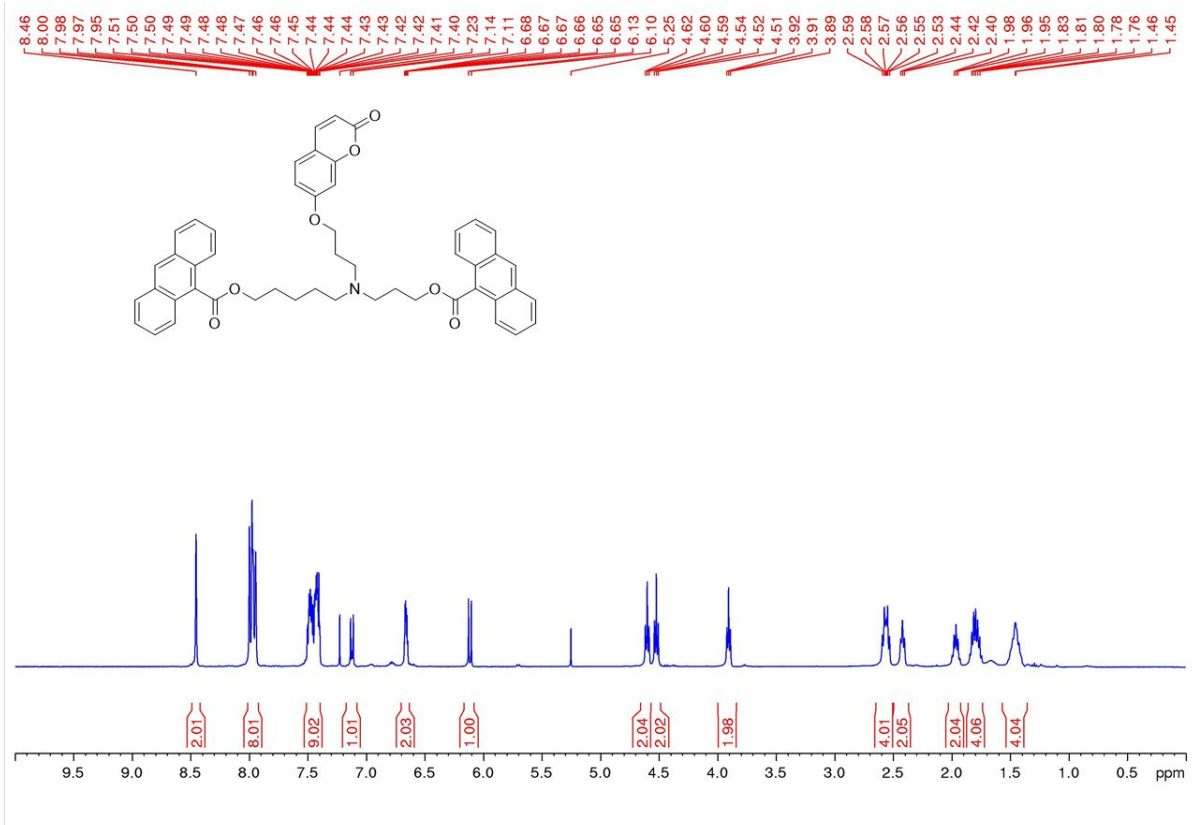
¹H-NMR spectrum of compound 7



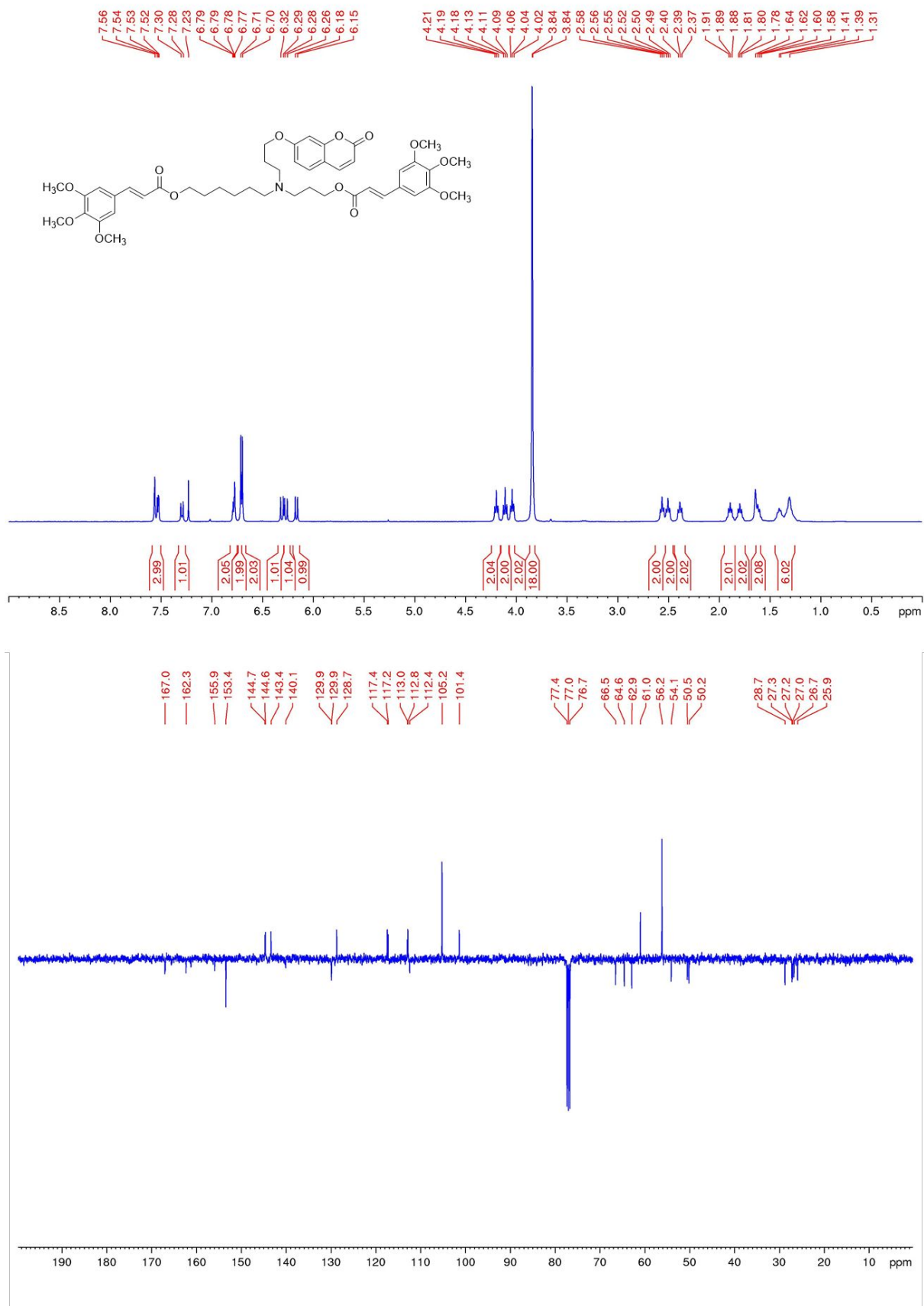
$^1\text{H-NMR}$ and $^{13}\text{C-APT-NMR}$ spectra of compound **8**



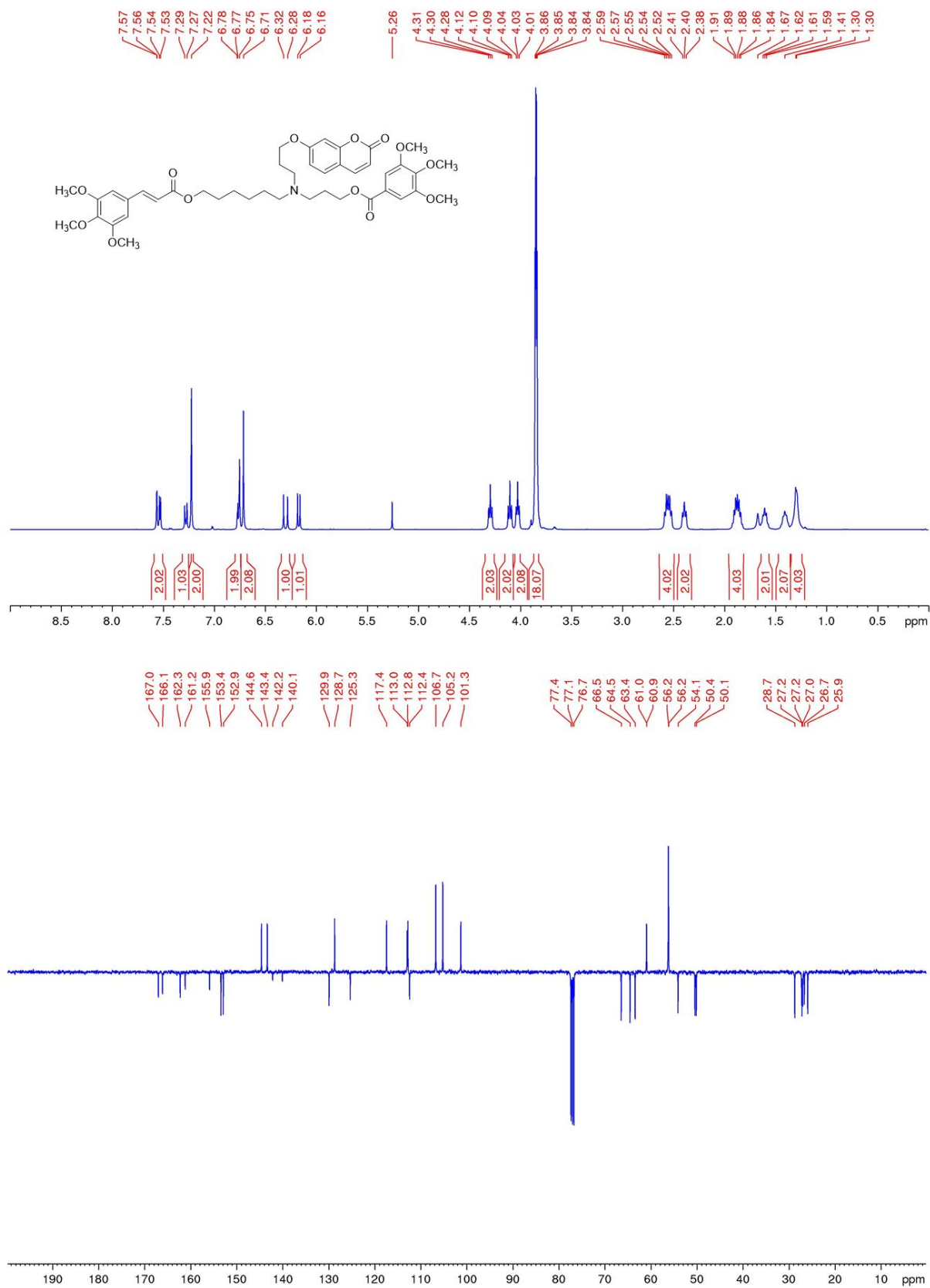
^1H -NMR and ^{13}C -APT-NMR spectra of compound **9**



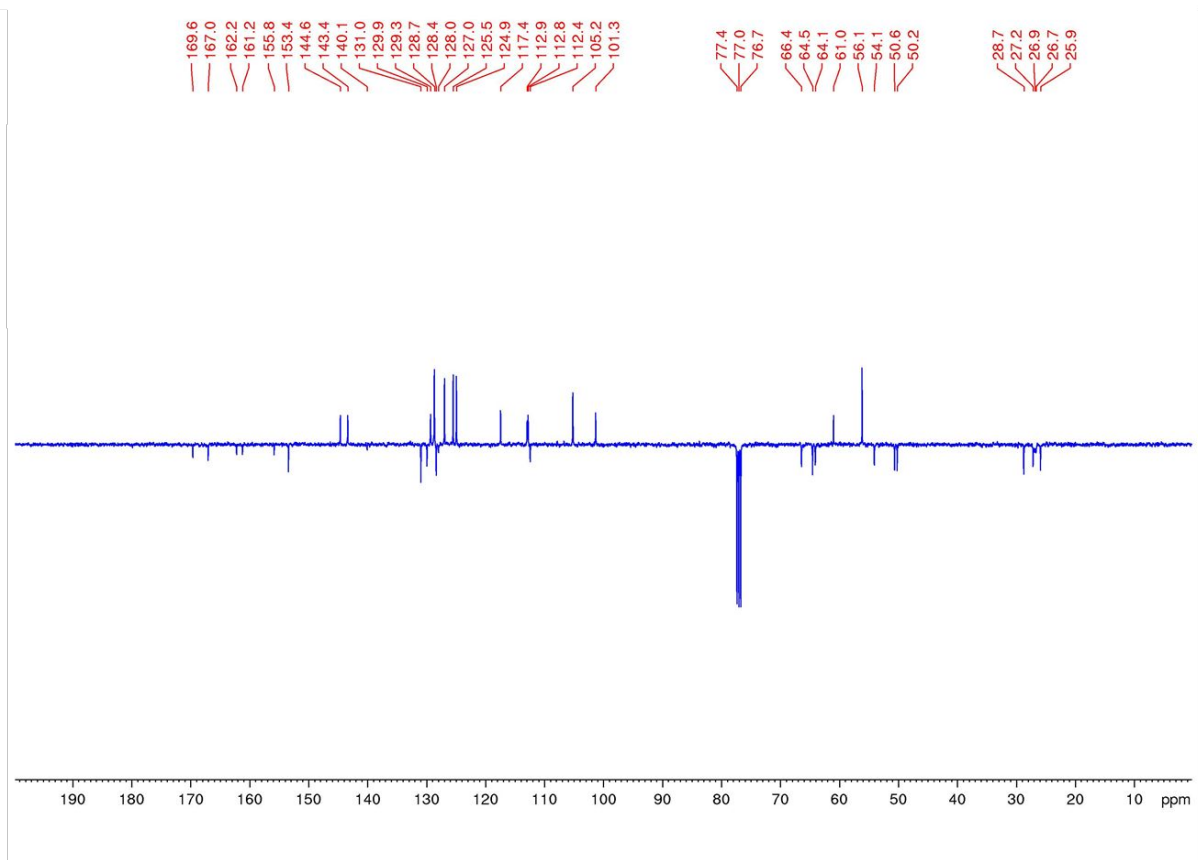
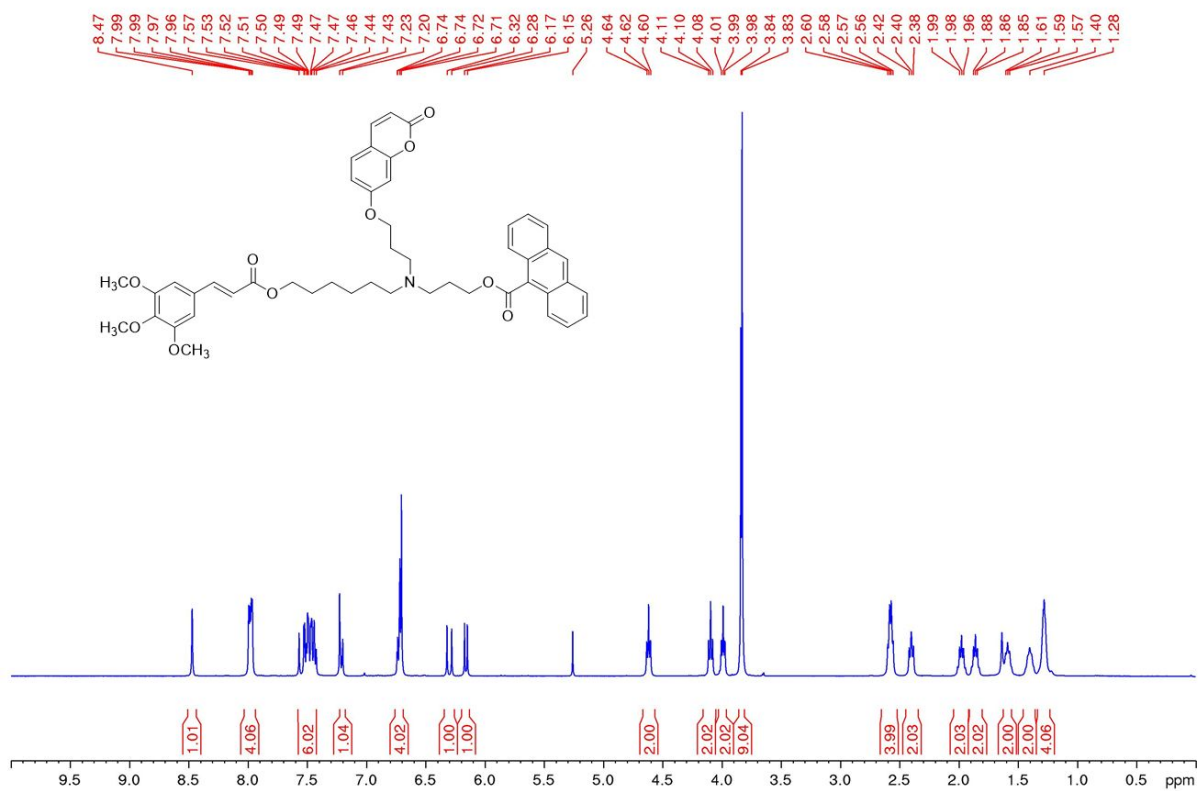
^1H -NMR and ^{13}C -APT-NMR spectra of compound **10**



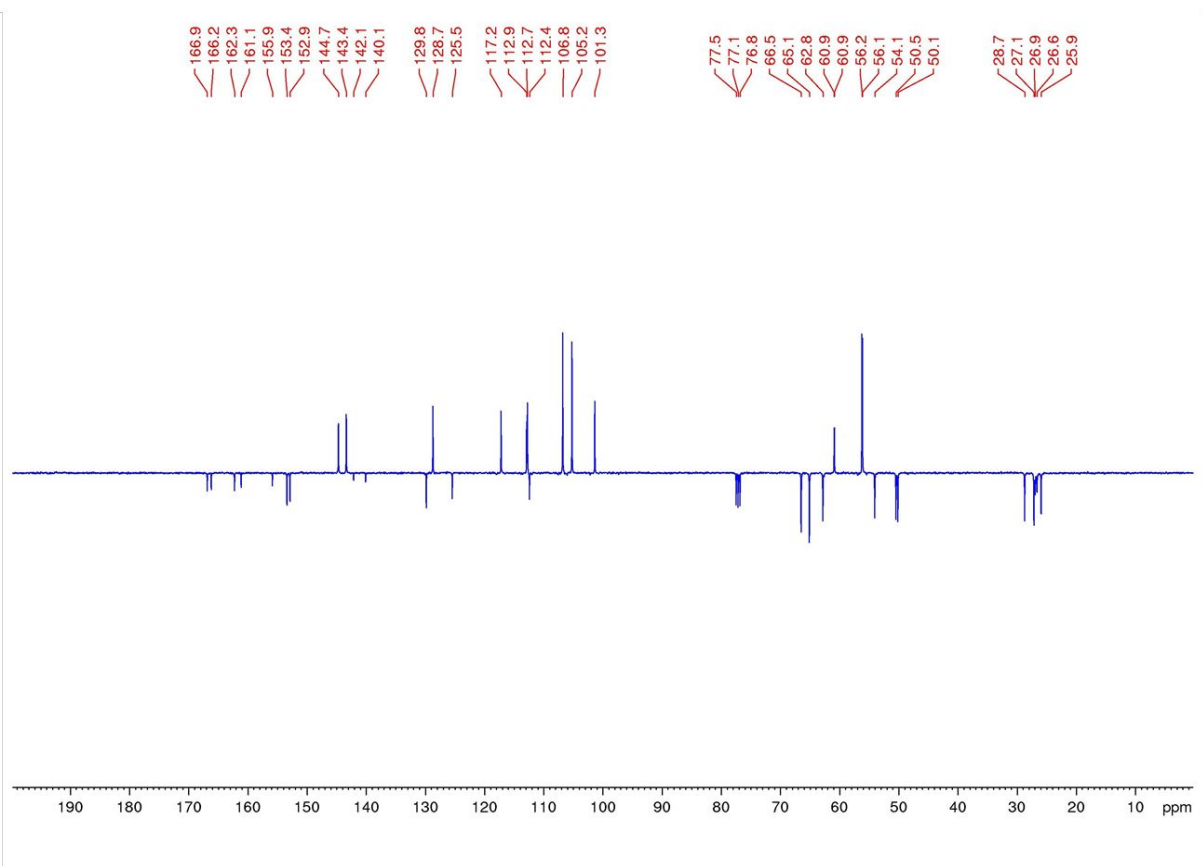
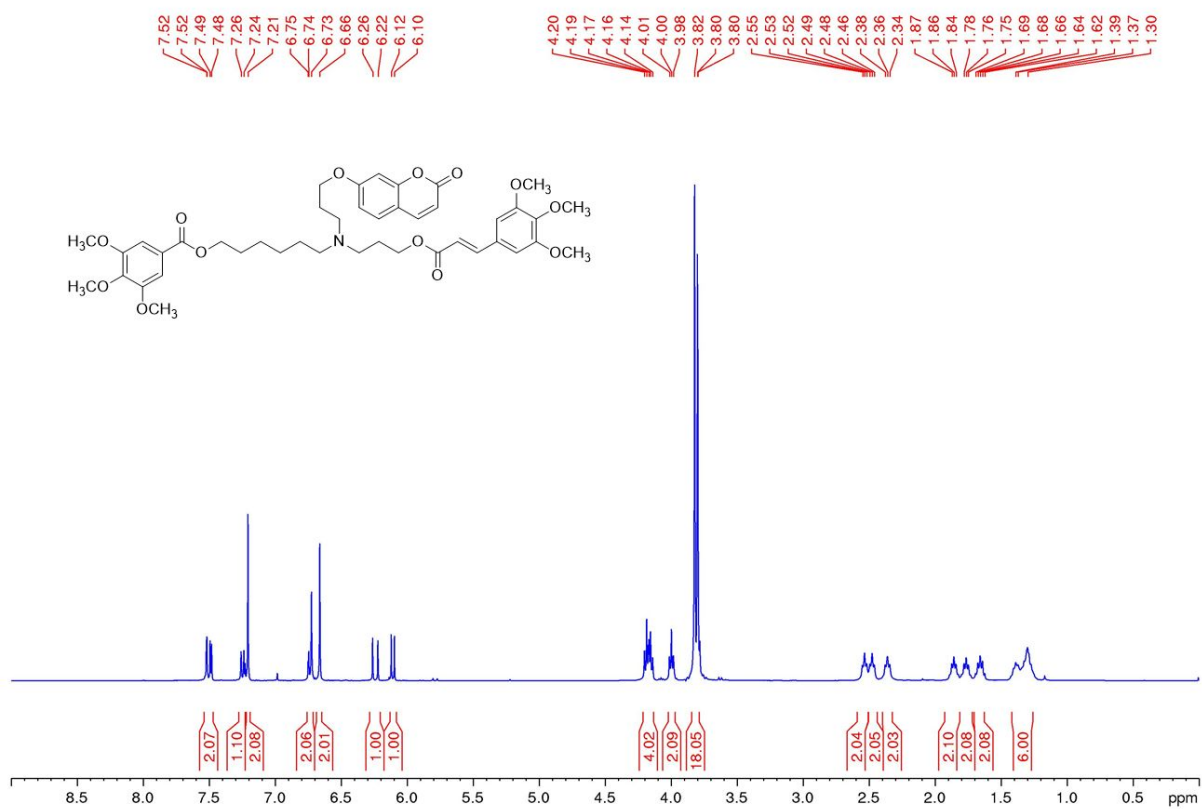
^1H -NMR and ^{13}C -APT-NMR spectra of compound **11**



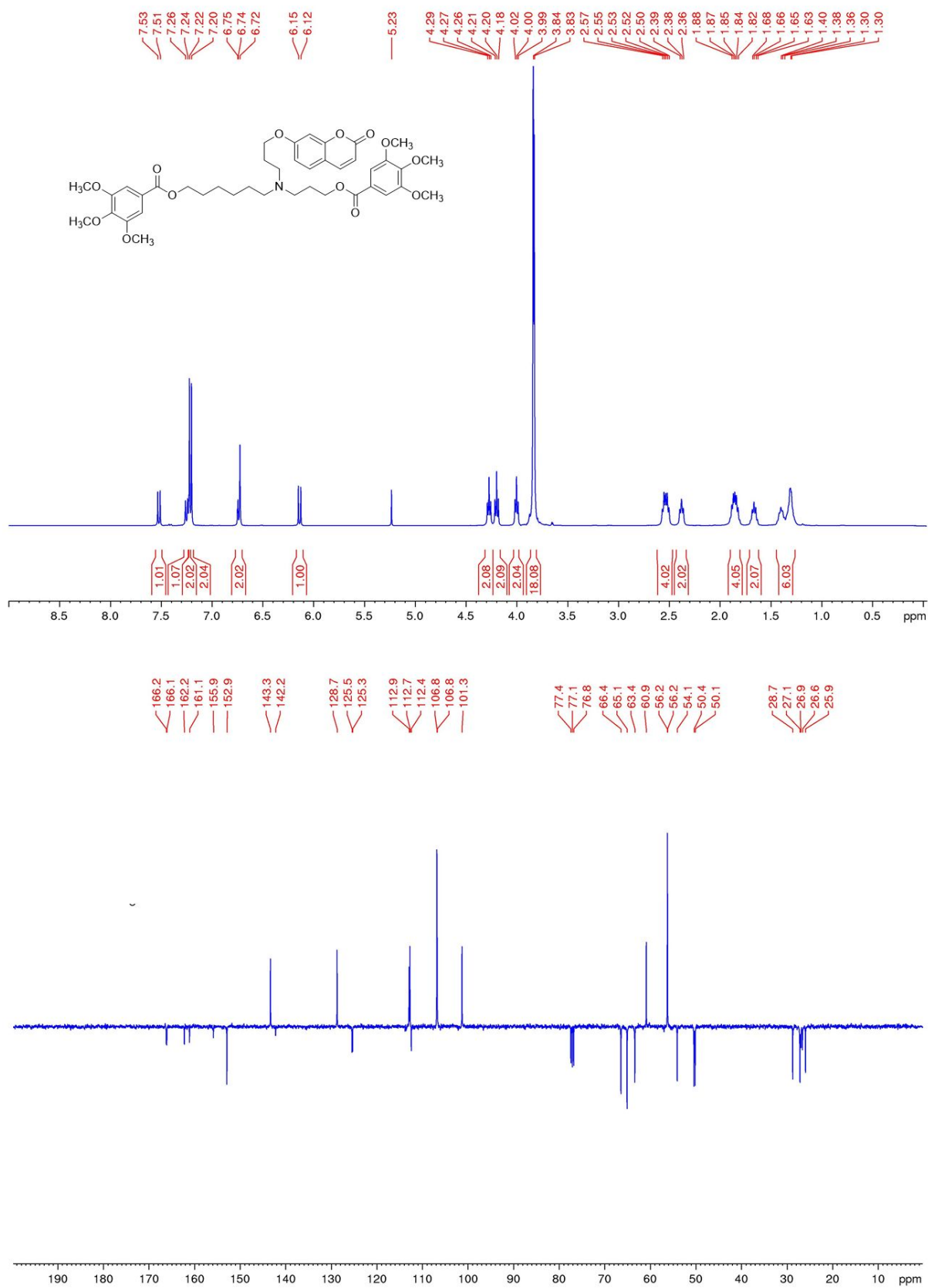
$^1\text{H-NMR}$ and $^{13}\text{C-APT-NMR}$ spectra of compound **12**



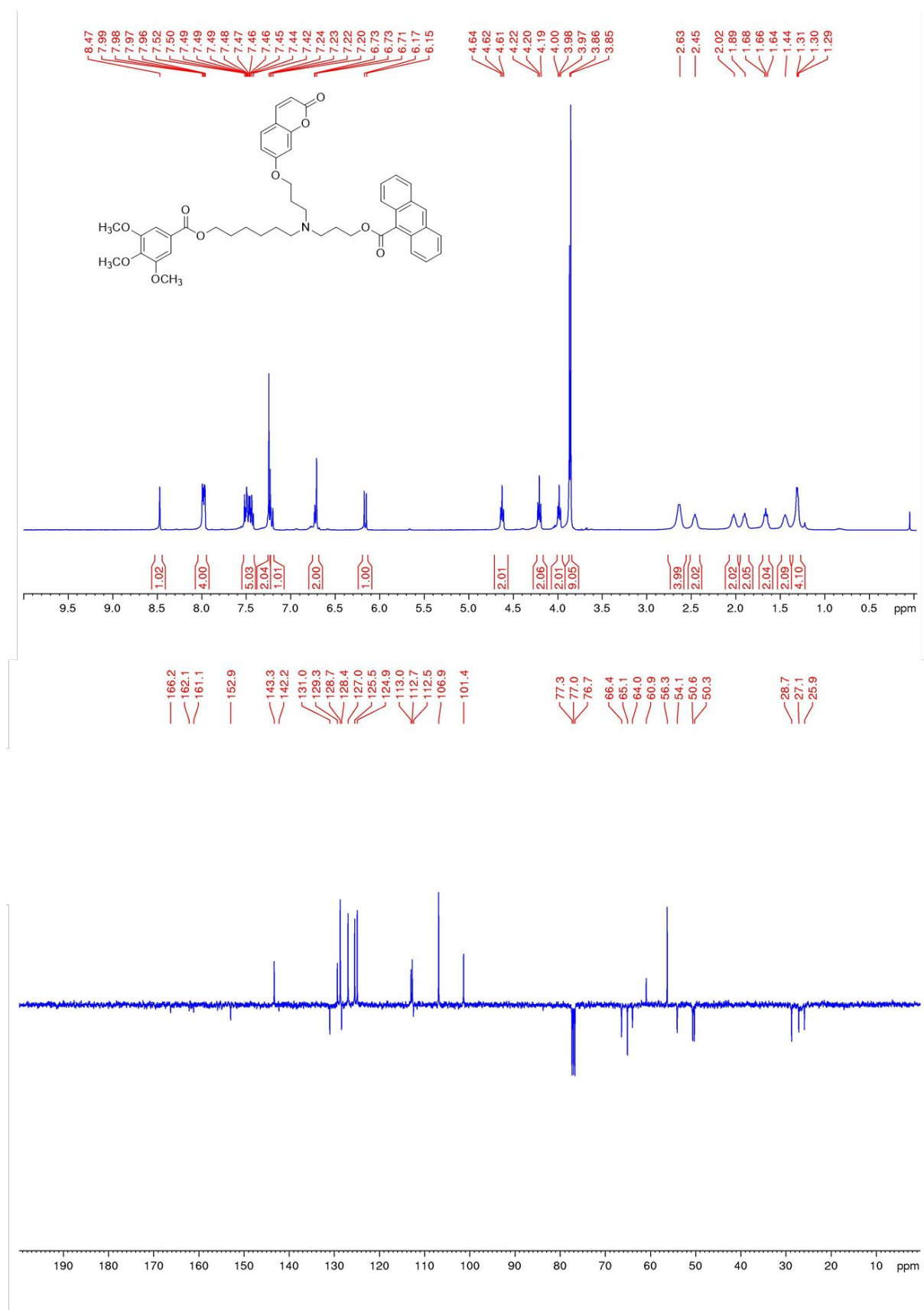
^1H -NMR and ^{13}C -APT-NMR spectra of compound **13**



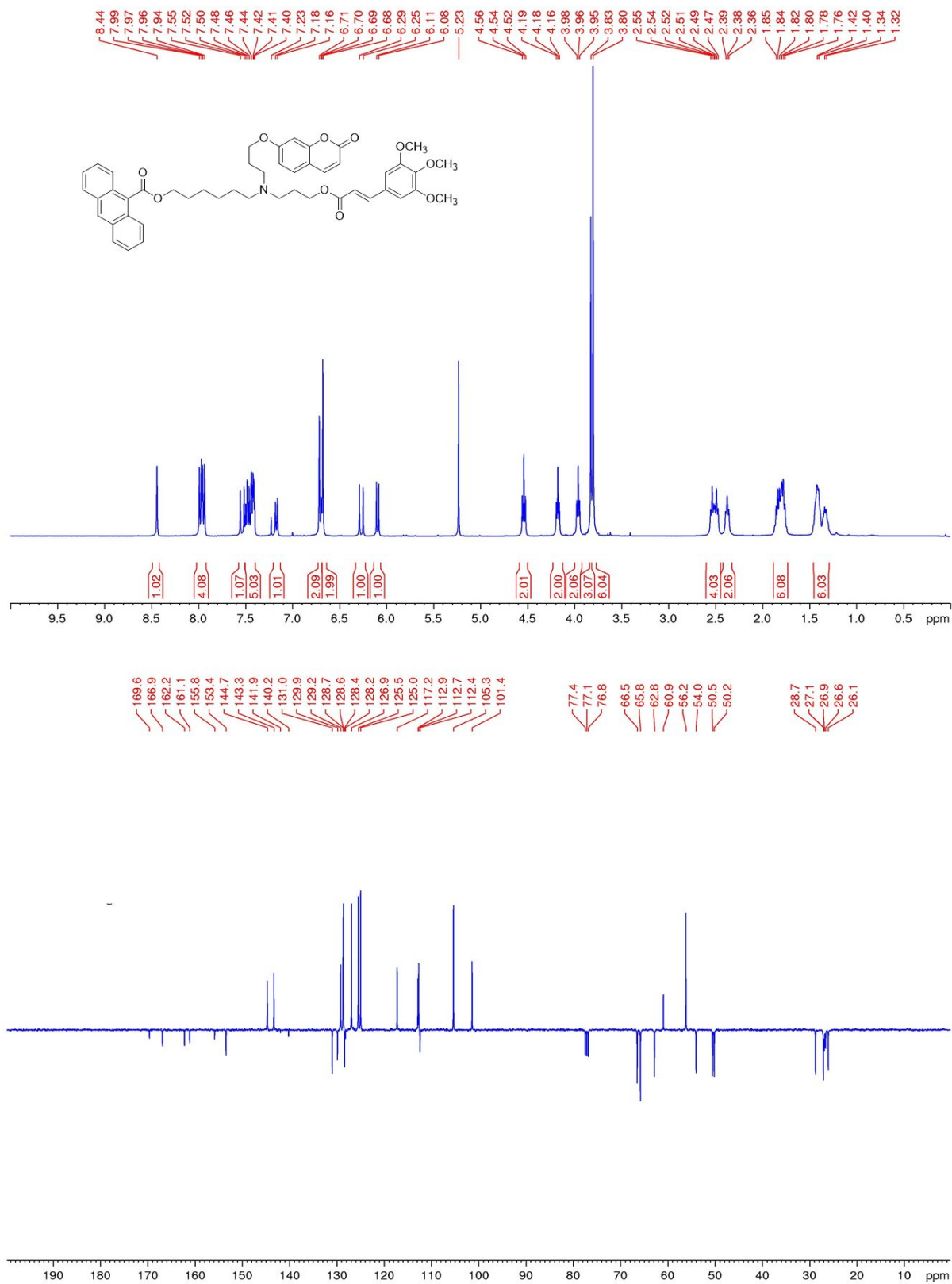
¹H-NMR and ¹³C-APT-NMR spectra of compound **14**



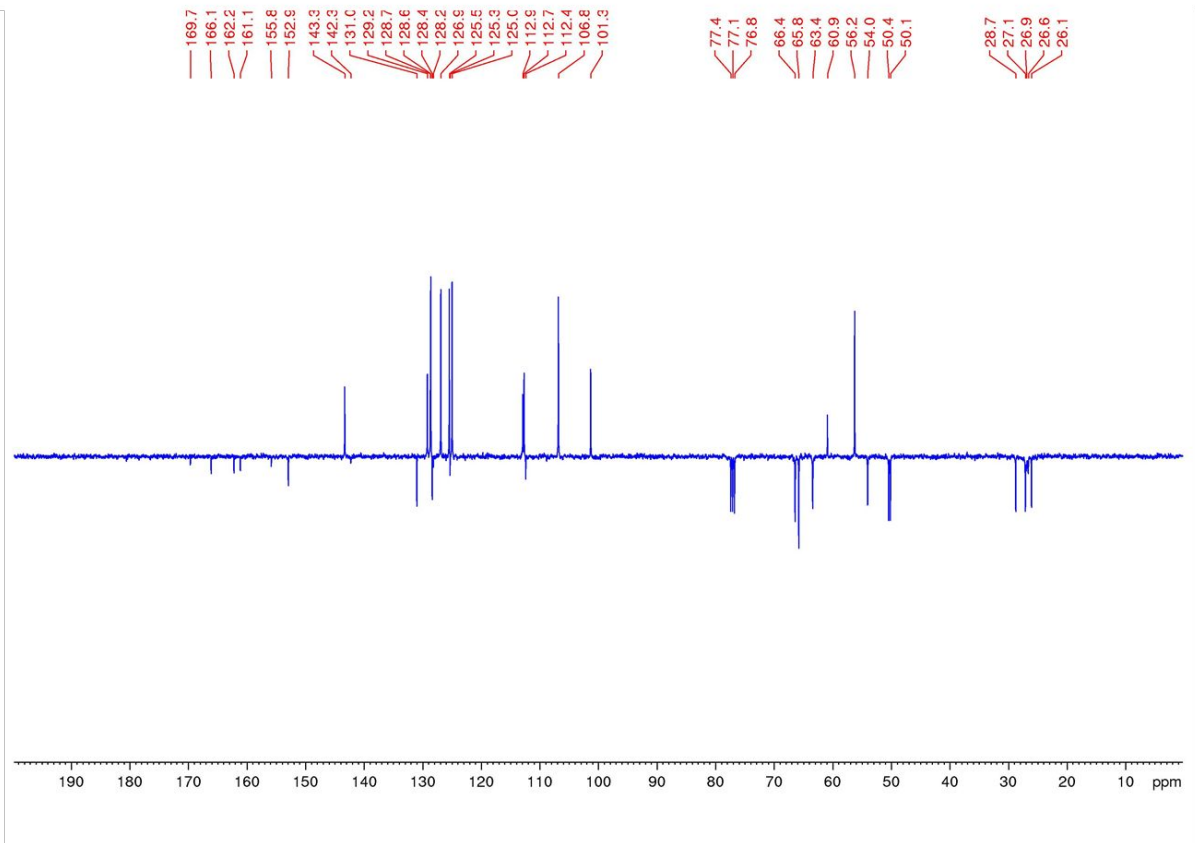
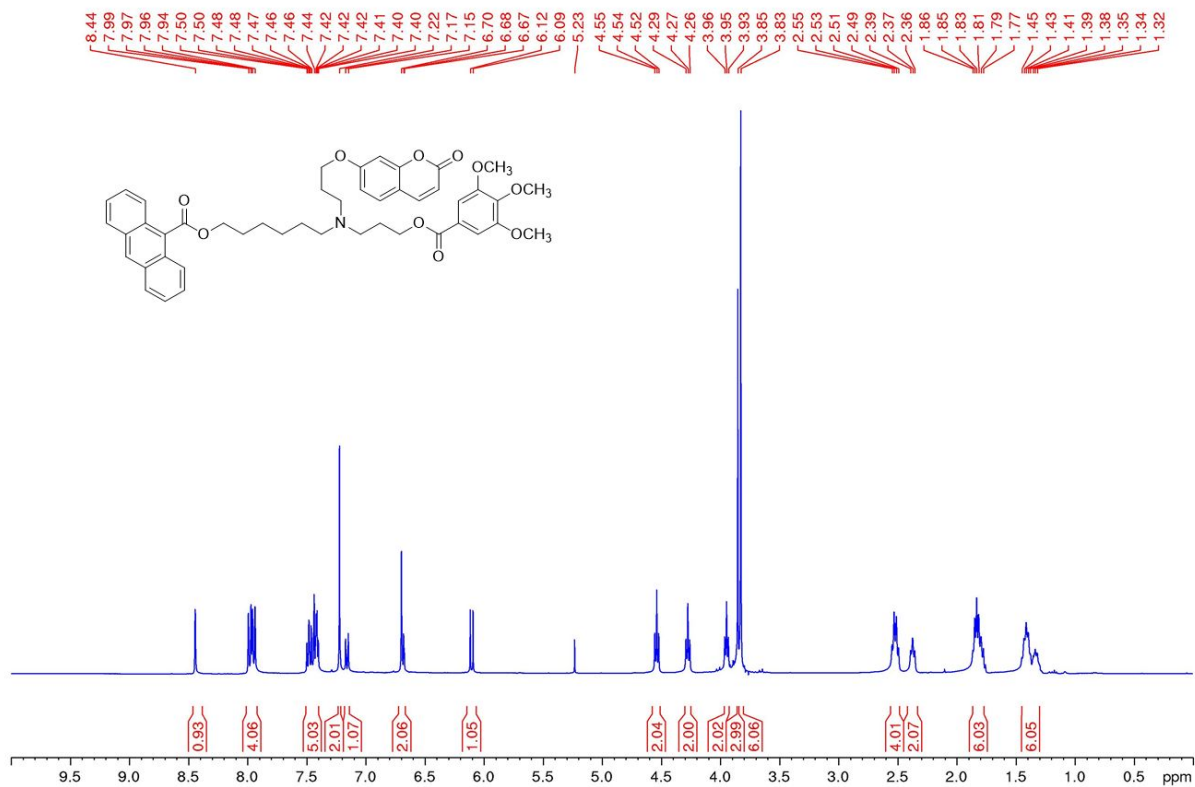
$^1\text{H-NMR}$ and $^{13}\text{C-APT-NMR}$ spectra of compound **15**



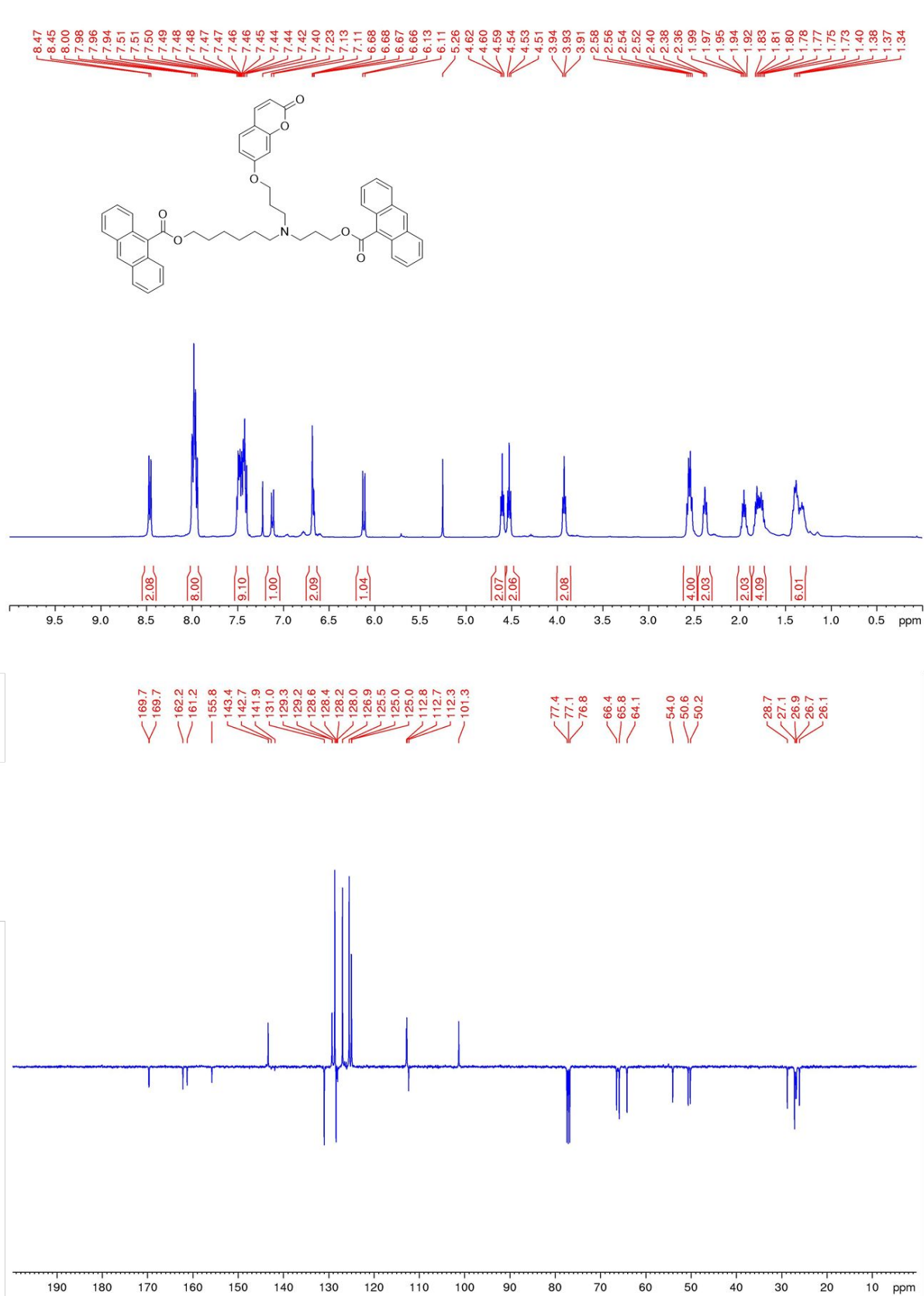
¹H-NMR and ¹³C-APT-NMR spectra of compound **16**



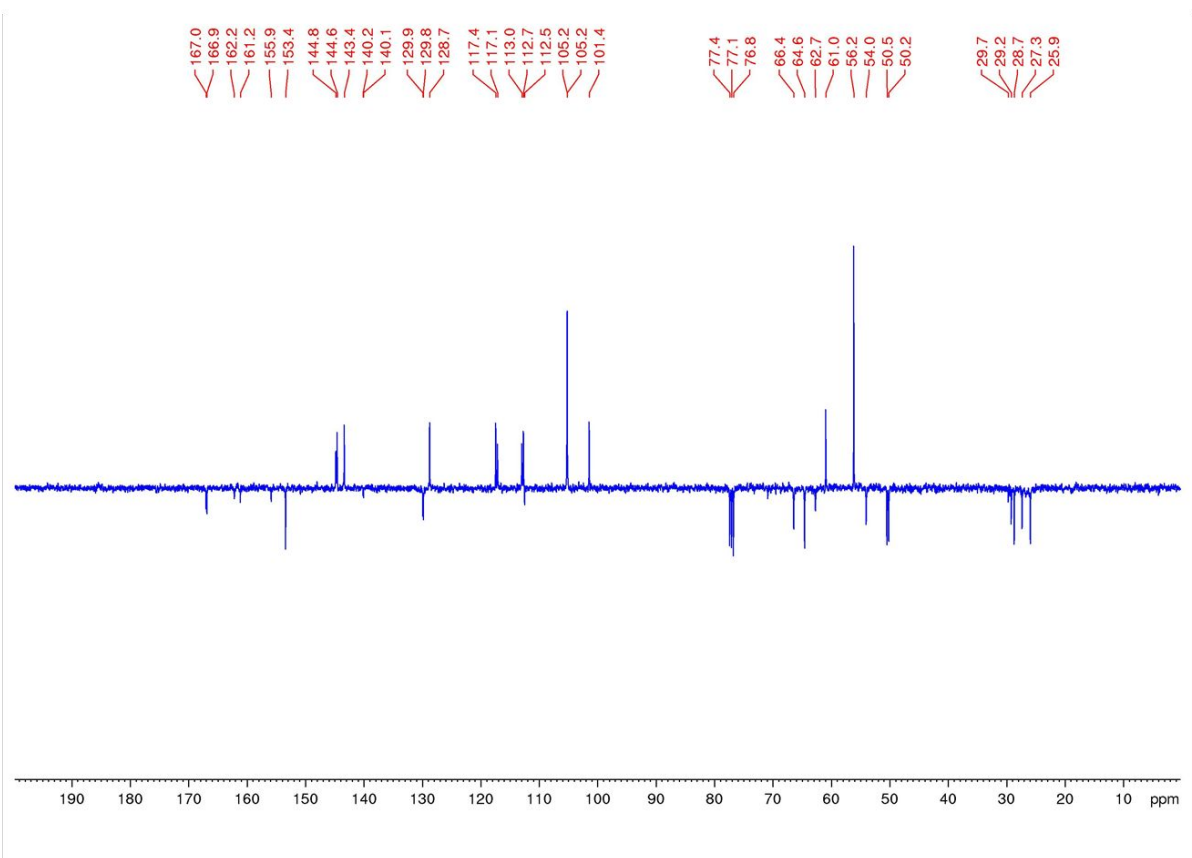
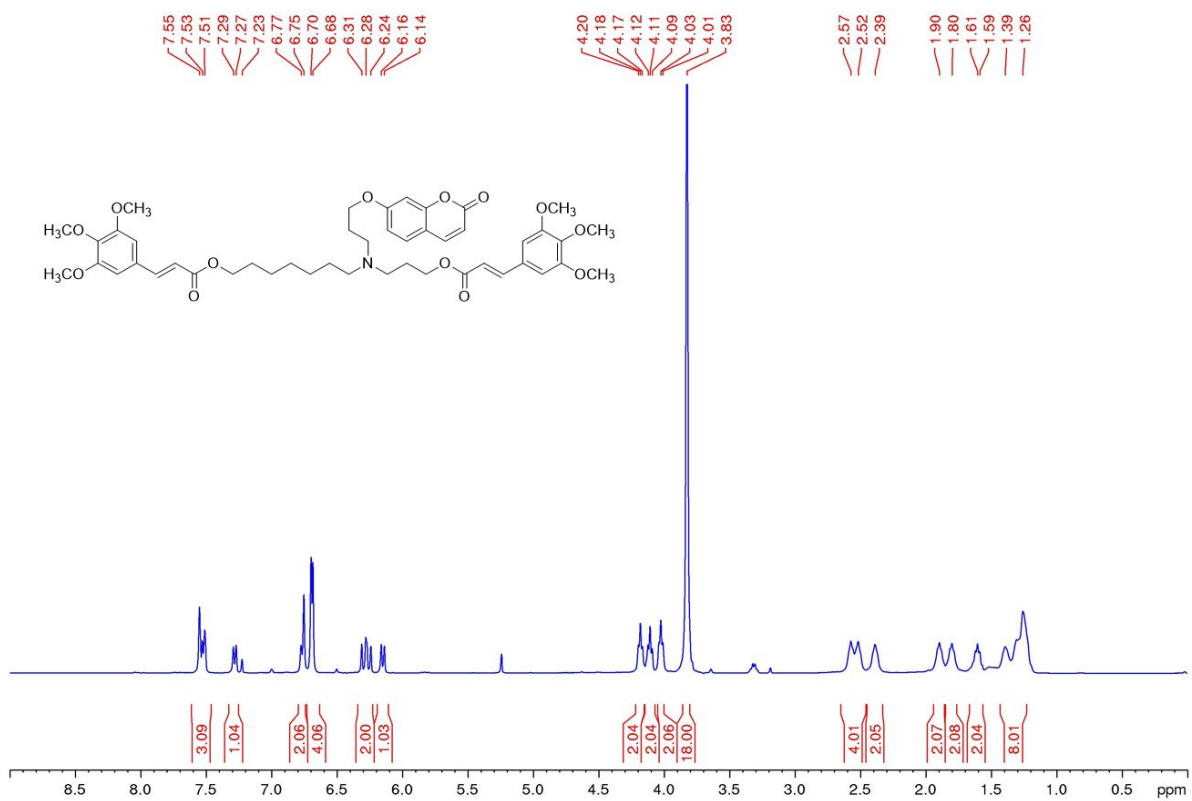
^1H -NMR and ^{13}C -APT-NMR spectra of compound **17**



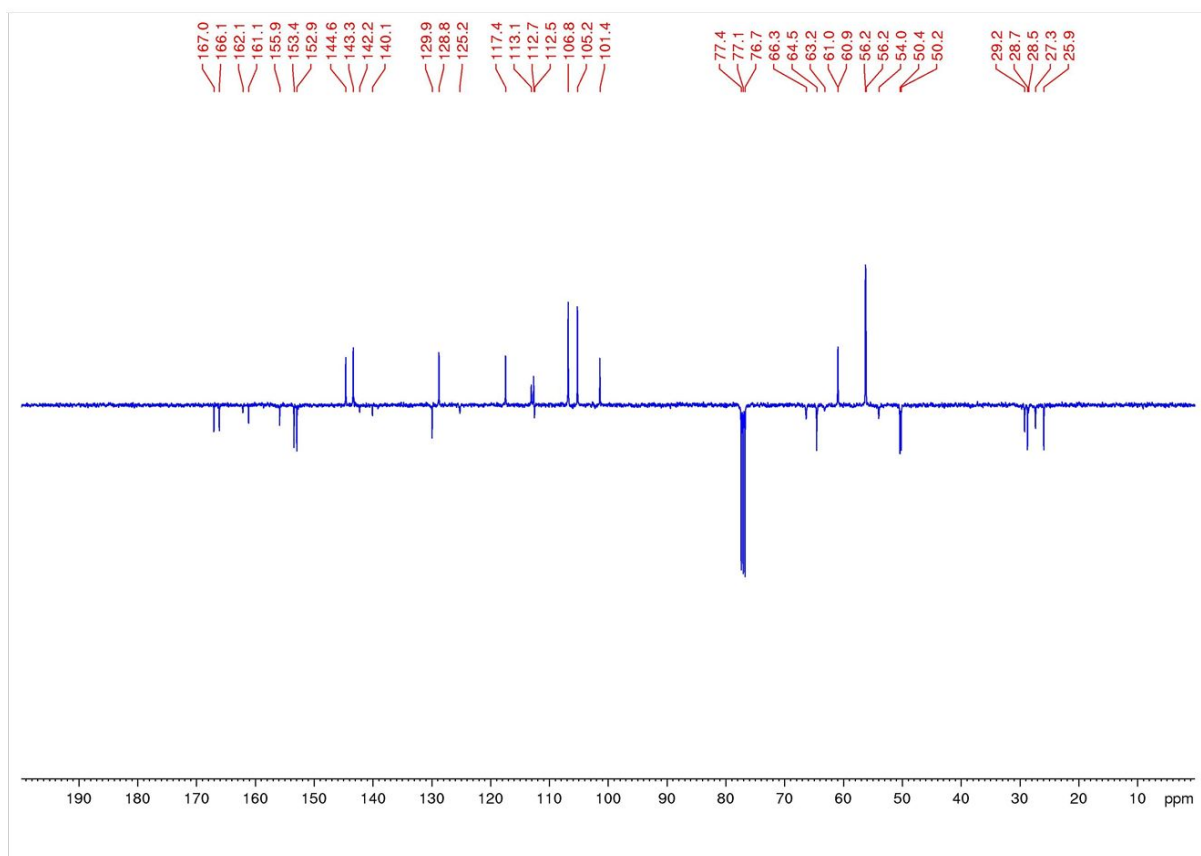
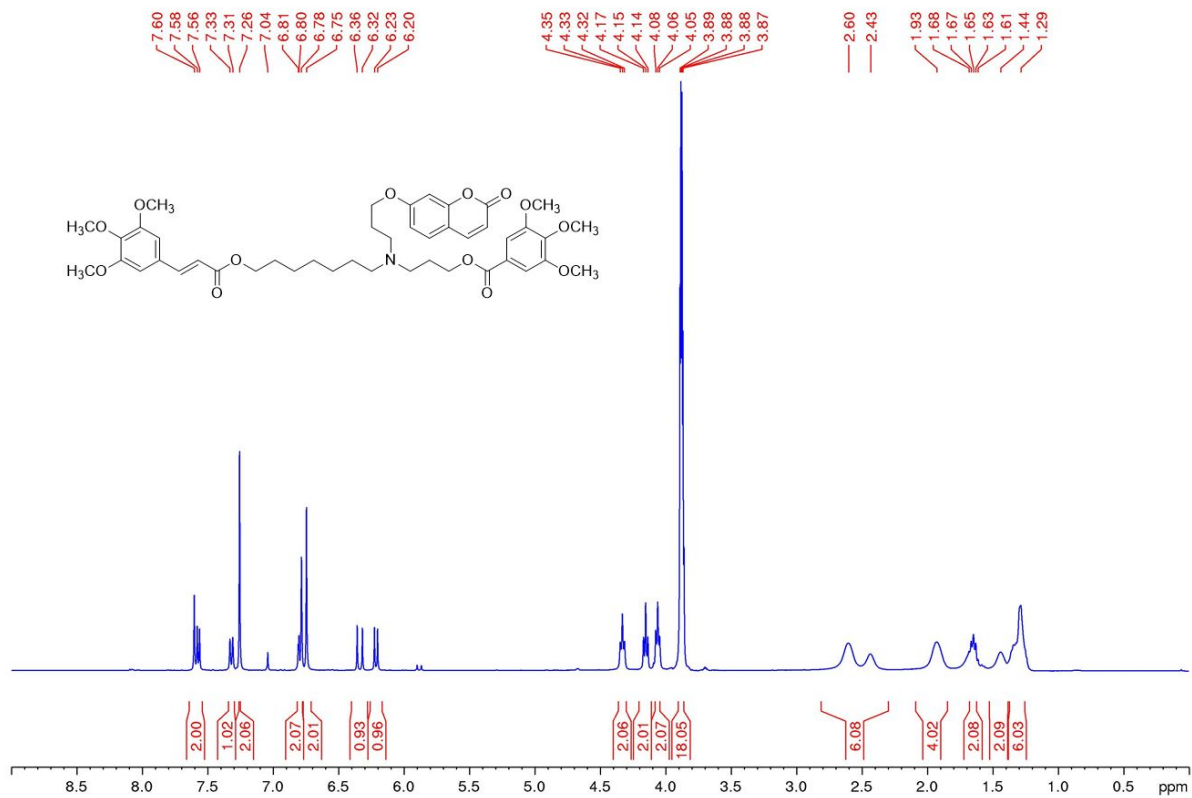
$^1\text{H-NMR}$ and $^{13}\text{C-APT-NMR}$ spectra of compound **18**



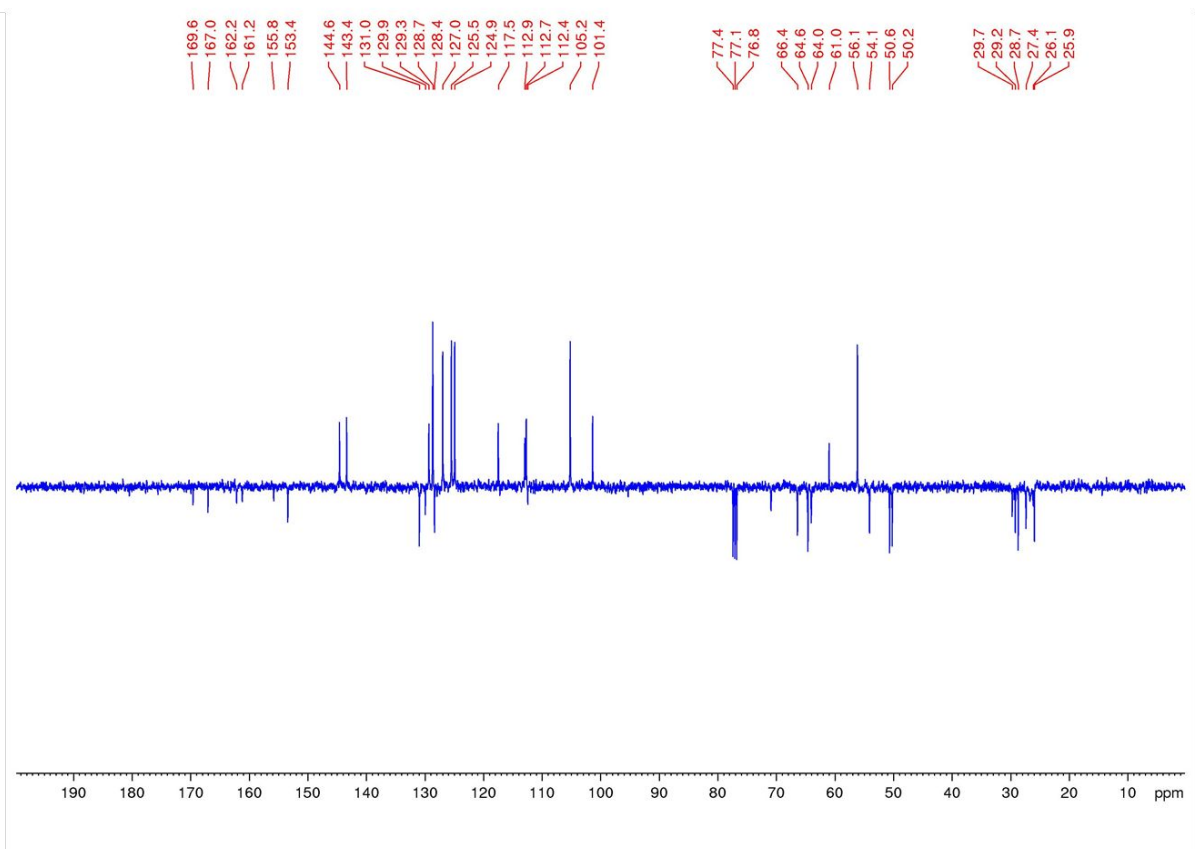
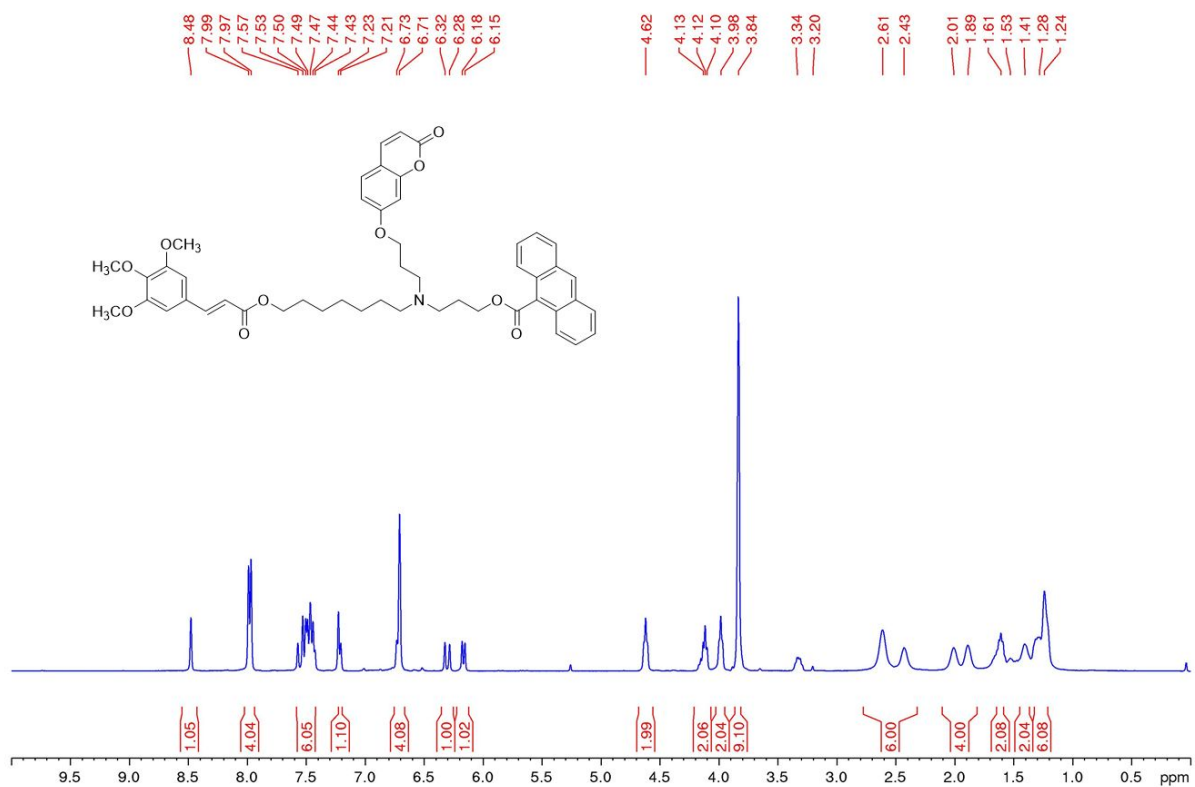
^1H -NMR and ^{13}C -APT-NMR spectra of compound **19**



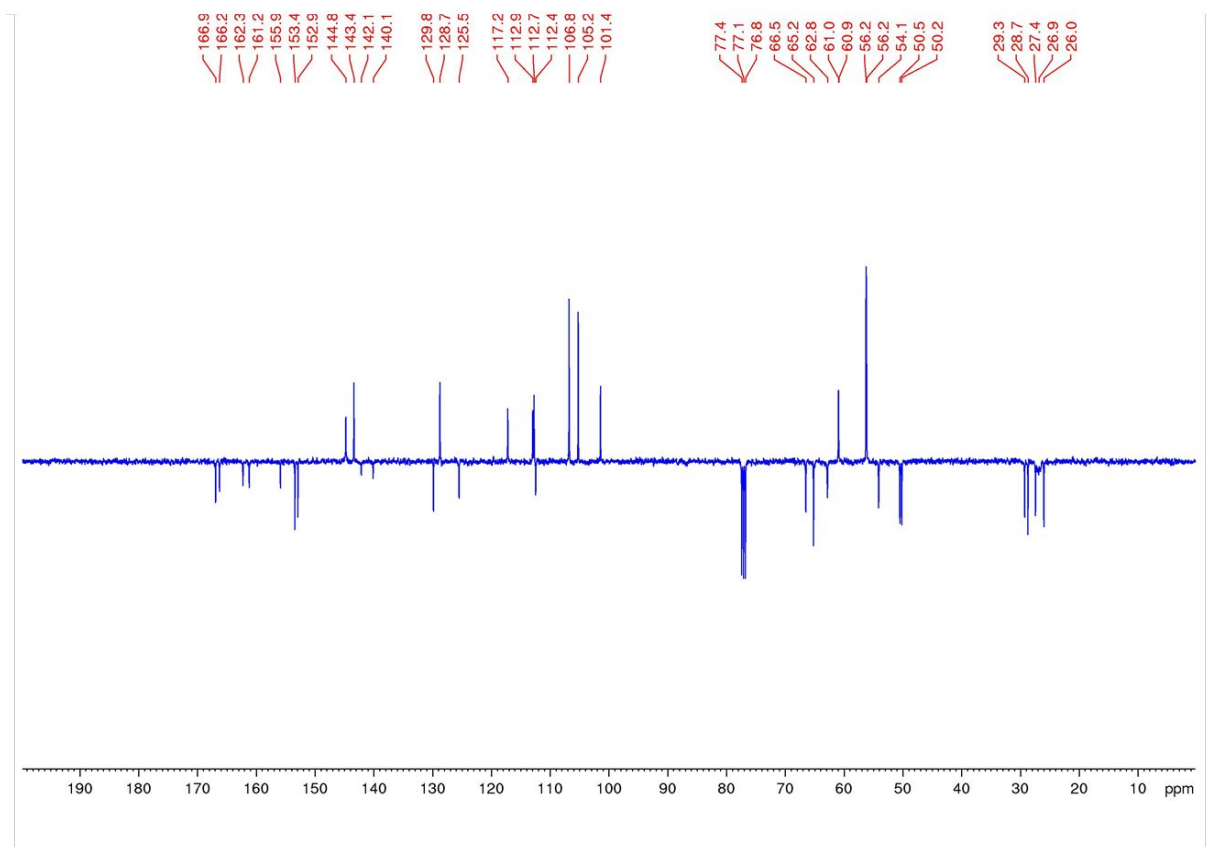
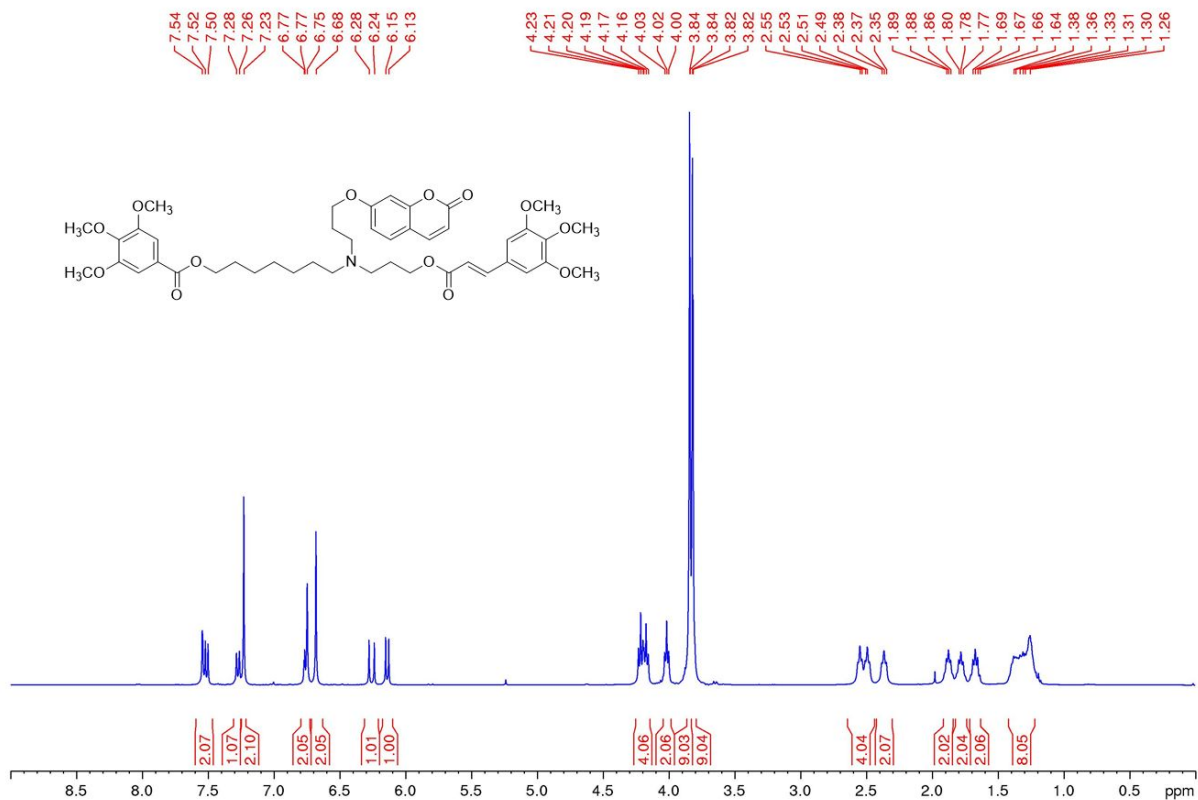
^1H -NMR and ^{13}C -APT-NMR spectra of compound **20**



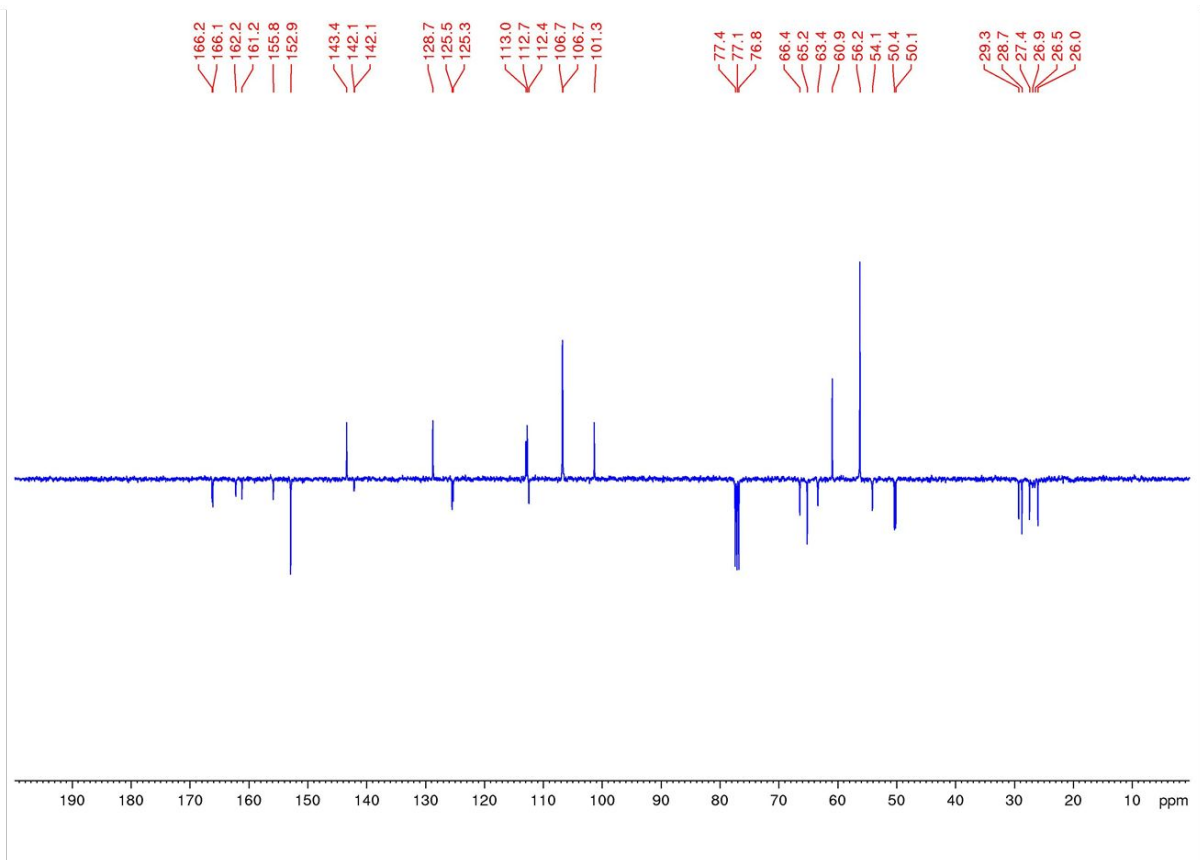
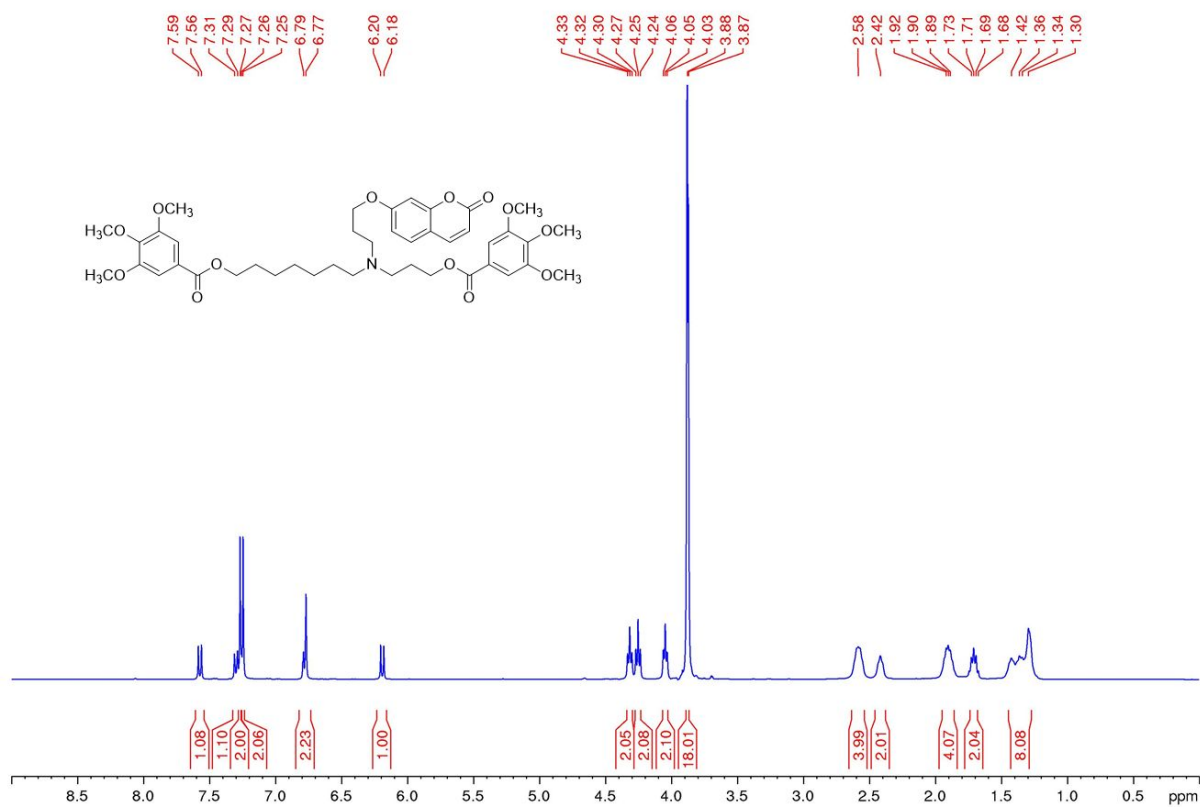
^1H -NMR and ^{13}C -APT-NMR spectra of compound **21**



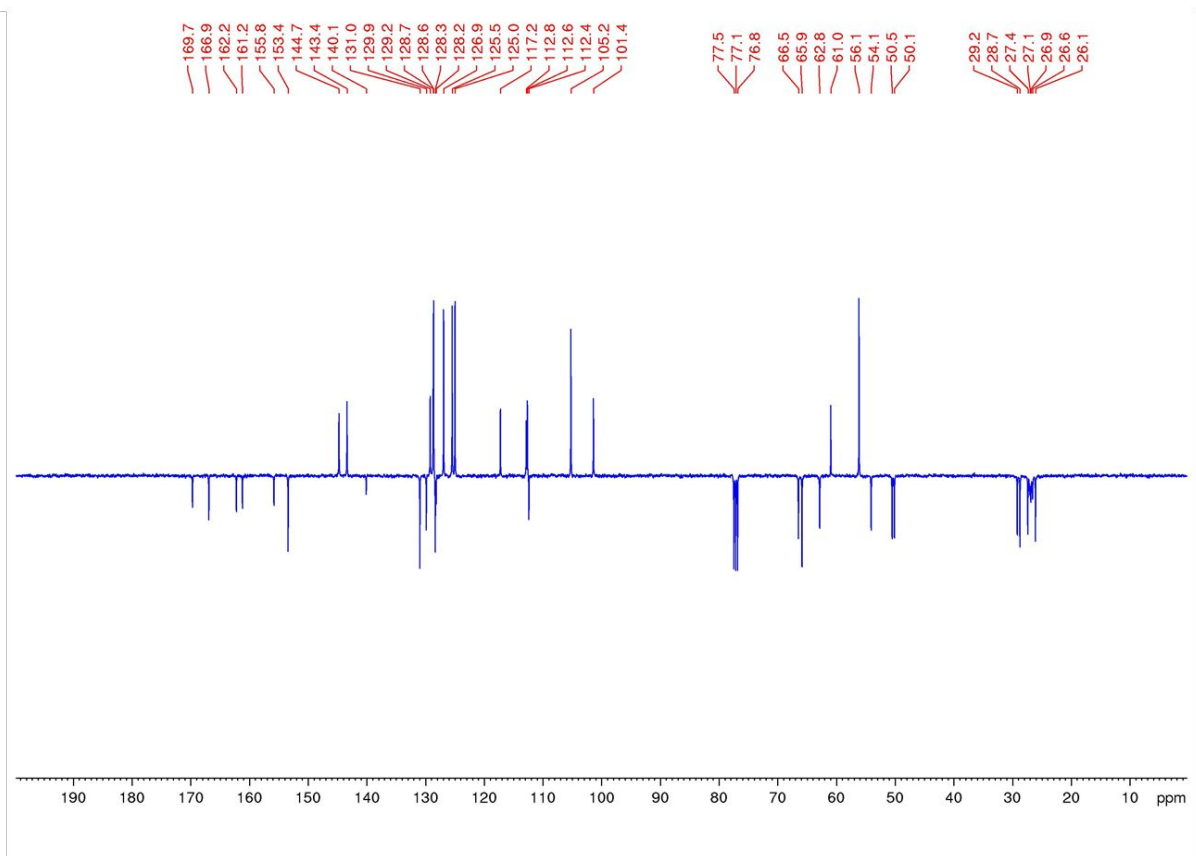
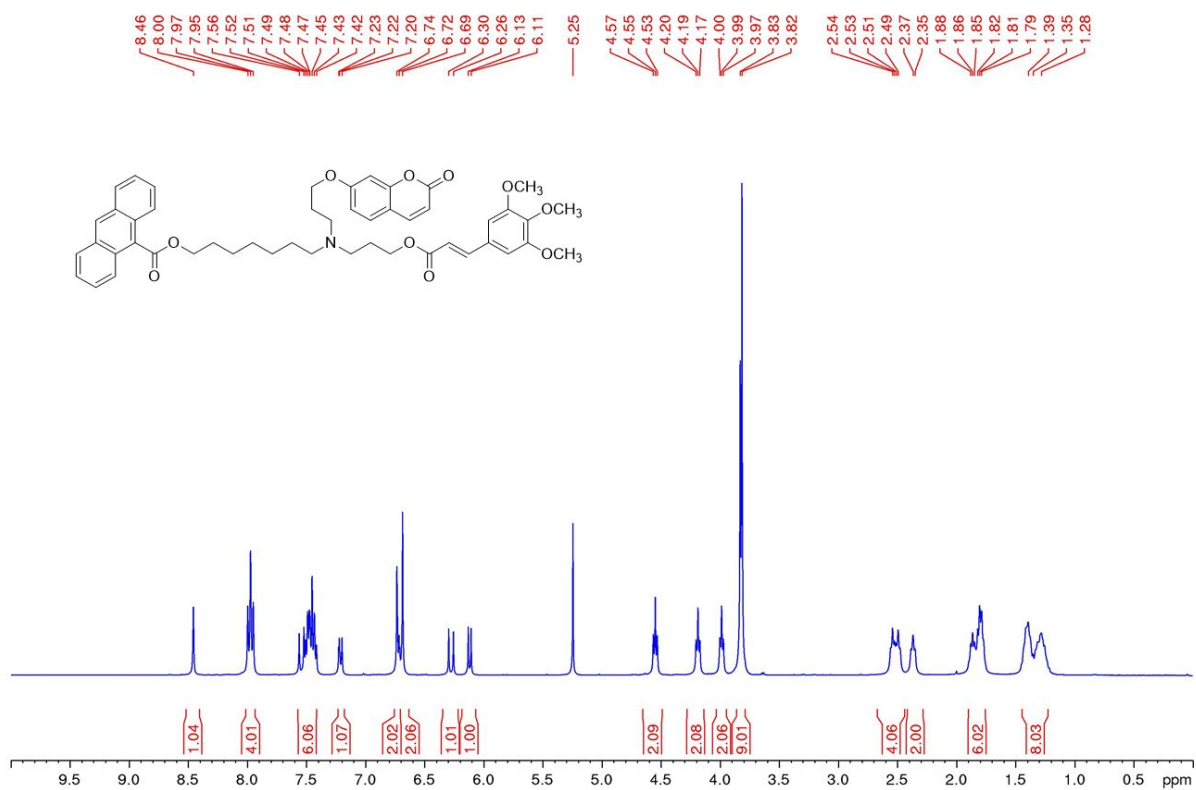
^1H -NMR and ^{13}C -APT-NMR spectra of compound **22**



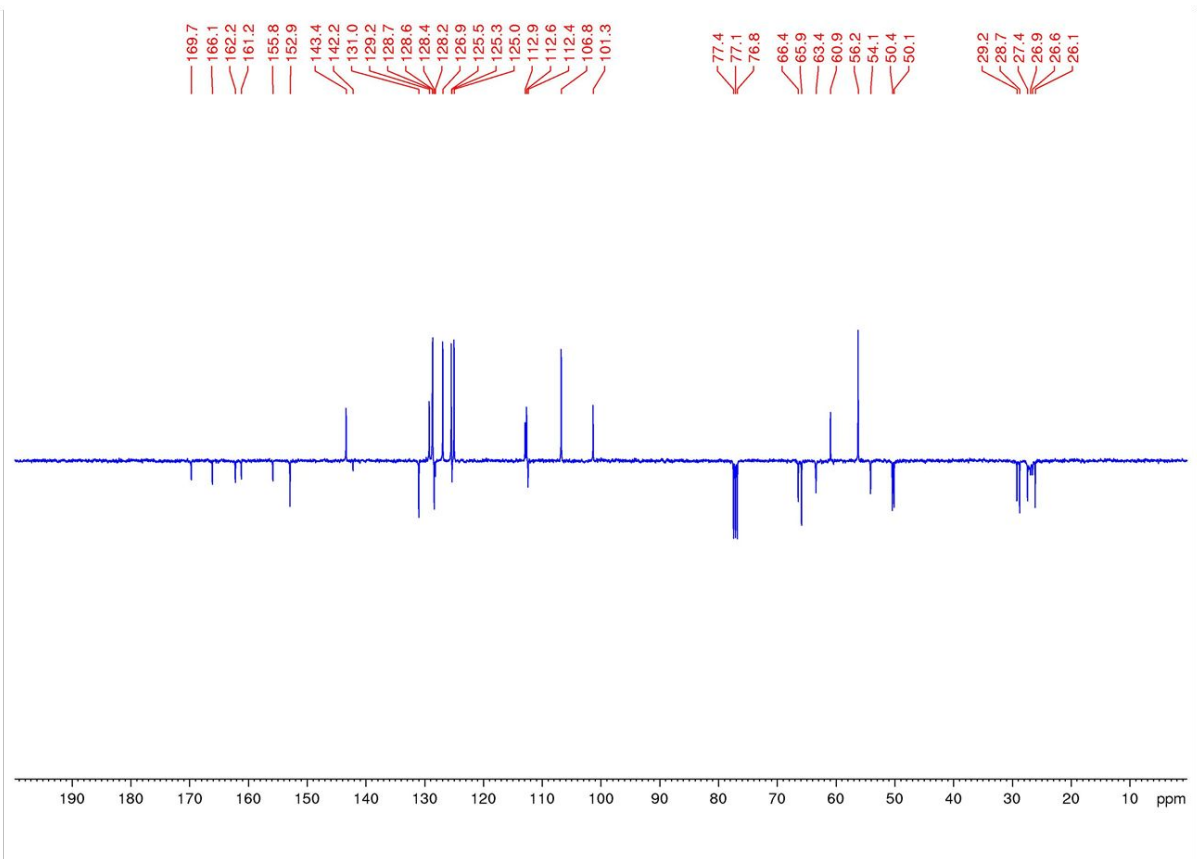
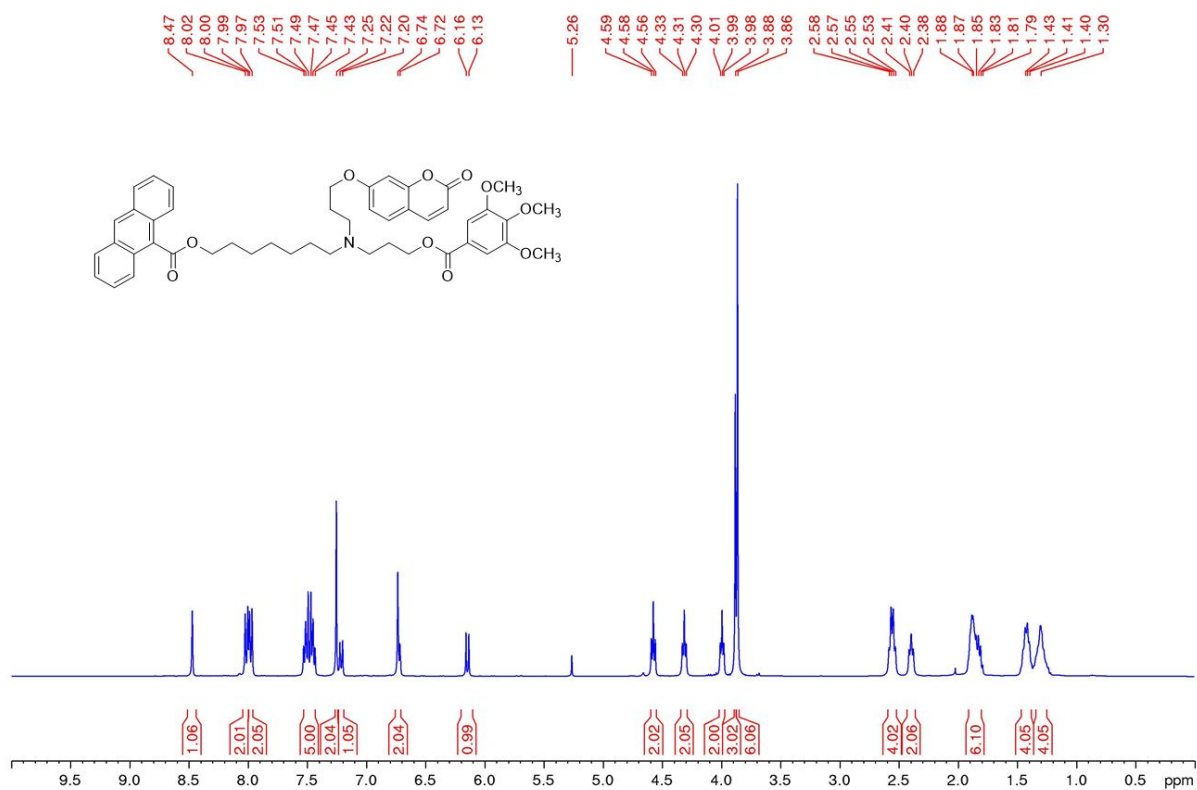
$^1\text{H-NMR}$ and $^{13}\text{C-APT-NMR}$ spectra of compound **23**



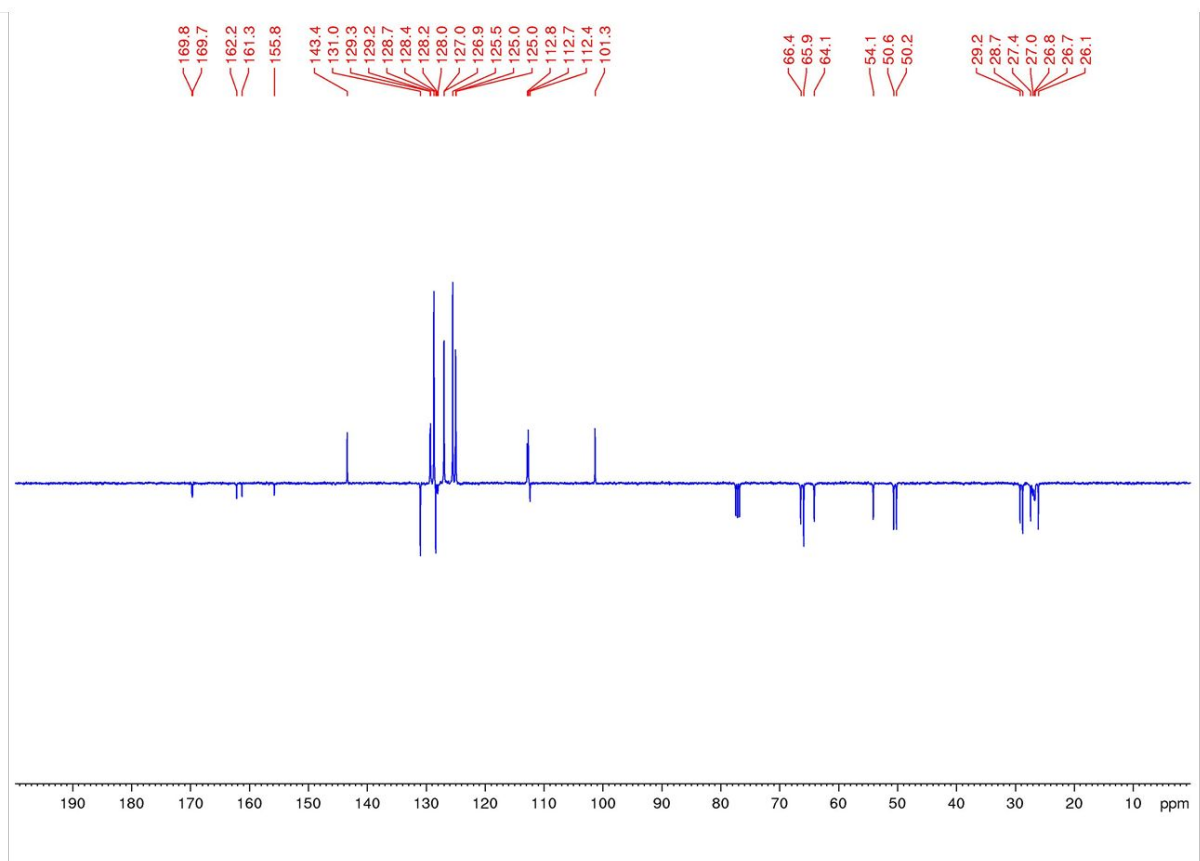
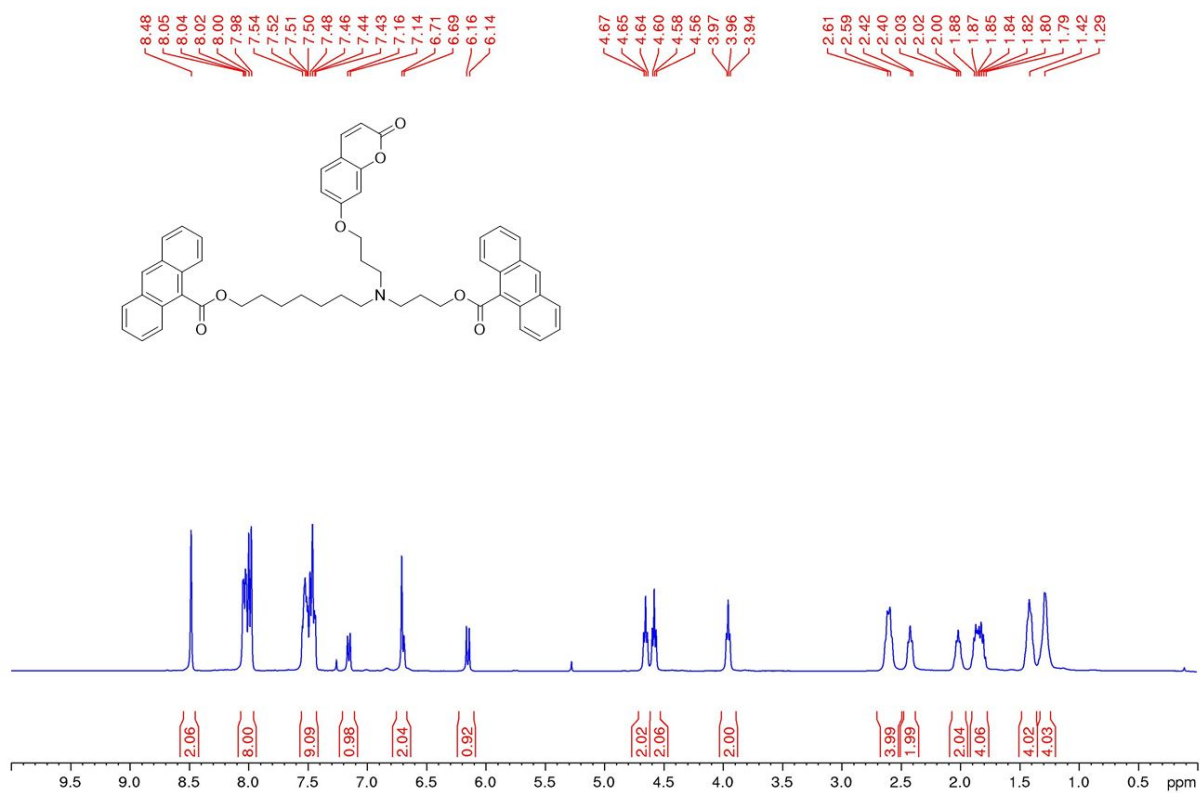
^1H -NMR and ^{13}C -APT-NMR spectra of compound **25**



$^1\text{H-NMR}$ and $^{13}\text{C-APT-NMR}$ spectra of compound **26**



^1H -NMR and ^{13}C -APT-NMR spectra of compound 27



Chemical stability data

Instrumental. The LC-MS/MS analyses were carried out using a Varian 1200L triple quadrupole system (Palo Alto, CA, USA) equipped by two Prostar 210 pumps, a Prostar 410 autosampler and an Elettrospray Source (ESI) operating in positive ions mode. Raw-data were collected and processed by Varian Workstation Vers. 6.8 software. G-Therm 015 thermostatic oven was used to keep the samples at 37 °C during the degradation tests. Eppendorf microcentrifuge 5415D was employed to centrifuge plasma samples.

Standard solutions and calibration curves. Stock solutions of analytes and verapamil hydrochloride (IS) were prepared in acetonitrile at 1.0 mg mL⁻¹ and stored at 4 °C. Working solutions of each analyte were freshly prepared by diluting stock solutions up to a concentration of 10 µM and 1 µM (working solution 1 and 2 respectively) in mQ water: acetonitrile 80:20 (v/v) solution. The IS working solution was prepared in acetonitrile at 20 ng mL⁻¹ (IS solution).

A seven levels calibration curve was prepared by adding proper volumes of working solution of each analyte to 500 µL of IS solution. The obtained solutions were dried under a gentle nitrogen stream and dissolved in 1.0 mL of 10 mM of formic acid in mQ water: acetonitrile 80:20 (v/v) solution. Final concentrations of calibration levels were: 0, 2.5, 5, 10, 25, 50 and 100 ng mL⁻¹ of analyte in the sample. All calibration levels were analysed by the appropriate LC-MS/MS method.

LC-MS/MS method. The chromatographic parameters were reported as follows:

- column, Phenomenex Luna C18 length = 20 mm; internal diameter = 2 mm; particle size = 3 µm, purchased from Merck.
- acidic mobile phase, composed by 5 mM of ammonium formate and 10mM of formic acid in mQ water: acetonitrile 90:10 (v/v) solution (solvent A), 5 mM of ammonium formate and 10mM of formic acid in mQ water: acetonitrile 10:90 (v/v) solution (solvent B).
- flow rate and the injection volume were 0.25 mL min⁻¹ and 5 µL, respectively.

The elution gradient is shown in Table S1.

Table S1: Elution gradient of mobile phase used for LC-MS/MS analyses

Time (min)	A (%)	B (%)
0.00	90	10
4.00	10	90
6.00	10	90
6.10	90	10
8.00	90	10

The analyses were acquired in MRM (Multiple Reaction Monitoring), using Argon as collision gas, and parameters are reported in Table S2.

Table S2: MRM parameters

Compounds	Precursor ion (m/z)	Quantitation ion (m/z) [CE (V)]	Qualification ion (m/z) [CE (V)]
KEE	283	209 [15]	105 [30]
1	804	221 [30]	279 [30]
2	778	221 [50]	195 [45]
3	788	205 [45]	221 [40]
4	778	221 [35]	195 [35]
5	752	195 [50]	253 [45]
6	762	205 [45]	195 [50]
7	788	205 [35]	221 [30]
8	762	205 [40]	195 [50]
9	772	205 [45]	263 [40]
10	818	221 [35]	279 [35]
11	792	221 [30]	195 [45]
12	802	205 [30]	221 [30]
13	792	221 [50]	195 [50]
14	766	195 [50]	253 [45]
15	776	205 [45]	195 [40]
16	802	221 [50]	205 [40]
17	776	205 [45]	195 [50]
18	786	205 [35]	177 [50]
19	832	221 [35]	279 [35]
20	806	221 [40]	195 [40]
21	816	205 [35]	221 [30]
22	806	221 [35]	195 [40]
23	780	195 [35]	253 [35]
24	790	205 [35]	195 [30]
25	816	221 [35]	205 [30]
26	790	205 [35]	195 [45]
27	800	205 [30]	177 [45]

Linearity and LOD. Calibration curves of analytes were obtained by plotting the peak area ratios (PAR), between quantitation ions of analyte and IS, versus the nominal concentration of the calibration solution. A linear regression analysis was applied to obtain the best fitting function between the calibration points.

The precision was evaluated through the relative standard deviation (RSD%) of the quantitative data of the replicate analysis of highest level of calibration curves.

In order to obtain reliable LOD values, the standard deviation of response and slope approach was employed. The estimated standard deviations of responses were obtained by the standard deviation of y-intercepts (SDY-I) of regression lines. The obtained linear regressions, the linearity coefficients, precision and the estimated LOD values for each analyte are reported in Table S3.

Table S3: Linear regressions data, linearity coefficients, precision and LOD values for each analyte

Compounds	Slope (PAR/ μ M)	Intercept (PAR)	R ²	Precision (RSD)	LOD (μ M)
1	2.53	0.04	0.999	5.5%	0.03
2	2.41	0.11	0.996	0.7%	0.04
3	5.35	0.07	0.996	3.3%	0.05
4	2.74	0.03	0.998	1.9%	0.04
5	5.86	0.14	0.998	8.1%	0.04
6	6.37	0.08	0.997	8.6%	0.06
7	4.22	0.08	0.996	2.7%	0.04
8	4.27	0.06	0.998	3.1%	0.06
9	3.29	0.05	0.998	6.7%	0.04
10	3.68	0.10	0.998	2.5%	0.04
11	3.72	0.08	0.999	6.7%	0.04
12	3.49	0.10	0.998	7.1%	0.04
13	3.92	0.13	0.999	4.7%	0.05
14	1.68	0.14	0.997	3.4%	0.04
15	6.83	0.15	0.998	4.7%	0.06
16	1.41	0.17	0.999	0.7%	0.05
17	1.43	0.11	0.997	3.3%	0.06
18	2.97	0.09	0.994	1.0%	0.07
19	3.97	0.12	0.991	0.8%	0.07
20	3.43	0.07	0.999	1.1%	0.03
21	2.93	0.14	0.996	5.6%	0.06
22	4.98	0.11	0.998	5.0%	0.04
23	5.8	0.12	0.998	1.4%	0.04
24	6.0	0.3	0.996	5.3%	0.06
25	3.6	0.29	0.991	4.9%	0.09
26	4.4	0.3	0.993	5.9%	0.08
27	5.7	0.3	0.991	2.1%	0.09

Solution stability profiles. The solution stability profiles in PBS and human plasma were obtained by monitoring the variation of analyte concentration at different incubation times. They are reported in Figures S1-S27.

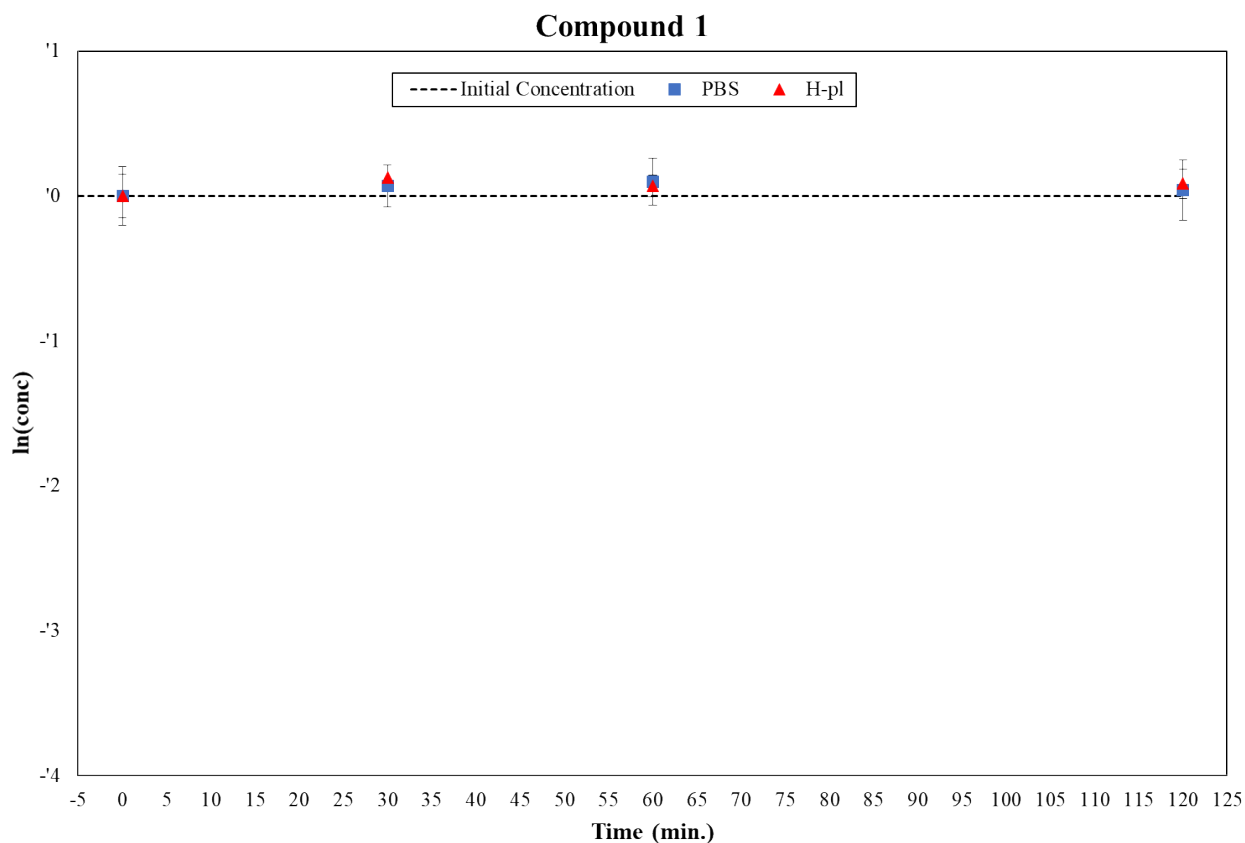


Figure S1: Degradation plots of **1** in PBS (blue square) and human plasma (red triangle), with the proper error bars.

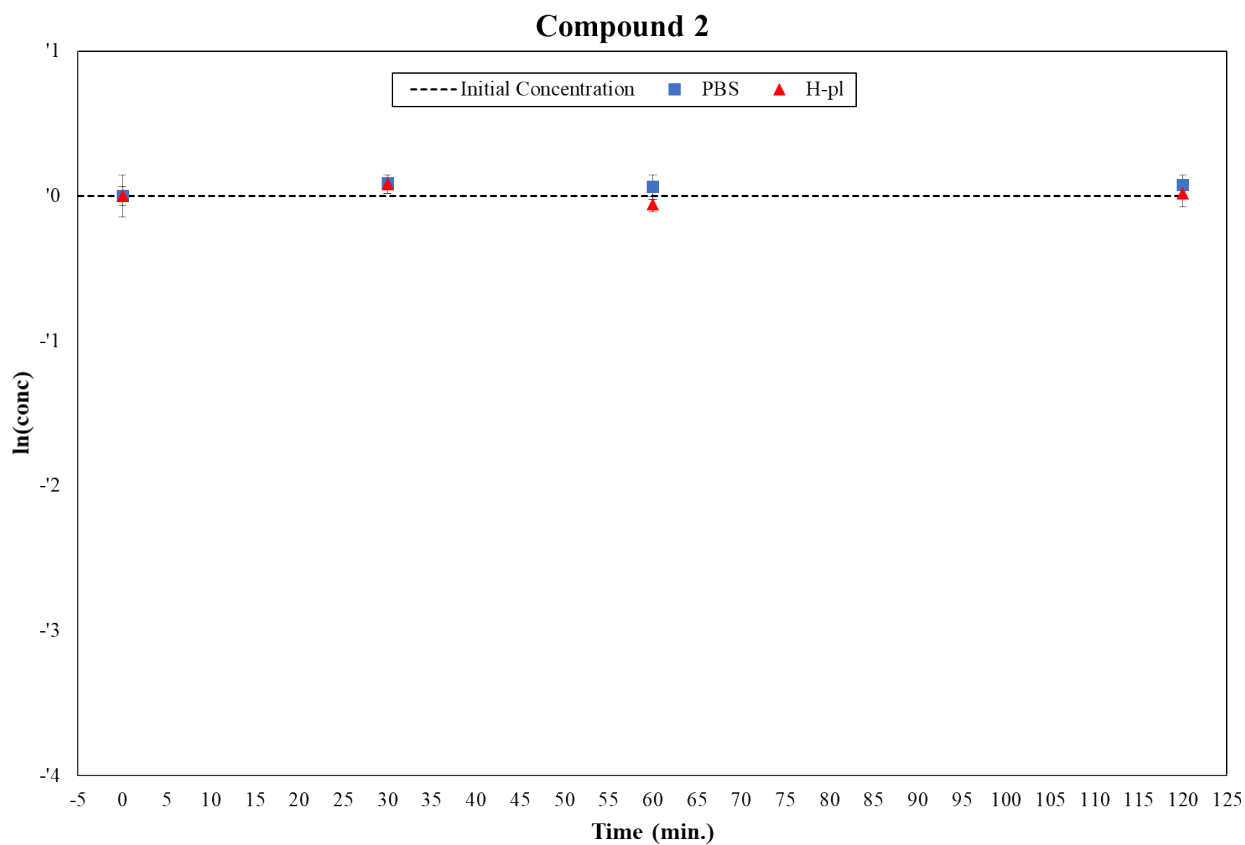


Figure S2: Degradation plots of **2** in PBS (blue square) and human plasma (red triangle), with the proper error bars.

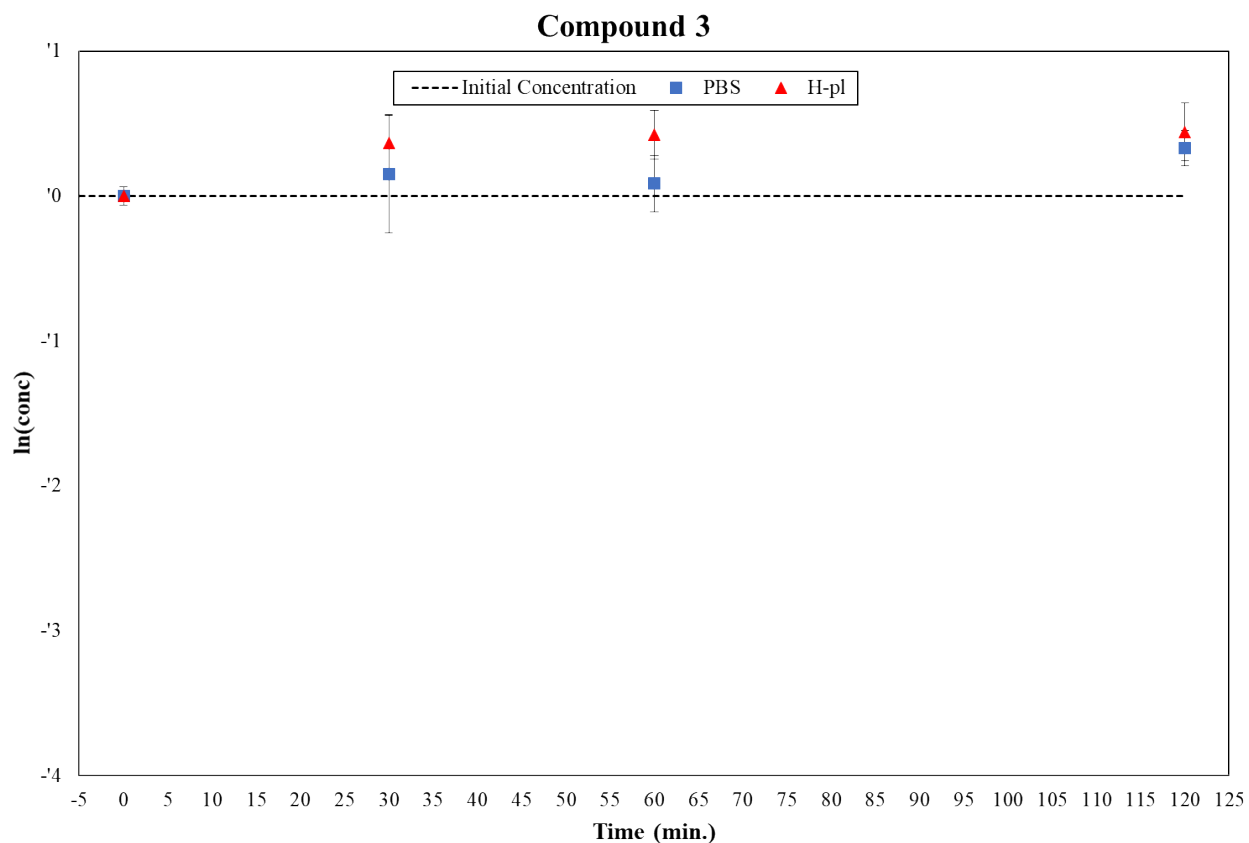


Figure S3: Degradation plots of **3** in PBS (blue square) and human plasma (red triangle), with the proper error bars.

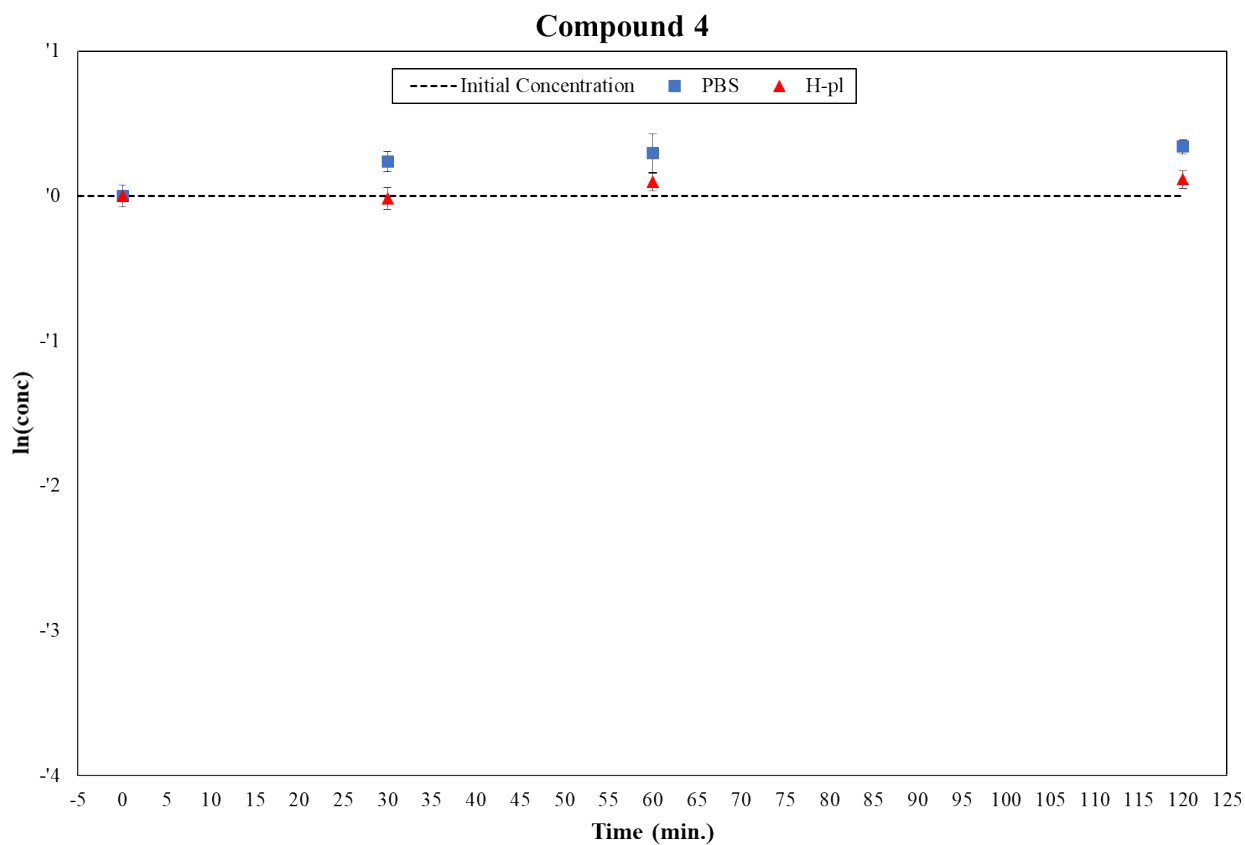


Figure S4: Degradation plots of **4** in PBS (blue square) and human plasma (red triangle), with the proper error bars.

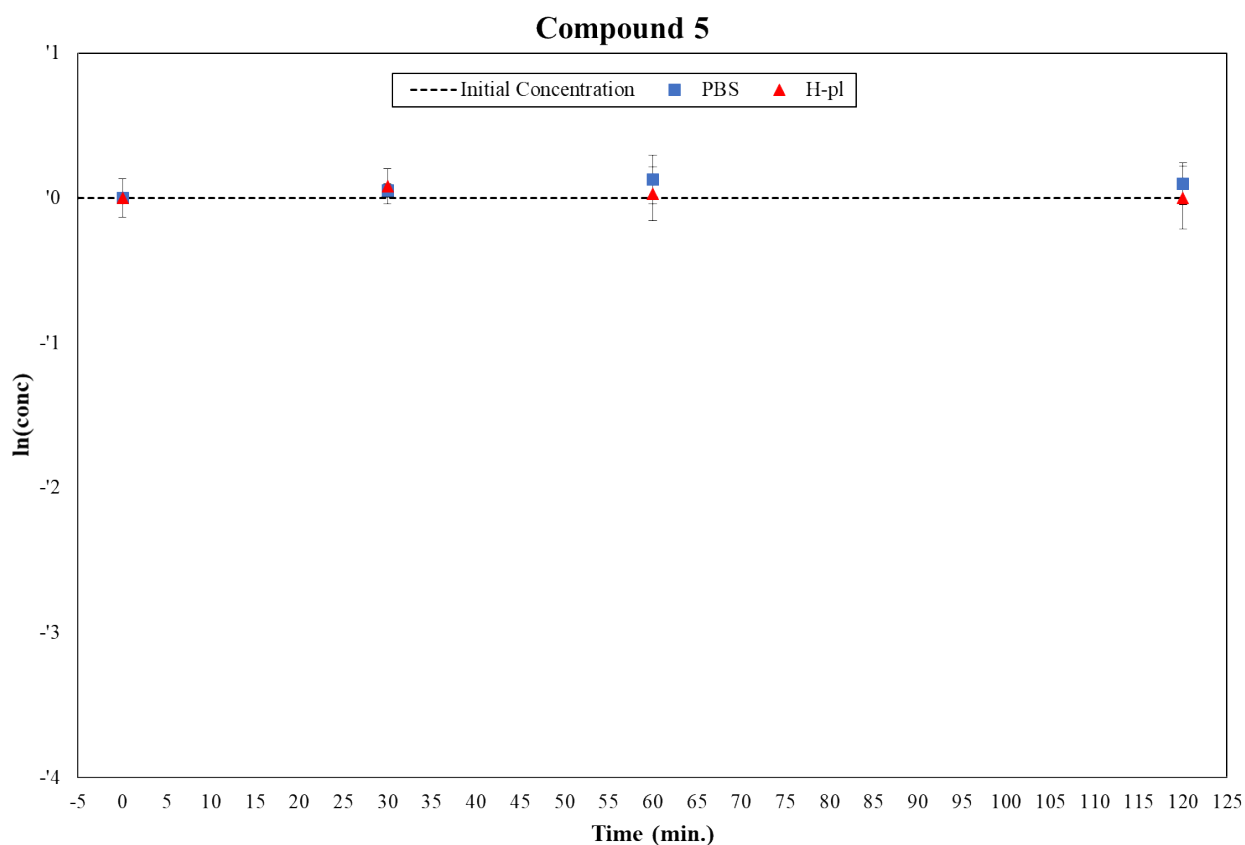


Figure S5: Degradation plots of **5** in PBS (blue square) and human plasma (red triangle), with the proper error bars.

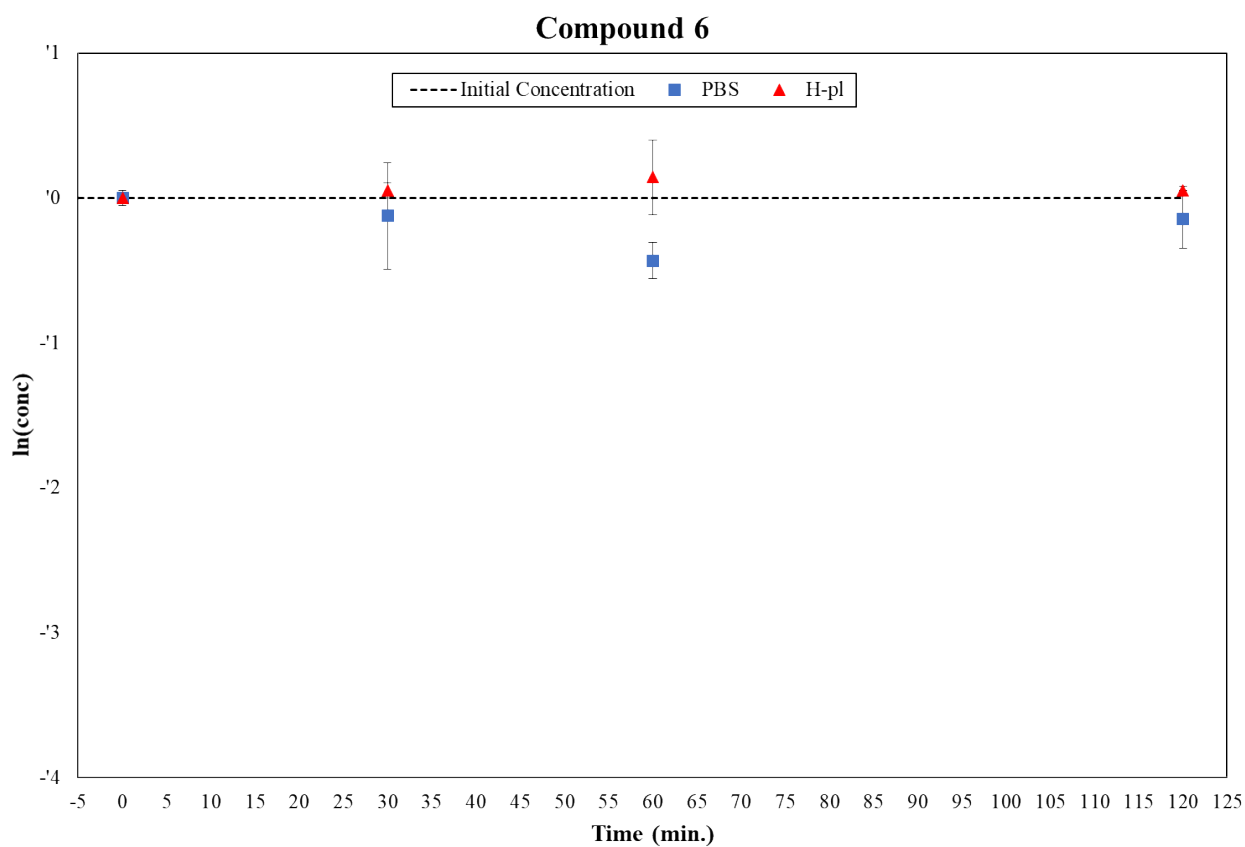


Figure S6: Degradation plots of **6** in PBS (blue square) and human plasma (red triangle), with the proper error bars.

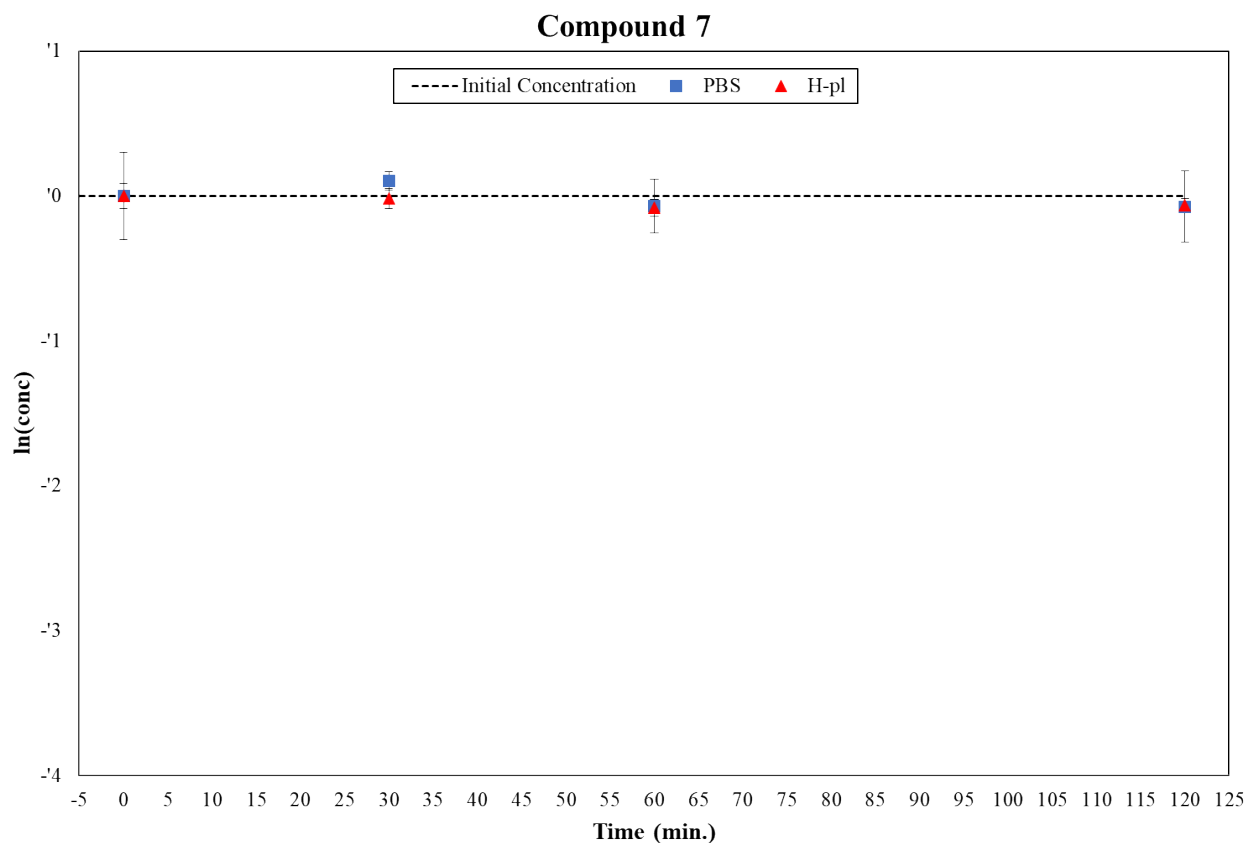


Figure S7: Degradation plots of **7** in PBS (blue square) and human plasma (red triangle), with the proper error bars.

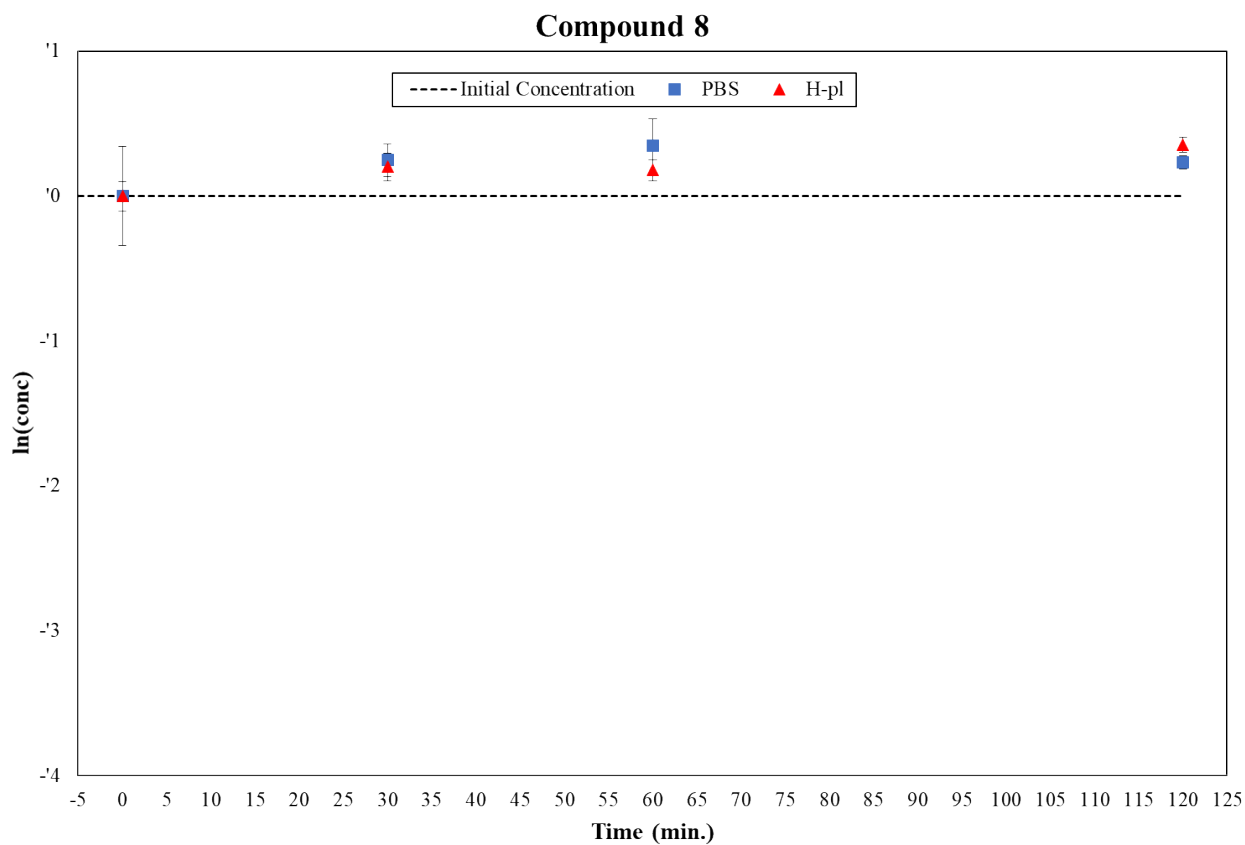


Figure S8: Degradation plots of **8** in PBS (blue square) and human plasma (red triangle), with the proper error bars.

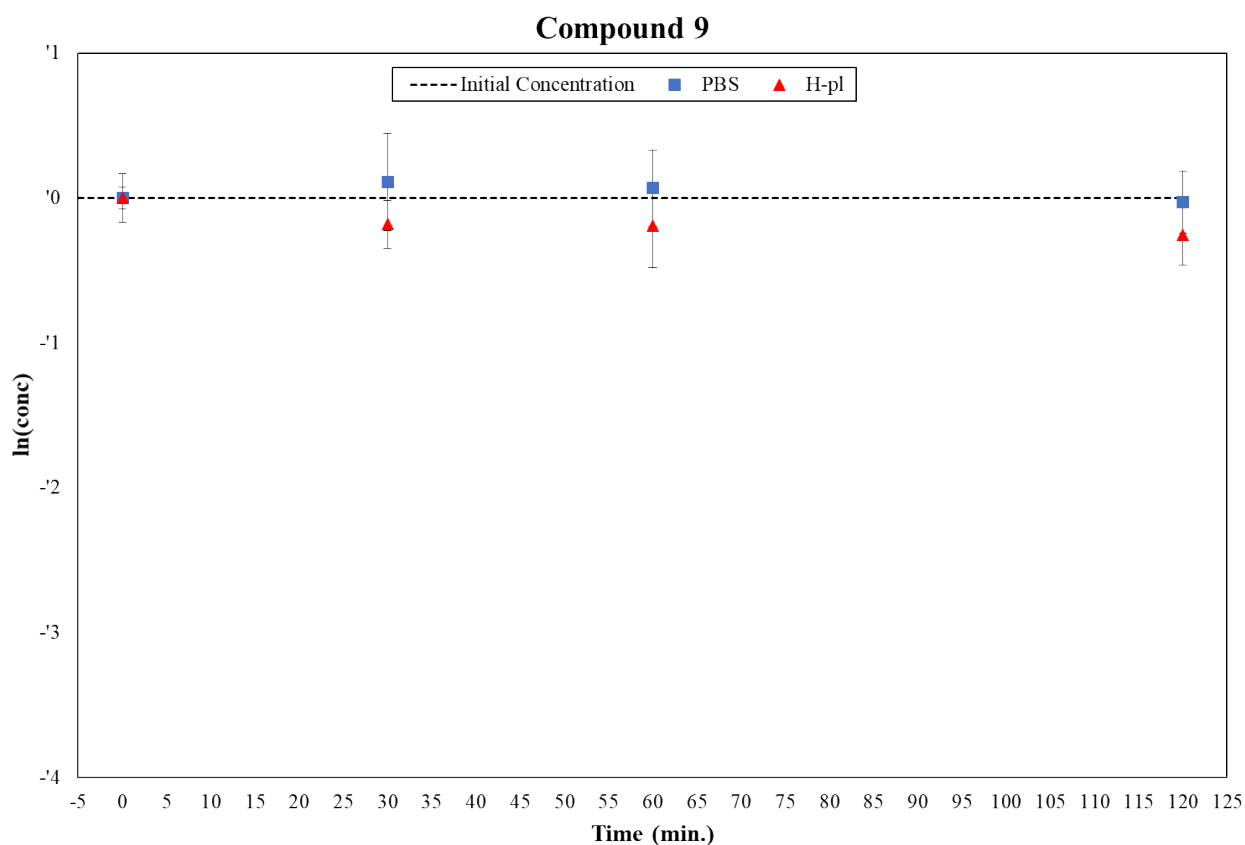


Figure S9: Degradation plots of **9** in PBS (blue square) and human plasma (red triangle), with the proper error bars.

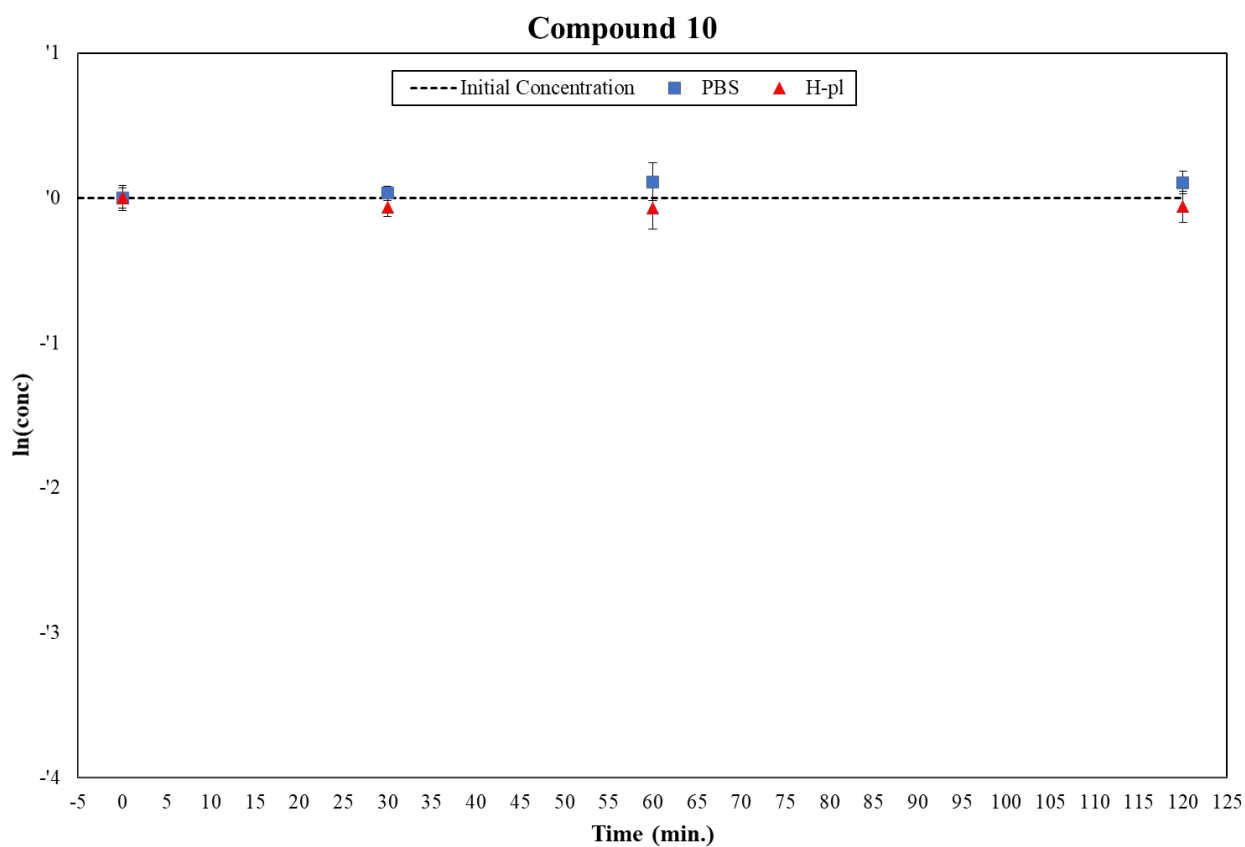


Figure S10: Degradation plots of **10** in PBS (blue square) and human plasma (red triangle), with the proper error bars.

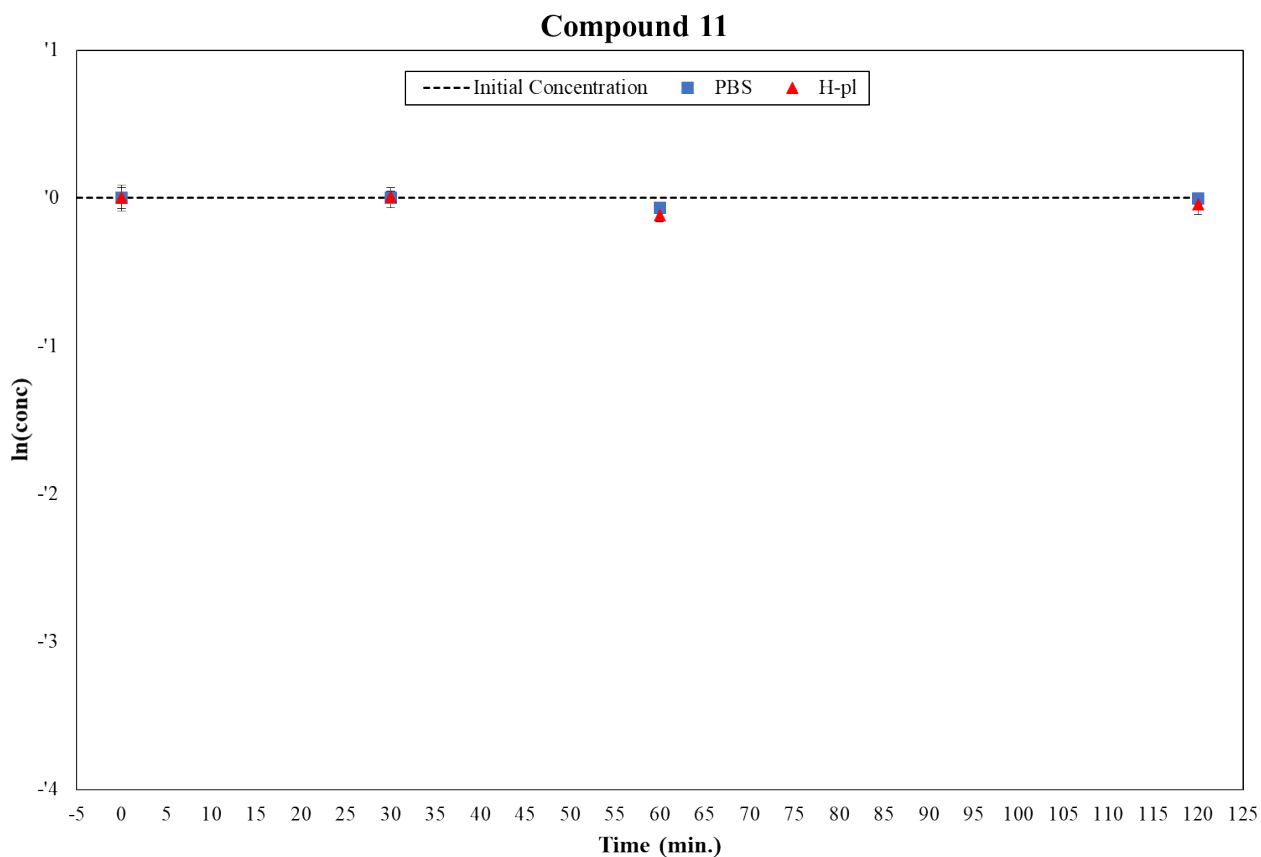


Figure S11: Degradation plots of **11** in PBS (blue square) and human plasma (red triangle), with the proper error bars.

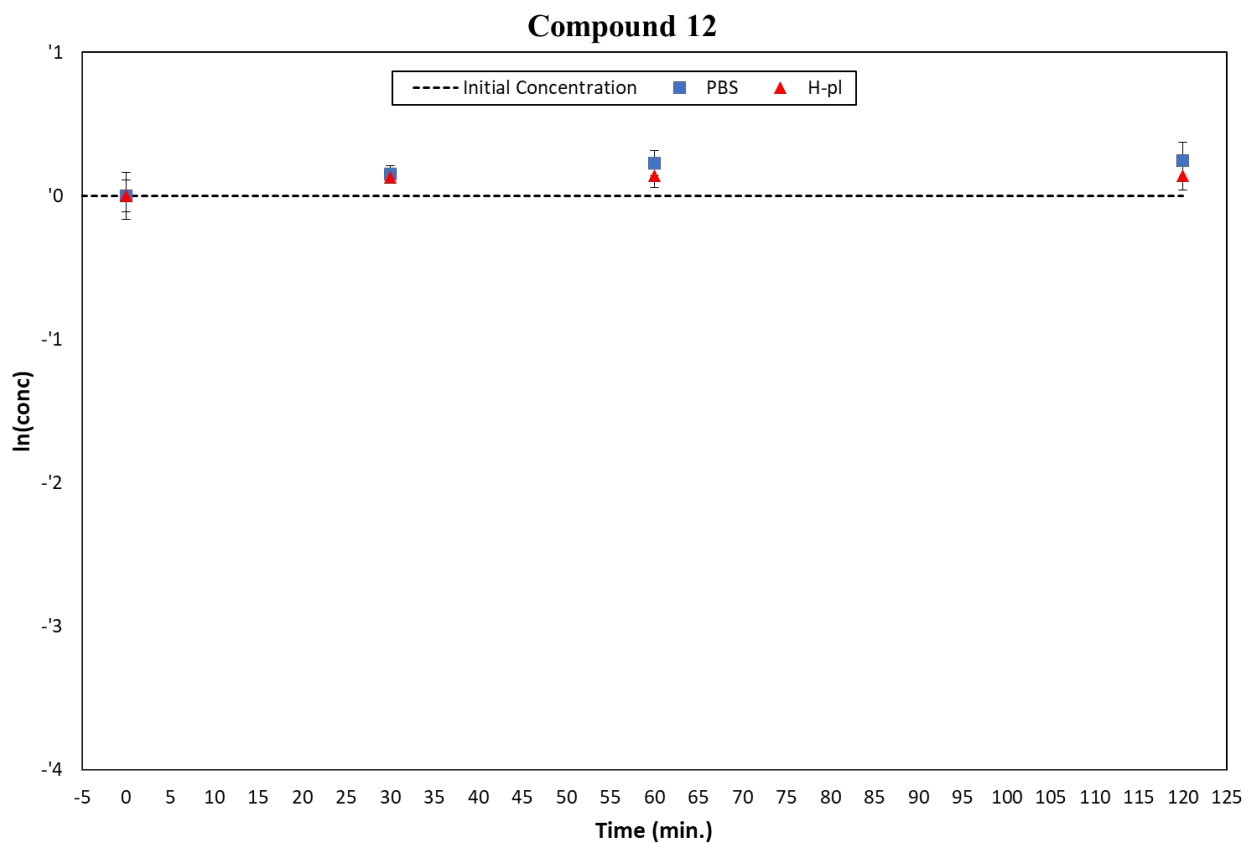


Figure S12: Degradation plots of **12** in PBS (blue square) and human plasma (red triangle), with the proper error bars.

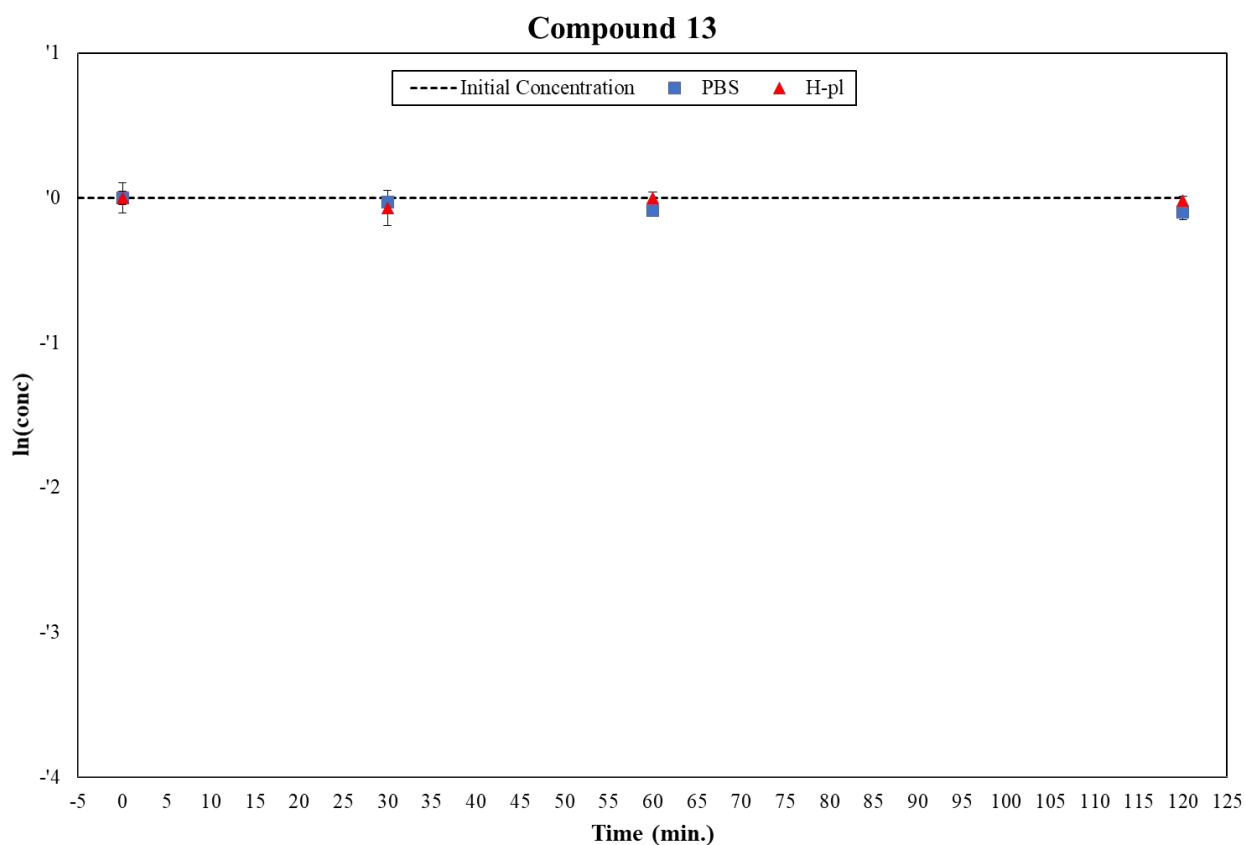


Figure S13: Degradation plots of **13** in PBS (blue square) and human plasma (red triangle), with the proper error bars.

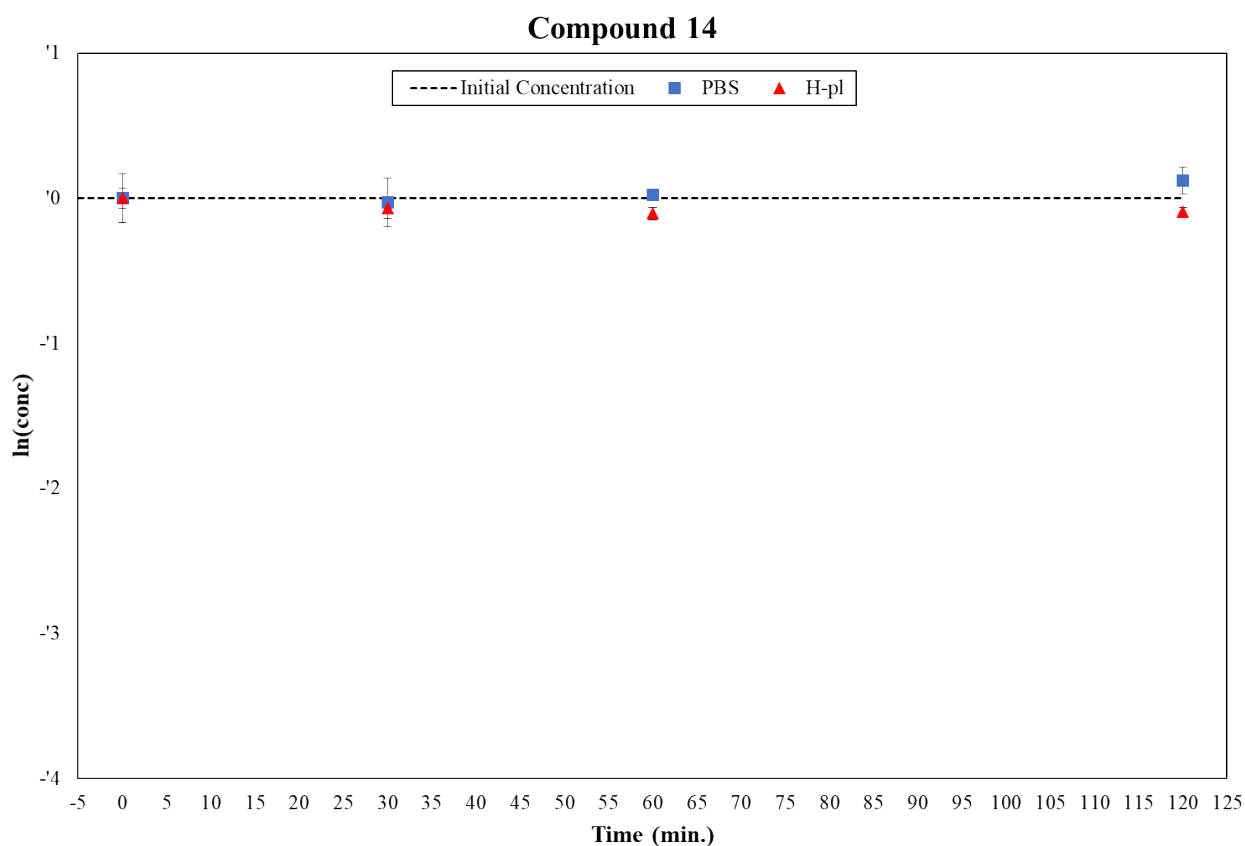


Figure S14: Degradation plots of **14** in PBS (blue square) and human plasma (red triangle), with the proper error bars.

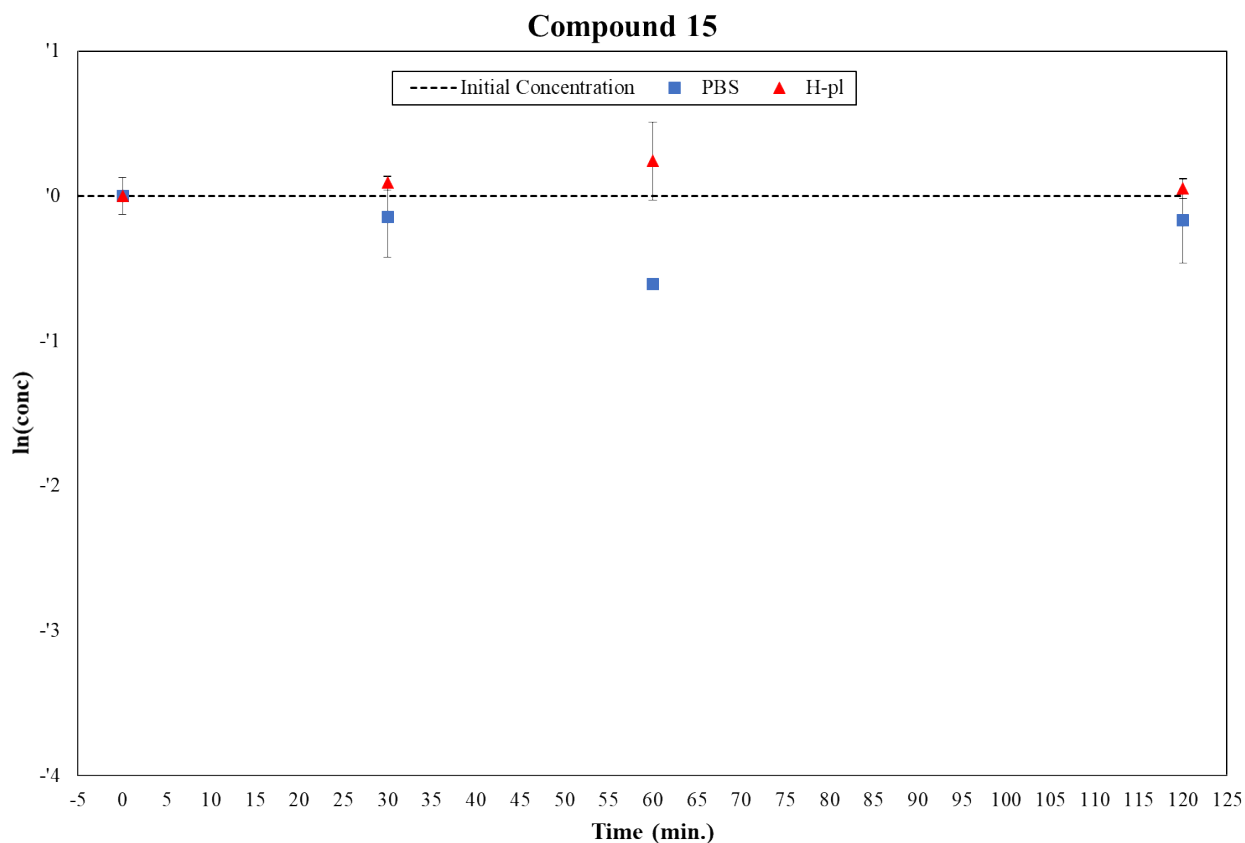


Figure S15: Degradation plots of **15** in PBS (blue square) and human plasma (red triangle), with the proper error bars.

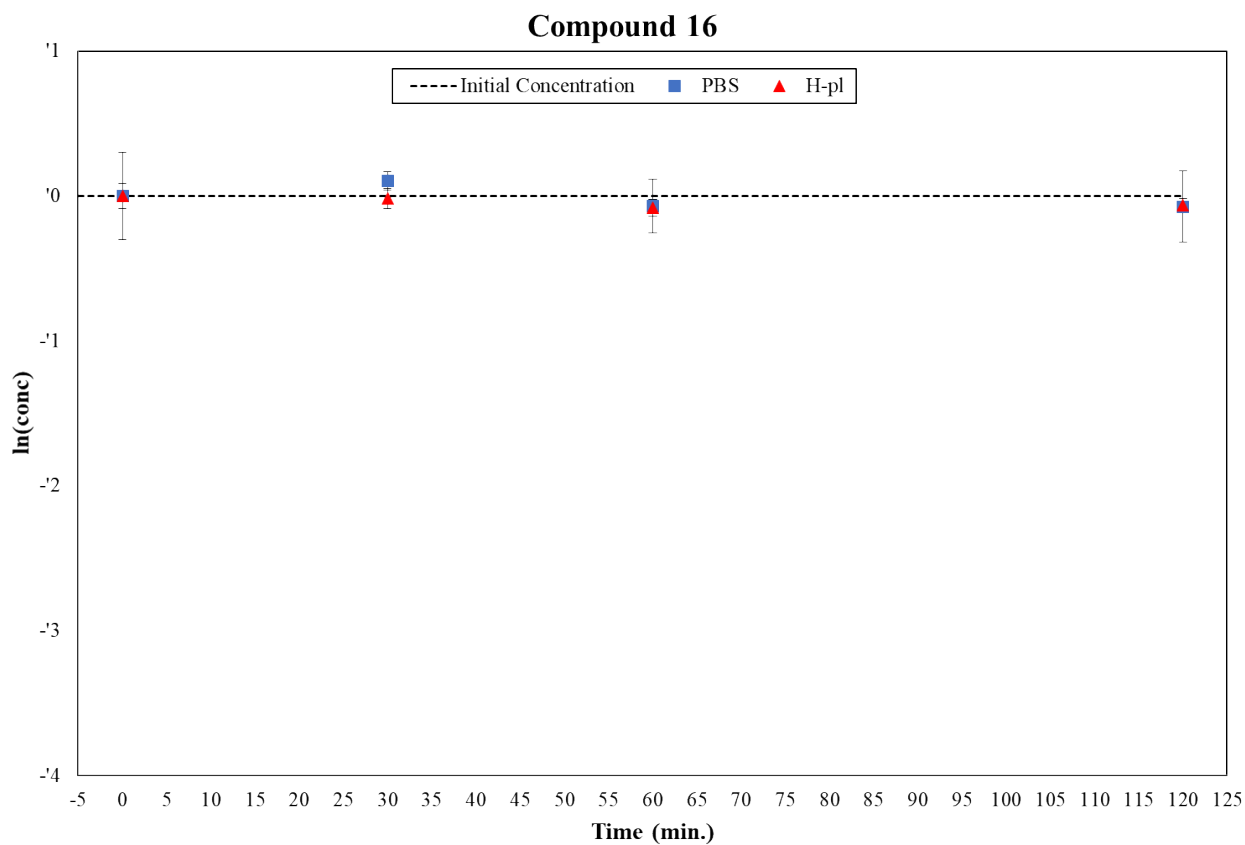


Figure S16: Degradation plots of **16** in PBS (blue square) and human plasma (red triangle), with the proper error bars.

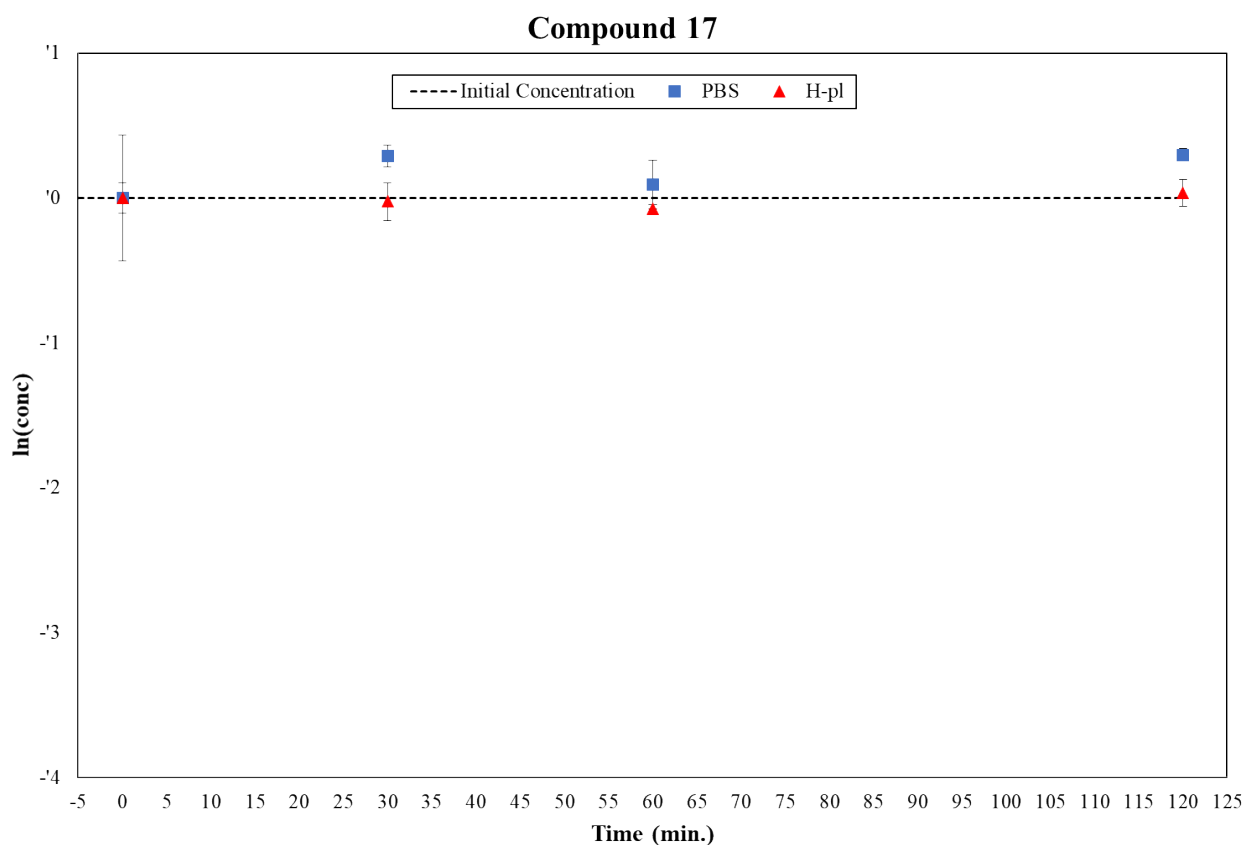


Figure S17: Degradation plots of **17** in PBS (blue square) and human plasma (red triangle), with the proper error bars.

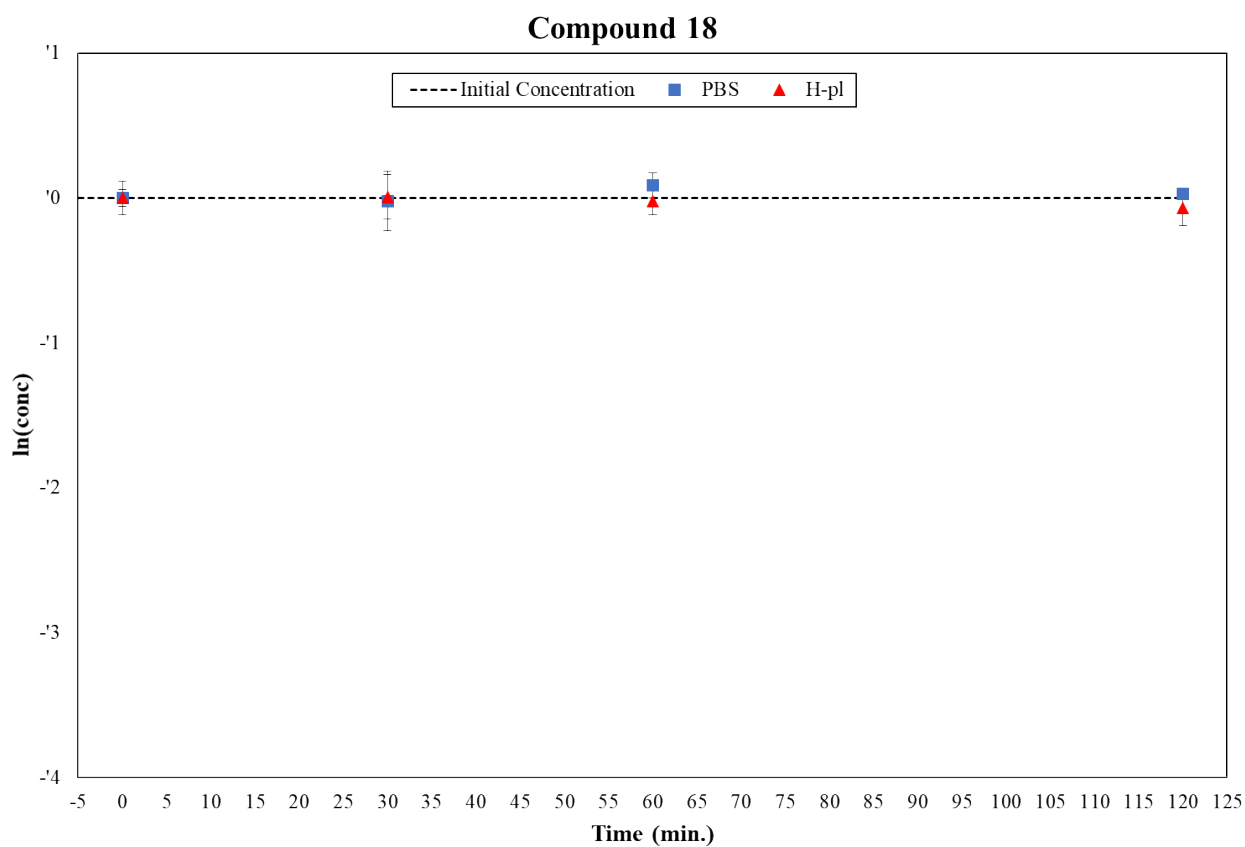


Figure S18: Degradation plots of **18** in PBS (blue square) and human plasma (red triangle), with the proper error bars.

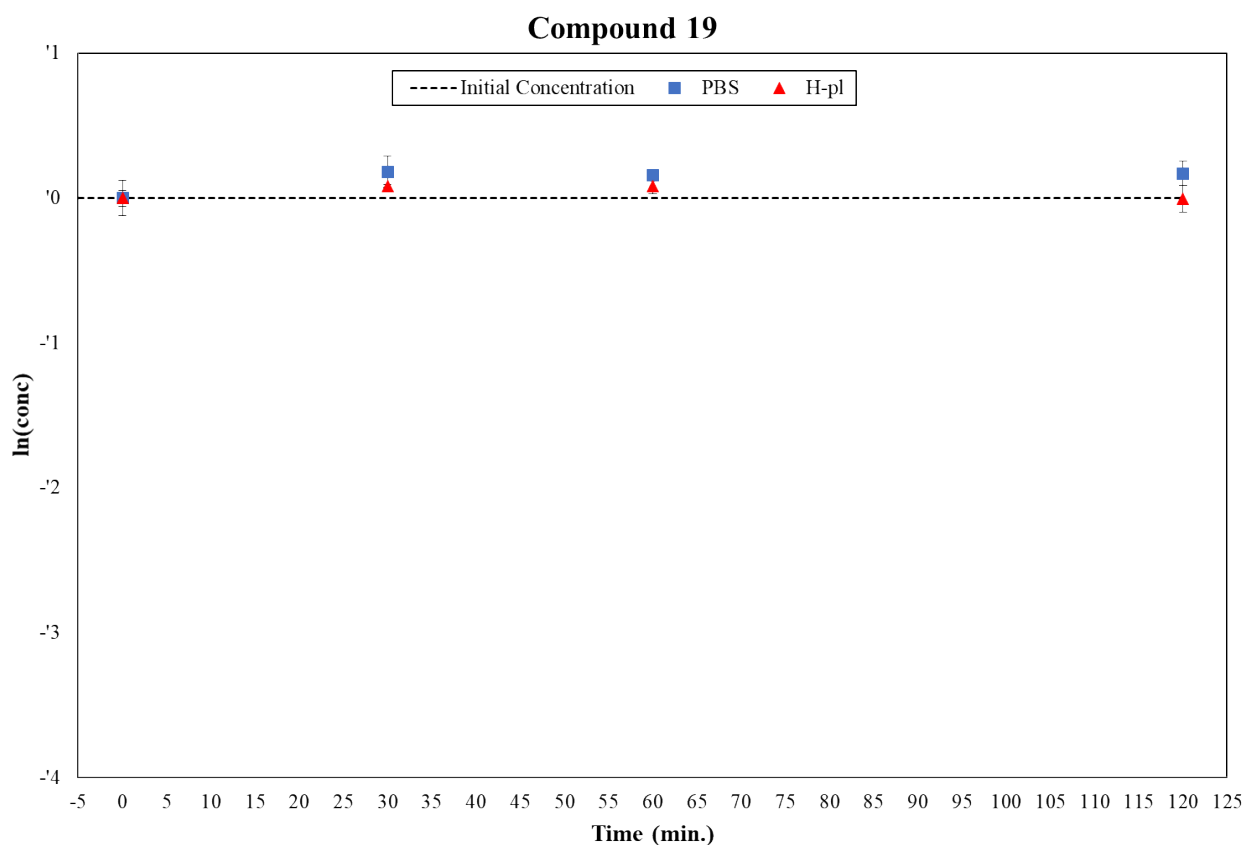


Figure S19: Degradation plots of **19** in PBS (blue square) and human plasma (red triangle), with the proper error bars.

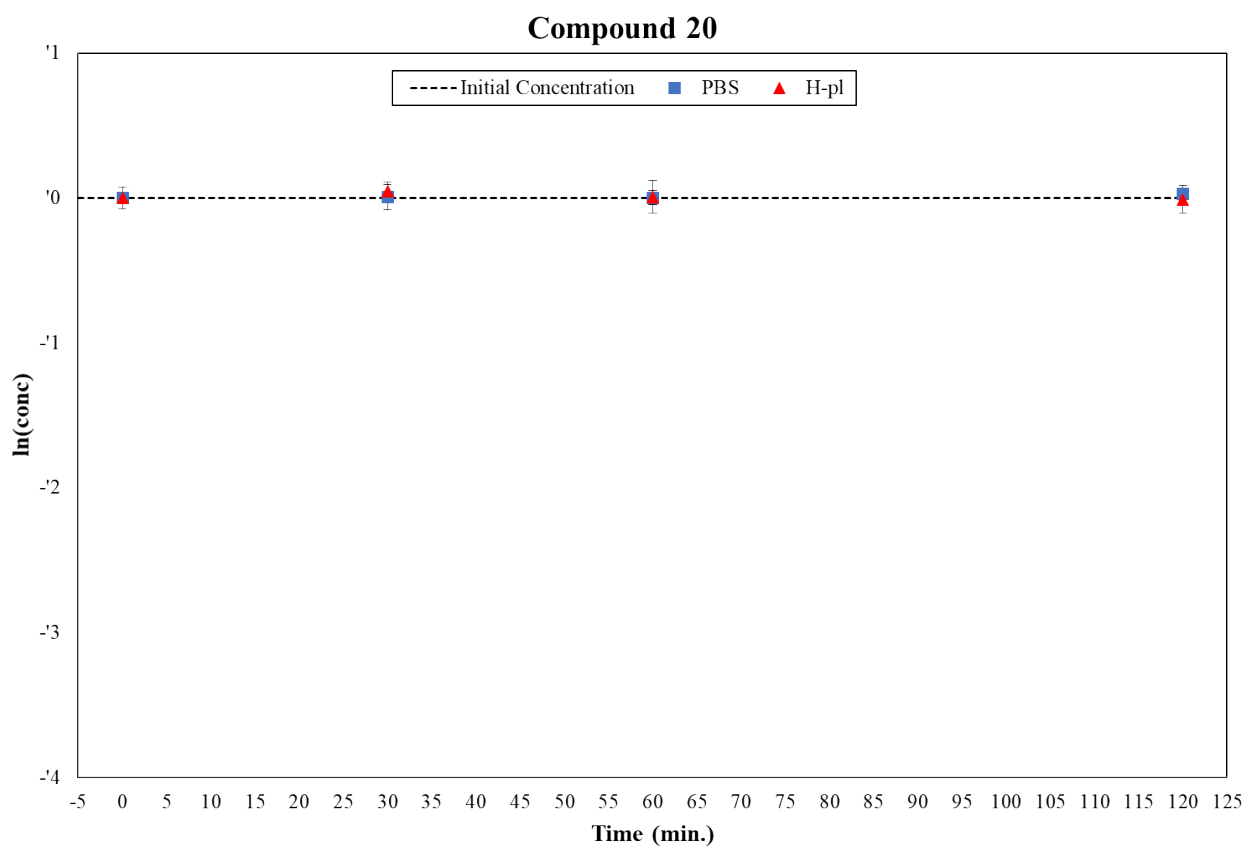


Figure S20: Degradation plots of **20** in PBS (blue square) and human plasma (red triangle), with the proper error bars.

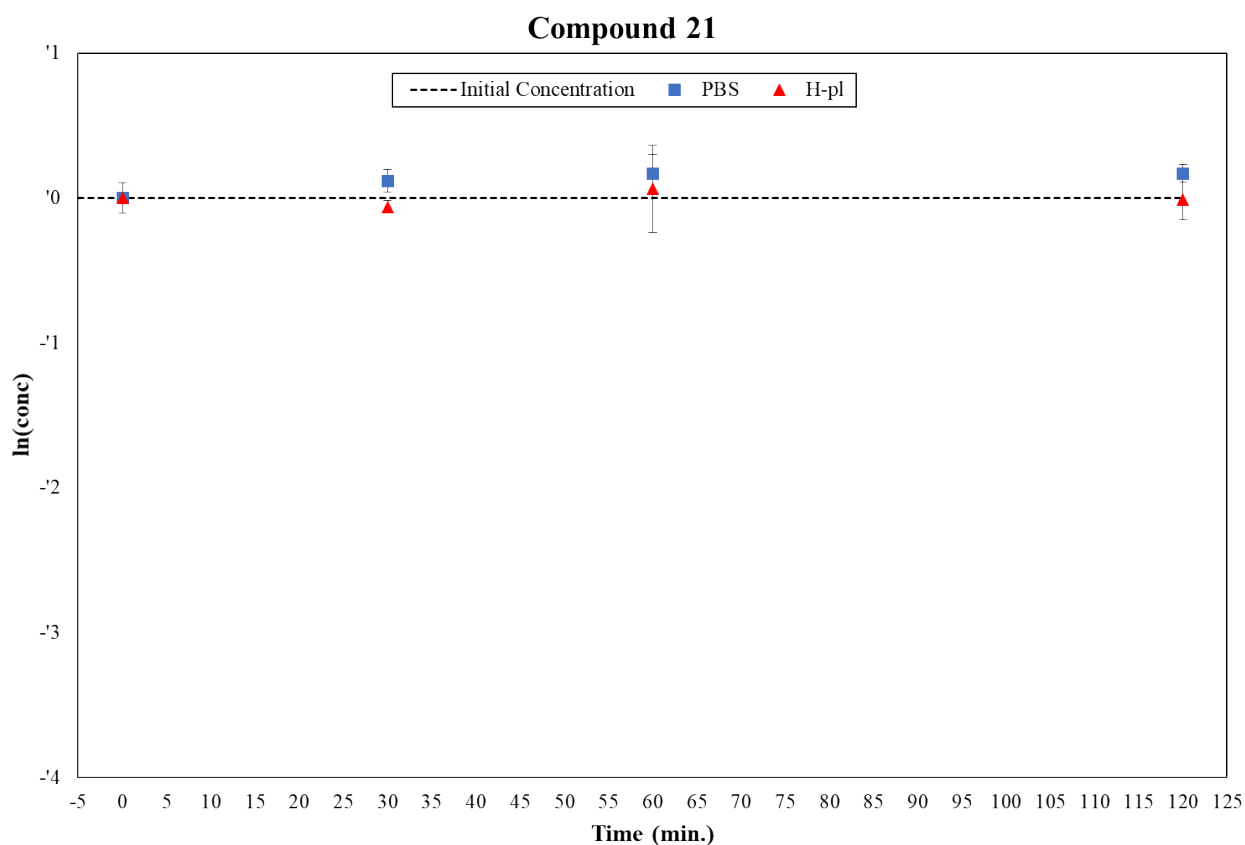


Figure S21: Degradation plots of **21** in PBS (blue square) and human plasma (red triangle), with the proper error bars.

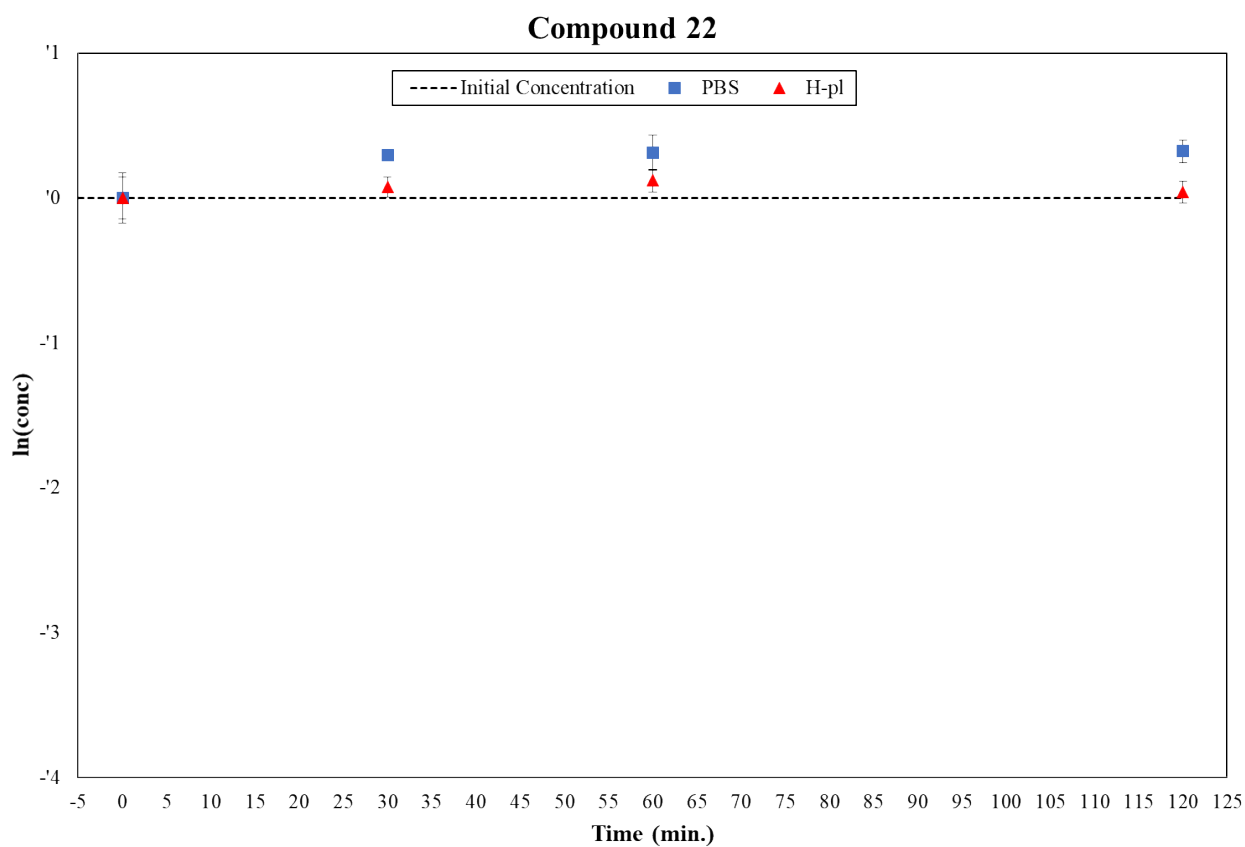


Figure S22: Degradation plots of **22** in PBS (blue square) and human plasma (red triangle), with the proper error bars.

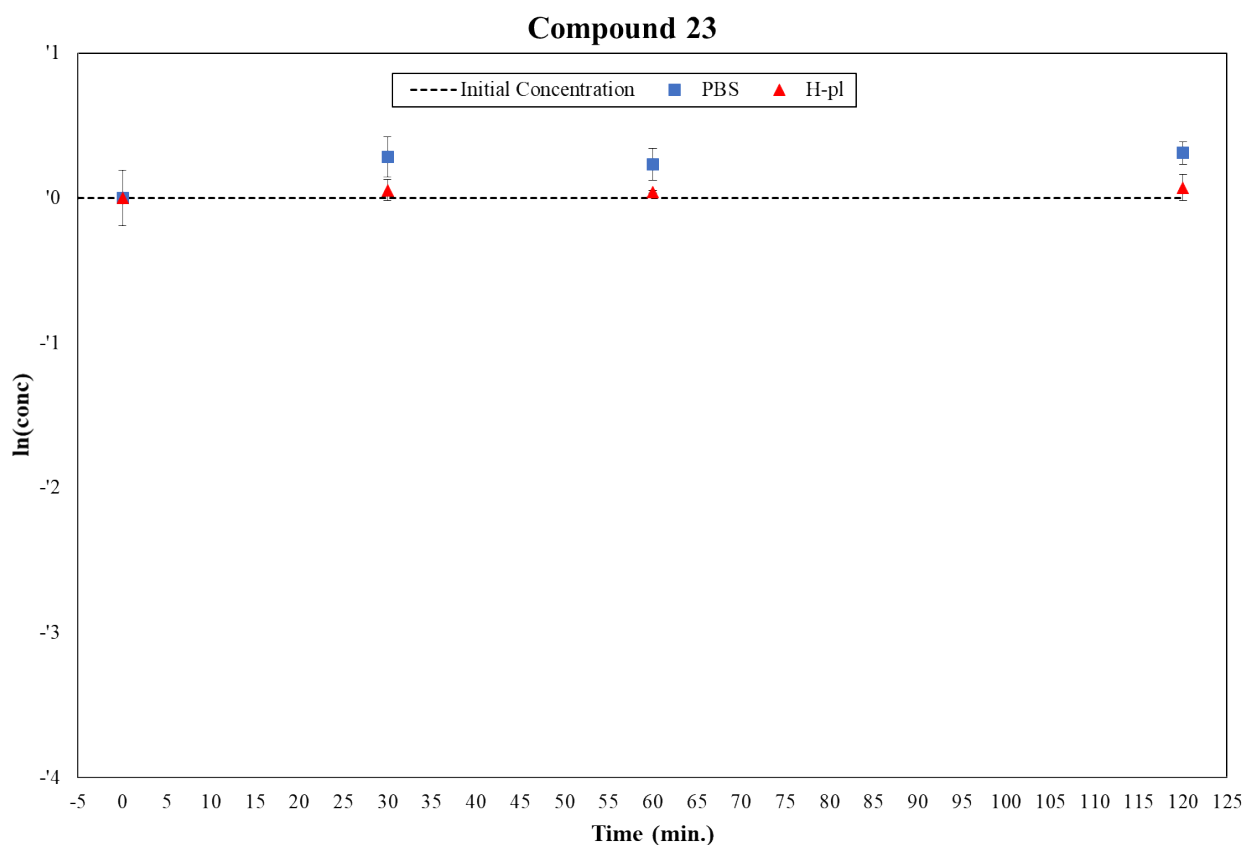


Figure S23: Degradation plots of **23** in PBS (blue square) and human plasma (red triangle), with the proper error bars.

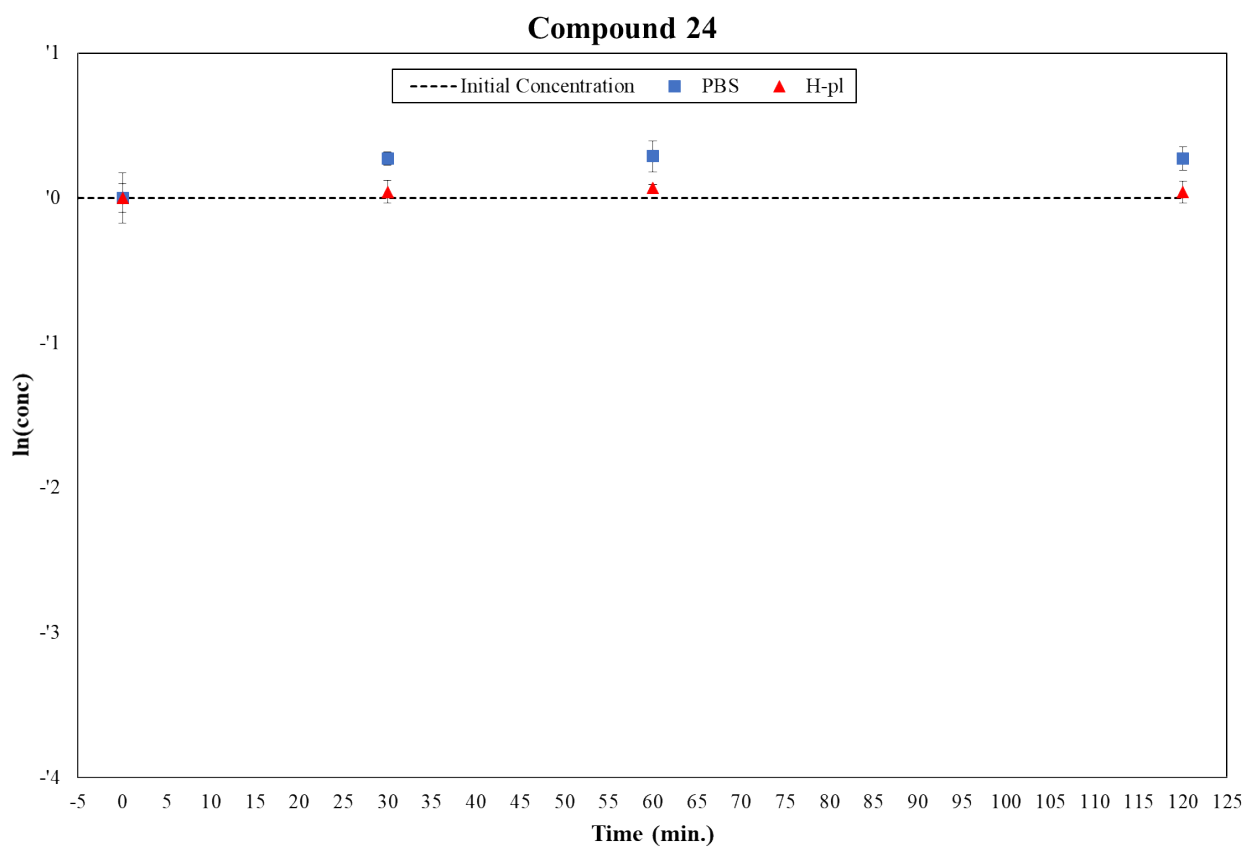


Figure S24: Degradation plots of **24** in PBS (blue square) and human plasma (red triangle), with the proper error bars.

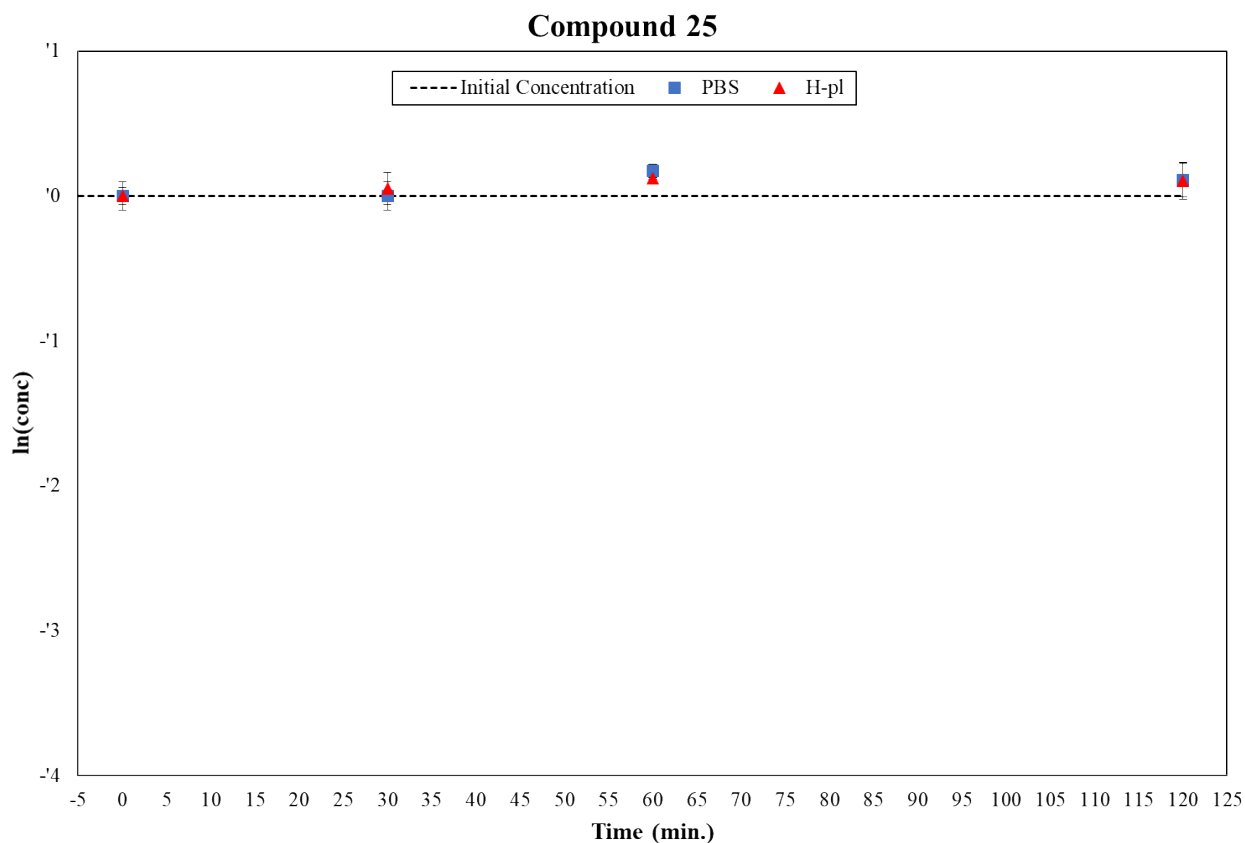


Figure S25: Degradation plots of **25** in PBS (blue square) and human plasma (red triangle), with the proper error bars.

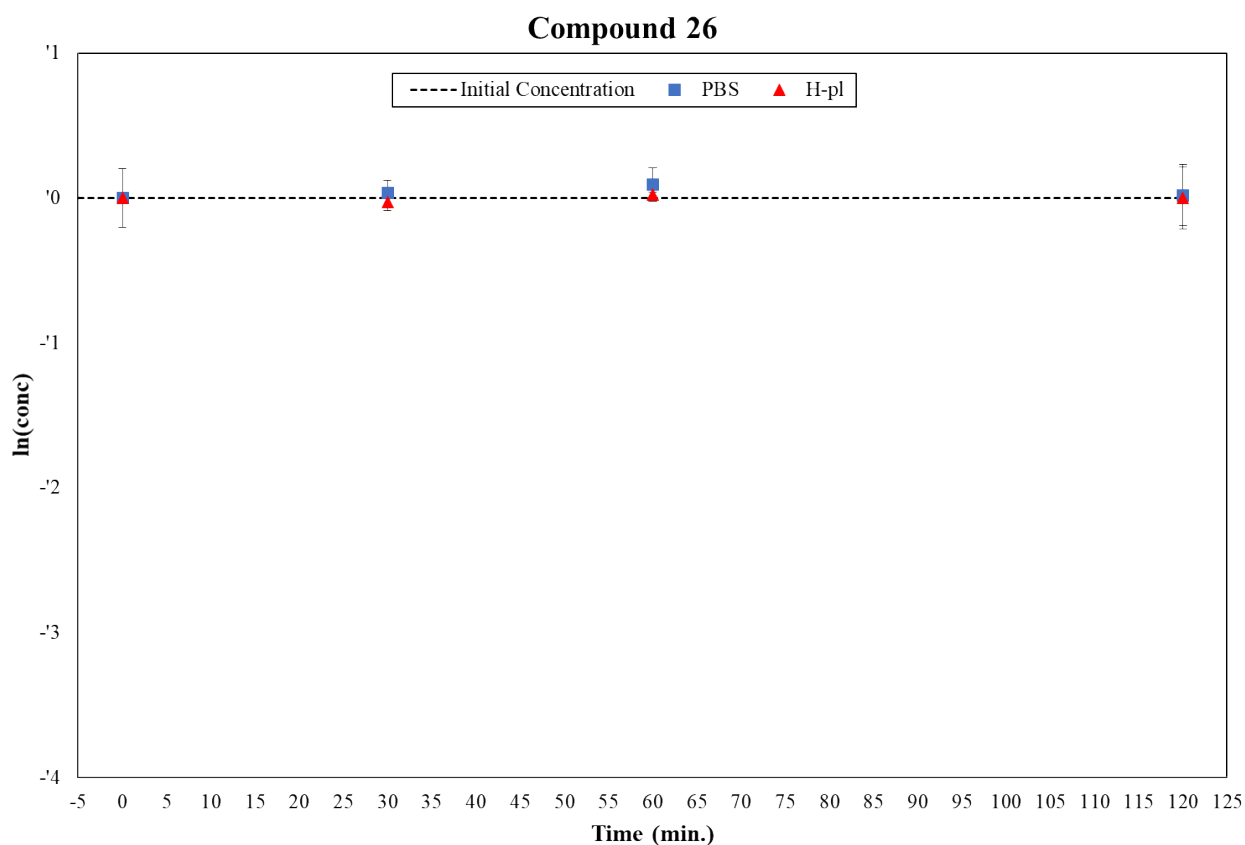


Figure S26: Degradation plots of **26** in PBS (blue square) and human plasma (red triangle), with the proper error bars.

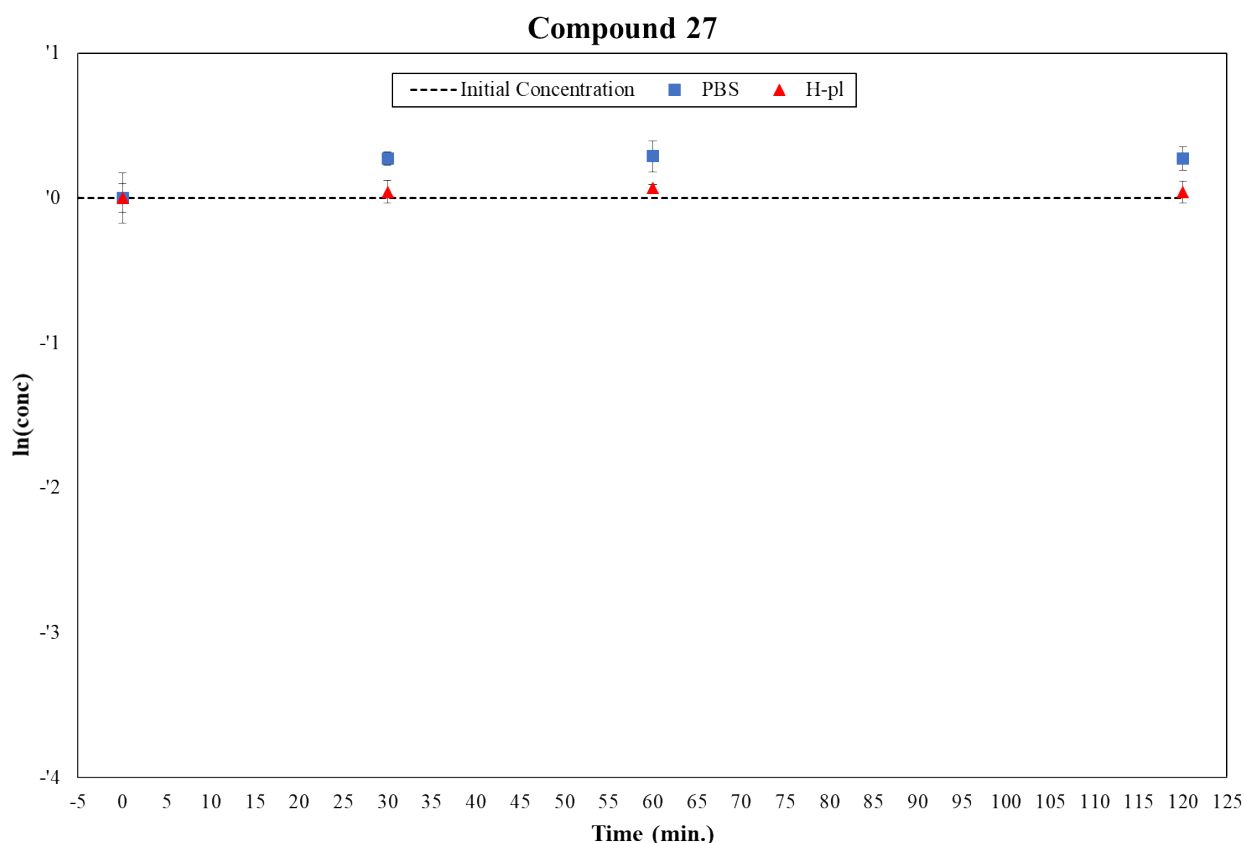


Figure S27: Degradation plots of **27** in PBS (blue square) and human plasma (red triangle), with the proper error bars.

HPLC-DAD method for purity analysis

The employed chromatographic parameters to check the purity of representative compounds were reported as follows:

- column, Pursuit C18 length = 50 mm, internal diameter= 2mm; particle size = 5 μ m purchased from Agilent Technologies (Palo Alto, CA, USA)
- acidic mobile phase, composed by 5 mM of ammonium formate and 10mM of formic acid in mQ water: acetonitrile 90:10 (v/v) solution (solvent A), 10 mM of ammonium formate and 5 mM of formic acid in mQ water: acetonitrile 10:90 (v/v) solution (solvent B).
- flow rate and the injection volume were 0.25 mL min⁻¹ and 5 μ L respectively.
- DAD detection set up was in the UV range between 210 to 400 nm. The chromatographic profile of each analyte was monitored at the λ of its maximum absorbance in acquired range.

The elution gradient is shown in Table S4.

Table S4: Elution gradient of mobile phase used for HPLC-DAD analysis

Time (min)	A (%)
0.00	90
8.00	10
13.00	10
13.01	90
18.00	90

The sample solution of each analyte/compound was prepared at $100 \mu\text{g mL}^{-1}$ in mQ water: acetonitrile 50:50 and analyzed by the HPLC-DAD method described above.

Chromatographic profiles of HPLC-DAD analysis of representative compounds (**2**, **3**, **5**, **6**, **8**, **9**, **13-17**) were reported in Figures S28-S38.

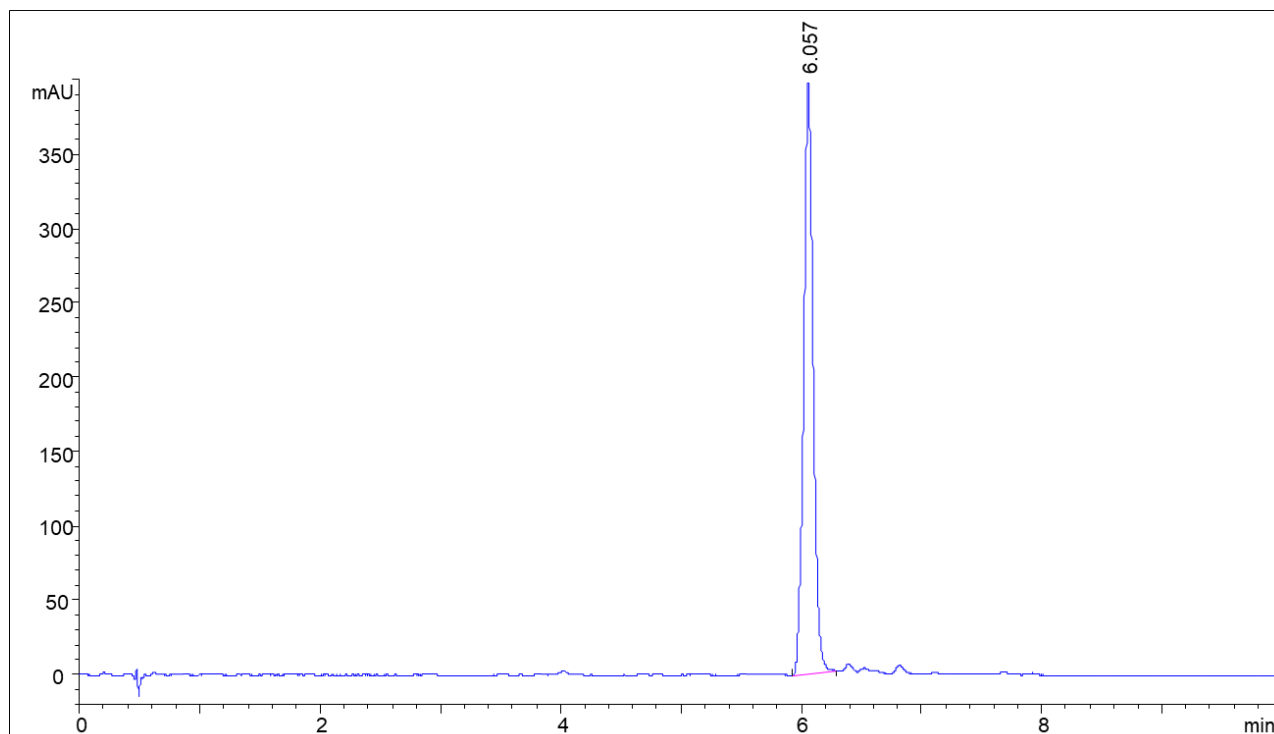


Figure S28: Chromatographic profile of compound **2** monitored at $\lambda=220$ nm.

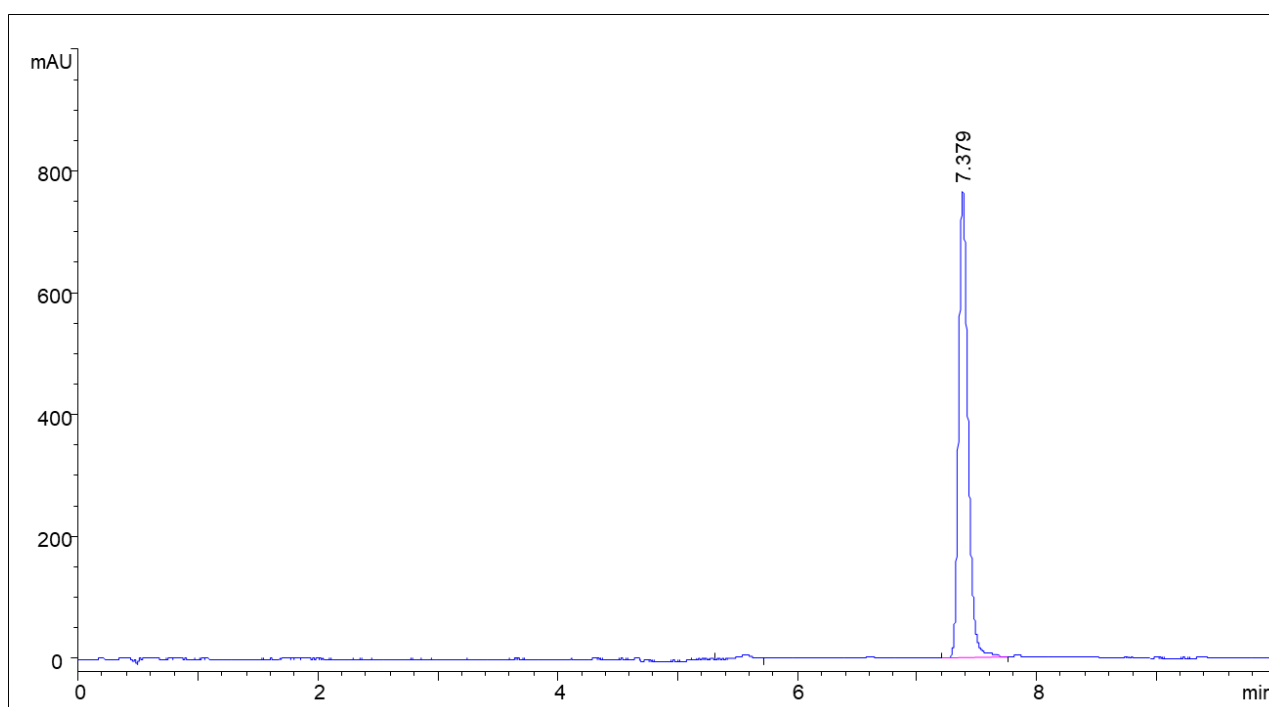


Figure S29: Chromatographic profile of compound **3** monitored at $\lambda=250$ nm.

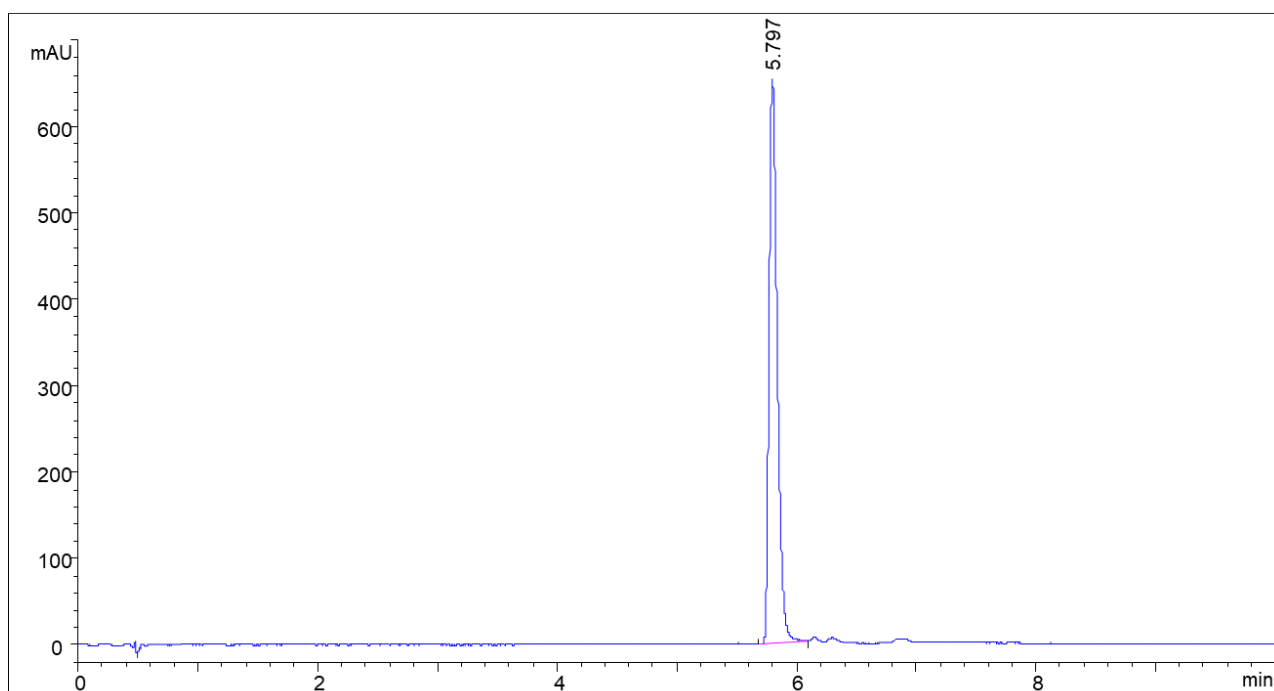


Figure S30: Chromatographic profile of compound **5** monitored at $\lambda=220$ nm.

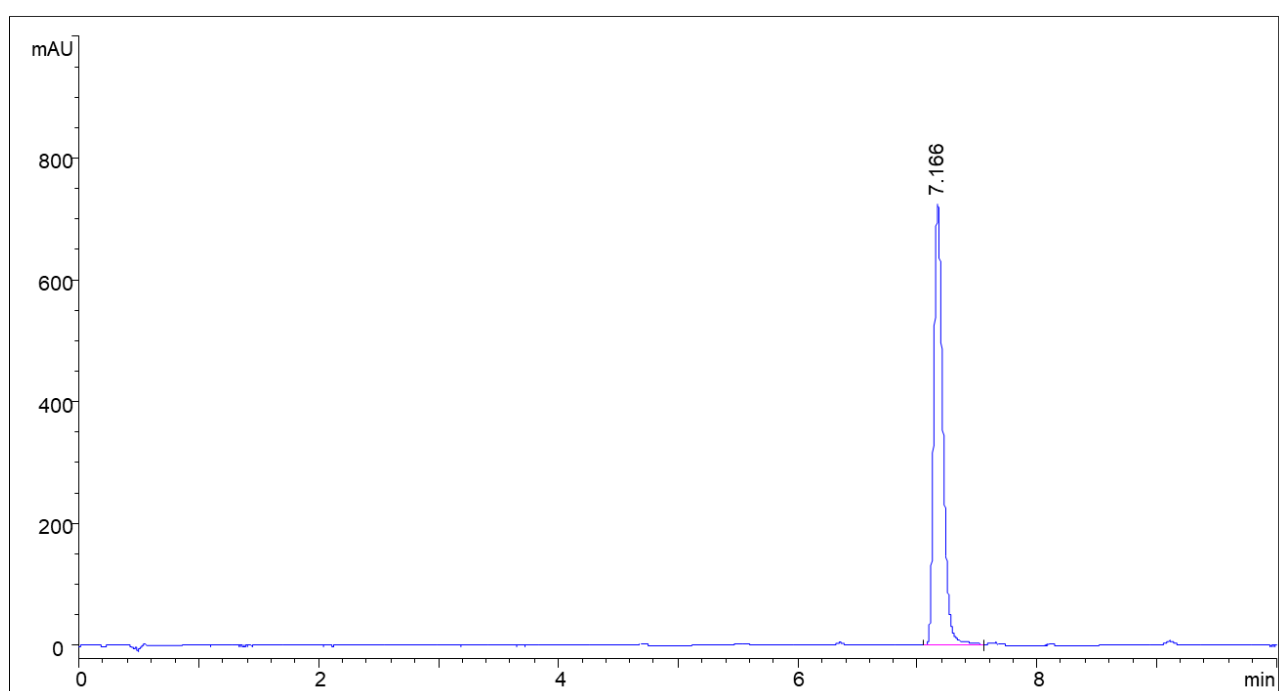


Figure S31: Chromatographic profile of compound **6** monitored at $\lambda=250$ nm.

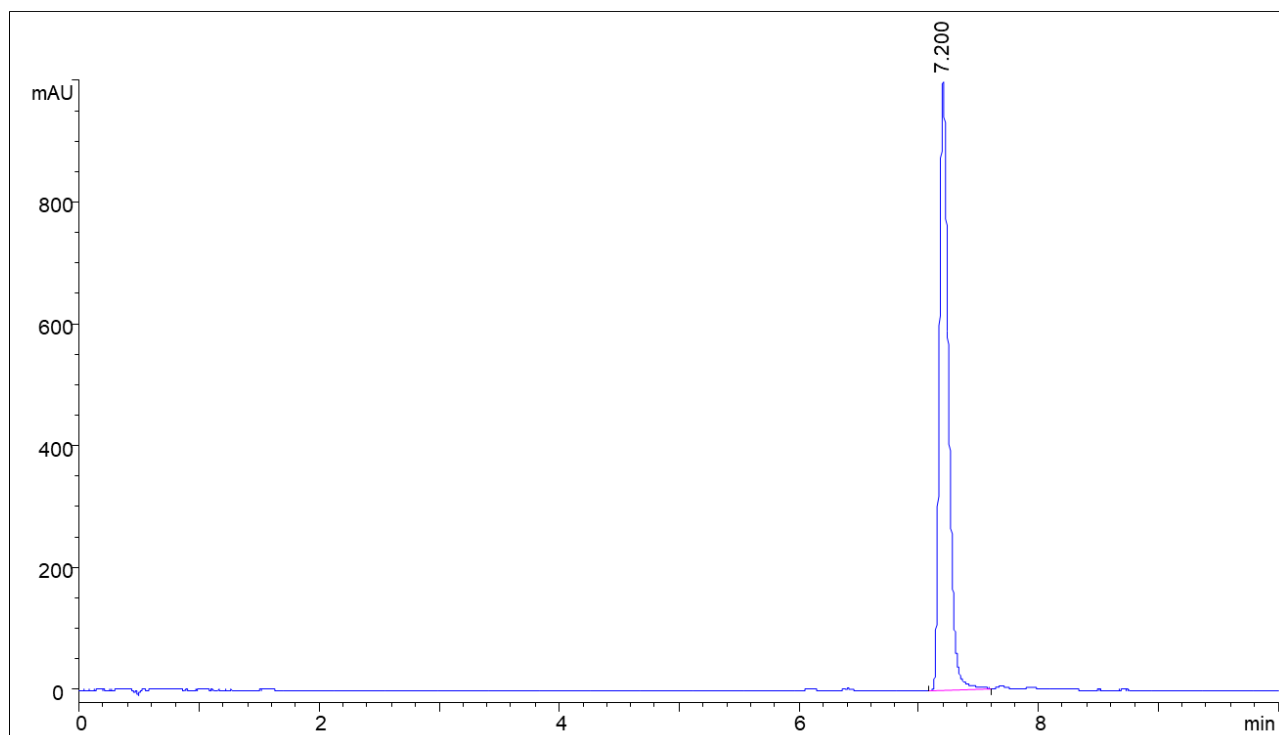


Figure S32: Chromatographic profile of compound **8** monitored at $\lambda=250$ nm.

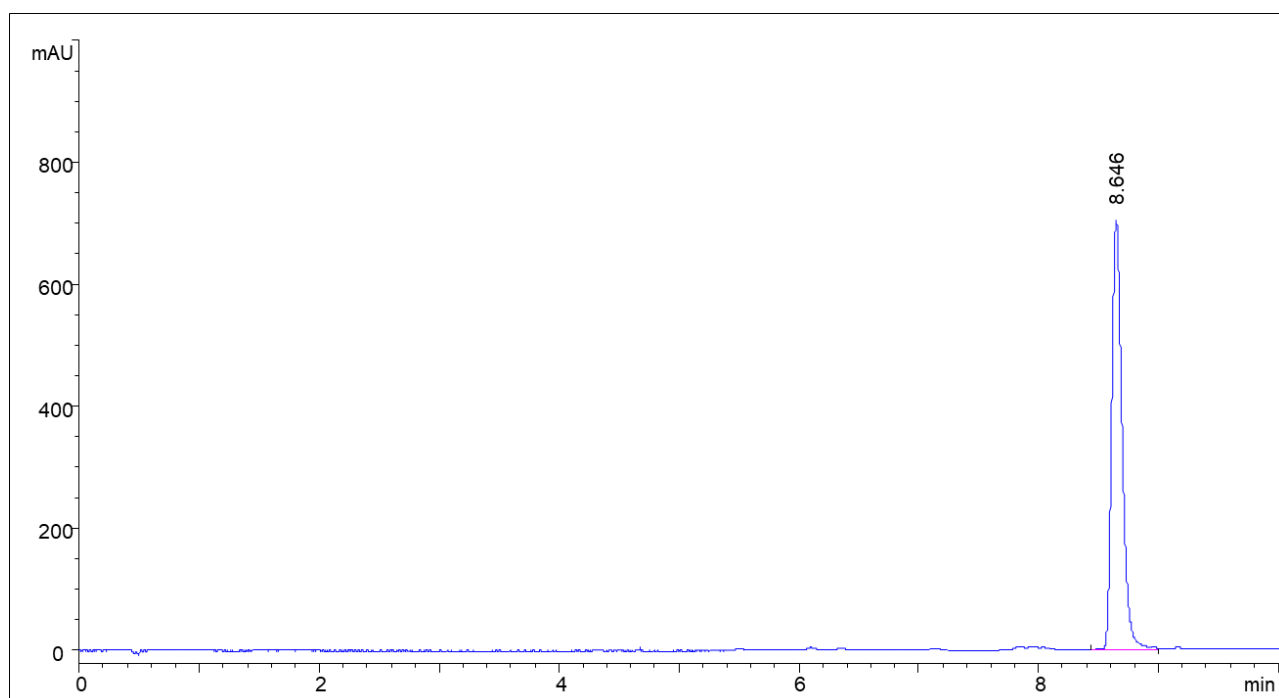


Figure S33: Chromatographic profile of compound **9** monitored at $\lambda=250$ nm.

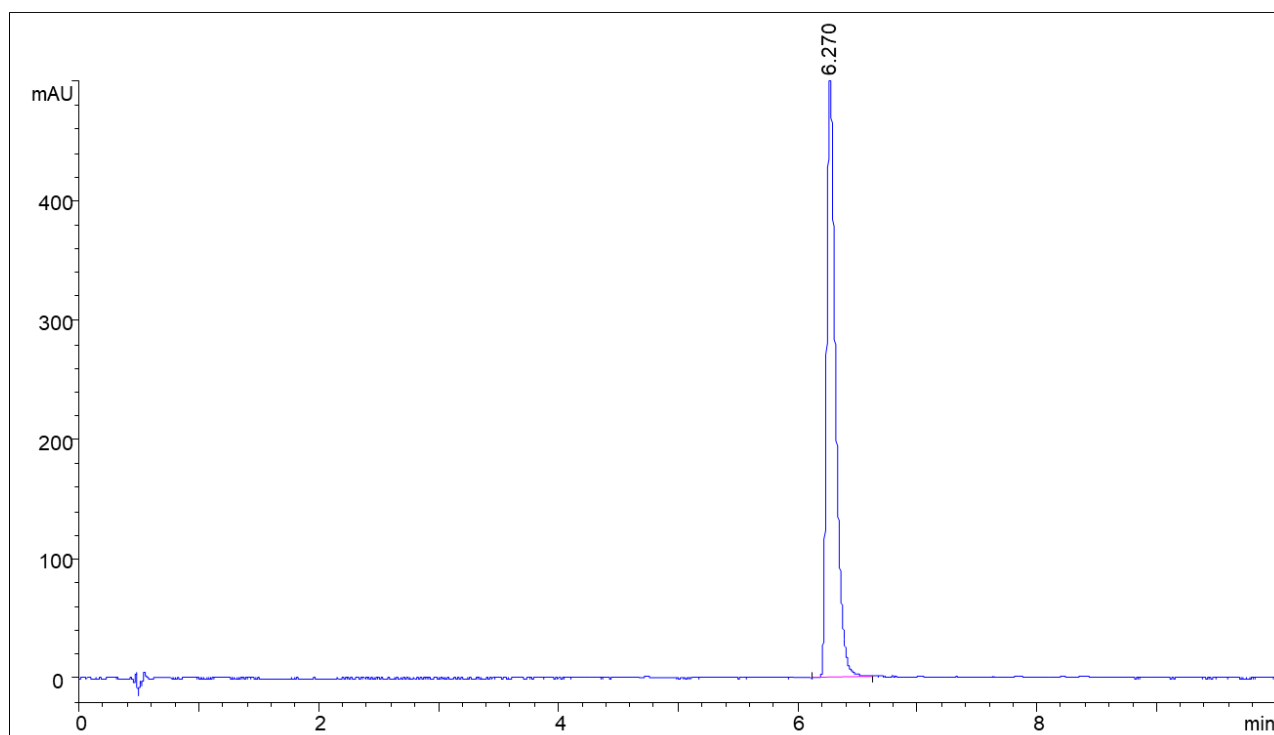


Figure S34: Chromatographic profile of compound **13** monitored at $\lambda=220$ nm.

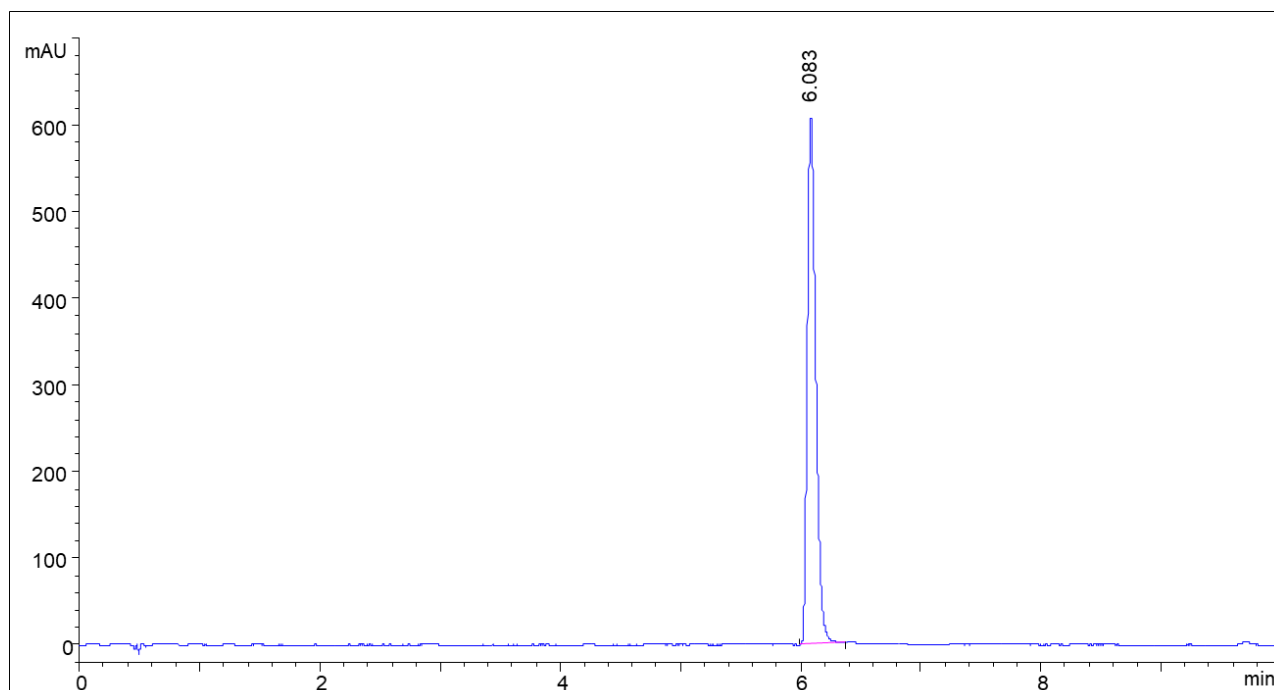


Figure S35: Chromatographic profile of compound **14** monitored at $\lambda=220$ nm.

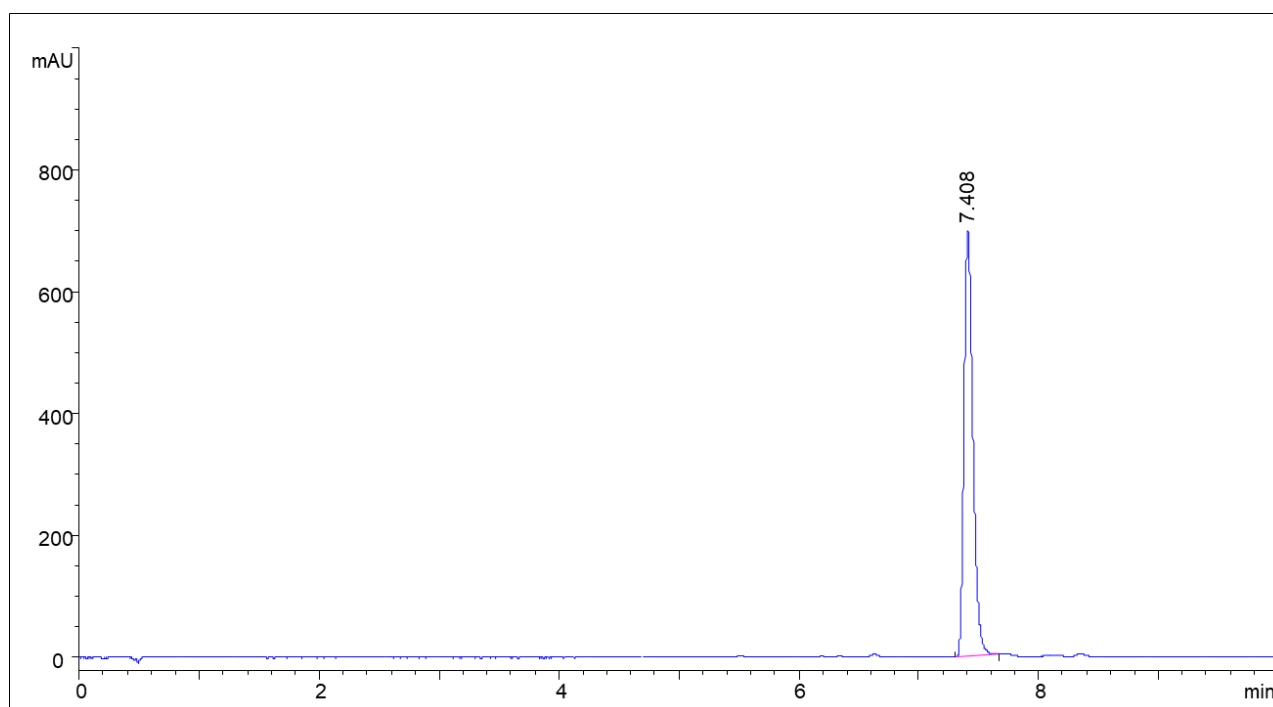


Figure S36: Chromatographic profile of compound **15** monitored at $\lambda=250$ nm.

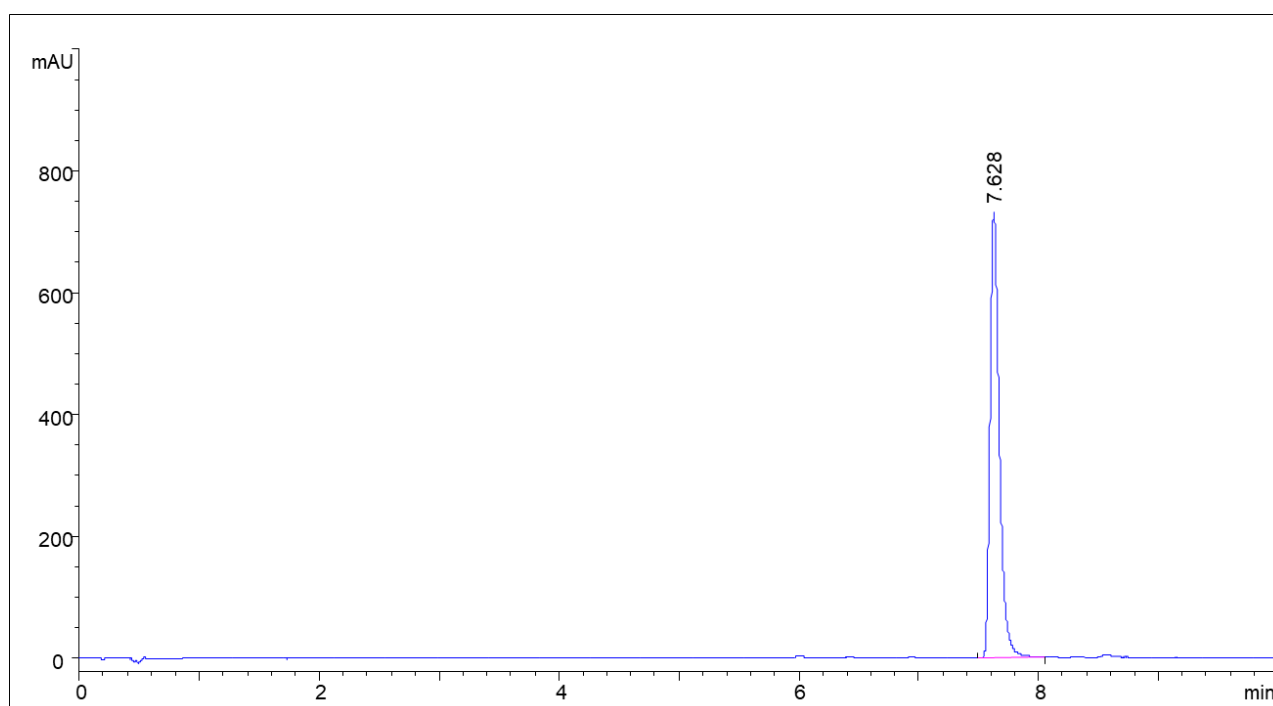


Figure S37: Chromatographic profile of compound **16** monitored at $\lambda=250$ nm.

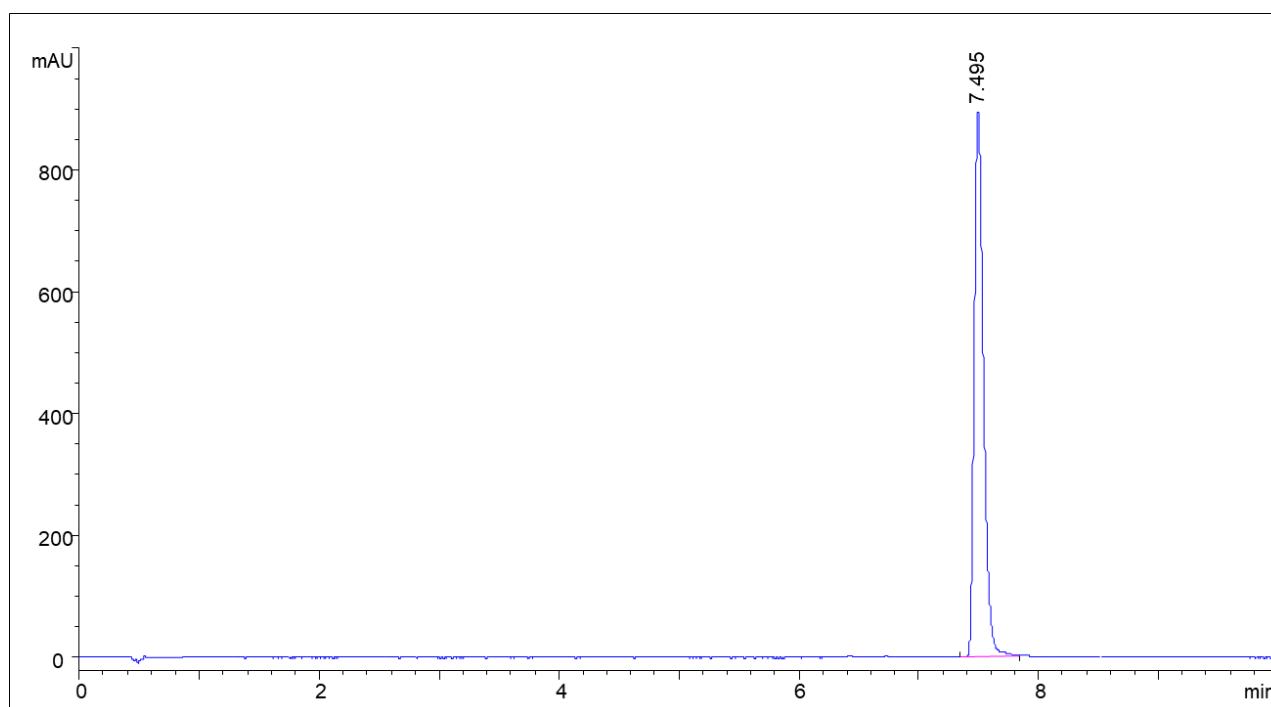


Figure S38: Chromatographic profile of compound **17** monitored at $\lambda=250$ nm.

UV spectra of compounds **2**, **3**, **5**, **6**, **8**, **9**, **13-17** were reported in Figures S39-S43.

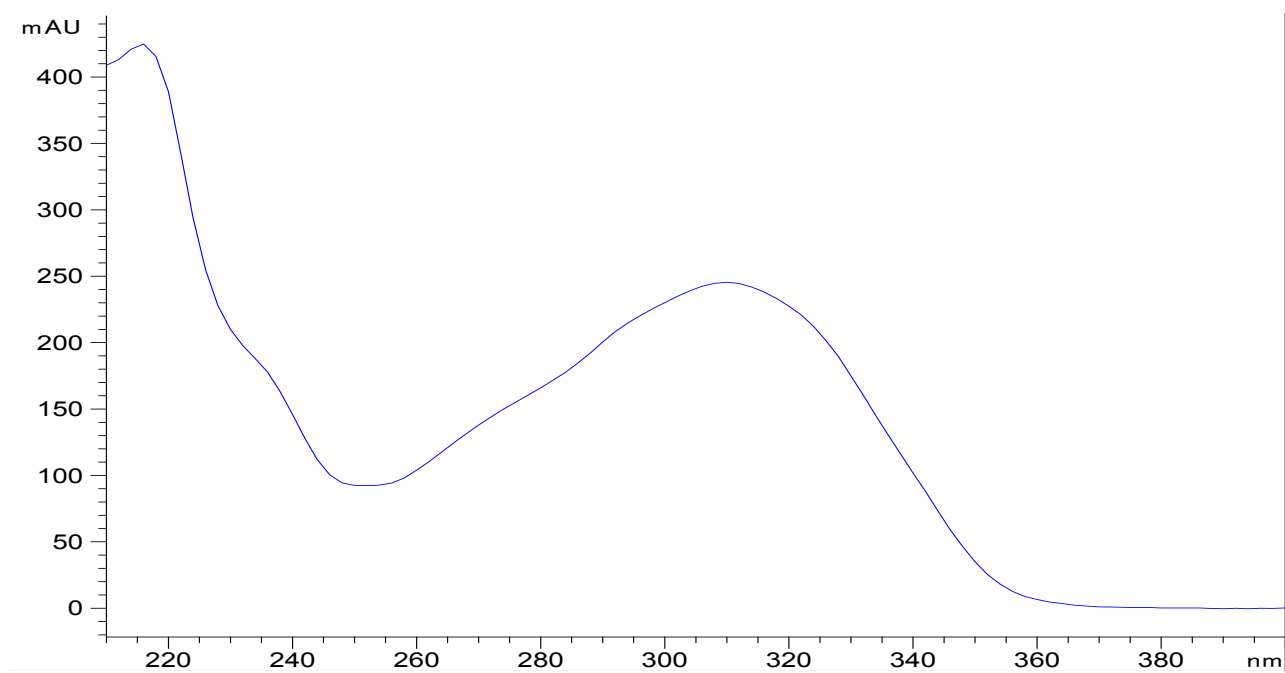


Figure S39: UV spectrum of compounds **2** and **13**.

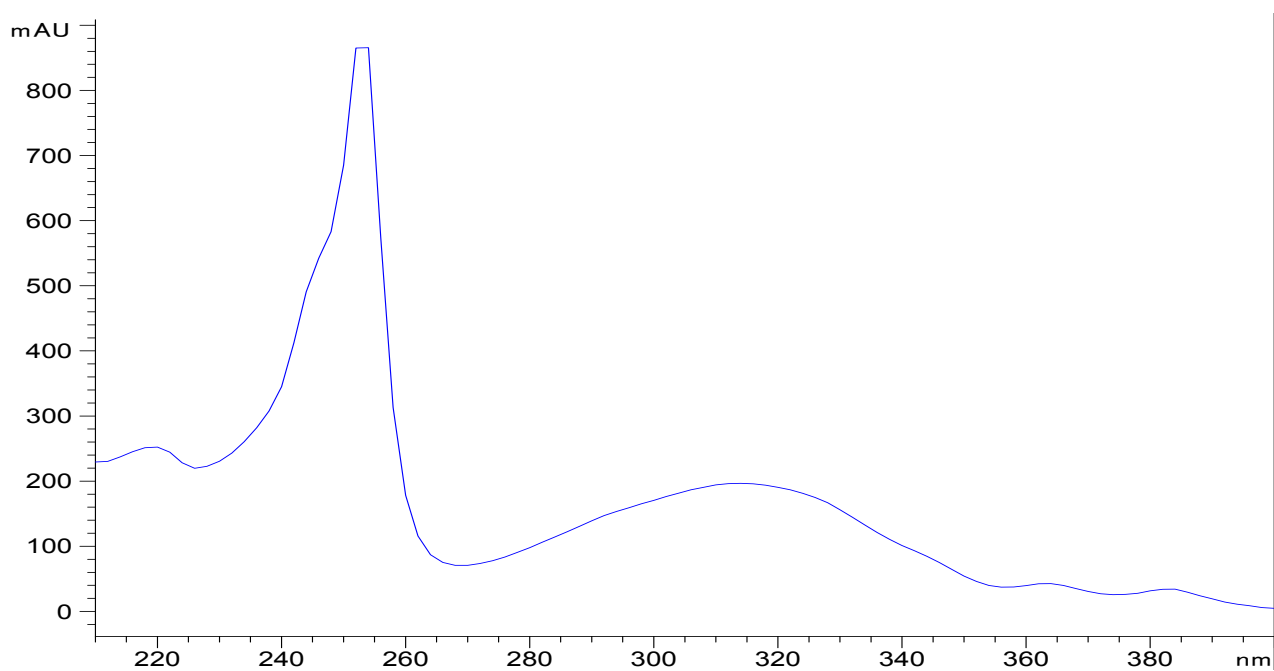


Figure S40: UV spectrum of compounds **3** and **16**.

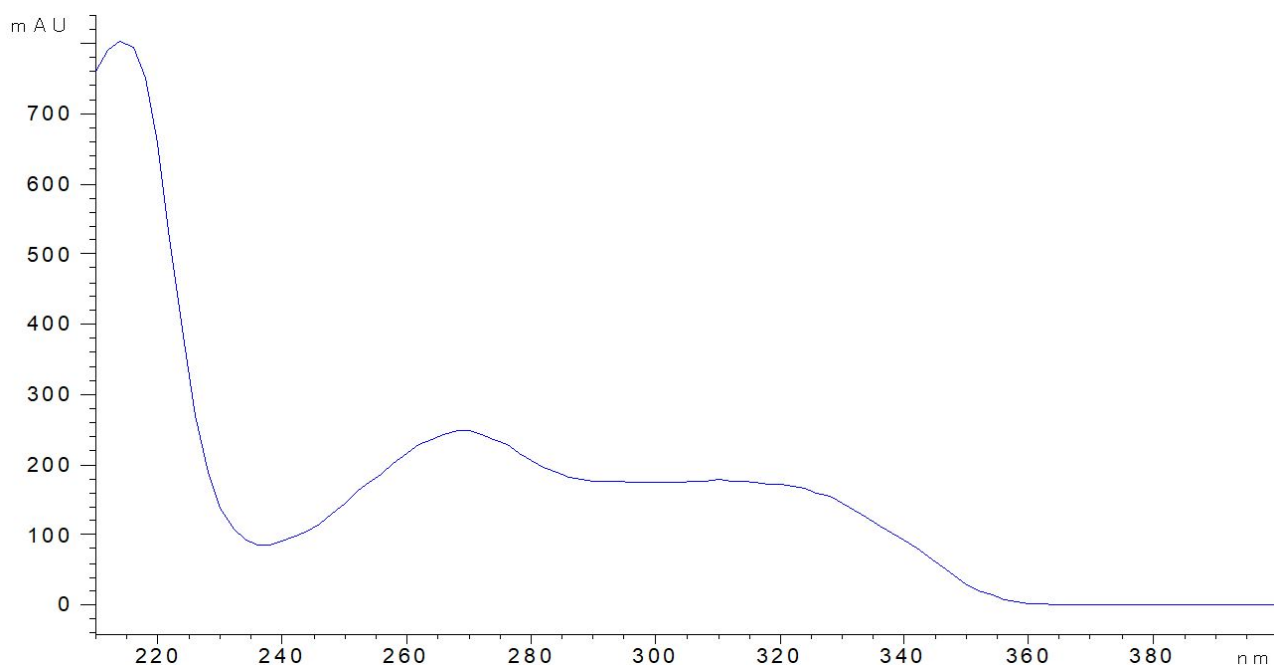


Figure S41: UV spectrum of compounds **5** and **14**.

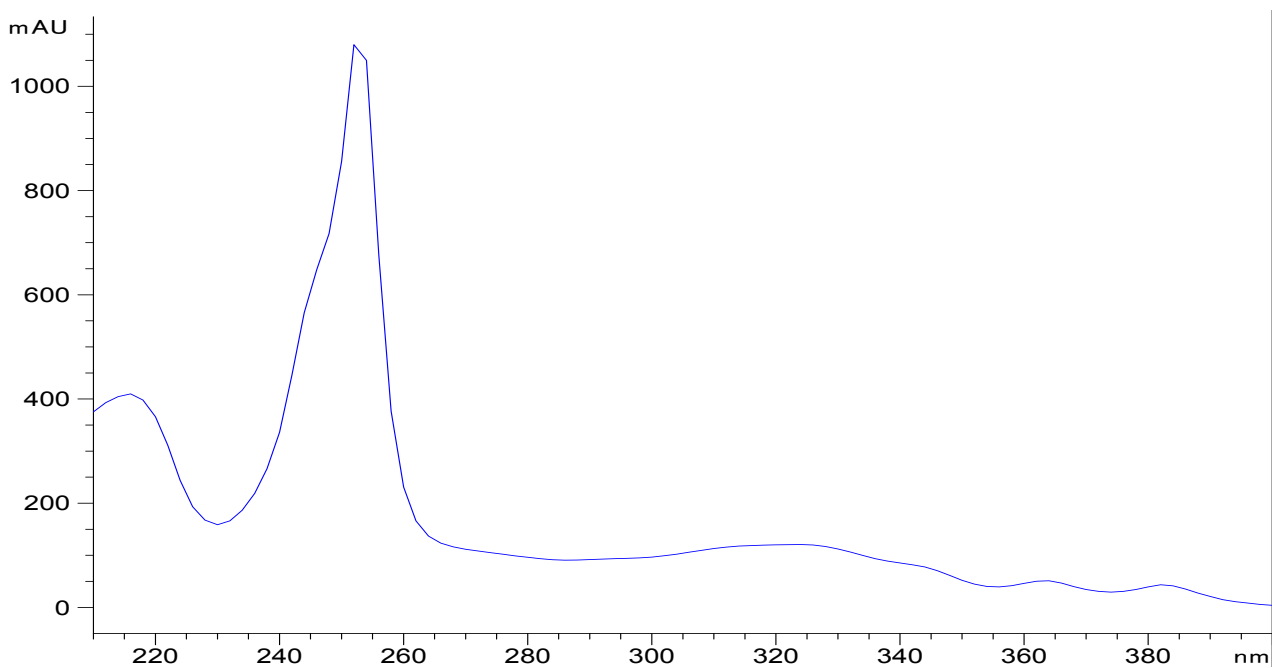


Figure S42: UV spectrum of compounds **6**, **8**, **15** and **17**.

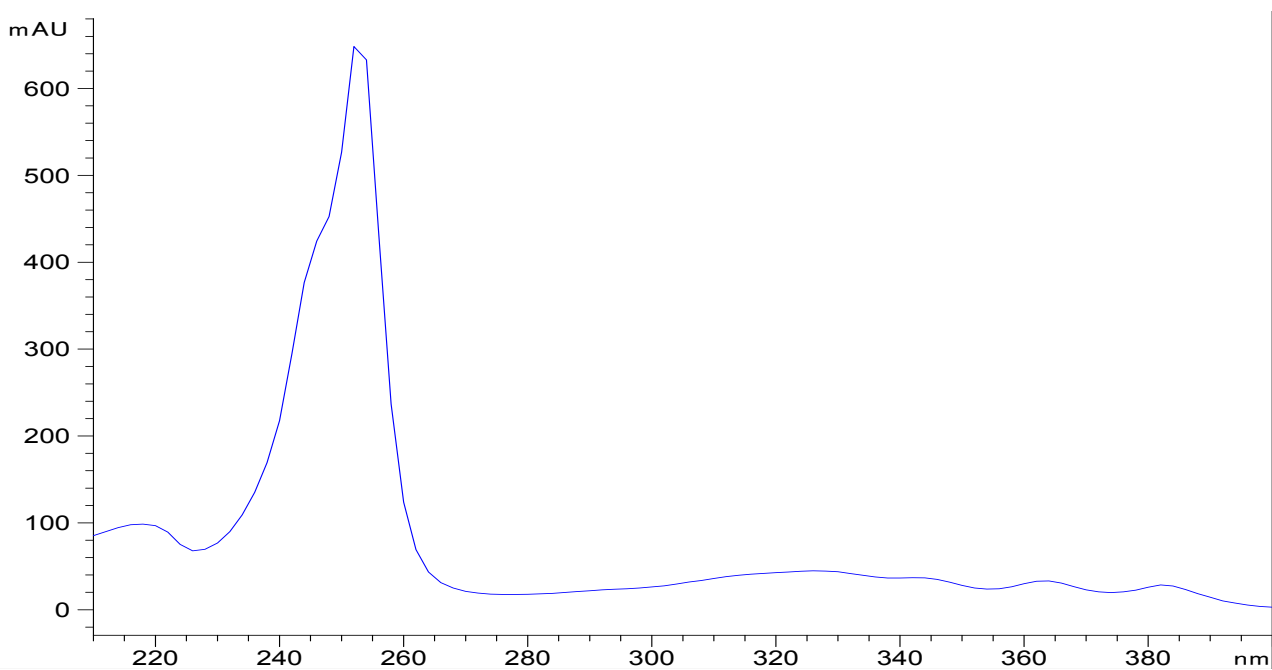


Figure S43: UV spectrum of compound **9**.

Expression levels of P-gp and hCA XII in sensitive HT29 and A549 human cancer cell lines, in resistant wild-type HT29/DOX and A549/DOX cells, and in their P-gp or hCA XII knock-out (KO) counterparts.

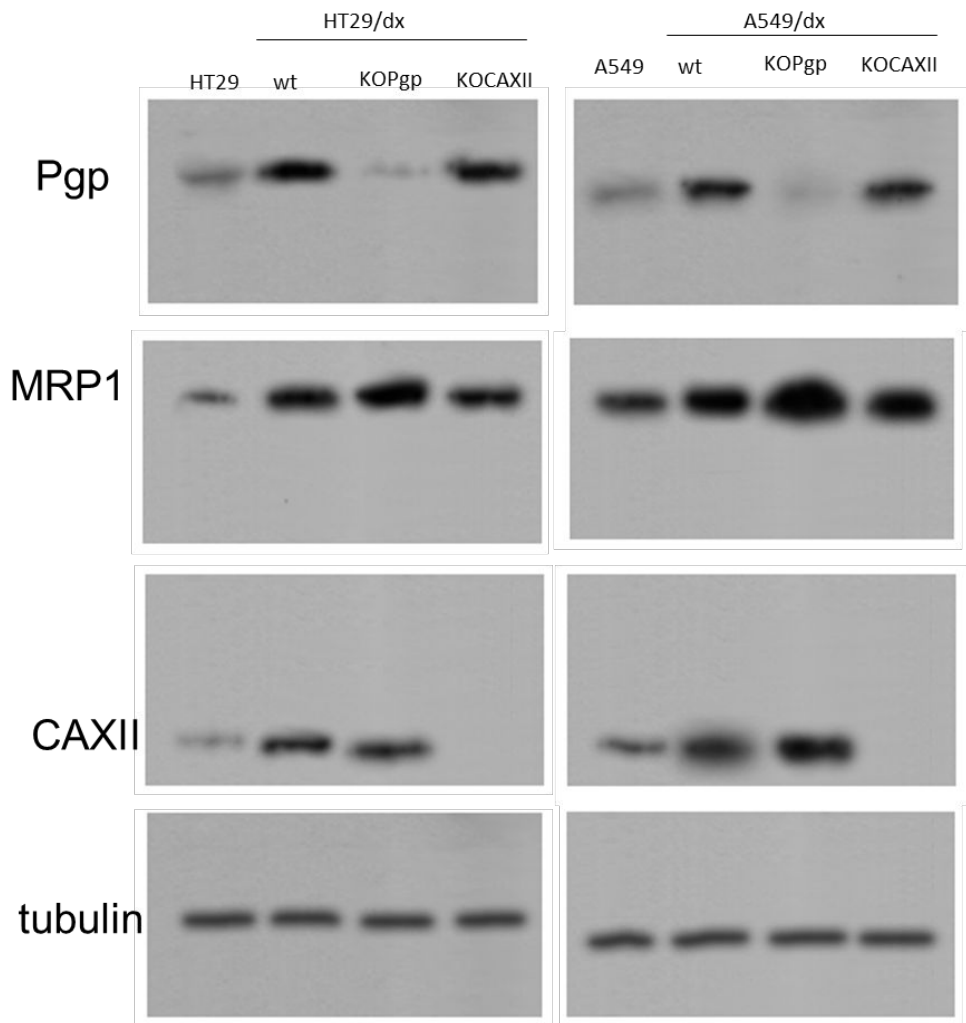


Figure S44. Immunoblotting analysis of P-gp and hCA XII in doxorubicin sensitive HT29 and A549 human cancer cell lines, in wild-type doxorubicin resistant HT29/DOX and A549/DOX cells and in their P-gp or hCA XII knocked-out (KO) counterparts. wt: parental wild-type HT29/DOX and A549/DOX cells. Tubulin was used as control of equal protein loading. The image is representative of three independent experiments.

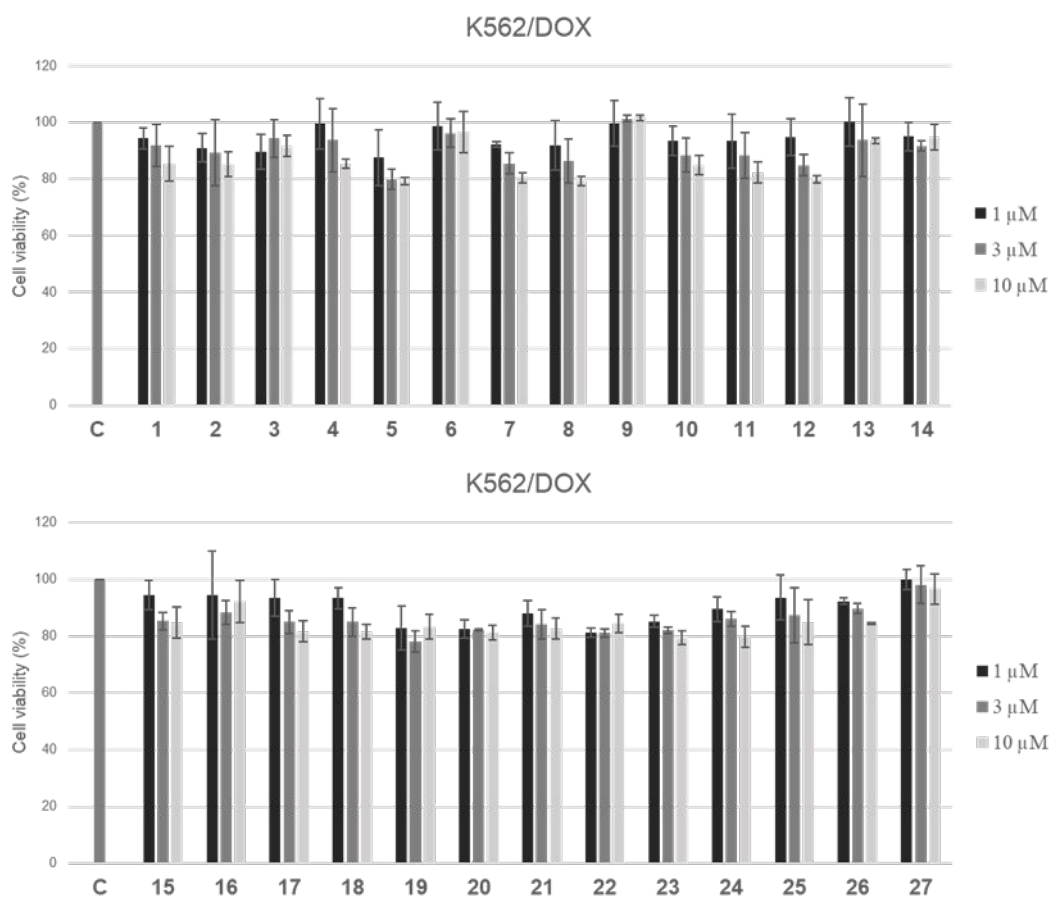


Figure S45. Viability of K562/DOX, cells incubated for 72 h with compounds 1-27 at 1, 3 and 10 μM, measured by the MTT assay, in triplicates. Data are the means \pm SD (n= 3).

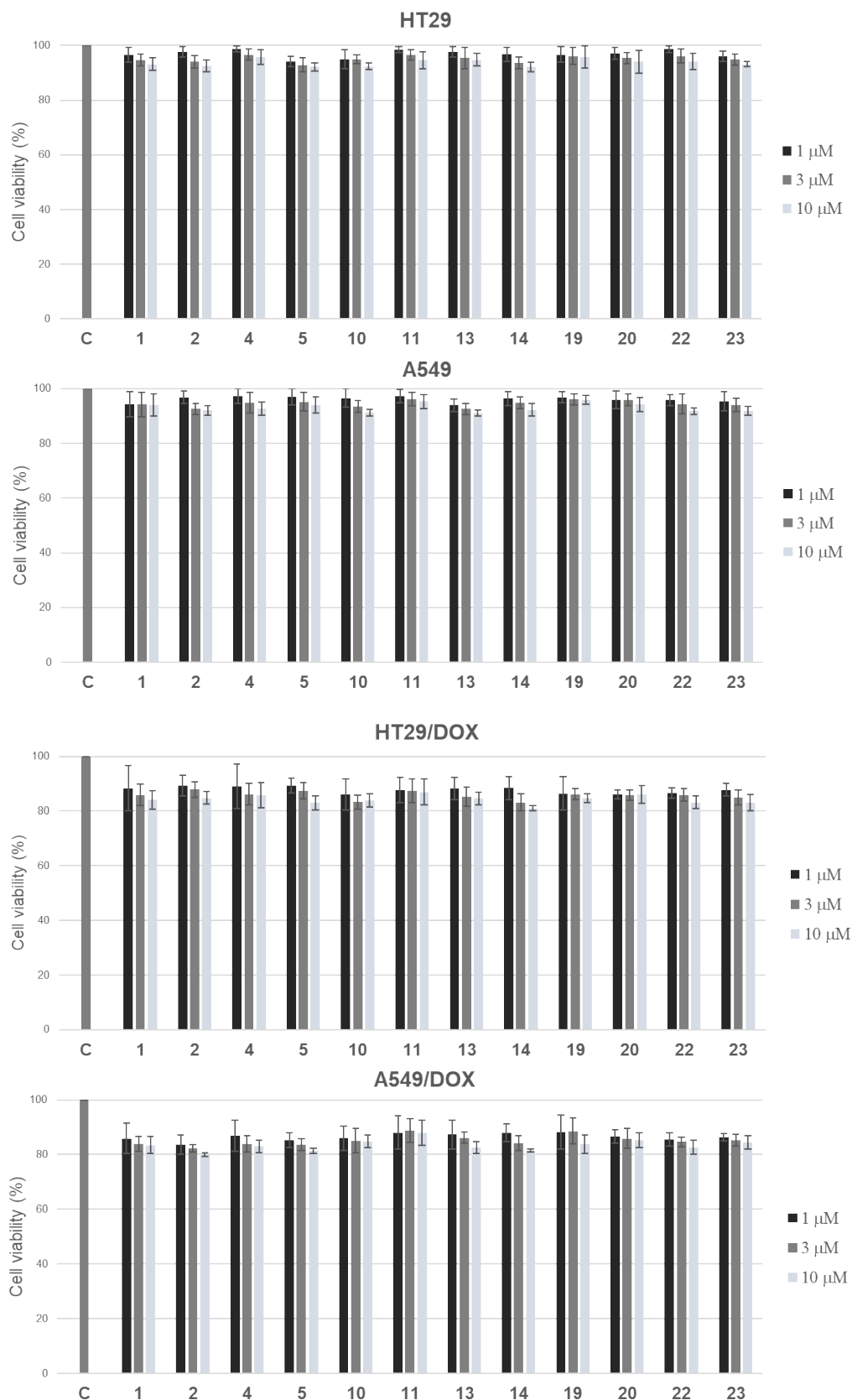


Figure S46. Viability of colon and lung cancer cells. Viability of HT29, A549, HT29/DOX and A549/DOX cells, incubated for 72 h with selected compounds at 1, 3 and 10 μM , measured by the MTT assay, in triplicates. Data are the means \pm SD ($n=3$).

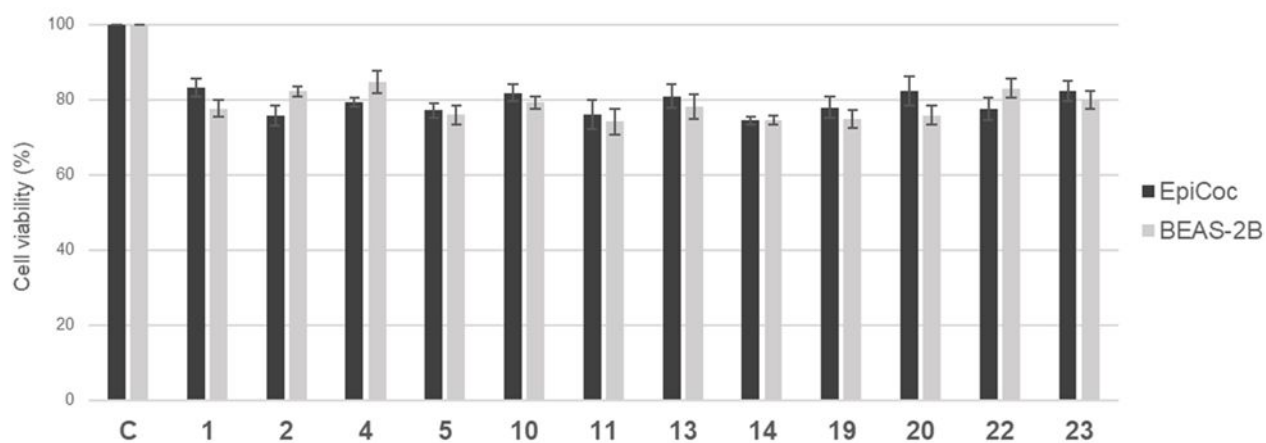


Figure S47. Viability of non-transformed epithelial colon and lung cells. Viability of EpiCoC and BEAS-2B cells, incubated for 72 h with selected compounds at 10 μ M, measured by the MTT assay, in triplicates. Data are the means \pm SD (n= 3).